

Investigation of natural fiber composites heterogeneity with respect to automotive structures

Proefschrift

ter verkrijging van de graad van doctor
aan de Technische Universiteit Delft,
op gezag van de Rector Magnificus prof.dr.ir. J.T. Fokkema,
voorzitter van het College voor Promoties,
in het openbaar te verdedigen

op 31 oktober 2005 om 10.30 uur

door

Kirill Gennadjevich KAVELIN

Master of Science in Mechanical Engineering,
Budapest University of Technology and Economics,
geboren te Izhevsk, Rusland

Dit proefschrift is goedgekeurd door de promotor:
Prof. ir. J. L. Spoormaker

Samenstelling promotiecommissie:

Rector Magnificus,	voorzitter
Prof. ir. J. L. Spoormaker	Technische Universiteit Delft, promotor
Dr. P. V. Kandachar	Technische Universiteit Delft
Prof. dr. ir. I. Verpoest	Katholieke Universiteit Leuven, België
Prof. ir. A. Beukers	Technische Universiteit Delft
Prof. dr. ir. A. Bakker	Technische Universiteit Delft
Prof. dr. ir. L. J. Ernst	Technische Universiteit Delft
Dr. G. T. Pott	Adviseur

ISBN-10: 90-9020036-3

ISBN-13: 978-90-9020036-1

Keywords: automotive design, composite, heterogeneity, natural fiber, spectral analysis

Copyrights © 2005 by K.G. Kavelin

Printed by PrintPartners Ipskamp, Enschede, Netherlands

Investigation of natural fiber composites heterogeneity with respect to automotive structures

Thesis

Presented for the degree of doctor
at Delft University of Technology,
under the authority of the Vice-Chancellor, prof.dr.ir. J.T. Fokkema,
to be defended in public in the presence of the committee
appointed by the Board of Doctorates

October 31, at 10.30

by

Kirill Gennadjevich KAVELIN

Master of Science in Mechanical Engineering,
Budapest University of Technology and Economics,
born in Izhevsk, Russia

To my lovely wife and my son

SUMMARY

This work is carried out within the scope of the program “Smart Product Systems” focusing on the life cycle efficiency of products. This program has emerged because of the growing interest towards environmental protection, which requires a sustainable development of the industrial progress. A Dutch-EVO concept car was taken as a vehicle for the research within this program.

One of the innovations in the Dutch-EVO project is the use of modern lightweight materials to reach the sustainability of the concept car. Thus, “Exploring the use of modern materials for automotive applications” project has been conducted as a part of the program. The purpose of this project is to explore new materials that have the potential to meet the requirements of modern automobile design.

In this research a number of modern materials applicable to automotive structures like magnesium alloys and composites are compared with the conventional materials like steel and aluminum alloys. Not only mechanical properties of the materials are compared, but also potential car weight reduction. However, the application of new materials requires sometimes a complete change in production technology. The costs of these changes are also discussed alongside with the mechanical properties of new materials. Complex interaction between economical, technological and environmental aspects is considered during the selection of suitable materials. As a result, a polymer composite reinforced with natural fibers is chosen as one of the most challenging materials to be applied in automotive structures of the future. Structural and semi-structural application of these materials is considered as challenging the car sustainability.

The mechanical properties of natural fiber composites are researched in detail. Polymer composites reinforced with randomly distributed natural fibers in form of non-woven mats are considered. A low price of these materials in combination with low density and good mechanical performance makes them especially attractive for automotive structures, where low cost and lightweight are the main issues. Some car manufacturers have already started to apply these materials in their cars. However, the current field of natural fiber composites application is limited to non-structural automotive components, partly because of the low impact properties, poor moisture resistance and difficulties to reach A-class surface quality. These are mainly technological problems, which sooner or later will be solved. But there is one more aspect, which is inherent in these materials. Large variation in mechanical properties is encountered in composites reinforced with natural fibers in the form of non-woven mats. The variation appears due to large heterogeneity of the reinforcement. This cannot be completely avoided by technology without substantial increase in price of final composite. The averaged values of mechanical properties derived from testing are usually used for engineering design of structures. However, mechanical properties determined by using traditional methods of testing of these materials can be unreliable. Therefore large safety coefficients are introduced to overcome the non-uniformity in material properties. As a result the material usage is far from optimal.

A reliable estimation of mechanical properties of heterogeneous natural fiber composites in combination with the new methods of engineering design is necessary for their successful application in automotive structures. The estimated heterogeneity can be incorporated in numerical engineering tools like finite element analysis (FEA) to enable engineering of structures using heterogeneous materials.

In this work a novel technique is proposed for quantitative estimation of heterogeneity in the properties of composites reinforced with natural fibers in the form of non-woven mats. The technique is based on the analysis of the digital image of the reinforcement using the signal processing technique. The digital image of the reinforcement could be obtained either by scanning of a non-impregnated fiber mat or X-raying the composite. It is found that the in-plane heterogeneity of the natural fiber composites is caused by the variation of local amount of fibers (fiber volume fraction variation), which is clearly seen in the images as the variation of image local brightness. In some places in material the natural fibers form clusters, while in

the others there are voids. Fiber clusters and voids are stochastically distributed in the composite. The heterogeneity through-the-thickness of material cannot be observed in X-ray images; therefore it is not taken into consideration.

Complex in-plane heterogeneity present in composites is described by the introduced approach of heterogeneity primitives. The heterogeneity primitives “hump” and “cavity” represent fiber clusters and voids correspondingly. And it is possible to describe the complex heterogeneity of natural fiber composite (or mat) by using simple equations.

Spectral analysis is employed for the estimation of the parameters of heterogeneity primitives. Several linear excerpts are stochastically chosen in X-ray image of the composite (or fiber mat) in order to perform the analysis. The excerpt represents the variation of the image’s brightness. Derived spectrograms are used to identify harmonics in excerpts. Harmonics are described by two parameters: wavelength and amplitude, which are linked to “size” and “intensity” parameters of the heterogeneity primitives correspondingly. The size parameter is used to determine the linear in-plane dimensions of the primitive, while the intensity – the magnitude of variation of the fiber volume fraction within the primitive. Harmonics with the major amplitudes are representative harmonics within the excerpt and are determined by the means of correlation. This set of harmonics is a quantitative characteristic of heterogeneity. Statistical parameters of harmonics: size and intensity are also estimated.

It is obvious that in order to carry out the FEA of structures made of heterogeneous materials, it is necessary to implement the variation in material properties according to the estimated characteristics of heterogeneity into a finite element model. However, the observed heterogeneity of considered material is rather difficult to implement directly into the finite element analysis. Therefore, a special procedure is developed in order to generate the heterogeneity using the derived characteristics.

A technique to generate the in-plane material heterogeneity is developed in this thesis. As the basis, the parameters of representative set of harmonics are used to generate stochastically distributed heterogeneity primitives. The heterogeneity primitives are described by a specially chosen mathematical function. The function describes the variation of material properties within the heterogeneity primitive. The harmonics parameters from the representative set are used to generate a low-order in-plane heterogeneity. Several low-order heterogeneities being generated simultaneously result in high-order in-plane heterogeneity. The generated high-order heterogeneity has characteristics similar to those observed in real composite materials and the similarity largely depends on the number of low-order heterogeneities involved. The simulated in-plane heterogeneity represents the variation of fiber volume fraction in the composite. This variation can be directly used to determine the mechanical properties of a composite material.

For linear elastic analysis the material model could be limited to the material modulus of elasticity. Modulus of elasticity of composite is assumed to be correlated with the fiber volume fraction variation. A reliable theoretical material model is required for a correct correlation.

In this thesis a vast number of theoretical models for estimation of elasticity modulus for natural fiber composites are evaluated to fit available experimental data on natural fiber reinforced composites with randomly distributed reinforcement. Three main parameters determine the modulus of elasticity of a composite: modulus of fibers, modulus of matrix and fiber volume fraction. It is discovered that no suitable model exists. The modification of one of the existing models is proposed. The modified model is successfully tested on available experimental data. This model is incorporated into the heterogeneity generation procedure. As a result the in-plane variation of modulus of elasticity of a composite can be simulated.

A method for implementing the simulated variation of material’s elasticity modulus into FEA of structures made of heterogeneous materials is developed in this thesis. This method is based on the assumption that most of the structures made of composites are thin-walled structures. Therefore they can be numerically simulated using shell finite elements with constant properties through their thickness. The variation in structure’s mechanical

properties is implemented as the variation in elastic properties of adjacent finite elements according to generated in-plane heterogeneity.

The required technique of appropriation of elastic properties of the finite element according to the generated in-plane heterogeneity is developed. It is based on geometrical primitives as plane and cylinder which are used to approximate the complex 3D shape of a real structure. The geometrical primitives are specified using the information derived from the finite element model of a structure in accordance to suggested principles. The developed method is suitable for simulation of 2D plane and 3D shell structures made of heterogeneous materials. The method is programmed as a FORTRAN procedure and implemented into MSC.MARC finite element code.

The developed approach is checked with available experimental data obtained from standard tensile tests of composite specimens. A contactless strain measurement system (ARAMIS) has been used during experiments in order to investigate the non-uniformity of strain at the surface of the specimens. The reinforcement in specimens made of natural fiber composite is investigated by using X-ray photographs and compared with the surface strain field obtained with ARAMIS. A good agreement of surface strain variation with the structure of the reinforcement is observed. The heterogeneity parameters of the material are estimated and implemented into the finite element model of plates with simulation conditions similar to a standard tensile experiment.

The surface strain field in modeled plates and in tested specimens is examined. Reasonable agreement between simulations and experimental data is observed. The effect of the finite element size on the results is investigated and a method for proper size estimation is suggested as the result.

An automotive component is chosen for a full-scale verification of the developed approach. A rear seat base structure is manufactured within the cooperation with the industrial partners. Certain numbers of structures made of two different composites are produced. Polypropylene reinforced with non-woven flax fiber mat and polypropylene glass mat thermoplastic (GMT) are used. The overall flexural stiffness of structures is tested using an experimental laboratory setup. It is found that the structure made of natural fiber composite can compete in stiffness/weight ratio with the structure made of GMT. However, the mechanical properties of the used natural fiber composite have to be improved to achieve the optimal performance.

The structure made of polypropylene reinforced with non-woven flax fiber mat while being flexurally loaded is also researched with contactless strain measurement system (ARAMIS). In these tests the non-uniformity of surface strain field is observed in the structure. However, the comparison the results of ARAMIS with X-ray photograph of the structure shows that the derived surface strain field can be unreliable. The image of the cross-section of the natural fiber composite is examined in order to find a reasonable explanation for this phenomenon.

The through-thickness heterogeneity of natural fiber composite appears to have great influence the surface strain results. This eventually results in the loss of correlation with the X-ray image of the reinforcement. Additional flexural tests of structure using strain gauges were performed in order to validate the results of ARAMIS locally. The conclusion drawn from the experimental result is that the contactless strain measurement system certainly has its limitations in measuring the surface strain in heterogeneous materials under complex stress states.

All the developed techniques can be summarized into a novel approach to model structures made of heterogeneous materials, which consists of the following steps: estimation of heterogeneity parameters, heterogeneity generation, tuning the model for the modulus of elasticity estimation and approximation of a complex geometry with geometrical primitives. The developed approach can be used for more reliable simulations of the structures made of heterogeneous materials through more accurate description of their local mechanical properties. Moreover, the estimated parameters of heterogeneity can be used for the proper choice of the specimens' dimensions for tests in order to avoid the so-called "size effect" and can improve the reliability of the results.

The developed approach to model structures made of heterogeneous material is successfully implemented into the FE model of the seat base structure. The heterogeneity parameters are estimated applying the developed technique based on the X-ray image of the structure. Reasonable agreement between simulation and experimental results is observed. Occurring problems and the possible ways of their solution are discussed.

The novel approach developed in this thesis, is a step towards a better understanding of the complex mechanics of natural fiber composites and behavior of the structures made of these materials. Using this approach one can perform more reliable simulations of structures made of heterogeneous materials resulting optimal material utilization in structures. Some future improvements of the developed approach are also suggested. General design guidelines using heterogeneous natural fiber composites are drawn in respect to design of automotive structures.

Kirill KAVELIN

SAMENVATTING

Dit onderzoek is uitgevoerd binnen het programma “Smart Product Systems” gericht op de efficiency van levensduurcyclus van producten. Dit onderzoeksprogramma is gestart vanwege de toenemende interesse voor de bescherming van het milieu, die een duurzame ontwikkeling van industriële vooruitgang vereist. Als carrier in dit onderzoeksproject werd de DutchEVO gekozen.

Één van de innovaties in het Dutch-Evo project is het gebruik van moderne lichtgewicht materialen om de duurzaamheidseisen van dit concept voertuig te halen. Het “Verkennen van de toepassing van nieuwe materialen in auto’s” is als een deel van het programma uitgevoerd. Het doel van dit project is om nieuwe materialen te exploreren die de potentie hebben om aan de eisen van modern auto-ontwerp te voldoen.

In dit onderzoek wordt een aantal moderne materialen, zoals magnesiumlegeringen en composieten, die toegepast kunnen worden in de constructie van auto’s, vergeleken met conventionele materialen zoals staal en aluminiumlegeringen. Niet alleen de mechanische eigenschappen van deze materialen worden vergeleken, maar ook de mogelijkheid van gewichtsreductie van auto’s. De toepassing van nieuwe materialen vereist soms een complete verandering van de productietechnologie. De kosten van deze veranderingen worden ook beschouwd samen met de mechanische eigenschappen van nieuwe materialen. De complexe interactie tussen economische, technologische en milieuaspecten wordt meegenomen gedurende de selectie van in aanmerking komende materialen. Als resultaat hiervan is een polymere composiet versterkt met natuurlijke vezels geselecteerd als één van de meest uitdagende materialen om gebruikt te kunnen worden in toekomstige autoconstructies. De toepassing van deze materialen in structurele en semi-structurele delen in auto’s wordt beschouwd als een uitdaging voor de duurzaamheid van auto’s.

De mechanische eigenschappen van composieten met natuurlijke vezels zijn gedetailleerd onderzocht. Polymere composieten versterkt met “at random” verdeelde natuurlijke vezels in de vorm van “non-woven” matten worden beschouwd. Een lage prijs van deze materialen gecombineerd met een lage dichtheid en goede mechanische eigenschappen maken hen heel aantrekkelijk voor constructies in auto’s waarvoor lage kosten en lichtgewicht de belangrijkste aspecten zijn. Enige autofabrikanten zijn al begonnen met de toepassing van deze materialen in hun auto’s. De huidige toepassingen van composieten met natuurlijke vezels zijn beperkt tot delen van de constructie die laag belast worden, gedeeltelijk vanwege de lage slagsterkte, slechte vochtbestendigheid en de moeilijkheden om klasse A oppervlaktekwaliteit te bereiken. Dit betreft voornamelijk technologische problemen die vroeger of later zullen worden opgelost. Grote variaties in de mechanische eigenschappen komt men tegen in composieten met natuurlijke vezels in de vorm van “non-woven” matten. Deze variatie ontstaat tengevolge van de grote heterogeniteit van de versterking. Dit kan niet volledig worden vermeden door technologie zonder een substantiële verhoging van de prijs van de uiteindelijke composiet. De gemiddelde waarden van de mechanische eigenschappen ontleend aan testen worden gewoonlijk gebruikt voor het technische ontwerp van constructies. Echter de mechanische eigenschappen bepaald met traditionele testmethoden aan deze materialen kunnen onbetrouwbaar zijn. Daarom worden hoge veiligheidscoëfficiënten gebruikt om rekening te houden met de niet-uniforme materiaaleigenschappen. Het resultaat hiervan is dat het materiaalgebruik verre van optimaal is.

Een betrouwbare schatting van de mechanische eigenschappen van heterogene natuurlijke vezel composieten samen met nieuwe methoden van technisch ontwerpen is nodig voor hun succesrijke toepassing in autoconstructies. De geschatte heterogeniteit kan worden ingebouwd in numerieke technische methoden zoals de eindige elementen methode (EEM) om het ontwerp van constructies met heterogene materialen mogelijk te maken.

In dit onderzoek wordt een nieuwe techniek voorgesteld om de heterogeniteit van de van de eigenschappen van composieten met natuurlijke vezels in de vorm van “non-woven” matten te kwantificeren. De techniek is gebaseerd op de analyse van het digitale beeld van

de versterking door gebruik te maken van signaalverwerking. De digitale afbeelding van de versterking kan worden verkregen of door het scannen van een niet geïmpregneerde vezelmat of door röntgenopnamen van de composiet. Er is gevonden dat de heterogeniteit in het vlak van de natuurlijke vezel composiet veroorzaakt wordt door de variatie in de lokale hoeveelheid vezels (variatie in de Vezel Volume Fractie), welke duidelijk zichtbaar is in de afbeeldingen als de variatie in de lokale helderheid in de afbeelding. Op sommige plaatsen in het materiaal vormen de natuurlijke vezels clusters, terwijl er op andere locaties er leemten zijn. Vezel clusters en leemten zijn stochastisch verdeeld in de composiet. De door de dikte heterogeniteit van het materiaal kan niet worden waargenomen in röntgenopnamen; daarom wordt dit niet in beschouwing genomen.

Er wordt voorgesteld om de complexe heterogeniteit in het vlak die aanwezig is in composieten te beschrijven door de introductie van de benadering met heterogeniteitprimitieven. De heterogeniteit primitieven “verhoging” en “holte” representeren respectievelijk vezel clusters en leemten. En het is mogelijk om de complexe heterogeniteit van een natuurlijke vezel composieten (of mat) te beschrijven door gebruik te maken van eenvoudige functies.

Spectrale analyse wordt gebruikt om de parameters van heterogeniteitprimitieven te schatten. Enkele lineaire excerpten worden at random gekozen in de röntgenopname van de composiet (of de vezelmat) om de analyse uit te voeren. Het excerpt representeert de variatie in de helderheid van de afbeelding. De afgeleide spectrogrammen worden gebruikt om de harmonischen in de excerpten te identificeren. De harmonischen worden beschreven door twee parameters: golflengte en amplitude, welke zijn verbonden met de “afmeting” en de “intensiteit” parameters van de corresponderende heterogeniteit primitieven. De afmeting parameter wordt gebruikt om de lineaire in het vlak afmeting van de primitieve te bepalen, terwijl de intensiteit de grootte van de avariatie van de Vezel Volume Fractie in de primitieve is. Harmonischen met belangrijkste amplituden zijn de representatieve harmonischen binnen een excerpt en worden bepaald door middel van correlatie. Het stelsel van harmonischen is een kwantitatieve karakterisatie van de heterogeniteit. De statistische parameters van de harmonischen: afmeting en intensiteit worden ook geschat

Het is vanzelfsprekend dat om de EEM uit te kunnen voeren op een constructie uit een heterogeen materiaal het noodzakelijk is om de spreiding in de materiaal eigenschappen te implementeren in een Eindige Elementen Methode model dat overeenkomt met de geschatte karakteristieken van de heterogeniteit. De waargenomen heterogeniteit van het beschouwde materiaal is echter tamelijk moeilijk direct te implementeren in een Eindige Elementen analyse. Er is daarom een speciale procedure ontwikkeld om de heterogeniteit te genereren met gebruikmaking van de afgeleide karakteristieken.

Een techniek om de materiaalheterogeniteit in het vlak te genereren is in deze thesis ontwikkeld. Het uitgangspunt is dat de parameters van een representatief stelsel van harmonischen gebruikt worden om de stochastisch verdeelde heterogeniteit primitieven te genereren. De heterogeniteit primitieven worden beschreven met een special geselecteerde wiskundige functie. De parameters van de harmonischen van het representatieve stelsel worden gebruikt om een in het vlak heterogeniteit van een lage orde te genereren. Verscheidene lage orde heterogeniteiten die simultaan worden gegenereerd resulteren in een hogere orde in het vlak heterogeniteit. De gegenereerde hogere orde heterogeniteit heeft karakteristieken die gelijkend zijn aan die van het reële gedrag van de composiet en de gelijkheid hangt grotendeels af van het aantal lagere orde heterogeniteiten dat wordt gebruikt. De gesimuleerde in het vlak heterogeniteit representeert de variatie van de volume fractie van vezels in de composiet. Deze variatie kan direct worden gebruikt om de mechanische eigenschappen van een composiet te bepalen.

Voor een lineair elastische analyse zou het materiaal model beperkt kunnen worden tot de elasticiteitsmodulus van het materiaal. Daarom wordt de elasticiteitsmodulus van een composiet verondersteld gecorreleerd te zijn met de variatie in de vezel volume fractie. Een betrouwbaar theoretisch materiaal model is vereist voor een correcte correlatie.

In dit proefschrift wordt een groot aantal theoretische modellen voor het schatten van de elasticiteitsmodulus van composieten met natuurlijke vezel geëvalueerd om de

beschikbare experimentele gegevens over composieten met natuurlijke vezels met at random verdeelde versterking te fitten. De drie voornaamste parameters die de elasticiteitsmodulus van een composiet bepalen zijn: de modulus van de vezels, de modulus van de matrix en de volumefractie van de vezels. Er werd ontdekt, dat er geen geschikt model bestond. De aanpassing van een van de bestaande modellen is voorgesteld. Het aangepaste model is met succes getest op de beschikbare experimentele data. Dit model is geïncorporeerd in de procedure van het genereren van de heterogeniteit. Het resultaat is dat de variatie van de elasticiteitsmodulus van een composiet in het vlak kan worden gesimuleerd.

In dit proefschrift wordt een methode voor het implementeren van de gesimuleerde variatie van de elasticiteitsmodulus van het materiaal in een EEM analyse van constructies uit heterogene materialen ontwikkeld. Deze methode is gebaseerd op de aanname dat de meeste constructies uit composieten dunwandig zijn. Daarom kunnen zij numeriek gesimuleerd worden door gebruik te maken van schaalementen met constante eigenschappen door de dikte. De variatie in de mechanische eigenschappen van een constructie wordt geïmplementeerd als de variatie in de elastische eigenschappen van aanliggende eindige elementen in overeenkomende met de gegenereerde heterogeniteit in het vlak.

De vereiste techniek van de benadering van de elastische eigenschappen van de eindige elementen overeenkomende met de gegenereerde heterogeniteit in het vlak is ontwikkeld. Het is gebaseerd op geometrische primitieven als vlakken en cilinders die worden gebruikt om de complexe 3D vormen van een reële constructie te benaderen. De ontwikkelde methode is geschikt voor de simulatie van 2D vlakke en 3D schaal constructies uit heterogene materialen. De methode is geprogrammeerd in een FORTRAN procedure en geïmplementeerd in het MSC.MARC eindige elementen programma.

De ontwikkelde benadering is geverifieerd met beschikbare experimentele gegevens verkregen uit standaard beproevingen van proefstukken composiet. Een contactloos rekmeet systeem (ARAMIS) is gedurende de experimenten gebruikt om de niet uniformiteit van de rek aan de oppervlakte van de proefstukken te onderzoeken. De versterking in proefstukken uit composieten van natuurlijke vezels is onderzocht door röntgenopnamen te gebruiken en deze te vergelijken met het rekveld aan het oppervlak verkregen met ARAMIS. Er werd een goede overeenstemming tussen de variatie in het rekveld aan het oppervlak met de structuur van de versterking waargenomen. De heterogeniteitparameters van het materiaal zijn geschat en geïmplementeerd in het Eindige Elementen model van platen met simulatie condities die gelijk zijn aan die van een standaard trekproefstuk.

Het rekveld aan de oppervlakte van gemodelleerde platen en in proefstukken is onderzocht. Een redelijke overeenstemming tussen de simulaties en de experimenten is waargenomen. Het effect van de afmeting van de eindige elementen op de resultaten is onderzocht en een methode om de juiste element afmeting te schatten is voorgesteld.

Een component uit een auto is gekozen voor een ware grote verificatie van de ontwikkelde benadering. De onderkant van de constructie van een zitting is gefabriceerd binnen de samenwerking met een industriële partner. Een aantal constructies gemaakt uit twee verschillende composieten zijn gefabriceerd. Polypropeen versterkt met "non-woven" vlasvezel mat en polypropeen met glasmatten (GMT) zijn gebruikt. De totale buigstijfheid van de constructies is getest gebruikmakend van een experimentele laboratoriumopstelling. Er is gevonden dat de constructie gemaakt uit composieten met natuurlijke vezels kan concurreren voor wat betreft de stijfheid/gewichtsverhouding met constructies gemaakt uit GMT. De mechanische eigenschappen van de gebruikte composiet met natuurlijke vezels moeten nog worden verbeterd om de optimale prestatie te bereiken.

De constructie uit polypropeen versterkt met "non-woven" vlasvezel matten is op buiging belast en is ook onderzocht met het contactloze rekmeetsysteem (ARAMIS). In deze proeven is het niet uniforme rekveld aan het oppervlak waargenomen. De vergelijking echter met de resultaten van ARAMIS met röntgenfoto's van de constructie toont dat de verkregen oppervlakte rek onbetrouwbaar kan zijn. De microscoop foto's van de doorsnede van de

composieten met natuurlijke vezels is onderzocht om een aanvaardbare verklaring voor dit verschijnsel te vinden.

De door de dikte heterogeniteit van composieten met natuurlijke vezels blijkt een grote invloed te hebben op de resulterende oppervlakte rek. Dit kan eventueel resulteren in een verlies in correlatie met de röntgenopnamen van de versterking. Er zijn aanvullende buigproeven uitgevoerd met rekstrookjes om de resultaten van ARAMIS lokaal te verifiëren. De conclusies van deze experimentele resultaten is dat contactloze rekmeet systemen hun beperkingen hebben in het meten van de oppervlakte rek in heterogene materialen in een complexe spanningstoestand.

De nieuwe benadering om constructies te modelleren uit heterogene materialen bestaat uit de volgende stappen: schatten van de heterogeniteit parameters, het genereren van de heterogeniteit, aanpassing van het model voor het schatten van de elasticiteitsmodulussen de benadering van een complexe geometrie met geometrische primitieven. De ontwikkelde benadering kan worden gebruikt voor een betrouwbaardere simulatie van constructies uit heterogene materialen door de accuratere beschrijving van de locale mechanische eigenschappen. Bovendien kunnen de geschatte parameters van de heterogeniteit worden gebruikt voor de juiste keuze van de proefstukafmetingen voor testen en kunnen de zogenaamde afmeting effecten worden voorkomen en kan de betrouwbaarheid van de resultaten worden verbeterd.

De ontwikkelde benadering om constructies uit heterogene materialen te modelleren is met succes geïmplementeerd in het EEM model van de onderkant van de constructie van de zitting. De heterogeniteitparameters zijn geschat door toepassing van de ontwikkelde techniek gebaseerd op Röntgen opnames van de constructie. Een redelijke overeenkomst tussen de simulatie en de experimentele resultaten is waargenomen. De opgetreden problemen en oplossingsmogelijkheden worden besproken

De nieuwe benadering die in deze thesis is ontwikkeld is een stap in de richting van een beter begrip van de complexe mechanica van composieten met natuurlijke vezels en het gedrag van constructies uit deze materialen. Door gebruik te maken van deze benadering is het mogelijk om betrouwbaardere simulaties uit te voeren aan constructies uit heterogene materialen en dit kan resulteren in optimaal materiaalgebruik in constructies. Enige verbeteringen van de ontwikkelde benadering worden ook voorgesteld. Algemene ontwerprichtlijnen voor het gebruik van heterogene composieten met natuurlijke vezels worden geschetst voor het ontwerp van constructies in auto's.

Kirill KAVELIN

Table of contents

SUMMARY	vii
SAMENVATTING	xi
1. INTRODUCTION	
1.1.BACKGROUND	1
1.2.OBJECTIVES	2
2. OVERVIEW OF MODERN STRUCTURAL MATERIALS	3
2.1. INTRODUCTION	3
2.2. CONVENTIONAL MATERIALS	4
2.2.1. Steel	4
2.2.2. Aluminum	4
2.2.3. Synthetic plastics	5
2.3. ADVANCED MATERIALS	5
2.3.1. Magnesium	5
2.3.2. Bioplastics	6
2.3.3. Composites	6
2.3.4. Synthetic composites	7
2.3.5. Biocomposites	8
2.4. NATURAL FIBER COMPOSITES	10
2.4.1. Natural fibers	10
2.5. PROPERTIES OF NATURAL FIBER COMPOSITES	16
2.5.1. Polymer matrix and processing technology	17
2.5.2. Length, quantity and orientation of fibers	18
2.5.3. Fiber-matrix adhesion and methods of its improvement	20
2.5.4. Moisture and temperature sensitivity	24
2.5.5. Discussion of mechanical properties	25
2.5.6. Heterogeneity	27
2.6. CONCLUSIONS	28
3. INVESTIGATION OF HETEROGENEITY OF NATURAL FIBER MATS AND COMPOSITES	33
3.1. INTRODUCTION AND HETEROGENEITY DEFINITION	33
3.2. HETEROGENEITY INVESTIGATION TECHNIQUE	34
3.2.1. Materials	34
3.2.2. Digital image processing	35
3.2.3. Spectral analysis	38
3.2.4. Excerpts	39
3.2.5. Analysis of spectrograms	40
3.2.6. Representative excerpt	43
3.3. CONCLUSIONS	45
4. SIMULATION OF MECHANICAL PROPERTIES OF COMPOSITES	47
4.1. INTRODUCTION	47
4.2.EXISTING MODELS FOR YOUNG'S MODULUS ESTIMATION	48
4.2.1. The rule of mixtures	48
4.2.2. Cox's model	48
4.2.3. Halpin-Tsai's model	49
4.2.4. Hirsch's model	49
4.2.5. Models based on micromechanics of materials	49

4.3. BENCHMARKING OF EXISTING MODELS	50
4.3.1. Approach 1	51
4.3.2. Approach 2	52
4.4. DEVELOPMENT AND VERIFICATION OF A NEW MODEL SUITABLE FOR NATURAL FIBER COMPOSITES	54
4.5. CONCLUSIONS	59
5. HETEROGENEITY SIMULATION	61
5.1. INTRODUCTION	61
5.2. HETEROGENEITY GENERATION APPROACH	61
5.3. VERIFICATION	66
5.4. CORRELATION WITH MECHANICAL PROPERTIES OF COMPOSITE	67
5.5. CONCLUSIONS	69
6. FINITE ELEMENT IMPLEMENTATION	71
6.1. INTRODUCTION	71
6.2. DEVELOPMENT OF THE USER'S SUBROUTINE	72
6.3. IMPLEMENTATION PROCEDURE	74
6.3.1. General approximation of the finite element model with geometrical primitives	76
6.3.2. Detailed description of the approximation procedure	78
6.3.3. Association of finite elements to the geometrical primitives	86
6.3.4. Heterogeneity generation procedure	87
6.3.5. Appropriation of properties of the finite elements according to generated heterogeneity	90
6.4. VERIFICATION OF FINITE ELEMENT IMPLEMENTATION	95
6.4.1. Material model	95
6.4.2. Experimental results	96
6.4.3. Simulation parameters	96
6.4.4. Results of the simulation trials	97
6.4.5. Size-effect	99
6.4.6. Influence of the finite elements' size	99
6.5. CONCLUSIONS	100
7. STRUCTURAL SIMULATION AND EXPERIMENTAL VERIFICATION	103
7.1. INTRODUCTION	103
7.2. TESTING AND SIMULATIONS OF SPECIMENS	103
7.2.1. Materials	103
7.2.2. Test setup	106
7.2.3. Results	106
7.2.4. Surface strain field analysis	112
7.2.5. Comparison of FE analysis results with the experimental data	115
7.3. TESTING OF THE STRUCTURE	118
7.3.1. Materials	119
7.3.2. Testing procedure and general results	119
7.3.3. Analysis of structure's heterogeneity	121
7.3.4. Measurements of the surface strain field	121
7.4. ESTIMATION OF HETEROGENEITY PARAMETERS FOR THE STRUCTURE	123
7.5. SIMULATION OF THE STRUCTURE	123
7.5.1. Geometry and boundary conditions	123
7.5.2. Tuning of material model	124
7.5.3. Approximation of the structure with geometrical primitives	124

Table of contents

7.5.4. General FE simulation results	124
7.5.5. Comparison of the local behavior of FE model with the local experimental results	125
7.6. DISCUSSION OF THE RESULTS AND CONCLUSIONS	127
8. CONCLUSIONS	135
9. REFERENCES	143
APPENDIX 1 Mechanical properties of natural fiber composites	155
APPENDIX 2 Algorithm of the finite elements' association with geometrical primitives	159
APPENDIX 3 Algorithm of heterogeneity generation procedure	163
ACKNOWLEDGEMENTS	165
CURRICULUM VITAE	167
ΡΕΦΕΡΑΤ	169

Chapter 1

Introduction

1.1 Background

This work is performed within the scope of the program “Smart Product Systems” focused on Life Cycle Efficiency of Products conducted at Delft University of Technology. In other words, the production of goods is performed with the minimal waste and maximum recycling of raw materials and reuse of components. The central objective of the program is a multidisciplinary research on the program level, which combines the expertise of at least several traditional technical disciplines.

Innovative technology, otherwise coined as ‘industrial progress’, continually delivers new products. Some of them even have become an essential part of everyday life in modern society. All products require both materials and energy for their production and usage phases, while at the-end-of life they all must eventually be discarded. Growing public concern about issues such as waste prevention and energy saving, however, has led to the emphasis on environmental issues within our consumer society. The concept has emerged which requires the industrial progress to be accompanied by sustainable development.

The following general understanding on sustainable development is used. “Humanity has the ability to make development sustainable - to ensure that it meets the needs of the present without compromising the ability of future generations to meet their needs. The concept of sustainable development does imply limits - not absolute limits, but limitations imposed by the present state of technology and social organization on environmental resources and by the ability of the biosphere to absorb the effects of human activities. But technology and social organization can be managed and improved to make way for a new era of economic growth. In the end, sustainable development is not a fixed state of harmony, but rather a process of change in which the exploitation of resources, the direction of investments, the orientation of technological development, and institutional change are made consistent with future as well as present needs.”

The co-operative challenge as a background of the program is to develop a scientific methodology able to assimilate the diverse knowledge about materials, products and processes, which can be used in various levels of optimization. This can help to understand the insights of the combined knowledge better and can lead to the improvement of the trade-off involved in economy, technology and environmental protection.

Sustainable development of products involves a delicate trade-off between the aspects related to the mass balance, consumed energy and economy, throughout all life cycle phases of products. It must be supported by sustainable technology, which strives towards the minimal use of raw materials and energy, minimal hazardous emissions, and maximal reuse and recycling in a balanced life cycle.

A concept car with a working name Dutch-EVO was taken as a vehicle of the research within the “Smart Product Systems” program. The concept has to meet the philosophy of the whole program on sustainable product development. The Dutch-EVO project aims at designing and building an affordable, lightweight car satisfying the current and/or future legislation on safety, emissions, recyclability etc.

One of the innovations in the Dutch-EVO project is the use of modern lightweight materials to reach safety and sustainability of the concept car. Therefore a project 3.2.1: “Exploring the use of modern materials for automotive applications” has been conducted as an important part of the project. The purpose of this project is to explore new materials that have the potential to meet the requirements of automobile design.

1.2 Objectives

Obviously, the main objective of the automobile industry is to deliver on the market cheap, reliable and economical cars. The cost aspects are very important especially for passenger cars. The price of raw materials has a major influence on the total price of a car assembly. Therefore, firstly the price of raw materials used in a passenger car design is the main issue. Secondly, the car structure has to fulfill the design requirements in the sense of strength, reliability and durability. Materials with sufficient mechanical properties have to be used. Saving fuel becomes more and more crucial nowadays. This makes car manufacturers look for ways to reduce the fuel consumption. According to the latest survey the fuel consumption, using current engine technology, mainly depends on the weight of the car, unless alternative energy source is used. Therefore, modern lightweight materials come to substitute the currently used materials.

The main aim of this thesis is to make an overview of modern lightweight materials, which have potentials to satisfy the automotive requirements in the sense of price, mechanical properties and sustainability. Then the properties of most suitable materials have to be analyzed in detail to find the boundaries of their application in cars.

Engineering design with new materials requires new methods. Therefore, the most challenging task is to develop an engineering design technique, which can be used in order to utilize the properties of modern materials efficiently. As a result of this thesis, general guidelines for product development using modern materials with respect to automotive design will be developed.

Chapter 2

Overview of modern structural materials

2.1 Introduction

Not so long ago automobiles were almost exclusively made from steel. But fierce competition and social push for lighter, more economical vehicles has led to the introduction and continuing usage of aluminium, plastics and various composites. The main driveline is to strengthen the technological base of the automotive industry with a primary focus on developing and implementing lightweight materials in order to reduce energy consumption of a car while taking into consideration safety and costs. Safety regulations, however, decrease weight reduction.

Major shifts in automotive materials are of vital interest to manufacturers in the raw materials industry, but are also of keen interest to the spare parts suppliers. Thus, the challenge for the automotive industry is to produce inexpensive, environmentally sustainable vehicles that are safe, attractive and economical to operate.

The environmental aspect of modern automobiles is very important nowadays. Automotive transport in Europe consumes about 9% of the total European material use, of which 63% by mass is needed for passenger cars. From the energy consumption point of view the transport sector is the third (16% of the total energy consumption) largest energy consumer (after industry and housing), where 80-85% of the total energy consumption happens during the use phase of a car [7, 76, 83, 87, 208]. According to recent studies the energy consumption of an automobile largely depends on its weight [1, 191, 219]. By weight reduction it is possible to reduce both the energy consumption and emissions substantially [159, 160]. It is shown in [40, 87] that the energy required for materials production and technological process is rather small in comparison with the energy consumed by a car during the use phase.

Over the last few years, ecological concern and global warming have initiated a considerable interest in using natural materials to produce “green” products and reduce carbon dioxide (CO₂) emissions by all possible means. Fossil fuel combustion is the main source of worldwide CO₂ emissions, which account for more than 99% of all green house gases [130]. It is estimated that about 75% of transport energy consumption and CO₂ emissions come from road transport and of this around 70% by cars [7, 40, 208].

Lightweight, high performance materials like aluminium, magnesium and composites enable lightweight design. However, the concerns about the waste generation in the transport sector should be taken into account. The EU has announced a waste management strategy resulting in the policy measures such as the End-of-Life-Vehicle-Directive [43]. This directive imposes a marked reduction in the use of virgin materials during the manufacturing process and a certain increase in the amount of recyclable materials recovered during dismantling. Thermal recycling is considered to be not sustainable and, therefore, not supported. In the present scenario, bio-materials based on renewable resources have excellent potential to reduce not only CO₂ emissions but also save non-renewable resources by substituting conventional mineral and petrochemical (fossil) materials. This appear to be quite efficient especially in the automotive sector due to large production scale [130].

Modern materials including metals, plastics and composites have excellent mechanical, ergonomic and eco-performance if properly assessed in lightweight design [44]. Structural and semi-structural materials in automobiles can be divided into conventional materials and advanced materials. Composite materials are considered as advanced because of the ultimate performance and are de-facto state-of-the-art materials nowadays. Also magnesium is a very lightweight material with good performance. This material is rather new in automotive applications.

A short overview of the properties of structural and semi-structural materials such as metals, polymers and composites, which applicable to car body and to other light- and medium-loaded structures in automobiles and perspectives of their usage in near future is made. This overview regards mechanical, environmental and economic performance of these materials.

2.2 Conventional materials

2.2.1 Steel

Steel is most widely used in automotive structures starting from the beginning of automotive era. Steel is being derived from iron ore and nowadays is available in many different grades by alloying it with other metals and by mechanical and heat treatment. Steel combines very good strength properties with ductility, which is very important for the automotive industry. Steel is relatively cheap and almost 100% recyclable, which is undoubtedly important for the eco-efficiency of cars.

Because mechanical properties of steel are well-known and engineering design rules well established it is feasible to design reliable and durable structures. Thus, a steel car might seem to be the best option ever. However, the main disadvantage of a steel car is its weight, which negatively affects the fuel efficiency and therefore eco-performance of cars. According to the recent studies on lightweight cars [1,130, 191] the weight reduction is beneficial. The same figure is estimated in the life cycle analysis presented in [87]. High strength steel enable thinner structures, which can contribute to the lightweight design [228]. However, even using high strength steel only limited weight savings are achievable [76].

Considering limited feasibility of eco-efficiency improvement of a steel car (due to its weight) the application of steel as the primary material in automotive structures in future is considered not very preferable.

2.2.2 Aluminum

The primary application of aluminum belongs to the area of aerospace structures. It offers very good mechanical performance, high corrosion resistance and low weight. The properties of aluminum, like that of steel can be modified to a large extent by alloying them with other metals as well as applying mechanical and heat treatments. The recyclability of aluminum is also quite good. The density of aluminum is three times less than steel; thus, it has great opportunities to be applied in lightweight automotive structures. These attributes are very attractive to automotive manufacturers. Weight saving in the whole car structure can be as high as 25% and for some structures as high as 52% in comparison with steel design. The optimal usage of aluminum requires a different approach to design structures. Thus, one of the latest achievements for cars is the recently developed new technology of Aluminum Space Frame (ASF) which allows to utilize most of the material performance [8, 15, 224]. Currently some car manufacturers like Audi (model A8), Honda (model NSX) and Lotus (model Elise) already use aluminum as primary material for the car body, but such design is quite expensive due to a high price of raw aluminum [27, 76]. Therefore only expensive, luxurious or racing cars are currently being made from aluminum.

The production of aluminum requires enormous amount of energy, which undoubtedly influences the price (about €4.41 per kilogram for aluminum sheet, compared to about €0.97 for steel). Unfortunately no breakthrough is foreseen to significant reduce the cost of raw materials. However, no high investments are needed to convert a “steel” technology equipment into an “aluminum” one [2].

Aluminum is produced from bauxite mineral ore. High material price limits a wide usage of aluminum as the primary material for mass automotive production in the future. Moreover extensive usage of limited mineral ore resources can hardly be considered as sustainable.

2.2.3 Synthetic plastics

A large number of plastics are available nowadays. Plastics produced by petrochemical industry from fossil oil are synthetic plastics. Plastics as engineering materials are widely used in various applications due to good mechanical properties, excellent aesthetics and low production price. This is mainly due to a low energy consumption during the production of raw material and subsequently component production. The main advantage of plastics is the possibility to manufacture very complex shaped products in one step, which considerably cuts the production costs [67, 76]. These attributes are very attractive for car manufacturers.

Therefore nowadays there are many plastics used in automotive structures carrying a wide range of functions. For example, internal panels in cars are made of plastics: the rear parcel shelf, door trim panels and the dashboard. Some of the structures can even carry limited load during the service, like the dashboard (light loads and thermal loads) and door trim panels (medium loads). Engine covers and liquids containers are external example of plastics applications. A light to a medium load is associated with these structures. Recently Daimler Chrysler has attempted to make a complete plastic car, where all body parts are made from polyethylene terephthalate (PET). But this is just a rare example because most of cheap plastics (commodity plastics) do not provide sufficient performance for heavy loaded applications [130].

With regard to chemical and technological behavior, plastics can be divided into two main groups: thermoplastics and thermosets. Thermoplastics become viscous at higher temperatures and solidify at lower temperatures. Therefore, they can be reversibly reshaped. Thermosets can flow only once and cross link with the applied heat and curing agents. Thermoplastics can be recycled, which is an advantage over thermosets because they can be reused several times, although their properties can degrade. The only way to reuse end-of-life thermoset parts can be as fillers (shredded material) in other materials; otherwise they can be thermally disposed or subjected to landfill [35]. The production of synthetic plastics results in much lower environmental impact than production of metals, because of the reduced energy consumption. Plastics can be recycled or their thermal energy can be utilized by incineration, which hence has questionable eco-performance.

Engineering and high-performance plastics can be used for structural automotive applications. They have very good mechanical properties, but the high price limits their usage. If their price would drop, the automotive components made from these materials can have mechanical performance close to those made of steel, but their weight will be much less. Thus, substituting steel components with plastics contribute to the weight reduction of the car. This scenario thus can be exploited in future.

2.3 Advanced materials

2.3.1 Magnesium

Magnesium is an even lighter construction material than aluminum and it offers comparable mechanical properties. The usage of magnesium in automotive applications can bring benefits from the point of view of weight, but it can also allow more extensive functions integration in a single part due to a better castability compared to that of aluminum and iron. Thus it will be possible for a single component to integrate the same functions performed presently by several different parts, leading therefore to considerable savings coming from assembly saving and machining costs. The cost of magnesium is the same as aluminum.

There are already some examples of magnesium applications in cars, like Mercedes Roadster (complete seat frame) and Mercedes SLK (petrol tank partition panel). In these cars magnesium components are made using the die-casting technology. The weight saving can be as high as 40% compared to a component made from steel. Door panels are also feasible applications of magnesium. However, the use of magnesium in sheeted panels is very complicated because a sheet has to be deformed at high temperatures (over 300 °C),

which requires heated tools [76]. Heated tools lead to large equipment investments, which are sometimes not economically efficient. Therefore processing of magnesium parts is very expensive. In addition structures made from magnesium corrode faster and therefore sufficient and reliable coating has to be provided [3, 47]. Thus, from the point of view of weight application of magnesium in automotive structures of the future can be beneficial, but it is still problematic technologically and economically.

2.3.2 Bioplastics

Biopolymers are based on renewable raw materials, which in this context we defined as “products derived from the agricultural and forestry sectors and being used for other purposes than nutrition”. The amount of carbon dioxide released in the atmosphere when products from renewable materials are disposed is equal to that absorbed from the atmosphere during plants growth. This is what is called “closed carbon cycle” [14, 156].

Such materials as starch, plant and animal oils, etc are used for production of biopolymers. The main advantage their usage is that only small amount of limited minerals and fossil resources are used for their production. Most of bioplastics are thermosets. Up to 98% bioplastics consists of renewable material and only 2% are synthetic components (usually catalyst). Their application in automotive structures can be considered as environmentally friendly, since they belong to lightweight renewable materials [38]. The advantage of bioplastics is that they can be either safely disposed or even self degrade after some time under certain conditions [14, 133].

The main disadvantage of bioplastics is their low mechanical performance, which is similar or worse than of commodity synthetic plastics. Moreover most of bioplastics are moisture, temperature and UV-radiation sensitive. These factors may cause rapid or unpredicted degradation of their mechanical properties. Nowadays bioplastics are mainly used in food packaging applications, where long life of the material and high mechanical performance are not necessary. The price of engineering bioplastics (see Table 2.1) whose performance is suitable for structural or semi-structural applications is quite high and can be up to 10 times higher than of similar synthetic ones (see Table 2.6) [133]. Engineering bioplastics was developed by several laboratories in recent time and not available on a mass production scale yet. High price and low production volume currently limit automotive application, where these issues hence are of a primary importance [133].

Table 2.1 The price for some of biodegradable plastics [after 120, 132, 133].

Material	Average price €/kg.
Polylactic acid (PLA) (Cargill Dow Polymers)	2.5 – 5
Starch-based resins (Novon/Novamont)	2.7 – 4.8
PHA (BIOTEC/Monsanto)	6.6 – 11
Cellulose acetate	2.8 – 3.1
Polycaprolactone (PCL)	~ 4.5
Polyster amide (Bayer's BAK)	~ 3.4
Alphatic aromatic copolyester (Eastman's Easter Bio)	~ 3.4

2.3.3 Composites

Composite materials consist of two or more rather than one material. They have a matrix material, which encapsulates discrete elements of one or more different materials. In general, composites are constructed by combining strong and stiff fibers with a lightweight matrix. The obtained material has better properties, than the matrix material alone, especially some specific properties (i.e. property-density ratio). The matrix material is usually tough and ductile rather than strong and brittle, while the reinforcing material is conversely strong, stiff and brittle. The resulting composite material has a good toughness due to the matrix material

and high strength due to the reinforcement. Fibers of different types and length are used as reinforcement in any composite material.

Nowadays synthetic composites are widely used. The synthetic plastics are usually used as matrix (based on fossil non-renewable resources) and glass or carbon (also synthetic, based on mineral resources) is used as fibers [76].

A new type of composites based on renewable resources has been recently developed. These composites are called biocomposites. In biocomposites the plastic matrix is based on starch, plant and animal oil, while plant or animal fibers are used as reinforcement [130]. Both types of composites (bio- and synthetic) will be discussed and the perspectives of their application in automotive structures will be presented.

2.3.4 Synthetic composites

The matrix material in synthetic composites is a synthetic polymer. The common fibers in polymer-matrix composites are glass, carbon and aramid. The properties of composite materials depend on many parameters. The material of matrix and fibers, the amount of fibers and their distribution are the most important of them [72]. Therefore, there are many possibilities to design the properties of composites adjusting them for specific needs, for example, orientation of fibers in the direction of maximum load etc. Thus, composites can be considered as materials with better designable properties [1].

Composite materials have had their first application in military aerospace technology, where fiber reinforced plastics are successfully used for various applications due to excellent specific properties, e.g. high strength and stiffness, low weight and the possibility of optimization by varying fibers orientations. Nowadays the application of composites is widely extended to civil areas like sport equipment and, of course, automotive structures [63]. They are used in those applications where lightness and high strength are required [229].

However, in automotive sector the application of composites started in early 1980's and after that has gradually increased [31]. Nowadays leading car manufacturers are applying more and more composites in their cars (see Fig. 2.1). However, there are difficulties in applying composites in ordinary cars. Most of them are due to high production costs of structures made from composites [1, 76, 207]. Usually it requires a complete upgrade of the production technology (more complex and expensive) and therefore large investments into the new equipment are required. Accordingly, the price of car increases, which negatively affects its market attractiveness.

Thus, considering eco-efficiency of a car, the application of composites can be considered as sustainable, but on the other hand synthetic composites contain a mixture of materials obtained from non-renewable resources. Therefore the reuse or utilization of composite structures at the end-of-life is questionable. None of the synthetic composites can be utilized without damage to the environment. The disposal of end-of-life composites, as these materials tend to be regarded as non-recyclable [25, 119], and much of the waste currently produced is ultimately sent to landfill sites for disposal. Composites with thermosetting matrices cannot be recycled otherwise than by landfill or incineration only, while composites with thermoplastic matrices are more attractive in that sense. Depending on composition they can be reused (recycled) up to several times, but with certain degradation of mechanical properties. When reuse is not possible any more, the only option to utilize them is to incinerate them (recycle into energy), but producing pollution as consequence. The slag remained after incineration of all types of synthetic composites has to be buried in landfill only.

A variety of ways of composite reuse at the end-of-life time have been developed recently. These methods include incorporating the end-of-life material into new composite materials [25, 193], recovery of the fiber reinforcement and filler material [25, 153, 158] and energy recovery through incineration [99, 158]. For example, a recycled carbon fiber thermoplastic composite material can be grinded into virgin composite to form high quality reinforcing material in injection moulds or as compression molding compounds [193]. By incinerating glass fiber reinforced thermosets in a fluidized bed the recovery of both glass

fibers and energy is possible [99, 158]. The latest method for recycling the sheet molding compound (SMC) utilizes solvent dissolution, hydrolysis and pyrolysis [153].

The development of composites with one material (the same materials for matrix and reinforcement) can help to achieve a better recycling performance. Such composites already exist, like all-polypropylene composite [155]. The polypropylene is used as a matrix material and as reinforcement. The technological know-how is to make the fibers stronger than the matrix by drawing the polymer to orient molecules. Also the fibers arrangement to specific orientation requires a sophisticated technology. All-polypropylene composites have slightly better mechanical properties than pure polypropylene [26, 155], but their properties are significantly worse than those reinforced with glass fibers. Thus, a low gain in mechanical properties limits the area of application of such composites. However, the problem of recycling has been reduced.

Fiber-reinforced composite plastics with appropriately oriented reinforcing fibers offer a suitable lightweight construction potential for a load-bearing body-in-white structures, even compared to aluminum and magnesium. Thus, in those structures where high stiffness is a major concern, carbon fibers are preferred, whereas glass or even natural fibers can be used if less stiffness is required. With this technology the achievable weight reduction is about 50%. Composites depending on the structure and orientation of the fibers not only have high stiffness and strength but also a much higher energy absorption potential than metals, that means in principle they can even be used as lightweight materials in crash-relevant structural areas (monocoque, bumper crash absorbing structures) [76].

Despite the negative factors due to recycling of synthetic composites and their high price, their applications in automotive structures is a good perspective due to a potentially reduced weight of future cars and therefore, better fuel economy.



Figure 2.1 Parts made of glass mat thermoplastics (GMT) in Mercedes A-class. (www.daimlerchrysler.com).

2.3.5 Biocomposites

The concern about the preservation of natural resources and recycling has led to a renewed interest in biomaterials with the focus on renewable raw materials. Application of composites based on renewable or easily recyclable materials in automotive structures allows to avoid (to some extent) the problems with recycling of components at the end of life.

New types of composites – biocomposites have been developed in recent time. Biocomposites offer a good mechanical performance and eco-efficiency at the same time.

Biocomposites application is rapidly growing nowadays. This is especially related to certain problems concerning the use of traditional fiber composites. They are often considerable with respect to reuse or recycling of traditional fiber composites at the end-of-life time, mainly due to the compound of miscellaneous and usually very stable fibers and matrices. A simple landfill disposal is more and more excluded in Europe due to the increasing environmental sensitivity. Therefore, environmentally compatible alternatives are being looked for and examined recently. This might be recovery of raw materials, CO₂-neutral thermal utilization, or biodegradation in certain circumstances. That is why composites based on renewable resources consisting of either natural fibers or co-called biopolymers or both at the same time are economically and ecologically acceptable [133].

In a biocomposite at least one component either matrix materials or reinforcement is based on renewable resources. Thus, several combinations of composite structure are possible:

- renewable bioplastic matrix reinforced with natural fibers (100% renewable composite);
- renewable bioplastic matrix reinforced with synthetic fibers (partly renewable composite);
- matrix material made from synthetic resources reinforced with natural fibers (partly renewable composite).

As mentioned above (see sect. “Bioplastics”) bioplastics do not sufficiently fulfill the requirements to be used as matrices in biocomposites in the sense of mechanical properties and durability. This main disadvantage is based on their historical development. These polymers have originally been designed for the packaging sector and therefore their properties were oriented for that purpose. In particular cheap bioplastics show either too high values of elongation at failure, low durability, fast degradation, or rheological behavior. Therefore they are not suitable for application in biocomposites. Automotive structures are often exposed to high humidity and/or elevated temperatures during service. Most of the bioplastics are critical to moisture, which may result in a great dimensional instability or properties degradation. Therefore, biocomposites with bioplastic matrix can be considered as very good materials from the eco-efficiency point of view, but their mechanical properties (especially their moisture, temperature sensitivity and fast degradation) in combination with high price (see in Table 2.1) at present do not make them attractive for automotive producers. These biocomposites based on bioplastics, especially those reinforced with natural fibers, have a great challenge to be applied in automotive structures, but not in near future [169].

Biocomposites based on synthetic plastic matrix and reinforced with natural fibers is the last type in the classification. Synthetic plastics both thermosets and thermoplastics can be used as matrix in these materials. Mechanical performance of synthetic plastics has been discussed earlier and considered as sufficient for the automotive application. The only disadvantage of synthetic plastics is a large environmental impact, especially when they are reinforced with synthetic fibers (glass, carbon, aramid).

Environmental impact of fully synthetic composites can be substantially reduced by the replacement of synthetic reinforcement by natural-based one. The natural fibers are a good option for that purpose. Natural fiber reinforcement can be derived either from animal or plant resources. They offer quite good mechanical performance and they are based on renewable resources. Some of the natural fibers have mechanical properties like strength and modulus comparable to that of glass fibers. Moreover, their density and price are much lower than of glass fibers [56, 143].

Natural fibers possess excellent sound absorption efficiency. They are more shatter resistant, and have a better energy management characteristics than glass fiber in their respective composite structures [137]. Thus, in automotive parts, compared to glass composites, the natural fiber composites reduce the mass of the component, lowering the energy needed for production by 80%. For example, it takes 3.1 MJ of energy to produce 1 kilogram of kenaf, whereas it takes almost four times the same energy (~12 MJ) to produce 1

kilogram of glass fiber [102]. Other studies [56, 143] also show low energy requirements of natural fibers over synthetic ones. A more detailed information is presented in Table 2.2.

Thus, biocomposites based on synthetic matrix and natural fibers demonstrate the mechanical performance comparable to that of completely synthetic composites, accompanied by low price and reduced environmental impact [225]. Although, they can be considered as the most promising materials to be applied in automotive structures their low impact strength and high moisture sensitivity require further investigations. This will be discussed further in detail.

Table 2.2 Comparison of properties of different natural fibers (after [143]).

Fiber type	Specific gravity	Modulus of elasticity, (GPa)	Specific tensile strength (GPa/kg)	Cost (\$/ton)	Energy to produce (GJ/ton)
Lignocellulosic	0.6 – 1.2	11 – 53	1.6 – 2.95	200 – 1000	4
Glass	2.6	70 – 85	1.35	1200 – 1800	30
Carbon	1.8	100 – 140	1.71	12500	130

2.4 Natural fiber composites

Biocomposites based on synthetic matrix and natural fibers or simply natural fiber composites are very promising materials to apply in automotive structures. They offer good mechanical performance in combination with a better eco-performance and lower price (in comparison to synthetic fiber reinforced composites) [130, 146, 156, 157]. Since these materials are rather new their behavior under different conditions is not fully researched yet. Properties of natural fiber composites with different types of fibers and matrices are still being researched in order to develop feasible design rules for automotive and other applications.

2.4.1 Natural fibers

Natural fibers have attracted the attention of scientists and technologists because of environmental advantages that these fibers provide over conventional reinforcement materials, and the development of natural fiber composites has been a subject of interest for the past 15 years. Natural fibers are low-cost fibers with low density and high specific properties. They are biodegradable and nonabrasive, unlike other man-made reinforcing fibers. Specific properties of some natural fibers are comparable to those of synthetic fibers used as reinforcements in composites [18, 56, 103, 143, 195, 220].

There are some difficulties, however, in dealing with natural fibers. Unlike manmade synthetic fibers (which have constant quality) natural fibers have large variation in mechanical properties; they are moisture and UV sensitive and they have low impact properties. Therefore, some problems have to be solved for successful application of natural fiber in composites.

Types of natural fibers. Natural fibers are based on renewable materials and depending upon the source can be subdivided mainly into two major groups: plant fibers (based on agricultural resources) and animal fibers (based on resources derived from animals). The group of plant fibers can be subdivided into several classes: straw, seed, bast, leaf and wood fibers as depicted in Fig. 2.2.

All mentioned above types of natural fibers are currently commercially available. For example, sisal fibers are widely cultivated in Tanzania and Brazil. Sisal plant though native to tropical and sub-tropical North and South America, is also widely grown in tropical countries of Africa, the West Indies and Far East [16]. Henequen is produced in Mexico, abaca and hemp in the Philippines and China [39]. The largest producers of jute are India, China and Bangladesh. Flax and hemp are largely being cultivated in Europe, Russia, Canada, Argentina and India. Kenaf is a crop grown commercially in the United States [186]. India is

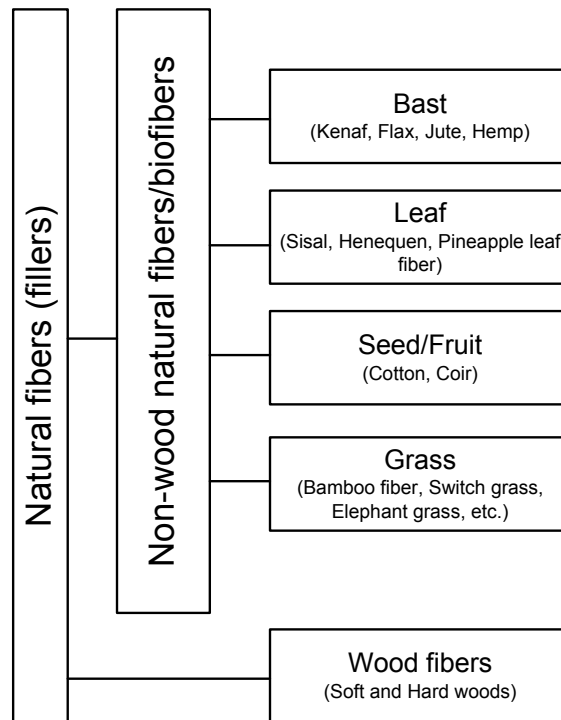


Figure 2.2 Classification of natural fibers derived from plants (after [130]).

also producing 20% of world production of coir [189]. Ramie fibers are the longest and one of the strongest fine textile fibers and mostly available and used in China, Japan and Malaysia [39].

Thus, each specific type of the fibers (plants) can be grown in these countries depending on favorable climate [20]. The prices of natural fibers vary to a large extent, because there are many factors influencing the price, they will be discussed further, but generally the price of plant fibers is much lower than that of animal fibers. The price of animal fibers can be up to up to 10 times higher (ex. wool and silk fibers) [133]. The animal fibers are not suitable because of high cost and low stiffness and therefore will no longer be discussed. The term “natural fibers” then implies in “plant fibers” in this thesis.

Chemical composition. The chemical composition and the structure of plant fibers depend to a large extent on climatic conditions, age and the digestion process of the plant, which they are derived from. Component values of some of plant fibers are presented in Table 2.3. With the exception of cotton, the major components of natural fibers are cellulose, hemicellulose, lignin, pectin, waxes and water-soluble substances. The physical properties of the fibers are mainly determined by cellulose (content and orientation of molecules), hemicellulose and lignin. Hemicellulose and pectin are responsible for the biodegradation, moisture absorption, and thermal degradation of fiber. Lignin is thermally stable, but degrades under UV radiation. Individual fiber properties and the structure of fiber bundles can vary widely depending on the plant, part of the stem (close to the roots or close to the top), age, extraction technique, moisture content, speed of testing, history of fiber, etc. Because of so many influencing factors there is a large variation in their properties.

Microstructure of natural fibers. A natural fiber in itself is composite. It consists of hollow cellulose fibrils held together by lignin and pectin in hemicellulose matrix. Each fibril has a complex, layered structure, consisting of a thin primary wall encircling a thick secondary wall (see Fig. 2.3). The secondary wall is made up of three layers and the thick middle layer determines the mechanical properties of the fiber. The middle layer consists of a series of helically wound cellular micro fibrils formed from long chain cellulose molecules; the angle between the fiber axis and micro fibrils is called a micro fibril angle (see in Table 2.3).

Table 2.3 Composition of different natural fibers (after [52, 133]).

Component	Natural fibers				
	Cotton	Jute	Flax	Hemp	Sisal
Cellulose, wt. %	82.7	61-71.5	64.1 – 71	70.2–74.4	65.7–78
Hemicellulose, wt. %	5.7	13.6–20.4	16.7–20.6	17.9–22.4	10.0–14.2
Pectin, wt. %	-	0.2	1.8-2.3	0.9	10
Lignin, wt. %	-	12-13	1.7-2.0	3.7–5.7	9.9
Wax, wt. %	0.6	0.5	1.5-1.7	0.8	2.0
Moisture wt. %	10.0	10.0-12.6	10.0	10.8	11.0
Microfibrillar spiral angle (degrees)	-	8.0	10.0	6.2	20.0

Component	Natural fibers				
	Kenaf	Coir	Ramie	PALF	Henequen
Cellulose, wt. %	31–39	36–43	68.6–76.2	70–82	77.6
Hemicellulose, wt. %	21.5	0.15–0.25	13.1–16.7	-	4-8
Pectin, wt. %	-	3-4	1.9	-	-
Lignin, wt. %	-	41-45	0.6-0.7	5-12	13.1
Wax, wt. %	-	-	0.3	-	-
Moisture wt. %	-	8.0	8.0	11.8	-
Microfibrillar spiral angle (degrees)	-	41-45	7.5	14.0	-

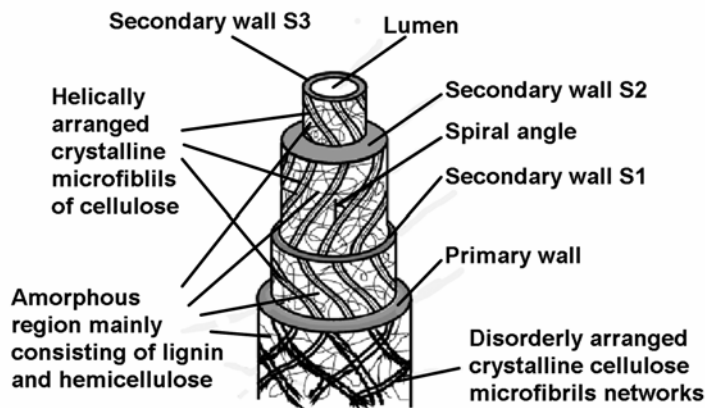


Figure 2.3 Structure of a natural fiber (after [172]).

The mechanical properties of natural fiber are dependent on the cellulose content in the fiber, the degree of polymerization of the cellulose and the angle of the micro fibrils [64, 178]. Fibers with higher cellulose content, higher degree of polymerization and a smaller microfibrillar angle exhibit higher tensile strength and modulus. Several studies on estimation of the mechanical properties of natural fibers have been carried out [20, 112, 145].

Processing of natural fibers. Processing of natural fibers is required in order to obtain fibers from a plant stem (or leaf) in the form suitable for composites. Technology for fibers processing determines their quality. Currently there are three main technologies: microbial deterioration (dew retting), hot water retting and hydrothermal treatment. The central problem of fiber production is its procurement. In order to obtain a maximum value gain, it is important to optimally use the facilities of nature. This means that the structure of the fibers should be retained and optimally used. The traditional dew-retting is one of the most important and widely used methods. This process is the only commercially developed by producers of plant stem fibers (at least for flax and hemp). It consists of simple and cheap procedures. Following this process freshly cut stems of a plant are left in the field for a

certain period of time (about 6 weeks). Under the natural condition they are exposed to combined deterioration of microbes, humidity and UV radiation. After that, the fibers reach the condition when they can be easily mechanically extracted from the stem, they will be collected and transported to the subsequent processing stage. The resulting fibers can have a large property variation and high moisture sensitivity due to non-optimal deterioration of hemicellulose and pectin (both influencing the fibers separation) and degree of cellulose crystallinity (responsible for mechanical properties) [101]. However, there are some developments in order to improve fiber quality.

Hot water retting is a technology, which can be used to extract natural fibers in a shorter time (several hours or days). However, this process requires much energy. The plants are processed in batches in tanks with hot water. After that the fibers can be separated from stem. This result in better mechanical properties of extracted fibers due more controlled processing conditions and therefore more optimal pectin and hemicellulose degradation.

New modern methods based on hydrothermal processes have been developed recently. One of the examples is Duralin® process [161 - 163]. Just harvested “green” plant straw can be directly processed, thus no dew retting is required. The technology has been proved on flax, hemp and jute fibers. Bundles of plant straw are heated in water in a pressure vessel at temperatures between 160-180°C for about 15 minutes (hydro-thermolysis). After drying, the plant straw is heated in the air or dry steam for about 30 min at temperatures of up to 180°C (curing). After that the fibers can be easier separated than after dew-retting process. A standard decorticator can be used. The fiber yield is considerably higher than after dew-retting. Also, this process results in less damage to the fibers’ structure than in traditional dew-retting process, which positively affects the quality of the extracted natural fibers and is therefore more consistent with their mechanical properties [100]. In addition extracted fibers become less sensitive to the moisture [162, 163, 208].

In order to obtain even more fine fibers the so-called “steam explosion” process can be applied to the fiber bundles obtained after decortification. In that process steam and additives (if necessary) under pressure and increased temperature penetrate into the space between fibers of the fiber bundle. As a result, the middle lamella and the fiber adherent substances are become “soft” and after pressure release can be removed by washing and rinsing [20]. The quality of natural fibers processed with steam explosion process is more constant than before the processing. Moreover, fine fibers when introduced into a composite result in better performance of the composite.

Geometrical properties. Unlike man-made synthetic fibers (glass, carbon) natural fibers extracted from plants have variable geometry. The fiber length and diameter are the main parameters, which have certain influence on reinforcing capabilities in composites. These geometrical parameters of the extracted fibers vary not only from one plant to another but even from one part of the plant to another (close to roots, middle and top of a plant stem) [112]. Typical geometrical parameters of some natural fibers are presented in Table 2.4. Stiffness, strength and impact resistance of composites increase fiber length and hence composites with flax and hemp (provide the longest fibers) can have the best mechanical properties [72].

Table 2.4 Geometrical parameters of some natural fibers.

Fiber type	Fiber dimension, mm	
	Length	Thickness
Cotton	10 to 60	0.02
Flax	5 to 60	0.012 to 0.027
Hemp	5 to 55	0.025 to 0.050
Jute	1.5 to 5	0.02
Deciduous Wood	1 to 1.8	0.03
Coniferous Wood	3.5 to 5	0.025

Mechanical properties. Mechanical properties of natural fibers alike geometrical properties vary to a large extent. Natural fibers exhibit considerable variation in diameter along with length of individual bundles. Quality as well as most their properties depend on the factors like size, maturity as well as processing methods adopted for the extraction of fibers.

Properties such as density, tensile strength, modulus, etc., strongly depend on the internal structure and chemical composition of fibers. It is known from the experiments that modulus of natural fiber decreases with increase of its diameter [112, 145].

According to the data collected from other scientific publications the strength of natural fibers is lower than that of glass fibers (see in Table 2.5), while the stiffness is on the same level. However, taking into consideration low density of natural fibers, which are up to 2 times lighter than glass, the resulting specific stiffness of natural fibers is substantially higher than the same parameter of glass fibers.

Flax, hemp and jute fibers are particularly standing out due to good specific stiffness. They are attractive candidates to be used as reinforcement in composites for automotive applications. Natural fibers like sisal, coir cotton and ramie are only beneficial if they are cheaper.

Wood fibers in the form of short fibers or flour are also used in natural fiber composites, but mainly as filler. The properties of natural fibers presented in Table 2.5 are mostly for those fibers extracted by using dew-retting process, and could be regarded as conservative.

Table 2.5 Properties of some synthetic and natural fibers [59, 120, 121, 133, 179].

Fibers	Tensile strength, MPa	Tensile modulus, GPa	Specific gravity	Specific strength	Specific stiffness	Failure strain, %	Price, Euro/kg
E-glass	2500-3500	70-73	2.56	27	29	2.5-3.0	1.5-2.5
Carbon	2500-6000	220-700	1.75-1.9	116	400	1.4 – 2	30-50
Flax	500-900	50-70	1.4-1.5	33	50	1.3 – 3.3	0.5-1
Sisal	80-840	9-22	1.3-1.45	6	17	3 – 7	0.3
Jute	200-450	20-55	1.3-1.4	14	42	1.16 – 1.5	0.12-0.5
Hemp	310-750	30-60	1.48	20	41	2 – 4	0.5-1
Banana	530-750	7-20	1.4	5	14	1 – 4	0.5
Coir	130-175	4-6	1.15	3	5	15-40	0.25
Cotton	300-600	6-10	1.5	4	7	7.0 – 8.0	1.6-4.6
Silk	-	-	1.34	-	-	-	18.3-36.7
Wool	125-200	-	1.31	-	-	-	Up to 15.4

Thermal stability. Natural fibers are complex organic materials and, higher temperature result in physical and chemical changes in their structure. The thermal stability of natural fibers can be studied using thermogravimetric analysis. From recent studies [51] it was learned that natural fibers start to degrade at temperatures between 170 – 260 °C (depending on chemical composition). Under these conditions natural fibers do not completely degrade immediately, but only start to do so.

The degradation level depends not only on temperature, but also on the duration of the exposure. The degree of thermal degradation of natural fibers is an important condition in the manufacturing of natural fiber composites. Thus, the curing temperature in case of thermosetting matrix and extrusion temperature of thermoplastic matrix should be within the limits. The process duration should be limited as well. Thermal degradation of natural fibers leads to emergence of poor organoleptic properties, such as odor and color change as well as deterioration of their mechanical properties. Changes in the surface of fibers due to thermal degradation cause changes in the bonding properties between fibers and polymer

matrix, which results in decrease of mechanical properties of a composite. The thermal stability of natural fibers can be slightly improved by chemical treatment [179].

Moisture content. All natural fibers derived from plants are based on cellulose, which is hydrophilic and hence absorb moisture. Usually a moisture content in natural fibers varies between 5 and 15%. It is higher in green natural fibers, but decreases during processing of natural fibers (after retting and drying). In composites a high moisture content in reinforcement can lead to dimensional variations and affects mechanical properties. During processing of thermoplastic composites, moisture can lead to poor processability and porous products. Therefore, natural fibers must be processed and stored under optimal conditions and must be dried before impregnating them with polymers.

Price of natural fibers. The price of natural fibers varies in a wide range depending on the economical wealth of the countries where fibers are grown (see in section “Types of natural fibers”) and applied processing techniques. In fact the price of raw natural fibers (i.e. just extracted from stem) is substantially lower than the price of glass fibers (see in Table 2.2). The price depends also on the length of fibers. Such difference originates not only from the techniques of handling the fibers, but also from the origin of fibers. For example, the flax fiber industry has already a well established infrastructure for fabrics (linen) production. Superior quality flax fibers are used for that purpose. They are long and handled in a way to keep the fibers parallel in bundles (for spinning). Such fibers are very expensive to apply in composites. However, the rest of fibers, such as tow fibers, are short. They are not suitable for linen production and usually thrown away. Tow fibers are cheap and can be successfully used as reinforcement for composites in the form of non-woven mats, for example. The price of natural fibers in woven form (fabric) is up to 10 times higher than that of non-woven.

The mechanical properties of composites with woven or unidirectional reinforcement are high due to good fiber orientation and better fiber quality, but the price is exceptionally high. Hence there are no economical benefits of woven natural fiber composites in comparison to synthetic ones, except the cases when an improved eco-performance needed. Therefore, natural fibers in non-woven form are more economically efficient as reinforcement in composites even if their reinforcing abilities in composites are lower than that of the woven ones.

Chemical treatment of natural fibers can improve their mechanical properties, thermal stability and reduce moisture content of natural fibers and, therefore, improve properties of the composite. However, additional processing of natural fibers increase their price. Therefore cheaper chemical treatment of natural fibers can be chosen in order not to affect the price too much.

Environmental and other properties. Plant fibers are renewable raw material and their potential availability is unlimited, as they can be grown every season. When natural reinforced plastics at the end of their life cycle are incinerated or naturally biologically decomposed in the soil the released amount of CO₂ of the fibers is neutral i.e. in balance to the assimilated amount during their growth [79]. This helps to reduce the so-called “Greenhouse effect”. The abrasive nature of natural fibers is much lower compared to that of glass fibers, which leads to advantages with regard to fibers extraction, material recycling or processing of natural fiber composite materials in general. Natural fibers do not cause skin irritation and therefore results the better labor conditions. Under the impact load the composite materials reinforced with natural fibers do not split into pieces. This helps to avoid additional injuries when natural fiber composites are applied in automotive structures (for example, in door panels).

2.5 Properties of natural fiber composites

The mechanics of natural fiber reinforced composites is largely similar to those reinforced with synthetic fibers. Like in a synthetic fiber reinforced composite the main parameters are the properties of matrix, fiber properties, fiber volume fraction, fiber aspect ratio, fiber orientation and fiber–matrix interface.

Most of the studies on natural fiber composites in existing literature have been carried out in order to determine their mechanical properties as a function of different types of fibers, fiber length [50, 218], fibers content [1, 27 - 29, 80, 146, 165, 171], effect of various treatments of fibers [13, 28, 29, 80, 85, 86, 166, 223] and optimal processing conditions [81, 217, 223]. The data from different sources are sometimes quite contradictory due to diverse properties of natural fibers and processing conditions of composites. This makes the information complex to analyze.

An overview of properties of some natural fiber composites is presented in Tables 1 - 3 in APPENDIX 1. The properties of some synthetic fiber composites are shown in the same table for comparison. Polypropylene (PP) matrix based composites reinforced with natural fibers are of prime interest, because PP is easy to process and it is one of the cheapest polymers on the market, which is of primary importance in the 'cost-performance' sector, like automotive. Therefore, particularly PP based composites will be in focus further. In the group of thermosets the unsaturated polyester (UP) has the similar price advantage over other polymers. It will be also discussed further.



Figure 2.4 Flax, hemp, sisal, wool and other natural fibers are used to make interior Mercedes-Benz E-Class components. (www.daimlerchrysler.com)

Several well-known automotive manufacturers like Daimler-Chrysler, Opel-GM and Volkswagen-Audi are already started to apply natural fiber composites in their series passenger cars. At the moment, mostly interior lightly loaded components like door trim panels, rear parcel shelf and seat squabs [114, 196] are in focus (see an example in Fig. 2.4). The lightweight design possibilities with plant fibers have already been proven, for example with the door panels and even exterior underbody panels of the Mercedes E-Class.

Volkswagen has also applied natural fiber composites (phenol-formaldehyde/Flax) in their door structures. Considering the specific properties of natural fiber composites, a weight saving of components potential of about 15% compared to glass fiber-reinforced is feasible. At the moment this is one of the most relevant technical driving forces for further developments in applying natural fiber composites for automotive applications [196].

2.5.1 Polymer matrix and processing technology

The matrix material in composites is a load transferring medium between fibers. The ability to transfer load between fibers is mainly characterized by mechanical properties of matrix (for example, modulus of elasticity, strength, etc.) and quality of its adhesion to the fibers [72]. Therefore, matrix plays a significant role in the performance of any composite. The main limitation in choosing a suitable polymer matrix for natural fibers impregnation is the processing temperature, which is restricted to temperatures below 170 - 260 °C to avoid thermal degradation of natural fibers. Both thermoplastic and thermosets offer significant advantages over metals, due to design flexibility and ease of molding of complex parts.

Drying of natural fibers is an important factor before processing of both thermoplastic and thermoset composites. Moisture on fibers surface can act as a separating agent in the fiber-matrix interface. Since most of thermosetting and thermoplastic resins have a processing temperature of over 100°C, water evaporates and voids in the matrix appear. This phenomenon leads to significant decrease of mechanical properties of natural fiber composites.

Thermoplastic matrix. The major advantage of thermoplastics over thermosets is in low cost of polymer itself and easy, fast and cheap processing technology. Methods such as extrusion, compression (NMT, similar to GMT) and injection molding can be used for processing of these composites [169]. In the field of thermoplastic composites most of the work reported so far deals with polymers such as polyethylene with different molecules weights (PE, LDPE, HDPE) [30, 42, 58, 60], polypropylene (PP) [28, 50, 84, 85, 123, 146, 156, 185, 226], polystyrene (PS) [188, 201], and polyvinylchloride (PVC) [104, 105, 115, 122]. Processing of natural fiber composites based on thermoplastic matrix involves extrusion of the ingredients (fibers mixed with polymer) at melt temperatures followed by shaping operations, such as injection molding or thermoforming (widely used in GMT). The induced flow of the melted material during the processing requires certain viscosity of the mass. Therefore there is a limitation of the amount of fibers and their length, especially in the injection molding process [174].

Natural fiber thermoplastic composites offer good recyclability perspectives. But, despite good process ability, they have not the best mechanical properties. This is mainly due to poor surface adhesion of thermoplastic polymer to natural fibers and some other features like absence of fiber orientation optimization. Therefore in most cases adhesion improvement is required.

Thermoset matrix. Thermoset matrix composites are processed by techniques such as hand layup and spraying, compression molding, pultrusion, resin transfer molding (RTM) and sheet molding compound (SMC) [169]. A few other methods such as centrifugal casting, cold press molding, continuous laminating, encapsulation, filament winding, and reinforced reaction injection molding are being used for composites, but the use of these methods for natural fiber composites are hardly reported. In composites with thermoset matrix, the fibers can be used as unidirectional tapes as well as woven and non-woven mats. First, they are impregnated with the thermosetting resins and then exposed to elevated temperature for curing to take place.

Natural fiber composite materials based on thermoset matrix usually have a very good mechanical performance, high solvent resistance, tough and creep resistant. Some research on thermosetting composites has been done, which covers the effect of process parameters such as curing temperature and various fiber treatments on the properties of composites [58, 74, 170, 187, 197, 213, 231].

The most popular thermosets for natural fiber composites are: unsaturated polyester (UP) [42, 58, 60, 68, 126, 141, 147, 151, 156, 170, 177, 197, 202, 214, 218, 231], epoxy (EP) [53, 54, 59, 148, 172, 173, 185, 202, 211] and phenol-formaldehyde (PF) [4, 64, 117]. These thermosets contain components, which have good compatibility with the surface material of natural fibers and therefore the adhesion is rather good.

The basic properties of some popular thermoplastic and thermosetting polymers are presented in Table 2.6.

Table 2.6 Properties of some polymers [120, 121, 215].

Polymer	Modulus, MPa	Tensile strength, MPa	Density, kg/m ³	Price, Euro/kg
Thermoplastics				
Polypropylene (PP)	800 – 1300	25 – 30	902 – 907	0.68 – 0.73
High density Polyethylene (HDPE)	600 – 1400	20 – 32	940 – 965	0.74 – 0.81
Low density Polyethylene (LDPE)	200 – 400	8 – 12	910 – 928	0.77 – 0.80
Polyvinylchloride (PVC)	2410 – 4140	35 – 65	1350 – 1550	0.79
Thermosets				
Epoxy (EP)	3100	65 – 79	1150	4.9
Unsaturated polyester (UP)	1400 – 2000	30	1170 – 1260	0.15 – 0.30
Polyurethane (PU)	3000 – 8000	20 – 45	1100 – 1700	0.4 – 1.9
Phenol-formaldehyde (PF)	5600 – 12000	20 – 25	1400 – 1800	0.35
Polyethylene terephthalate (PET)	3100	70	1370	2.55

2.5.2 Length, quantity and orientation of fibers

Fiber aspect ratio is very important to achieve sufficient strength and impact properties of composites. This parameter is determined by the ratio of fiber length to its diameter. Unlike synthetic fibers, which can be made continuous, natural fibers are usually not longer than 50 mm. This is mainly because of natural fibers are being extracted from the stem for technical applications are often residual fibers (tow) from the textile industry [64] or waste from the wood products industry [78]. Wood fibers are short fibers or fillers. Thus, natural fibers with a length in range of 5 – 50 mm are considered as long, fibers with length in range of 0.5 – 3 mm are considered as short and even shorter fibers are considered as fillers. The higher aspect ratio the better mechanical properties of the composite. But the material cost is also gets higher.

Another important parameter to achieve significant reinforcement of polymer matrix by fibers is the critical fiber length [42, 77, 110]. If the length of fibers in a composite is shorter than critical length then failure in the fiber-matrix interface can occur even at low stresses due to debonding (resulting in a weak composite), whereas if the fiber length is greater than the critical length, the fiber-matrix load transfer is better and therefore fibers are better stressed under the applied load (resulting in a strong composite). The critical fiber length is different for every combination of fibers and plastic matrix.

Higher fiber contents and longer fibers in composites usually lead to improvement of mechanical properties of both, thermoplastic and thermosetting composites [42, 77, 110]. But the composite processing technology limits the length of natural fibers. For example, in composite structures made by injection molding, fibers should be short (not longer than 0.5 - 1 mm) in order to allow the flow of the melted material [174]. Long fibers as well as high volume fractions increase the viscosity of melted composite mass and, therefore, might cause bad filling of mold and inhomogeneity of the structure (thus, worsening processability of the composite). In other processing methods like compression molding, RTM, SMC, NMT etc. there is no limitation on fiber length, but the limitation on fiber volume fraction still remains. Therefore, a balance between the mechanical performance and the processability of the material must be found [53, 54, 139].

Thermoset matrix. Technologies like resin transfer molding (RTM), vacuum injection, hand lay-up and similar ones are applicable for thermoset natural fiber composites.

Using thermoset matrix in a composite the amount of fibers can be increased (up to 75 vol. % as reported in [173]). The movement of fibers during the impregnation is minimal and therefore better properties of composites can be achieved. This allows a local optimization of the performance of a composite structure by preliminary (before impregnation) fibers orientation.

The values of strength and Young's modulus of natural fiber reinforced thermosets are rather high and even comparable to those reinforced with glass fibers. Thus in [64] it is reported modulus 10 – 13 GPa and strength 37 – 43 MPa for MF/flax with 22wt. % of fibers in form of non-woven mat. In other study of Epoxy/flax with 30 vol. % of non-woven fibers it is reported 7.8 GPa modulus and 54 MPa strength [59]. For comparison, these properties of glass fiber composite with 15 – 65 wt.% of randomly distributed fibers are in range of 5,4 – 7.0 GPa for Young's modulus and 85 – 144 MPa for strength [68, 143, 177].

Since the processing techniques of the thermosets based composites sometimes allow to preserve the fiber orientation, there are numbers of research papers about determination of mechanical properties of natural fiber composites with unidirectional fibers (see in Table 1 – 3 presented in Appendix 1). The strength of Epoxy/flax fiber composites reinforced with unidirectional fibers is reported in [59, 148, 171, 217]. It is as high as 50-130 MPa and modulus 8-30 GPa with fiber volume fraction at 30 – 48 vol. %. There is a significant improvement in the properties of the composite with at higher fiber volume fraction. A similar improvement in the mechanical properties of an unidirectional Epoxy/sisal composite with higher fiber volume fraction is reported in [173], where levels of modulus up to 8 – 10 GPa and strength up to 160 – 300 MPa are reached at fiber volume fraction 25 – 75 vol. %. In [148] for UP/sisal composite at least 40% increase in tensile strength, modulus and impact strength with increase of amount of fibers from 22 to 46 vol. % is reported.

The impact properties of a composite also largely depend on fiber length. In [218] at least 130% improvement of impact strength of UP/flax composites with fiber length 38 mm rather than 13 mm is reported. But, still, the impact strength of the natural fiber reinforced thermosetting composites is quite low in comparison with those reinforced with glass fibers. In [143] at least 10 times difference in impact properties between UP/jute and UP/glass composites in favor of those reinforced with glass fibers is observed. Fiber volume fraction in both composites is equal to 15%, which, however, can be considered rather low. Very likely the low amount of natural fiber reinforcement does not improve quite brittle polyester matrix sufficiently and the impact energy absorbed by a composite is mainly due to a brittle matrix fracture. On the contrary the impact strength of UP/coir composites is rather high and significantly increases (by 50%) after increasing the amount of long fibers (150 mm) from 17 wt. % to 33 wt.% [176].

Thermoplastic matrix. Thermoplastic composites can be processed using compression molding or GMT (in other words, NMT – natural mat thermoplastics), vacuum forming and technologies, in which the fibers have been pre-mixed with the polymer or preimpregnated in form of sheets (prepregs). These technologies allow processing of long natural fibers.

Most of the research on thermoplastic natural fiber composites is concentrated on the usage of non-woven fibers or needle-punched mats. This is, of course, due to cheap fibers and low processing costs. In [146] a good comparison has been made of the mechanical properties of PP reinforced with 25 - 50 wt. % non-woven flax fibers available from different manufacturers. All investigated natural fiber reinforced composites have quite good modulus up to 2.9 – 6.5 GPa which is comparable to PP/glass fiber (typical GMT), which has modulus about 5.1 – 5.4 GPa. The strength of tested PP/flax composites is also rather high up to 21 – 56 MPa (74 – 77 MPa for GMT). Most of the tested PP/flax composites have 38 – 200 J/m of Izod impact parameter, which is rather low in comparison with GMT composite (Izod impact 410 J/m). The only PP/flax composite from Mühlmeier GmbH, Germany has its impact properties in the range of 266 – 403 J/m, thus comparable to GMT.

The influence of fiber volume fraction is researched in [28, 80, 123, 146, 156, 157, 165, 171]. Most experiments have been done using composites with the fiber weight fraction up to 10 – 60 wt. %. Increasing the amount of fibers in a composite produced a positive

effect on its stiffness, strength and impact performance. For example increase in fiber volume fraction in PP/flax composites from 30 to 60 vol. % results in 100% improvement in the modulus and 50% of its strength. However, there is a certain limit of fiber volume fraction, beyond which the properties of composite will go down. This limit is induced by a poor impregnation of fibers with polymer. The thermoplastic polymer has a high viscosity and hydrophobic nature, which bring porosity in composite. Thus, in [157] it is reported 10 – 150 % drop in mechanical properties of PP/Hemp composite while increasing fiber weight fraction from 57 to 68 wt. %.

The fiber length has an effect on mechanical properties of thermoplastic composites. In [50] it is reported that an increase can be achieved of up to 100 % in impact properties and up to 20 % in stiffness and strength in PP/flax composite (20 vol. % fibers) with change of fiber length from 6 to 13 mm. Also the influence of fiber length on the properties of UP/palm leaf fiber composite is investigated in [110]. It is reported that 180% improvement in strength and 250% in modulus at constant fiber volume fraction can be achieved just by changing fiber length from 5 mm to 30 mm.

Different types of fibers certainly play a role in properties of the composite. Thus, good results are achieved by [123] with 60 wt. % of randomly oriented flax fibers embedded in PP (without using any copolymer) reaching levels of modulus 8 GPa and strength 60 MPa. While in [165] PP (with 3% MAPP)/Jute composite (randomly oriented fibers) reaches levels of modulus up to 11 GPa and strength up to 73 MPa. These are quite remarkable properties and they are comparable to PP composite reinforced with randomly distributed glass fiber, which has the modulus about 5.4 – 9 GPa and the strength about 77 - 110 MPa [29, 146].

A newly developed process applicable for natural fiber composite production is thermoplastic pultrusion [57, 125, 216]. Using this process it is possible to produce unidirectional composites on a continuous basis. The reinforcement can be in form of preimpregnated yarns, tapes or interweaved prepregs. The resulting composite quality is very high because continuous feed of the reinforcement is used. Long and oriented fibers secure very good mechanical properties. Using this process, composite profiles with tailored mechanical properties can be produced [57, 125, 216]. Unfortunately this process is not on the commercial scale yet.

2.5.3 Fiber-matrix adhesion and methods of its improvement

Achieving good bonding between fibers and matrix polymer is one of the major problems in composites engineering. In synthetic fiber reinforced composites this problem has been researched since the beginning of composites era. Therefore there have been some solutions already found to handle the problem, while natural fibers are more recently being introduced and for them the problem still exists. According to the latest research studies, the mechanisms of fiber-matrix adhesion in natural fiber composites are rather different from synthetic fiber composites. This is due to a large difference in chemical composition of natural fibers and synthetic polymer matrix. This problem is especially relevant for thermoplastic polymer based composites. The difficulties are associated with highly polar character (hydrophilic) of natural fibers, making them less compatible with weakly polar (hydrophobic) synthetic polymers (like polypropylene, polyethylene) [46]. This results in poor load transfer and therefore poor mechanical performance of the composite. Therefore, new physical and chemical methods to improve fiber-matrix adhesion for natural fiber composites have been developed. They optimize the interfacial characteristics and improve the properties of natural fiber reinforced polymer composites [19, 21, 203].

The purpose of the physical methods, such as stretching, calendering [197, 198], thermotreatment [167], and the production of hybrid yarns [41] is to change structural and surface properties of the fiber and, thus, improve the adhesion to polymers. Electric discharge (corona, cold plasma) is another way of physical treatment of fibers. Corona treatment is one of the most interesting techniques for surface oxidation activation. This process changes the surface energy of cellulose fibers before impregnation [9] and makes it

more compatible to the polymers. Electric discharge methods are known [62] to be very effective for certain polymers such as polypropylene, polyethylene and etc.

The old chemical method of cellulose fiber modification is mercerization [107, 140, 180], it has been widely used on cotton textiles. Mercerization is an alkali treatment of cellulose fibers; it depends on the type and concentration of the alkaline solution, its temperature, time of treatment, tension of the material and on the additives [140, 166, 180].

Thus, strongly polar cellulose fibers [222] are inherently incompatible with weakly polar synthetic polymers [9, 116, 192]. When two materials are incompatible, it is often possible to bring about compatibility by introducing a third material that has properties intermediate between them. There are several mechanisms [128] of coupling in materials:

- Elimination of weak boundary layers – coupling agents eliminate weak boundary layers;
- Creation of deformable layers – coupling agents produce a tough, flexible layer;
- Creation of restrained layers – coupling agents develop a highly crosslinked interphase region, with a modulus intermediate between fiber and polymer;
- Improve the wettability – coupling agents improve the wetting between polymer and fiber;
- Chemical coupling – coupling agents form covalent bonds with both materials;
- Changing of acid-base effect – coupling agents alter acidity of fiber surface.

The mechanism of bonding by coupling agents in composites is very complex. In spite of the large variety of methods the most popular technique applied by different researchers belongs to chemical coupling methods. Chemical coupling improves the interfacial adhesion by forming chemical bridges between fiber and matrix. These methods include treatment of either fiber (ex. graft copolymerization [107]) or polymer (compatibilizing agents). The compatibilizing agents, which are added to the matrix polymer can be a polymer with functional groups grafted onto the chain of the matrix polymer. The most popular and commercially available compatibilizing agents are presented in Table 2.7 [179].

Table 2.7 Some typical representative commercial coupling agents [179].

Functional Group	Applicable Polymer
Vinyl	Elastomers, polyethylene, silicone elastomers, UP, PE, PP, EPDM, EPR
Chloropropyl	EP
Epoxy	Elastomers, especially butyl elastomers, epoxy, phenolic and melamine, PC, PVC, UR
Methacryl	Unsaturated polyesters, PE, PP, EPDA, EPM
Amine	Unsaturated polyesters, PA, PC, PUR, MF, PF, PI, MPF
Cationic styryl	All polymers
Phenyl	PS, addition to amine silane
Mercapto	EP, PUR, SBR, EPDM
Phosphate (titanate)	Polyolefins, ABS, phenolics, polyesters, PVC, polyurethane, styrenics
Neoalkoxy (zirconate)	Polyolefins, ABS, phenolics, polyesters, PVC, polyurethane, styrenics

The grafting of natural fibers involves attaching a suitable polymer with a solubility parameter similar to that of the polymer matrix to the surface of a fiber/filler. This polymer acts as an interfacial agent and improves the bonding between the fiber and the matrix. The resulting co-polymer possesses properties characteristic of both, fibrous cellulose and grafted polymer. In this case the cellulose fibers are treated with a suitable solution (compatible with the polymer matrix), for example vinyl monomer [107], methyl methacrylate [61], polystyrene [116], maleic anhydride [45] etc. An example of grafting scheme is presented in Fig. 2.5, where the compatibilizing agent possess at one end a functional group *F* able to react with hydroxyl groups (OH) of cellulose and at the other end an alkyl chain of varying length. The polymeric chain has a structure similar to that of the matrix.

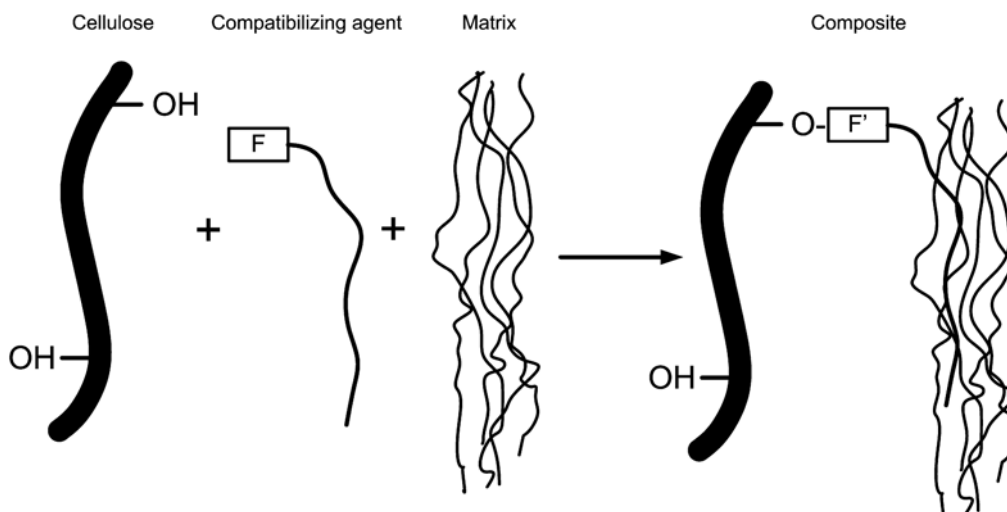


Figure 2.5 Chemical modifications of cellulose for compatibilization with matrix in composites. (after [55]).

Table 2.8 Chemical treatments used for modification of natural fibers (table after [179]).

Fibers	Chemical treatment	Coupling agents (compatibilizers)
Wood flour	Succinic acid, EHMA, styrene, urea-formaldehyde, m-phenylene bismaleimide, acetic anhydride, maleic anhydride, itaconic anhydride, polyisocyanate, linoleic acid, abietic acid, oxalic acid, rosin	Maleated PP, acrylic acid grafted PP, Silane A-174, Epolene C-18, Silane A-172, A-174, and A-1100, PMPPIC, zirconates, titanates
Jute	Phenol-formaldehyde, malemine-formaldehyde, cardanol-formaldehyde	-
Sisal	NaOH, isocyanate, sodium alginate, N-substituted methacrylamide	-
Pineapple	p-phenylene diamine	-
Banana	Sodium alginate	-
Coir	Sodium alginate, sodium carbonate	-

The important parameters for such treatment are the degree of grafting and the length of the grafted alkyl chain. The modification of natural fibers is attempted to make the fibers more hydrophobic (to change surface tension) and to improve interfacial adhesion between the fiber and the matrix polymer. Chemical treatments such as dewaxing (defatting), delignification, bleaching, acetylation, and chemical grafting are used for modifying the surface properties of the fibers and for enhancing its performance in a composite [5, 21, 73, 111, 118, 134, 154, 181 – 184, 203]. The summary of the various chemical treatments and coupling agents used so far for the modification of natural fiber surface is presented in Table 2.8. As a result, composites reinforced with treated natural fibers might have better mechanical properties (strength and modulus as well as impact strength) due to better fiber-matrix adhesion [20, 53, 54, 165, 223]. The research is mainly concentrated on the finding of the best chemical coupling agents for natural fiber composites [28, 29, 42, 68, 71, 80, 86, 131, 132, 143, 202].

A more detailed experimental information on the chemical way of improvement of mechanical properties of natural fiber composites with thermoset matrix is presented in [10, 13, 29, 42, 68, 85, 86, 123, 143, 146, 165, 176, 202]. The positive effect of using chemically (silane, glycol or methacrylamide) treated natural fibers on all mechanical properties

(modulus, strength and impact) of composites is reported. But in [68, 143] a slight decrease of impact and strength properties of UP/jute composite is observed if glycol treated fibers are used. The results of experiments reported in [143] are quite contradictory to the other papers [42, 85, 202] with regards to strength. In [143] it is reported that the strength of UP/jute composite does not change when treated fibers are used. But the results in [143] are similar to the other papers with regards to decrease of the impact strength if treated fibers are used in comparison with those composites with untreated fibers.

Since PP is the most popular resin used in natural fiber reinforced composites, many researchers [28, 29, 80, 85, 86] study the influence of copolymer (maleic anhydride polypropylene - MAPP) on mechanical properties of the composite. Thus, in [28, 29, 85, 86] a significant improvement in modulus (up to 15 – 50 %) and strength (up to 10 – 80 %) in PP/kenaf, PP/sisal and PP/jute composites with addition of MAPP copolymer is reported. Also, the impact properties of PP/kenaf are improved up to 10 – 90 % [29, 86] using the same copolymer. In [28] it is also reported, that the increase of concentrations of MAPP from 0 wt. % to 4 wt. % results in the improvement of strength and modulus, but deterioration in impact properties of PP/sisal composites.

Different chemical treatments of natural fibers and the resulting effect on the thermal stability of composites are being studied in [127, 138, 156, 223, 227]. It has been reported [42, 202, 209], that the treated natural fibers have lower moisture absorption than untreated ones. Lower moisture absorption results in better behavior of structures made from natural fiber composite subjected to humid environment [53]. An increased dimensional stability and unchanged mechanical performance are expected. A better wetting (and therefore mixing) of chemically treated natural fibers with thermoplastic polymers enables an improvement of formability of a composite and helps towards homogeneity of a final component [179].

Some examples of the applied treatments to some natural fibers and the gain in mechanical properties are presented in Table 2.9, but there is a lack of economical data on these treatments. However, a value of about 20% of untreated natural fiber price can be taken as an approximate indication of fiber treatment costs.

Table 2.9 Influence of coupling agents on the mechanical properties of natural composites [52].

Fiber/matrix	Coupling agent	Increase in properties, %		
		Tensile strength	Young's modulus	Impact energy
Thermosets				
Jute/EP	Acrylic acid	Constant	-	100
Jute/UP and EP	Polyesteramid Polyol	10	10	-
Sisal/EP	Silane	25	-	-
Cellulose/UP	Dimethanolmelamine	Constant	-	100
Thermoplastics				
Cellulose/PS	Isocyanate	30	Constant	50
Cellulose/PP	Stearinic acid	30	15	50
	Maleicanhydride PP-copolymer	100	Constant	
Flax/PP	Silane	Constant	50	Constant [71]
	Maleicanhydrid PP	50	100	Constant [71]
Hemp/PP [131]	Maleicanhydrid PP	30	15	- 30 (negative)
Henequen/PP [131]	Maleicanhydrid PP	70	70	- 5 (negative)

2.5.4 Moisture and temperature sensitivity

Moisture sensitivity. Natural fibers are quite hydrophilic and their properties are moisture sensitive. As they absorb water easily their mechanical as well as geometrical properties change, resulting in degradation and rotting, or swelling correspondingly. This has a great effect on the polymer matrix, which surrounds fibers in composite. Cracks can appear in a polymer around fibers due to their swelling and, therefore, worsen the mechanical properties of the composite. Fibers on the surface of a composite are subjected to moisture influence most of all. Natural fiber composites with high fiber volume fraction have more fibers in the core of composite as well as on its surface. Therefore, higher fiber volume fraction results in more moisture sensitive composite, because the fibers simply can absorb more moisture. The moisture soaked by fibers on the surface can go deep into the composite via interfacial areas (capillary effect) [108]. Studies on unmodified Epoxy/jute composites regarding their moisture absorption (in distilled water at 23 °C) reported in [53] show, that the kinetics of absorption and the moisture content at equilibrium distinctly increase with increasing fibers content. Similar results are shown in [129] on Epoxy/jute composites and in [197, 198] on UP/jute composites.

Therefore, in general, natural fiber composites should be prevented from moisture exposure. Some techniques to reduce moisture sensitivity of natural fiber composites are already under development. There are two different approaches to reduce moisture uptake by natural fibers:

- Chemical treatment that reacts with OH-groups present on the surface of the cellulose fibers and thereby increase its hydrophobicity (silane, acetic anhydride);
- Hydrothermal treatment, for which no chemicals are used, only water and energy.

Chemical treatment of natural fibers, for example, with silane or acetic anhydride can be applied to reduce fibers moisture gain [152]. For example, composites with silanized jute fibers have about 20% lower moisture gain at equilibrium [53]. The applied silane reduces the amount of hydroxyl groups (OH) on the surface of cellulose fibers, which are free to bind moisture. An increase at about 30 % (compared to composite with unmodified fibers) of modulus and strength at standard humidity of composites made of treated fibers is observed. Researchers in [124, 197] have also observed an improved water repellence in UP/jute composites treated with polyvinylacetate.

In [52] it was observed that the tensile strength of the composites reinforced with silanized fibers is nearly independent of the moisture content in the composite (see Fig. 2.6). A similar effect has already been known for glass fiber reinforced plastics: the usage of silane coupling agents reduces the dependence of the mechanical properties in glass fiber composite on moisture content. Unmodified Epoxy/jute composites reach only 65% of the values of their dry-strength at the maximum moisture content of 5.2 wt. %. In [41] similar results were reported on composites without any coupling agents. The used materials were unidirectional Epoxy/jute (fiber content ~ 33 vol. %) and UP/jute (fiber content ~ 22 vol. %) composites, which were stored for 2 hours in boiling water. Tensile strength of these composites was reduced by 10 – 16 % and the decrease of the modulus by 13 – 25% was observed [41].

The improved moisture resistance caused by the application of coupling agents is explained by the improved fiber-matrix adhesion. The coupling agent builds chemical silanol and hydrogen bonds, which reduce the moisture penetration between fiber and matrix and prevent fiber-matrix debonding.

Applying hydrothermal treatment (has been discussed earlier, see section “Processing of natural fibers”) for natural fibers preparation such as the Duralin® process, one can reduce moisture content (up to 3 times) as well as moisture uptake in natural fibers [17, 162, 163].

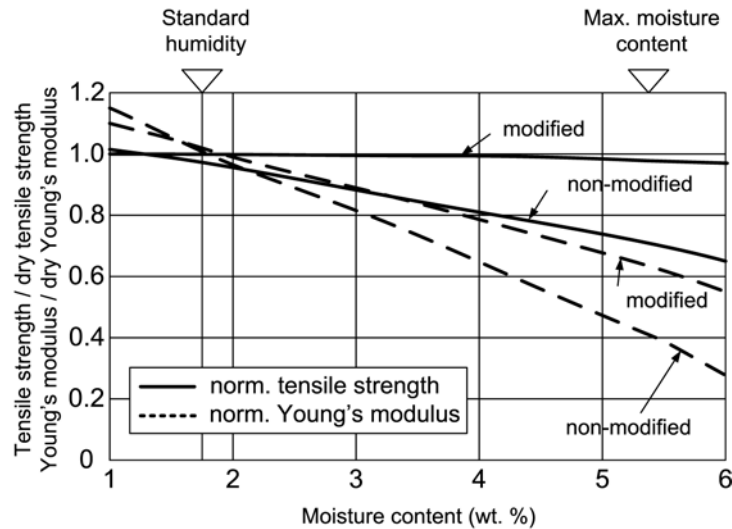


Figure 2.6 An example of the influence of silane coupling agents on the strength and stiffness of Epoxy/jute composites at different moisture contents (after [52]).

Temperature sensitivity. In principle, composites reinforced with natural fibers have similar temperature sensitivity as the original natural fibers and polymer matrix. Thus, structures made from thermoplastic polymer reinforced with natural fibers should be prevented from higher than maximum allowable service temperature of the polymer matrix to avoid melting, if its melting temperature is lower than the maximum service temperature of fibers. In case of thermoset the maximum service temperature of natural fibers determines the maximum allowable service temperature of a composite to avoid fiber degradation.

2.5.5 Discussion of mechanical properties

The properties of matrix and fibers as well as processing conditions are very important in achieving good mechanical properties of the composite. The strength parameter is more sensitive to matrix properties, whereas the modulus is dependent on the fiber properties. A strong fiber-matrix interface, low stress concentration and better fiber orientation are required to achieve good strength of composite, whereas the fiber concentration, fiber wetting in the matrix and high fiber aspect ratio determine stiffness [72]. An optimum bonding level, possibly long natural fibers and stronger fibers are necessary in order to achieve a good impact performance of the composite. The degree of adhesion, fiber length and mechanism to absorb energy are the parameters that have the major influence on the impact strength of a composite.

Processing of short natural fiber composites (ex. injection molding) is not complex and, therefore, and economically attractive. However, the mechanical performance of injection molded composites is rather low and suitable only for non-loaded applications. Whereas composites reinforced with long natural fibers are better suitable for medium and heavily loaded applications.

Thermosetting composites. It is clear that thermosetting polymer based composites have better mechanical properties than thermoplastic ones. First of all, due to better mechanical properties of thermosetting polymer itself and secondly due to presence of reactive groups in its formulation, which aid the interfacial adhesion. The reported work on the composites based on thermosetting matrix covers the effect of fiber contents and various treatments on the properties of composites. Reported strength of the composites reinforced with randomly distributed flax fibers varies (Epoxy or UP matrix) in range 40 – 80 MPa and modulus is in range 7 – 12 GPa at 25 – 40 wt. % fiber volume fraction. Thermoset matrix composites have better mechanical properties than thermoplastic ones. First of all, this is

due to better mechanical properties of polymers and secondly, thermosets contain reactive groups, which aid the interfacial adhesion.

Obviously, there is a strong relationship between the fiber volume fraction and modulus and the strength of composite, the more fibers in composite the better mechanical properties are. However, the fiber length is also one of the important parameters which have an influence on the composite properties. For example, the influence of the fiber length on the properties of UP/palm leaf fiber composite is studied in [110]. It is reported that 180% improvement in strength and 250% in modulus can be achieved at the constant fiber volume fraction just by changing the fiber length from 5 mm to 30 mm.

The processing technique of thermosetting polymers based composites sometimes allow to preserve the fiber orientation, therefore there is a number of research papers on based determination of mechanical properties of the natural fiber composites with unidirectional fibers. The values of strength and modulus of natural fiber reinforced thermosets are rather high and comparable to those reinforced with glass fibers. Thus in unidirectional composites modulus and strength can be improved at least 100% in comparison to randomly oriented ones (see in Table 1 – 3 presented in Appendix 1). Of course, the manufacturing technology for unidirectional composite is much more complex and expensive than that for composite with randomly oriented fibers.

The fiber volume fraction here plays a quite important role in mechanical properties of the natural fiber composites (random or unidirectional): the higher parameters the better properties. Particularly, the fiber volume fraction in thermosetting matrix composites can be very high (up to 75 vol. % as reported in [173]), due to benefits of technology, like lower viscosity of polymer and elevated temperature which allow good fibers impregnation (ex. hot pressing technology, resin transfer molding, etc.).

Thermoplastic composites. In spite of the fact that thermoplastic natural fiber composites have lower performance than thermosetting ones, they offer other benefits, like easy and cheap processing, as well as possible recycling or reuse of the end-of-life material. The major problem is that thermoplastic natural fiber composites demonstrate poor fiber-matrix adhesion. Current research in this area is mainly focused on that aspect.

Obviously, when fiber-matrix interface is improved, the load is better transferred to the fibers. In this case the stiffening potential of the fibers is better utilized, resulting in a better performance of the composite in stiffness and strength. However, the decrease of impact strength in treated natural fiber composites can be explained by the fact that loose natural fiber itself has a poor impact strength (at least it is lower than that of a glass fiber). In composite with improved interface a different mechanism of energy absorption appears. Thus, the fibers due to good bonding with matrix easily break (small energy required) than pull-out (large energy required), while absorbing impact results in low impact performance of composite. However, the decrease in impact strength is not due to a negative effect of compatibilizer applied, but weak fibers.

The strength of thermoplastic composites reinforced with randomly distributed flax fibers (PP matrix) varies in range 20 – 60 MPa and Young's modulus is in range 3 – 7 GPa at 25-50 wt. % of fibers.

The impact properties of thermoplastic composites can be improved by modification of matrix with additives. For example, in [13] up to 130 % improvement in impact properties of composite based on PP with 30 % of rubbery additive and reinforced with random flax fibers is reported, while a negative effect on the strength and stiffness is observed. However, it is reported in [10] that the impact strength of natural fiber composites can be improved by adding small amount of glass fibers resulting in hybrid composite.

Although positive effects of application of chemical treatment to natural fibers used as reinforcement in composites are known, deep understanding of the complex nature of natural fiber and its surface properties is still needed in order to optimize the natural fiber treatment processes. Undoubtedly this will help to increase the usefulness of natural fibers as reinforcing material for plastics and to gain insights in the interaction between these materials [46].

The application of non-woven natural fiber mats in composites is economically attractive, but the efficiency of fibers usage is not optimal, which results in poor mechanical properties of the composite (especially impact properties). Therefore, in [157] the possibility of application of chopped loose fibers in combination with non-woven mats as reinforcement in composites has been studied. This may result in even cheaper composite (loose bast fibers are twice cheaper than non-woven mat) with a better mechanical performance. The increase in the impact strength is feasible while applying long loose bast fibers in combination with non-woven natural fiber mat. However, new technology has to be developed yet in order to handle loose fibers effectively.

The overview of natural fiber composites are made by different researchers and under various conditions. The overall tendency is quite clear: natural fiber composites with thermoplastic matrix produced under optimal conditions (fiber length, fiber volume fraction, using compatibilizers, etc.) can compete with glass fiber composites in stiffness and can be used in those applications where stiffness is of a primary importance. A low weight and a low price of natural fiber composites make them good alternative to synthetic composites in lightweight and cost effective applications.

2.5.6 Heterogeneity

A major disadvantage associated with the use of natural plant fibers is the variation in fiber quality. Important parameters are the type of ground on which the plant grows, the amount of water the plant receives during growth, the year of the harvest, and, most importantly, the kind of processing and production route. A possible approach to solving this problem is in mixing batches of fibers from different harvests. Manufacturing of the composite, especially the quality of the fibers distribution in the polymer matrix plays even more important role in the lowering of the properties variation.

We have proved with several experiments on PP composite reinforced with 30% flax fibers in form of non-woven mats that it has a significant variation in its mechanical properties [97]. Determining tensile mechanical properties (strength and modulus) of that material by using a standard procedure (ISO-527), large variation in their properties has been found. The experimentally obtained stress-strain diagrams are presented in Fig. 2.7. It was determined, that modulus and strength of specimens cut out from one sheet of material varies up to 20%.

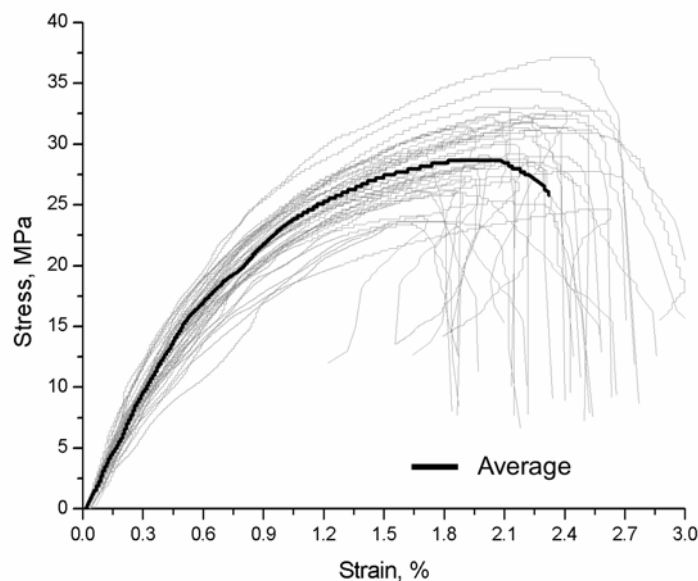


Figure 2.7 Experimentally obtained stress-strain diagrams as an example of heterogeneity in the properties. The number of curves detects the number of tested specimens (after [97]).

Following the standard ISO-527 averaged properties of the tested material can be taken as reliable characteristics. However, due to a large scatter observed in the testing diagrams the usage of such material in structural applications with averaged characteristics is unreliable. This effect is hardly covered in the literature and, therefore, should be discussed in more detail.

Although, heterogeneity in natural fiber composites is currently rarely being researched, it has a direct influence on the reliability of the products. Therefore we consider this issue as an important component in the design using natural fiber composites and will discuss further in detail.

2.6 Conclusions

Having been almost completely replaced by their synthetic counterparts in the sixties and seventies of the last century, natural materials are regaining ground in the automotive applications. The use of renewable materials has gathered much momentum throughout the nineties of the last century. One of the major reasons for this renewed growth is an increased awareness of environment protection, reflected by protection of resources, reduction of CO₂ emissions and recycling. Plant fibers are brought in focus because they are renewable, have low production costs and good mechanical properties. The use of plant fibers as insulating or damping materials or as fillers and as reinforcement in polymeric materials plays an important role nowadays.

The overview of modern materials showed, that not only conventional materials like metals and synthetic composites are suitable for automotive application. Recent independent studies [56, 157, 169, 194] including giant automotive suppliers like Johnson Controls Interiors [114, 168] show much interest in application of natural fiber reinforced composites in cars. Thus their characteristics such as:

- Low density (weight savings);
- Low price;
- High specific properties;
- Not brittle fibers (no skin irritation, better post-impact behavior);
- Non abrasive;
- Possible recycling;
- Low energy consumption [23].

make them attractive for car producers [23].

At the moment, composites with thermosetting binders such as Epoxy or Phenols fulfill the requirements for high-performance applications. They provide sufficient mechanical properties, in particular stiffness and strength, at acceptably low price levels. Compared to compounds based on thermoplastic polymers such as polypropylene, thermosetting compounds have a superior thermal stability and lower water absorption. However, the demand for improved recycling concepts and alternative processing techniques is expected to result in a substitution of the thermosetting polymers by thermoplastic ones. Considering the ecological aspects of materials selection, the substitution of synthetic fibers by plant fibers is only the first step. The pressure to curb the emission of greenhouse effect causing gases such as CO₂ into the atmosphere and an increasing awareness of the finiteness of fossil energy resources are leading to the development of new materials, that are entirely based on renewable resources. But all that kind of materials developed until now (based for example on starch, cellulose, sugar) do not fulfill the requirements for automotive applications [23].

Apart from the well-known methods such as dumping, incineration, and recycling, the so called "biocomposites" could offer a new way of disposing industrial waste: biological decomposition. Prototype materials, some of which are already established in other industries, are under consideration, but not yet available at acceptable properties and prices for automotive applications.

Modern technologies applicable for natural fiber composites processing are as follows:

- Compression Molding of
 - Pre-impregnated plant fiber mats;
 - plant fiber/PP hybrid mats;
 - NMT (Natural fiber Mat reinforced Thermoplastics) comparable to GMT (Glass fiber Mat reinforced Thermoplastics);
 - EXPRESS Process (extrusion-compression molding);
- Structural Reaction Injection Molding (S-RIM);
- Injection Molding with short fiber reinforcement.

The applicable processing technology depends on the used polymer and the form of natural fibers (mat, loose fibers, fiber length, etc.) and the geometry of the structure to secure homogeneity. The technology based on pre-impregnated materials has a number of advantages in view of processing and allows a commercial production of materials with good and constant quality mechanical performance. The technology that can handle long fibers and preserve their orientation is rather time consuming and costly, therefore its applicability for mass production is limited.

Processing short natural fiber composites by using, for example, injection molding, is not complex and economically attractive. However, the mechanical performance of injection molded composites is rather low and suitable only for non-loaded applications, whereas composites reinforced with long natural fibers are better suitable for medium and heavily loaded applications due to good mechanical properties. In unidirectional natural fiber composites modulus strength can be improved by at least 100% and their impact properties are much better in comparison to randomly oriented ones, but the manufacturing technology for unidirectional composite is much more complex and expensive, than for a composite with randomly oriented fibers.

The most promising technology is undoubtedly compression molding. Different variations of this process depending on the company are available for processing natural fiber composites. As almost all processes use the fibers in the form of mats decortications of the fibers and the processing of the mats are key issues for the technology.

Natural fibers in form of non-woven mats are the most economically advantageous in polymer composites due to low production costs. Roving and weaving is expensive. Loose fibers are bulky and difficult to handle. Therefore, techniques such as needle punching and air laying have been developed to aggregate fibers into non-woven mats. The non-woven fiber mats can be made entirely of plant fibers or a mixture of plant fibers, plastic fibers and resin in various amounts depending on the required properties of the end product [149]. Handling and processing of reinforcement in form of non-woven mats is much easier and can be highly automated (composites reinforced with unidirectional natural fibers are usually hand made, except for pultrusion). They can be used well as in thermoplastic as in thermoset based composites. Currently natural fibers in the form of non-woven mat are commercially available (ex. HempFlex BV, Netherlands, Muhlmeier GmbH, Germany) [64]. Therefore, the application of natural fiber composites based on non-woven fiber mats is considered most suitable for automotive applications [196].

However, the efficiency of the usage of fibers potentials in non-woven composites is not optimal, which results in poor mechanical properties of composite (especially impact properties). Recent studies show that there is a possibility of application of chopped loose fibers in combination with non-woven mats as reinforcement in the composites. This may result in even cheaper composite (loose bast fibers are twice cheaper than non-woven mats) with a better mechanical performance. The increase in impact strength is feasible while applying long loose bast fibers in combination with non-woven natural fiber mat. However, new technology has to be developed yet in order to handle loose fibers effectively.

The amount of natural fibers in composites fibers can be as high as 25 - 50 vol.%, in exceptional cases up to 60 vol.%. The usage of pre-impregnated materials helps to reduce the extended flow of the material in moulds during processing and, therefore, secures a better mould filling resulting in a more homogeneous material.

One inherent characteristic of plant fibers is their ability to take up and store humidity. For example, in seat cushions this characteristic is desired, but for other applications

(especially structural), water absorption must be prevented. This is the main reason why until now plant fiber applications have been limited to the interior of the vehicles (see in Fig. 2.4). However, several methods like acetylation, hydrothermal treatment of natural fibers and/or protective layers can be used to improve the moisture repellence of composites.

As to any internal application (such as a cabin), unpleasant smell and fogging must be prevented. It has been found that the use of plant fiber materials in standard production does not present a problem in this respect. The best results, however, were achieved with the natural fibers embedded in thermosetting matrix. In terms of fogging these materials are often better than conventional synthetic materials.

In the discussed literature no examples of medium-loaded or highly-loaded automotive structures made of natural fiber reinforced composites have been found. Probably, this is due to marketing policy and absence of experience of automotive designers in dealing with such materials and, therefore, fears of possible unreliability in their design. However, as it was discussed earlier in this chapter, the mechanical properties of natural fiber composites are rather sufficient for medium- and even for highly-loaded components and can satisfy the automotive design restrictions [124, 168, 194, 205]. But considering low impact properties of the natural fiber composites their application in components subjected to impact loads is questionable.

During the assessment of natural fiber reinforced composites properties it was found that first of all these materials are quite new for researchers and designers [92]. Most of the research work related to the estimation of the mechanical characteristics of natural fiber composites deals with hand-made specimens and trial-and-error methods of improvement of their mechanical properties. Many researches try to optimize the processing conditions of composites and test them afterwards, while others - try to predict their mechanical properties using various theoretical approaches. In those papers where authors perform mechanical testing of natural fiber composites the testing is performed using standard methods. This is reasonable when conventional composites are being tested, but for natural fiber composites not all existing standards are suitable.

This point of view originates from basic understanding that natural fibers are not like synthetic man-made fibers. By nature their geometrical and mechanical properties as well as surface properties are different from one fiber to another. Therefore, when natural fibers with variable properties are used as reinforcement they cause large variation in properties of composite. This variation is not taken into account by any of the existing standards yet. Hence, using them for testing of natural fiber composites a large variation in their properties can be underestimated. This results in unreliable mechanical properties estimation and might cause unpredicted failure of the designed structures.

For example, ISO 527 is a standard for determination of tensile properties of composite materials [75]. Following that standard, only 7 specimens are offered for a test in order to obtain reliable results. However, for the testing natural fiber composites this is not enough to due to large variation in their properties. Unfortunately in most papers based on determination of their mechanical properties, there is not enough information published on the testing conditions, like, for example, the number of tested specimens. After that the authors give determined mechanical properties with standard deviation, which might be not reliable. Therefore, either a deep understanding of mechanics of natural fiber composites or a careful and confident testing is required in order to obtain reliable characteristics.

Due to high safety consideration, automotive components should be engineered using reliable methods and made from materials with reliably determined properties. Thus, in order to apply natural fiber composites (for example, investigated in [97] non-woven PP/flax composite) in automotive components it is required that their homogeneity is approved or new technique is introduced taking into account variation in their properties. The improvement of the material properties requires the upgrade of the production process, which is rather costly. A new technique of engineering (design rules) can be suggested instead. A research on heterogeneity in the properties of natural fiber composites should be performed in order to develop new design rules.

This will allow the extension of application of natural fiber reinforced composites in a larger number of components including load bearing automotive structures. This, in its turn, can help towards a lightweight and cheap car design and lead to other benefits.

Chapter 3

Investigation of heterogeneity of natural fiber mats and composites

3.1 Introduction and heterogeneity definition

In the previous chapter it was shown that composites reinforced with non-woven fiber mats have large variations in their mechanical properties, i.e. they are non-uniform. Therefore there is a lot of uncertainty about the mechanical behavior of these materials when they are applied in load-bearing structures. During the engineering design of non-loaded or lightly loaded structures non-homogeneity in material properties can be neglected, because of low levels of stresses in structures [97]. Average properties of material, determined from simple mechanical tests, can be used in this case. However, in medium-loaded structures the variation in strength due to heterogeneity in material properties is high. Sometimes it plays a significant role in the structural performance and might even cause unpredicted failure under adverse conditions. In this case heterogeneity in properties of the material should be taken into account.

The analysis of the material's heterogeneity should be performed keeping in mind a considerable scatter in natural fibers properties. For composites with randomly distributed natural fibers there are several main parameters that may have influence on their non-uniformity:

- a) Properties of the natural fibers. Natural fibers have extremely high variations in geometrical and mechanical properties due to the difference in their growth and extraction process conditions. Moreover, natural fibers are not solid fibers but they consist of smaller fibers (fibrils), which are bonded together;
- b) Distribution of fibers. This parameter plays a most significant role in non-uniformity, since in the manufacturing stage it is hard to distribute natural fibers uniformly at reasonable costs;
- c) Fiber-to-matrix bonding variation. The surface condition of natural fibers is not constant along its length which influences adhesive ability of fiber to a polymer resin. Moreover, the seizing (wetting) of natural fibers is less than that of synthetic fibers;
- d) Air and moisture entrapment. Natural fiber always contain some amount of air (in lumen) and moisture (in cellulose and hemicellulose), which is different for each fiber and cause its degradation in a long term; etc [89].

All mentioned above parameters have different magnitudes and scales. In order to simplify the material description the parameters can be ranged into three scale categories. The variations of the properties of the natural fibers (fibrils), condition of their surface and bonding conditions with resin are on a **microscale** (several microns). The microscale in this case is comparable to the scale of fibers diameter (i.e. several micrometers). But, the variations in fiber distribution in composite are on the so-called "**mesoscale**". The mesoscale is much larger than the scale of fibers on the one hand, but from the other hand it is smaller than the size of a structure (macroscale). For example, the mesoscale in non-woven natural fiber mat can be defined with the reference to the fiber length. Usually, fibers with the length ~5...30 mm can be observed in non-woven natural fiber mat, so the mesoscale for such a mat corresponds to this range. **Macroscale** properties in this case can be defined as properties which determine the overall properties of the structure made of natural fiber composite.

The variation of properties in natural fiber composites on microscale is hardly predictable due to natural scatter in the properties of the natural fibers and their low magnitudes of influence on meso- and macroscale properties of the composite. Therefore,

from the meso- and, therefore, macroscale point of view the microscale property variations are uniformly distributed through the whole material domain. The possible weakness in defect areas is hence compensated by strong areas and these areas are quite small (several micrometers). On the meso- and macroscale these variations are relatively small and therefore can be homogenized. Thus, it is possible to assume that microscale variations can be neglected to a certain extent (unless the micromechanics of a composite is under investigation). However, property variation on the mesoscale is much larger, than microscale. The variation of properties in areas with dimensions in range of ~3...30 mm is quite a significant contribution to the macro-scale properties variation, because in some cases the dimensions of a structural element, which is made from such non-uniform material, might lay within that range. This might lead to unpredicted unbalance of relatively weak and strong areas, which lead to uncertainties in overall mechanical performance of the whole structure. Thus, the property variations in natural fiber composite material on mesoscale during structural design cannot be neglected [88].

In general, the mesoscale property variation can be found in any kind of composites. Like, for example, amount of fibers which is present in certain volume in the material can vary from one area to another. Fiber volume fraction of the composite material is an important characteristic and it has large influence on most of properties of a composite material.

The fiber volume fraction variation is low (less than 5 % [72]) for those composites reinforced with woven or aligned long fibers, because fibers usually have better quality and therefore the manufacturing process is more controllable. But, in composites with randomly distributed fibers (i.e. non-woven) the fraction of fiber volume variation might be high. This is due to non-uniformities in the non-woven reinforcement itself. Some areas in the mat have more fibers than others. Therefore, there is a direct influence of the natural fiber mat structure on the fiber volume fraction in composite materials. Obviously non-uniform properties of the fiber mat result in the variation of fiber volume fraction in a composite. In order to estimate the variation of the fiber volume fraction in a composite material it is necessary to analyze the structure of its reinforcement.

3.2 Heterogeneity investigation technique

3.2.1 Materials

A non-woven natural fiber mat is usually produced by a process of compaction and needling of carded layers of natural fibers. During that process fibers interweave with each other in stochastic way and form a mat. Natural fibers are bound together in the form of bundles. Since natural fibers have different properties (length, diameter and surface quality), they interact with each other in unique manner which leads to the variation in interweaving process from one fiber bundle to another. This forms a mat which consists of fiber clusters with various amounts of fibers in them. It is suggested that fiber clusters can be characterized by two parameters: **size and intensity**. Thus, linear dimensions of cluster can be considered as the **size**, where as the amount of fibers in a cluster can be considered as **intensity**. The clusters with different size and intensity are stochastically distributed along the mat, resulting in heterogeneous structure. **Size and intensity of clusters can be considered as heterogeneity parameters**. It is important to notice that the heterogeneity parameters of mats, produced from different fibers are not the same due to diverse properties of the fibers. Moreover the mat production technology also has even greater effect on the heterogeneity parameters of mats.

A special procedure is needed in order to estimate heterogeneity parameters of the non-uniform materials. The estimated properties can be used further for the simulation of structures with heterogeneous materials. The procedure should be suitable to estimate the heterogeneity properties of the non-impregnated fiber mat (if one available) as well as composite material (thus applicable to evaluate heterogeneity of final structures). The ability to estimate the heterogeneity properties of a final composite material gives the possibility to

study the composite materials, which are not based on non-woven fiber mats but have randomly distributed fibers. Injection molded and long fiber thermoplastics (LFT) composites are examples of such composite material.

Four different types of non-woven fiber mats have been chosen for the analysis of their structure. Three of them were made from natural fibers (Flax, Duralin® Flax and Coir), the fourth mat was made from randomly distributed chopped short (20 mm) glass fibers. Such set of fiber types was chosen in order to study the influence of different fibers and production techniques on mats' structure. The first two mats both made of flax fibers, but derived by using different fiber extraction techniques, which might have an effect. The first flax fibers were extracted from a flax plant by using dew-retting technology, while the Duralin® flax fibers were extracted by using novel Duralin® process. The third mat has been made from Coir fibers. The properties of the Coir fibers are rather different from the flax fibers. They are much thicker than flax fibers. Thus, the Coir mat properties are expected to be different from flax fiber mat. The non-woven glass fiber mat was chosen in order to ensure the developed analysis technique is suitable for synthetic fiber mats as well. All fiber mats were supplied by industry.

3.2.2 Digital image processing

A digital image can be used in order to estimate the heterogeneity parameters of non-woven fiber mats or composites reinforced with non-woven fiber mats. The digital image can be obtained using several techniques:

- a) Optical scanning;
- b) X-ray photography;
- c) Ultrasonic technique.

The applicability of optical scanning is very limited, since the light intensity emitted by cold cathode lamps (used in scanners) is very low. Low intensity causes a poor light penetration through the material thickness. Thus it is suitable only for studying thin non-impregnated fiber mats. But there is a great advantage of this technique because it does not require complex equipment. Scanners with optical resolution of 600dpi or more are applicable. In order to use this method the reinforcement not impregnated with the resin should be available. Due to this there is a chance that the property of the final material (i.e. after impregnation of reinforcement with resin or subsequent component molding) will be different from that initially determined.

The X-ray photography is the best method to use. The penetrating abilities of X-rays is high, therefore it can be used for any materials: fiber mats as well as final composite specimens or even ready components. The quality of the derived images is very high. Hence a complex equipment is required. After the X-ray images (usually on wide format film) are obtained it is necessary to transform them into digital form by means of scanning. A regular desktop scanner with slide-module adapter can be used for that purpose. The scanning resolution should be 600 dpi or higher.

The application of ultrasonic techniques is also accompanied by the usage of sophisticated equipment. This method works only with finished composite material. The quality of the image might be the poorer than that of the two previous techniques due to a larger size of the receiver sensors. The image can be obtained directly in the digital form, therefore scanning is not necessary.

Since non-impregnated fiber mats were available for investigation the optical scanning technique has been chosen. An ordinary desktop scanner with maximum optical resolution 1200x1200 dpi has been used. Scanning of the mats was performed at maximum scanner resolution in grayscale mode with 256 gradations (8-bit mode). Pieces of fiber mats with dimension at least 100 x 100 mm were placed into scanner one by one. Non-woven fiber mat is a dense structure and during scanning the image appeared to be very dark, since the light from the lamp of the scanner has to pass through the mat twice. This causes a small range of brightness between the completely translucent and completely non-translucent parts in the image. This characteristic is called optical density. In order to extend

optical density of the image it is necessary to apply additional external source of light during scanning (see the scheme in Fig. 3.1). A regular desktop daylight lamp is suitable for that purpose. The shape of the lamp is rectangular and gives more or less uniform light on large area (in comparison to incandescent lamp). One more important parameter of daylight lamp is its low temperature. This allows attaching the lamp closer to the fiber mat without overheating the fibers and mechanisms of the scanner.

The resulting image is much better than without a lamp, but further image improvements are still necessary. The improvements can be made by using a raster image editing software, like Adobe Photoshop®, for example. It has a large set of tools to work with raster images. In particular the histogram of the images should be stretched in order to use the full range of brightness levels (256 levels in 8-bit grayscale scanning mode). This procedure is called “level-correction” and it is depicted in Fig. 3.2. Further, the image inversion should be performed in order to put in correspondence the brightness of pixels in the image and the amount of fibers in the mat. Thus, the areas in a mat with small quantity of fibers should correspond to a lower brightness of pixels and therefore should be black in the image and vice versa. The fragments of the digital images of fiber mats after the improvement and the inversion are presented in Fig. 3.3. It should be noted that a better image quality can be obtained by using higher scanning resolution accompanied with 16-bit grayscale mode.

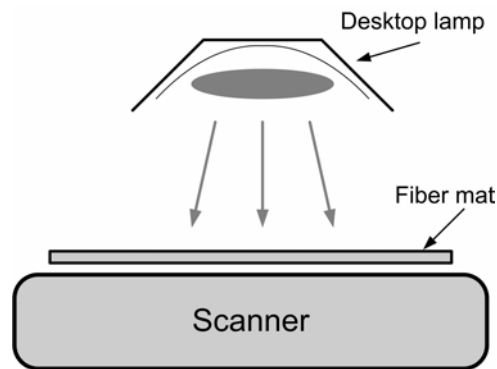


Figure 3.1 Scanning technique with applied back light.

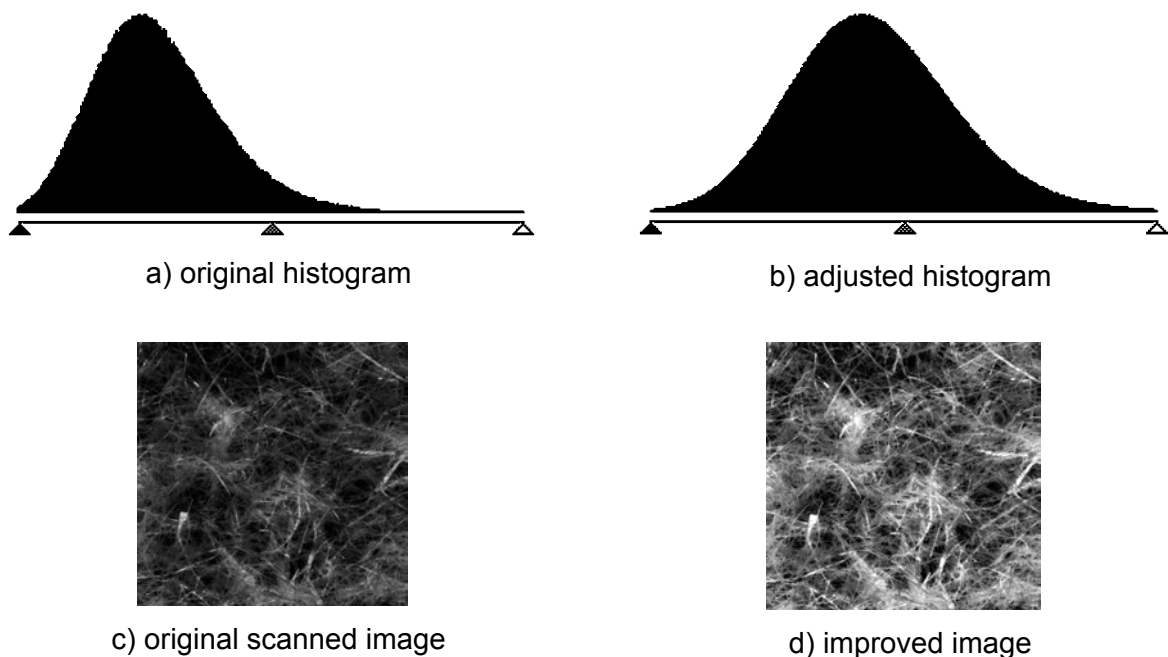


Figure 3.2 Improvement of image via histogram stretching.

X-ray investigations of some of natural fiber composites are performed along with optical scanning. Several wide format films were obtained as a result of X-raying of composites. Each film was scanned using a scanner with slide module adapter at the resolution of 1200 dpi in 16-bit grayscale mode (due to very high optical density of films). The correction of scanned image (similar to described above) has been performed in Adobe Photoshop®. The digitized images of X-ray films for some natural fiber reinforced composites are presented in Fig. 3.4. The similarity of the optically scanned flax fiber mats and X-rayed flax fiber composite can be observed.

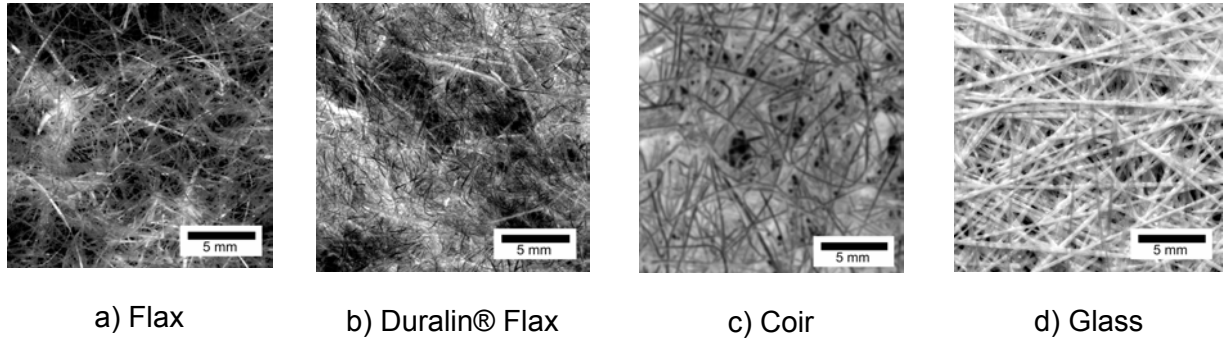


Figure 3.3 Fragments of digital images of different fiber mats.

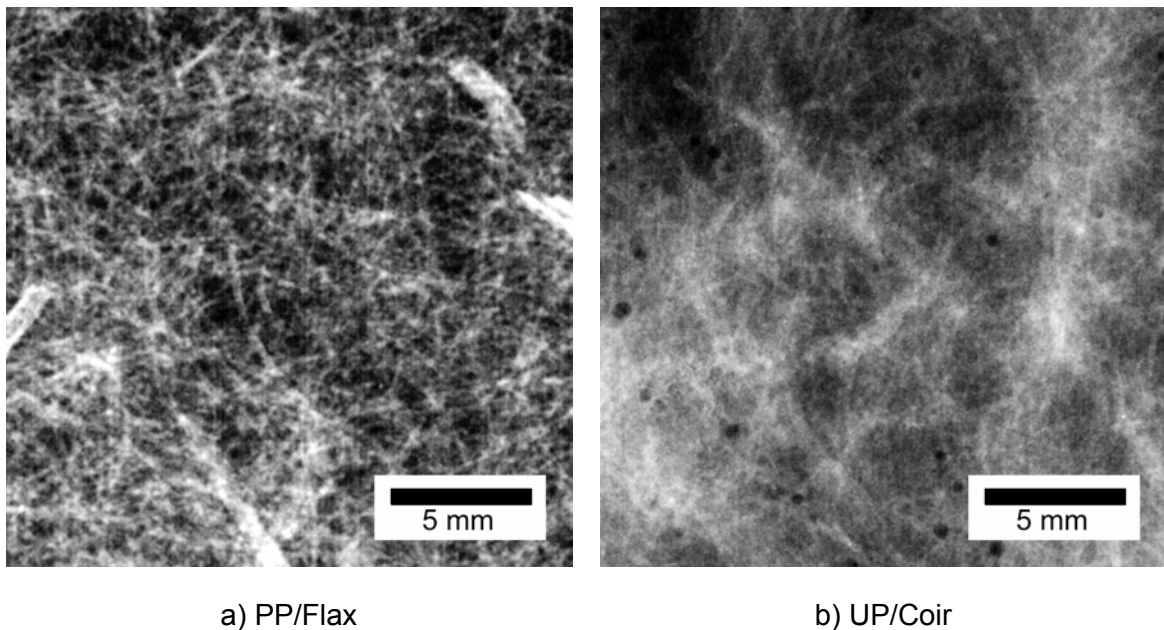


Figure 3.4 Fragments of digitized X-ray images of different natural fiber composites.

3.2.3 Spectral analysis

A closer look at the images of fiber mats confirms that the distribution of fibers in mats is not uniform (see Fig. 3.5). All fiber mats are heterogeneous, at least on mesoscale. The shape and intensity of fiber clusters should be estimated in order to evaluate the heterogeneity of each mat.

There are number of techniques to perform the analysis of the existing images. The chosen technique should be capable to work with grayscale images. The integral brightness (optical density) of the images is different. Therefore the technique should be invariant to this

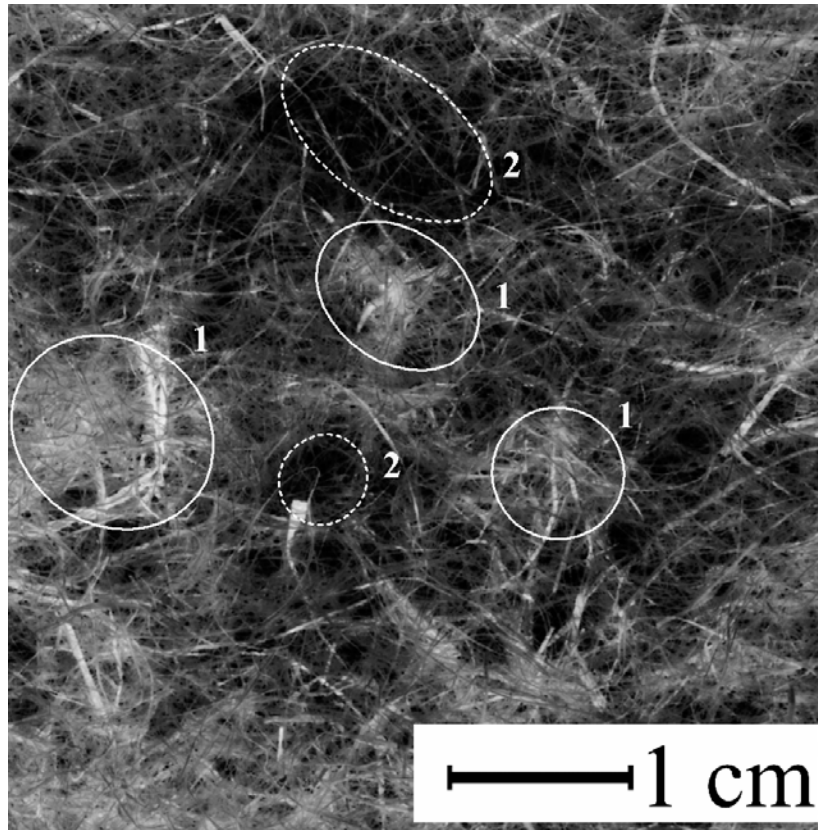


Figure 3.5 Fragment of scanned image of flax fiber mat with indication of clusters (1) and voids (2).

characteristic. Most of the techniques, which meet the mentioned criteria, are based on methods of photogrammetry. They require either special commercial software or complex programming, if commercial software is not available. However, there are other methods which are simple and reliable, for example, spectral analysis. This method is capable to decompose the complex data series into simple components. Brightness series taken from images can be used as an input for spectral analysis.

The spectrum of brightness series can be calculated in the same way as for time series. The linear coordinate along the excerpt line in this case corresponding to the time and the brightness of the pixels is a variable. The spectral analysis is known as harmonic analysis or frequency approach to time series analysis [150]. Suppose that a series X_t , contains a periodic (cyclic) component. A natural model of the periodic component would be:

$$X_t = R \cos(ft + d) + e_t, \quad (3.1)$$

where R – amplitude of the component; f – frequency of the periodic component, measured in number of radians per unit time; d – phase; e_t – random error (noise) of the series about the periodic component; t – the time period number.

Since $\cos(ft + d) = \cos(ft)\cos(d) - \sin(ft)\sin(d)$, the Eq. 3.1 can be written as follows:

$$X_t = a \cos(ft) + b \sin(ft) + e_t, \quad (3.2)$$

where $a = R \cos(d)$ and $b = -R \sin(d)$.

This model is a multiple regression model with two independent variables. In this case, the independent variables are $X_1 = \cos(ft)$ and $X_2 = \sin(ft)$. The regression

coefficients are $B_1 = a$ and $B_2 = b$. In other words, the variation in a time series may be modeled as the sum of several different individual waves occurring at different frequencies.

The generalization of the model Eq. 3.1 to the sum of n frequencies may be written as follows:

$$X_t = \sum_{i=1}^n R_i \cos(f_i t + d_i) + e_t \quad (3.3)$$

or, using the alternative form Eq. 3.2, as follows:

$$X_t = \sum_{i=1}^n (A_i \cos(f_i t) + B_i \sin(f_i t)) + e_t, \quad (3.4)$$

where A_i and B_i – the regression coefficients to be estimated; i – number of frequency.

This is an example of a harmonic regression. After performing the analysis we get a table of frequencies with A_i and B_i coefficients corresponding to particular frequencies. A spectrogram is the common way to visualize the results. The equation to estimate spectrum is as follows:

$$S_i = \frac{N}{2} (A_i^2 + B_i^2), \quad (3.5)$$

where N – the length of the series [150].

In general, the spectrum S_i can be plotted vs. frequency f or vs. wavelength $\lambda = 2\pi/f$. The spectrum plotted vs. wavelengths will be used because the frequencies which are present in the brightness series are expected to be mostly in the range of low frequencies and therefore can be better visualized.

3.2.4 Excerpts

The structure of a fiber mat image is complex and it contains information about the fiber clusters size and intensity. Therefore the brightness of the image can be used as an input for a spectral analysis. Since simple spectral analysis uses one dimensional data series (image is two dimensional) it is necessary to derive that information from images. The excerpts were employed as an input data for the analysis of images.

The excerpt is a series of pixels' brightness along the line drawn in the image. Several excerpts (up to 7...15), with equal lengths were randomly chosen (see white lines in Fig. 3.6) in each image. The minimum length of the excerpts has been estimated beforehand. The excerpt with the length of 2000 pixels (approx. 42 mm) is enough to contain at least one visible large fiber cluster. An example of brightness series of an excerpt is presented in Fig. 3.7.

3.2.5 Analysis of spectrograms

A well-known NCSS statistical analysis & data analysis package the product of NCSS Statistical Software Company has been used to perform spectral analysis. The brightness series of each excerpt was taken as input data series for the analysis. An example of a spectrogram for one of the excerpts is presented in Fig. 3.8.

The spectrogram consists of harmonics, which are present in the brightness series of an excerpt. The spectrum of excerpts is quite complex and consists of large number of humps (see Fig. 3.8). The humps on the spectrum consist of number of harmonics. Each harmonic is characterized by a wavelength (or frequency), amplitude and phase. The peaks of the humps represent the most probable harmonics which exist in the brightness pattern of excerpts. The tails at both sides of each peak represent the scatter of harmonics wavelengths.

Since the brightness pattern of an excerpt contains information about the fiber clusters in a mat the spectrum of such excerpt contains decomposed information about fiber clusters. This allows assuming that harmonics in spectrum with different wavelength represent the size of fiber clusters and the amplitude of the harmonics represents the intensity of the fiber clusters.

The analysis of spectrums of different excerpts showed the similarity in the harmonics which belong to major humps. Therefore it is possible to subdivide the whole range of harmonics into several groups. The groups were formed according to the wavelengths of the harmonics (see Fig. 3.8). The depressions in spectrum were used as separators between groups. The harmonics, which are at the peaks of the humps, are considered the most probable for a certain group.

The obtained images of fiber mats have quite high resolution; thus, even information about fibers' sizes is presented in a spectrum of excerpts by a bunch of corresponding harmonics with short wavelengths up to 0.2 mm (diameter of the fibers). This results in a large number of peaks in the spectrums, but it is not necessary to process all of them. Since the scope of the fiber mat analysis is to determine meso-scale heterogeneity (~3...30 mm) it is possible to neglect some of the harmonics with wavelengths shorter than ~3 mm.

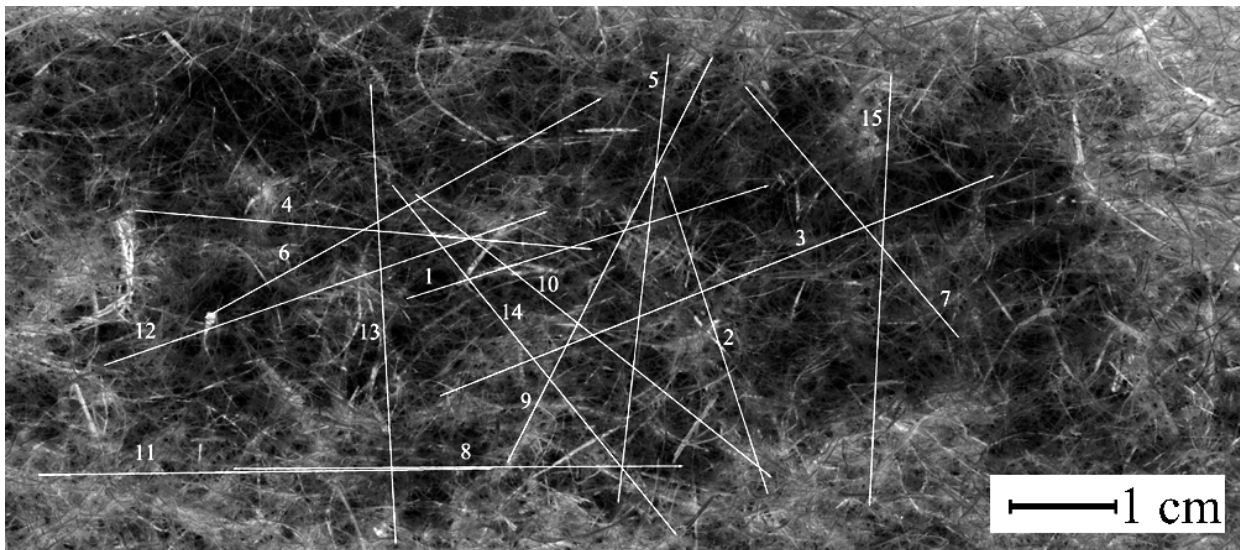


Figure 3.6 Fragment of the digitized image of Flax fiber mat with indication of excerpts locations.

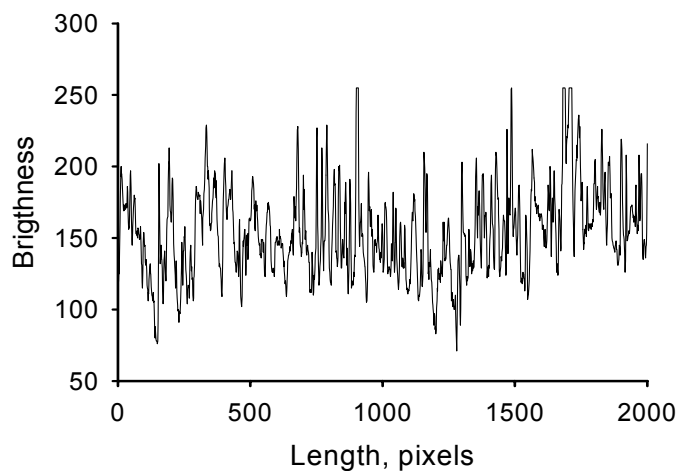


Figure 3.7 Example of brightness distribution along linear excerpt.

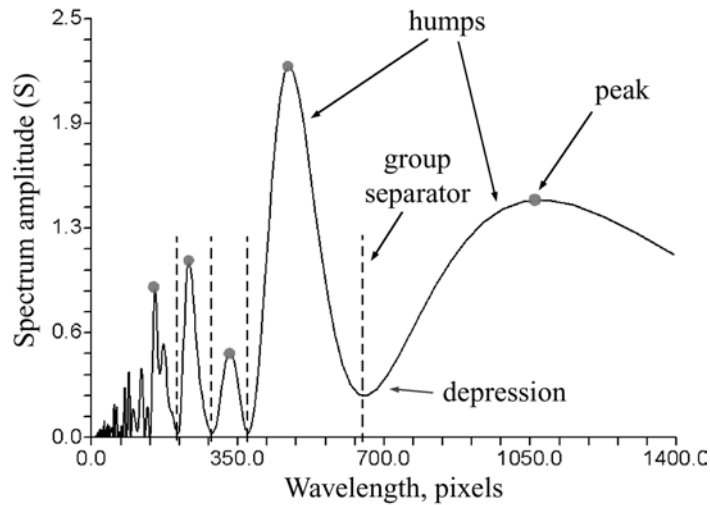


Figure 3.8 Example of spectrogram.

Consider the lower bound of the harmonics wavelength is limited to 130 pixels (see Fig. 3.8). This limit corresponds to the fiber clusters' size of about ~5 mm. Those harmonics present in spectrum with the wavelengths less than this limit are neglected. Up to 5 most probable harmonics (at peaks in spectrum) from each excerpt were taken into consideration.

Each harmonic has its own amplitude, which determines the significance of a particular harmonic in forming the mat's heterogeneity. Higher harmonic amplitude means a higher variation in the image brightness or, in other words, higher variation of amount of fibers in the clusters (which excerpt passes through). Thus, the harmonic amplitude determines the second important parameter of heterogeneity - fiber cluster intensity.

For a limited number of harmonics within one excerpt it is possible to normalize their amplitudes in order to simplify their further analysis. The following equation can be used for that purpose:

$$A_i = \frac{S_i}{\sum_{i=1}^n S_i} \quad (3.6)$$

were A_i - the amplitude of the i -th harmonic, S_i - the spectrum of the i -th harmonic and n - the number of harmonics determined in one excerpt. After such normalization the amplitudes of harmonics within one excerpt are in range from 0 to 1, which makes them easy to analyze. The parameters of excerpts for flax mat are presented in Table 3.1. Graphically the determined harmonic wavelengths of excerpts are presented in Fig. 3.9.

In each excerpts the set of harmonic wavelengths was analyzed in order to highlight the common behavior of the excerpts. Visually it is possible to find out some similarity between the parameters of harmonics of a different order. In the graph (see Fig. 3.9) there are the so-called first-order harmonics with the wavelengths in the range of 760 – 1154 pixels, second-order harmonics with the wavelengths in the range of 450 – 700 pixels, third-order harmonics with the wavelengths in the range of 300 – 420 pixels, fourth-order harmonics with the wavelengths in the range of 200 – 300 pixels and fifth-order harmonics with the wavelengths in the range of 130 – 200 pixels (see Fig. 3.9). The difference in harmonic wavelengths between excerpts can be explained. Obviously there are no fiber clusters with the same parameters present in a mat, they have quite complex shapes and their sizes are different. Therefore, even if two different excerpts are passed through the

same cluster in different directions they will contain different information about the same cluster. This explains the difference in sets of harmonic wavelengths between excerpts.

Thus, harmonics within the defined limits have been processed for each excerpt for each fiber mat. After that several most probable harmonics for each excerpt were determined. There is similarity in harmonic wavelengths in those excerpts taken from the same fiber mat, so there is difference in harmonic amplitudes. Unfortunately each excerpt has a unique set of harmonic amplitudes. This makes it difficult to determine the parameters of a fiber mat heterogeneity, since there is no obvious similarity between the excerpts. In order to resolve this problem a representative excerpt for each fiber mat should be chosen.

Table 3.1 Parameters of excerpts for non-woven flax fiber mat.

Harmonics at peaks	Excerpt 1		Excerpt 2		Excerpt 3		Excerpt 4	
	Wave, pixels	Amplitude (normalized)						
1	1091.31	0.23	1154.2	0.54	1034.91	0.19	857.63	0.31
2	472.87	0.36	422.94	0.07	461.97	0.19	600.48	0.06
3	331.84	0.08	292.99	0.11	349.19	0.13	432.07	0.26
4	234.64	0.17	197.60	0.12	280.68	0.21	255.60	0.20
5	152.47	0.15	136.84	0.15	190.10	0.28	157.26	0.17

Harmonics at peaks	Excerpt 5		Excerpt 6		Excerpt 7	
	Wave, pixels	Amplitude (normalized)	Wave, pixels	Amplitude (normalized)	Wave, pixels	Amplitude (normalized)
1	937.96	0.18			759.99	0.41
2	682.31	0.18	619.04	0.41	484.31	0.33
3	361.81	0.23				
4	226.67	0.32	293.00	0.22	203.62	0.07
5	138.74	0.07	207.85	0.37	145.86	0.20

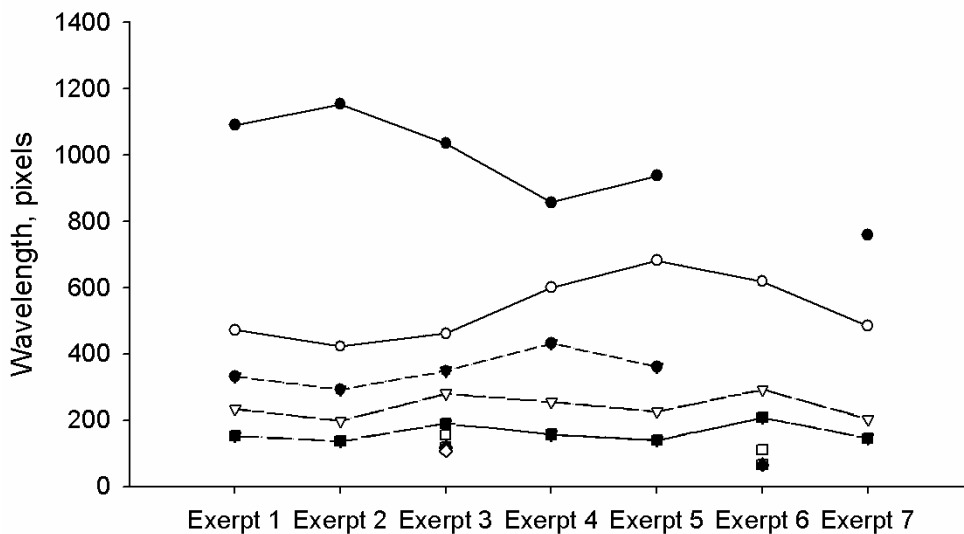


Figure 3.9 Wavelengths of excerpts for flax fiber mat.

3.2.6 Representative excerpt

A correlation technique can be employed in order to determine the representative excerpt. The characterization of excerpts involves a few parameters (up to 5 harmonics, where each of harmonic has wavelength and amplitude); using this technique is essential since it helps to estimate the similarity between two or more variables. Correlation coefficient is the measure of similarity of two excerpts containing several variables (amplitudes in this case). If it is necessary to compare more than two excerpts a correlation matrix will be built. The harmonic amplitudes of all excerpts, taken from flax fiber mat, were analyzed. A correlation matrix for Flax fiber mat is presented in Table 3.2 as an example. It is obvious that large correlation coefficient (up to 1) shows higher similarity between the excerpts.

Table 3.2 Example of correlation matrix for amplitudes for flax fiber mat.

	Excerpt 1	Excerpt 2	Excerpt 3	Excerpt 4	Excerpt 5	Excerpt 6	Excerpt 7
Excerpt 1	1	0.49	-0.12	0.43	0.58	0.18	0.86
Excerpt 2	0.49	1	-0.12	0.80	0.37	-0.43	0.76
Excerpt 3	-0.12	-0.12	1	-0.30	-0.49	0.74	0.03
Excerpt 4	0.43	0.80	-0.30	1	0.67	-0.49	0.46
Excerpt 5	0.58	0.37	-0.49	0.67	1	-0.29	0.27
Excerpt 6	0.18	-0.43	0.74	-0.49	-0.29	1	0.05
Excerpt 7	0.86	0.76	0.03	0.46	0.27	0.05	1
Sum	3.42	2.87	0.74	2.57	2.11	0.76	3.43

The sum of correlation coefficients for each excerpt is calculated in order to determine the excerpt which parameters are similar to those of the other excerpts. The excerpt with the maximum sum of coefficients can be taken as a representative. In this example Table 3.2 excerpts 1 and 7 can be considered as representative for Flax fiber mat.

The harmonic amplitudes of chosen excerpt are considered as representative for a particular fiber mat. They characterize the intensities of fiber clusters with certain size. Since all fiber clusters a mat have different size and intensity the distribution of these parameters is stochastic and, therefore, can be correlated to Gaussian (normal) distribution. Thus, parameters of the representative excerpt can be taken as mean values. The standard deviation value can be determined using all other excerpts. The wavelength and amplitude of the determined harmonics can be easily correlated to physical parameters (size and intensity) of fiber clusters present in a mat. The mean values of size and intensity for each harmonic are equal to those determined for the representative excerpt only. But the standard deviation of size and intensity is calculated by using those parameters determined for all excerpts.

The harmonic wavelengths in the spectrograms are determined in pixels. Hence in order to determine this parameter in millimeters the following equations can be used:

$$L = \frac{L_p}{N_s} K, \quad (3.7)$$

where L – the cluster size (in mm); L_p – the wavelength of harmonic (in pixels); N_s – the length of data series (number of data points in the excerpt); K – the scale parameter (in mm), which can be estimated as follows:

$$K = L_e \cdot R, \quad (3.8)$$

where L_e – the physical length of the excerpt line (in pixels); R – the resolution parameter (in mm/pixels), which can be estimated as follows:

$$R = \frac{1(\text{inch})}{1200\left(\frac{\text{pixel}}{\text{inch}}\right)} = \frac{25,4(\text{mm})}{1200\left(\frac{\text{pixel}}{\text{inch}}\right)} = 0.021167\left(\frac{\text{mm}}{\text{pixel}}\right). \quad (3.9)$$

The procedure of determination of the representative excerpt has been performed for each fiber mat. The determined mat characteristics are presented in Table 3.3. These parameters can be used further for simulation of heterogeneous properties of composites reinforced with randomly distributed fibers.

Table 3.3 Parameters of clusters for some non-woven fiber mats.

Fiber mats	Harmonics	Size (St. dev) , mm	Intensity, normalized (St. dev)
Flax	1	23.43 (3.87)	0.23 (0.14)
	2	13.57 (1.81)	0.36 (0.14)
	3	9.10 (1.45)	0.08 (0.07)
	4	5.91 (0.67)	0.17 (0.12)
	5	3.8 (0.91)	0.15 (0.11)
Duralin® Flax	1	25.41 (2.39)	0.24 (0.27)
	2	14.57 (2.15)	0.09 (0.23)
	3	8.61 (1.56)	0.21 (0.20)
	4	5.53 (0.52)	0.15 (0.14)
	5	3.10 (0.65)	0.31 (0.08)
Coir	1	32.8 (3.08)	0.30 (0.09)
	2	15.73 (2.59)	0.02 (0.09)
	3	9.32 (2.17)	0.31 (0.14)
	4	5.62 (0.91)	0.24 (0.05)
	5	0.39 (0.74)	0.13 (0.07)
Glass	1	23.00 (5.59)	0.09 (0.13)
	2	13.7 (1.51)	0.41 (0.13)
	3	8.86 (1.89)	0.08 (0.17)
	4	5.55 (0.67)	0.21 (0.11)
	5	3.92 (0.45)	0.20 (0.10)

3.3 Conclusions

The basis of the high non-uniformity of mechanical properties of natural fiber reinforced composites was discussed in this chapter. It was shown that certain non-uniformity can appear on different scales. All natural fibers are different in the micro-scale due to natural scatter. Their mechanical properties and surface quality vary. The fibers are processed into non-woven natural fiber mats before being impregnated with resin. The non-uniformity of the natural fiber mats characterizes the mesoscale properties variation. Sometimes it is very high due to different abilities of the fibers to interweave with each other during the mat production process. The fiber clusters with different size and intensity are stochastically distributed in a mat. Size and intensity are the parameters of fiber clusters and they can be used to characterize the heterogeneity of fiber mat.

A technique has been developed in order to determine the parameters of fiber clusters in non-woven fiber mats. The technique is based on the digital image of fiber mats. The image can be obtained, as suggested, using optical scanning, X-ray photography or ultrasonic methods. The X-ray is preferable. The suggested technique should be invariant to optical density of the digital image which might appear due to its high variability from one fiber mat to another. Spectral analysis is successfully applied for that purpose. Using this method the decomposition of a complex structure of the image into simple basic components (harmonics) has been done.

The parameters of harmonics in spectrum are correlated to certain physical parameters of fiber clusters. Thus, the wavelength of harmonic determines the size of a cluster and the amplitude of harmonic determines its intensity. It is determined that the set of representative harmonics can be highlighted in each fiber mat. The set consists of several harmonics with different parameters. This allows to characterize the difference in heterogeneity of different fiber mats.

The derived parameters can be used both for modeling heterogeneous materials as well as for planning experiments. The estimation of geometrical parameters of the specimens in order to avoid the influence of a size-effect on the results is essential when working with such heterogeneous materials. It was shown that the developed technique is suitable for natural and synthetic fiber non-woven mats. This gives the possibility to characterize almost any type of composites with heterogeneous reinforcement.

Chapter 4

Simulation of the mechanical properties of composites

4.1. Introduction

Heterogeneity by definition can represent variation in physical, mechanical, acoustical or other material properties. Various material properties can be put into correspondence with the generated heterogeneity. Since mechanically loaded natural fiber composites are under consideration here it is reasonable to choose one of the mechanical properties of a material to vary according to the generated heterogeneity.

The variation of the amount of fibers in a natural fiber composite has been analyzed in Chapter 3 and the results of the analysis were used to develop the technique describing that variation. Therefore this characteristic can be successfully chosen to correlate with the mechanical properties of composite. The amount of fibers is one of the most important characteristics of any composite material since their mechanical properties are strongly dependent on it. The amount of fibers in a composite material can be characterized either by the volume fraction or by weight fraction of fibers. One of these parameters (its average value, of course) is usually available in specifications of any composite, together with fiber type, fiber distribution and resin type. The volume fraction value can be recalculated into weight fraction using the following equations [221]:

$$V_i = \frac{W_i / \rho_i}{\sum_i W_i / \rho_i}, \quad (4.1)$$

where V_i - volume fraction, W_i - weight fraction and ρ_i - density of i -th component.

Composite producers generally use the weight fraction value since during production they operate with mass quantities of fibers and resins. But the volume fraction value is used by mechanical engineers to estimate the mechanical properties of the composite material and to perform the engineering design of structures. Therefore, only the volume fraction value will be considered further.

The volume fraction of fibers is commonly used to estimate certain mechanical properties of the composite material. Besides, the type of fibers distribution (aligned or random) and their mechanical properties as well as properties of resin should be available. The modulus of elasticity and strength can be considered as the most significant mechanical properties of materials required for engineering design of structures. These properties of composite materials in particular, depend on many parameters, the most important of which are:

- a) fiber type;
- b) resin type;
- c) volume fraction of fibers;
- d) fibers length;
- e) fibers distribution;
- f) adhesive properties between fibers and resin
etc.

The fiber and resin types, fiber volume fraction, the length and distribution of fiber are commonly used to estimate the modulus of elasticity or strength of a composite material [221]. The rest of the mentioned parameters can be regarded not as variables but as constants in modulus of composite estimation. In this work it is rather important to find an existing or to develop a new reliable method for elastic modulus estimation of composites

material with the known properties of fibers, matrix and fiber volume fraction. Composites with randomly oriented natural fibers are considered.

4.2 Existing models for Young's modulus estimation

Several methods are available, but due to the complexity of the natural fiber composites not every method is suitable. It is necessary to perform comparison of the methods in order to determine the best. In general the existing methods can be divided into two groups. The first and major group of the methods is based on theories which take into account basic properties of fibers (including length) and the resin and their mixing conditions:

- 1) The rule of mixtures (RoM) [200];
- 2) Cox's model (modified rule of mixtures) [34];
- 3) Halpin-Tsai's model [65, 66];
- 4) Hirsch's model [70].

The other group of methods is based on micromechanics of fibers and resin polymer interaction [22, 32, 48, 69]. Let us review some of the methods.

4.2.1 The rule of mixtures

The rule of mixtures (RoM) is the most popular method to estimate the modulus of elasticity and the strength of unidirectional composite material. This method was developed a long time ago and has been successfully used for composite materials with long unidirectional synthetic fibers. The standard representation of the rule of mixtures is the following:

$$E_c = V_f E_f + (1 - V_f) E_m \quad \text{- parallel model,} \quad (4.2)$$

$$E_c = \frac{1}{\frac{V_f}{E_f} + \frac{(1 - V_f)}{E_m}} \quad \text{- series model,} \quad (4.3)$$

where E_c is the elastic modulus of a composite, V_f is the fiber volume fraction, E_f is the elastic modulus of fibers, and E_m is the elastic modulus of matrix.

The modified representation of the RoM which was adopted to estimate the modulus of elasticity of a composite material with long randomly distributed fibers is as follows:

$$E_c = \eta V_f E_f + (1 - V_f) E_m. \quad (4.4)$$

It takes into account the weakening of the composite due to fibers orientation and fiber length factors through introduced additional coefficient, $\eta < 1$. Some attempts by other researchers have been done in order to estimate η . For example, in [230] it is suggested to apply $\eta = 0.2$ for a composite reinforced with randomly oriented natural fibers.

4.2.2 Cox's model

The Cox shear lag theory [34] adds to the RoM the shear lag analysis, which includes a fiber length and a stress concentration rate at the fiber's ends. The model is described by Eq. 4.4, in which the coefficient η is written as follows:

$$\eta = 1 - \frac{\tanh\left(\frac{\beta l}{2}\right)}{\left(\frac{\beta l}{2}\right)}, \quad (4.5)$$

where l is the length of fibers and β is the coefficient of stress concentration rate at the ends of the fibers, which can be described by the following equation:

$$\beta = \frac{l}{r} \sqrt{\frac{E_m}{E_f(1+\nu) \ln \sqrt{\frac{\pi}{4V_f}}}}, \quad (4.6)$$

where ν is Poisson's ratio of fibers and r is the fiber radius.

4.2.3 Halpin-Tsai's model

This model was developed to estimate the elastic modulus of a composite material with aligned short fibers [65, 66]. Its representation is as follows:

$$E_c = E_m \frac{1 + ABV_f}{1 - BV_f}, \quad (4.7)$$

where, $A = \frac{2l}{d}$ is the aspect ratio of fibers that can be considered here not only as a measure of fiber geometry but also as a characteristic of fiber loading conditions, d is the diameter of fibers, and $B = \frac{E_f/E_m - 1}{E_f/E_m + A}$.

4.2.4 Hirsch's model

Hirsch developed the model for the elastic modulus prediction of a composite material, which is a weighted combination of RoM parallel and series models [70]. Indeed, the natural fiber reinforced composite, where the embedded fibers are usually in a random mat form, can be represented as the combination of parallel and series loaded fibers. The representation of Hirsch's model is as follows:

$$E_c = x[V_f E_f + (1 - V_f)E_m] + (1 - x) \left[\frac{1}{V_f/E_f + (1 - V_f)/E_m} \right], \quad (4.8)$$

where x is the empirical coefficient. It is assumed that the controlling factors for x are mainly the fiber orientation, fiber length and stress amplification at fiber ends.

4.2.5 Models based on micromechanics of materials

One of the models within the group of models based on micromechanics is the aggregate model. This model uses the concept of subunits (unit cells). Each of these units possesses the elastic properties of the composite in which the fibers are continuously and fully aligned. Usually it is applicable to polymer composites reinforced with unidirectional synthetic fibers. The interpolative aggregate model, which is discussed in [212], was simplified and adopted to short-fiber reinforced composites. A formal equation for this model is as follows:

$$\{C\} = [F][R] \begin{Bmatrix} T \\ L \end{Bmatrix}, \quad (4.9)$$

where $\{C\}$ represents the stiffness of the composite (stiffness tensor); $[F]$ is the fiber orientation distribution (FOD) matrix; $[R]$ is the constant, essentially determined by Poisson's ratio of a unit cell; T and L are the transverse and longitudinal stiffness of a unit cell

incorporating constituent and interface properties, fiber aspect ratio, fiber volume fraction etc, but independent from the FOD.

The group of methods based on micromechanics is potentially applicable to the natural fiber reinforced composites, but the complexity of their construction and verification is a barrier for this application. As the aggregate model all other methods in this group require the FOD matrix data. There are some methods which determine the FOD and take into account a fiber length distribution (FLD) [22, 32, 48, 69]. However, due to the complexity of the FOD determination for randomly distributed natural fibers in composites in particular, this group of methods is less preferable than simpler methods. Simple models described above can be more successfully applicable for mechanical engineers. Therefore, it was decided not to consider the group of methods based on micromechanics, but models based on rule of mixtures.

4.3 Benchmarking of existing models

In order to perform benchmarking of models under consideration, it is necessary to analyze the experimental information on natural fiber composites. Here the experimental studies determining mechanical properties of natural fiber composites with known fiber and resin properties are considered. A large number of sources including literature, Internet sites, datasheets from companies and own experimental data are analyzed [89, 90].

It appears that the reported properties of natural fiber composites are quite diverse. Moreover, most of the reported studies do not contain all necessary characteristics of fibers and resins for the comparison. Therefore it is not possible to accept the found data as a reference. The systematization of the sources has been done. The available information has been arranged by type of resin, type of natural fibers and fiber volume fraction. Polypropylene (PP) is widely used as a matrix in composite materials due to good mechanical properties, low weight, low processing temperature (especially important for processing of natural fibers) and low price. Composites reinforced with various natural fibers embedded into PP matrix have been chosen as a case study. Three parameters of the composites material are under consideration: moduli of elasticity of fibers and matrix as well as fiber volume fraction.

The modulus of elasticity of natural fibers basically depends on the type of the natural fibers (flax, hemp, jute, etc.), but it can vary in a wide range even for the same types of fibers. Therefore the maximum, minimum and the average values are important. The modulus of elasticity of PP also varies (depending on manufacturer and processing conditions), but the range of this variation is small. Thus, only mean value is considered. The information collected is presented in Table 4.1.

Table 4.1 Values of modulus of elasticity for several types of natural fiber composites (randomly oriented fibers) and per component [89, 90].

Material	Modulus of elasticity				
	Fiber, GPa	Matrix, MPa	Composite, MPa		
			Min	Max	Average
PP / Flax 40%	48.8	1050	3290	6000	4645
PP / Hemp 40%	60.0	1050	n/a*	n/a*	n/a*
PP / Kenaf 40%	n/a*	1050	3550	3550	3550
PP / Jute 40%	37.5	1050	1480	3340	3960
PP / Sisal 40%	27.0	1050	1040	2060	1550

It is important to note, that the benchmarking of the theoretical models for composite modulus estimation can be performed under certain conditions. Two of three mentioned parameters (matrix modulus, fiber modulus and fiber volume fraction) should be fixed and one can be a variable. Since all the composites under research have the same PP matrix, the modulus of matrix is fixed. Therefore there are two possible approaches:

- 1) Fiber volume fraction is fixed and modulus of fibers is a variable;
- 2) Modulus of fibers is fixed and fiber volume fraction is a variable.

4.3.1 Approach 1

The first approach was used for primary benchmarking, since enough data on composites materials with different types of natural fibers and certain fiber volume fraction (40 % vol.) are available. The experimental and estimated values of the modulus for some natural fiber composites are presented in Fig. 4.1. In this graph the modulus of composites (with the same fiber volume fraction) is plotted against the modulus of fibers. The experimental data of PP/Flax 40%, PP/Jute 40% and PP/Sisal 40% composites with randomly oriented fibers found in literature are plotted with black dots and error bars. For each composite the averaged experimental values are used as input parameters in the theoretical models. The theoretically predicted values are represented by different lines in that graph. These lines are based on data interpolation between reference (data) points.

In the presented graph (see Fig. 4.1) it is clear that the values estimated by the RoM models (Eq. 4.2 and 4.3) are quite different from the data that have been found in literature. The possible reason for poor prediction by the RoM models (Eq. 4.2 and 4.3) might be that it was initially developed for a continuous aligned fibers reinforced composite material. The distribution of fibers in non-woven natural fiber composites is far from aligned; moreover

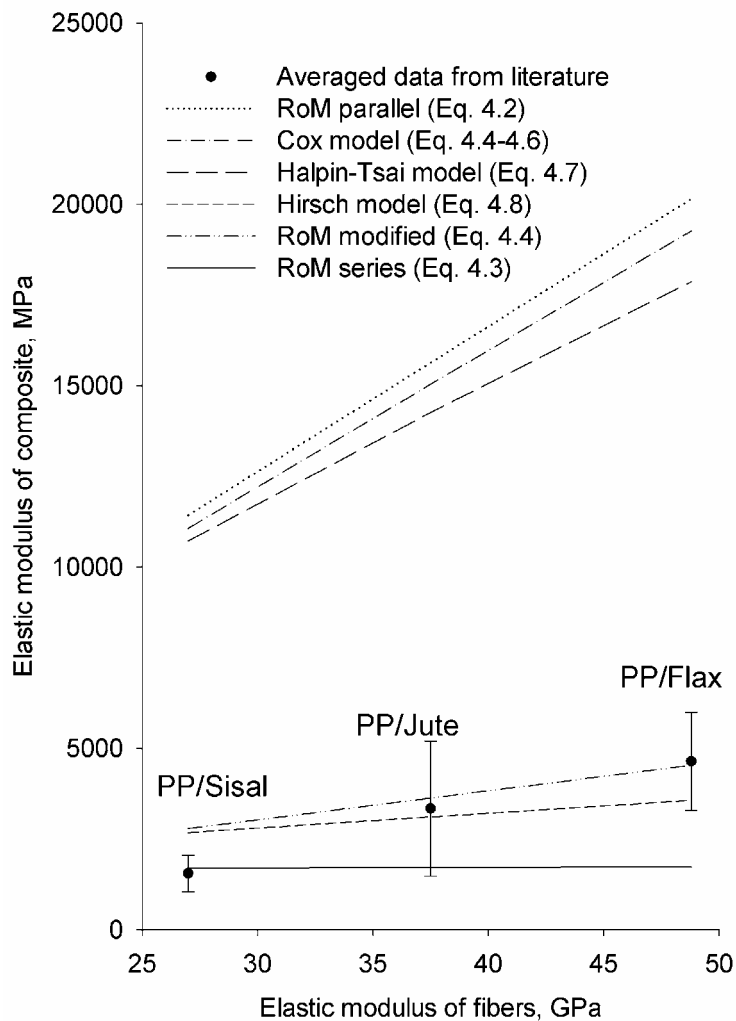


Figure 4.1 Estimated modulus of elasticity of composites using different theoretical models in comparison with experimentally obtained data for composites reinforced with 40 vol.% of fibers. (Error bars show the scatter of reference data).

The estimated values of modulus of composite using the modified model of the RoM model (Eq. 4.4) with $\eta = 0.2$ are quite close to those experimentally obtained, but the inclination of interpolation curve is, however, different. The error between the theoretically estimated modulus and experimental data is quite high for Sisal fiber reinforced composite. Taking into account a lack of sources of experimental studies on Sisal fiber composites the scatter in properties can be much larger. In this case it can occur that the theoretically estimated modulus of Sisal reinforced composite lies within that scatter. Considering the maximum observed error of 10% (between theoretically and experimentally estimated values) the modified RoM model, hence, can be used for limited types of natural fiber composites. As follows from the performance analysis, reliable estimation using Eq. 4.4 can be achieved for those composites in which the modulus of natural fibers are in range of about $E_f = 35 - 50$ GPa.

The moduli of elasticity were also estimated according to Cox's model (Eq. 4.4, 4.5, and 4.6). The values for Poisson's ratio and fibers geometrical parameters are: $\nu = 0.3$, $l = 20$ mm and $r = 0.1$ mm. Poisson's ratio and radius were averaged over the data from literature sources [6, 36, 89, 113]. A poor elastic modulus prediction (see Fig. 4.1) might be explained by the involved Poisson's ratio and fiber diameter in this model. The Poisson's ratio and fiber radius are extremely difficult measurable parameters for the natural fibers due to heterogeneity of their structure and may vary to a large extent. In the work of [82] a poor agreement of the predicted value of modulus based on Cox's model with the experimental results for composites reinforced with misaligned short Sisal fiber is registered.

The modulus of natural fiber PP-based composites has also been calculated using Halpin-Tsai's model (Eq. 4.7) with the aspect ratio $A = 200$. This value is based on $l = 20$ mm and $d = 0.2$ mm as a result of averaging the reference data [89]. Unfortunately, the agreement of theoretically estimated values with experimentally obtained is very poor. A possible explanation might be that this model was initially developed for composite materials with aligned fibers and does not take into account the bonding between fibers and matrix. However, for unidirectional Jute fiber reinforced composites with different volume fraction of fibers the model of Halpin-Tsai was successfully applied [11].

The estimated modulus of natural fiber composites under consideration using Hirsch's model (Eq. 4.8) is also plotted in Fig. 4.1. The estimated modulus is quite close to the obtained with modified RoM (Eq. 4.4). But the inclination of curve is even more different than the trend resulting from the experimentally obtained data. Thus, this model gives even less accurate result than modified RoM (Eq. 4.4). Actually, both models use the similar principle of accounting random fibers distribution. The principle is based on the insertion of an additional weakening coefficient (η – in RoM and x – in Hirsch's model) to the part of equation responsible for the strengthening of matrix material due to presence of fibers in it. In Hirsch's model such coefficient plays the role of weighting factor in both parts of the model: parallel and series. Usually, this coefficient is empirically estimated and less than the unity.

The results of the benchmarking by using the first approach showed that RoM (Eq. 4.4) and Hirsch's (Eq. 4.8) are the most promising to be applied for natural fiber composites. However, additional benchmarking of these models is necessary.

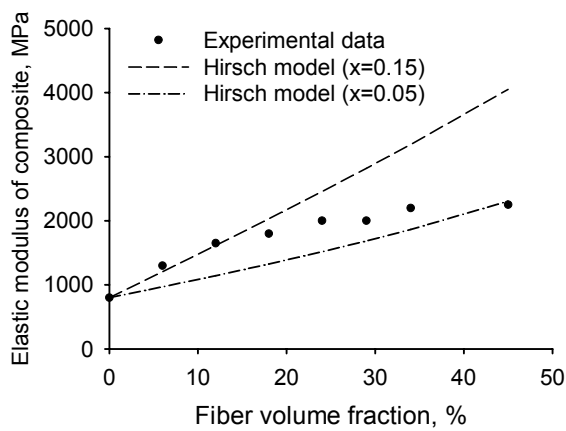
4.3.2 Approach 2

It was discussed in Chapter 2 that heterogeneity in natural fiber composites is associated with variation of fiber volume fraction. Thus, for successful application of the selected models their benchmarking using the second approach has to be performed. In this approach the moduli of fibers and matrix remain constant, while fiber volume fraction is varies. The most promising models from the previous benchmarking were chosen.

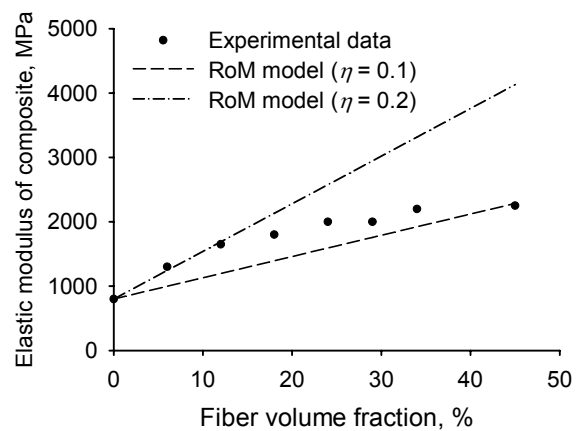
Experimental data on investigation of natural fiber composite properties with different fiber volume fraction used here for comparison was obtained in [11]. The experiments were carried out for composites reinforced with randomly distributed Jute fibers embedded

Table 4.2 Experimentally obtained modulus of PP/Jute composite reinforced with randomly oriented fibers with different fiber volume fraction, where $E_f=41$ GPa, $E_m=800$ MPa (after [11]).

Fiber volume fraction	Modulus of composite, MPa
0	800
0.06	1300
0.12	1650
0.18	1800
0.24	2000
0.29	2000
0.34	2200
0.45	2250



a) Hirsch's model (Eq. 4.8)



b) RoM model (Eq. 4.4)

Figure 4.2 Comparison of experimentally obtained (after [11]) and theoretically estimated modulus of PP/Jute composite reinforced with randomly oriented fibers.

into PP matrix for fiber volume fraction $V_f=0\dots45$ vol. %. The used experimental data are presented in Table 4.2.

Experimental data and theoretically estimated values for composite modulus using Hirsch's model (Eq. 4.8) are shown in Fig. 4.2a. Two curves represent the behavior of the model with different parameters x (see Eq. 4.8). The *min* and *max* values of x presented in that graph were adjusted such a way that the theoretical model overlaps at least in two points with the experimental data. The theoretical model with parameter $x=0.15$ has reasonable correlation with the experimental data only in a narrow range of fiber volume fraction $0 < V_f < 0.12$ (0 ... 12 vol. %). Beyond this range the theoretical model gives a large error and cannot be applied. With lower $x=0.05$ the curve has smaller inclination (relatively horizontal axis of the graph), but still the behavior of the curve is quite different from the experimental data.

Comparison of experimentally obtained and theoretically estimated modulus of the PP/Jute composite has been also performed using RoM model (Eq. 4.4). The graphs of the theoretical model with $\eta=0.1$ and $\eta=0.2$ are presented Fig. 4.2b. The good agreement with experimental data can be achieved with $\eta=0.2$, but only in quite narrow range of fiber volume fraction i.e. $0 < V_f < 0.12$ (thus in range of 0...12 vol. %). The behavior of the curve of this model is rather similar to that of Hirsch's model. This means that neither RoM model (Eq.

4.4) nor Hirsch's model (Eq. 4.8) can be used for estimation of the modulus of natural fiber composite with a wide range of fiber volume fraction at least $0 < V_f < 0.45$ (thus in range of 0...45 vol. %). Therefore, a new theoretical model is required in order to obtain a better correlation with experimental data at least within the specified range of fiber volume fraction.

4.4 Development and verification of a new model suitable for natural fiber composites

A new theoretical model of the modulus estimation for natural fiber composite is necessary, since the existing models (at least those found in literature) are not suitable. A new model should be able reliably estimate the modulus of composite with a different fiber volume fraction and with different elastic properties of fibers (with constant volume fraction) as well. The development of a new theoretical model from scratch is not reasonable, while one of the existing models can be used as the basis for a new model.

During the benchmarking of the existing theoretical models it was found that Hirsch's model (Eq. 4.8) and RoM model (Eq. 4.4) give the modulus estimation quite close to the experimentally obtained data. Therefore, the equations of these models can be used as a reference for the development of a new model. In composites with randomly distributed fibers there are fibers which are parallel, series and under an angle orientated to the chosen main direction. Unfortunately RoM model (Eq. 4.4) does not take into account the influence of fibers which have series orientation to the chosen main direction, because in its equation the series part is absent. Therefore the equation of this model has a linear behavior with respect to V_f variable which does not give enough flexibility to adjust the model's behavior to interpolate the non-linear trend of experimentally obtained data (see Fig. 4.2b). Hirsch's model (Eq. 4.8) in that sense seems to be more applicable, since it takes into account both parallel and series orientations of fibers. This model (Eq. 4.8) has two parts, which take into account different fiber orientations, but reflect this with only by one weight coefficient x . In order to increase flexibility to adjust the model it is necessary to introduce two independent weight coefficients instead of one. The following equation can be proposed:

$$E_c = \alpha[V_f E_f + (1 - V_f)E_m] + \beta \left[\frac{1}{V_f/E_f + (1 - V_f)/E_m} \right], \quad (4.10)$$

where α and β are the weight coefficients. These coefficients can be independently adjusted to reach the desired convergence with the experimentally obtained data. The experimental data presented in Table 4.1 can be used for this purpose. The curve fitting can be performed using available experimental data on the modulus of composites in dependence on modulus of fibers at constant fiber volume fraction. At the beginning of the fitting the analysis of the model (Eq. 4.10) sensitivity to different values of coefficients α and β has been done. It was found, that α contribute to the parallel offset of the curve (Eq. 4.10) in vertical direction. But β influences both: the slope of the curve and its vertical offset, at the same time. The behavior of the model with several values of α and fixed β is presented in Fig. 4.3 and Fig. 4.4. Thus, in order to adjust the curve to the maximum convergence with experimental data it is necessary to adjust coefficient β first and only then α . While adjusting β it was discovered that the best result can be achieved if $\beta < 0$. Thus, the series part of equation lowers the modulus of composite. This can be explained by the fact that those fibers, which do not coincide with the load main direction, do not strengthen, but weaken the whole composite. In fact, natural fibers and a synthetic resin due to difference in chemical composition have quite poor adhesion to each other. Therefore, this combination when transversally loaded does not contribute positively to the load bearing performance of the material. It was found, that the best correlation of the proposed

theoretical model with experimental data is achieved with $\alpha = 0.34$ and $\beta = -1.34$. Apparently, β can be written as follows: $\beta = -(\alpha + 1)$.

In addition to fibers distribution in matrix, the inherent anisotropy of natural fibers can contribute to the composite properties. There are recent studies on the properties of natural fibers, where high anisotropy in their properties is discussed [210]. For example, the modulus of elasticity of fibers is quite different in longitudinal and transverse directions. Thus, for Jute fibers the determined longitudinal modulus is about $E_f^L = 38.9\text{--}39.4$ GPa, while their transverse modulus is about $E_f^T = 3.8\text{--}5.5$ GPa. Such extreme anisotropy can be reflected in the new model. The proposed Eq. 4.10 can be rewritten as follows:

$$E_c = \alpha [V_f E_f^L + (1 - V_f) E_m] + \beta \left[\frac{1}{V_f / E_f^T + (1 - V_f) / E_m} \right], \quad (4.11)$$

where E_f^L and E_f^T - are the longitudinal and transverse moduli of fibers correspondingly. The new model according to Eq. 4.11 was tested on the same set of experimental data. The constant transverse modulus of the fibers equal to $E_f^T = 4$ GPa was used during fitting. The behavior of the curve did not vary much (see Fig. 4.5) and the best agreement with the experimental data can be achieved with slight correction of the coefficient $\alpha = 0.32$ (then $\beta = -(\alpha + 1) = -1.32$). Thus, with properly determined coefficients the proposed model gives reliable result at least within given range of fibers longitudinal modulus variation $E_f^L = 27\text{--}50$ GPa.

The subsequent testing of the modified proposed model should be performed with a constant longitudinal modulus of fibers where the fiber volume fraction is a variable. Experimental data obtained in [11] can be used (see Table 4.2). The comparison of theoretically predicted using the developed model (Eq. 4.11) and experimentally obtained modulus of PP/Jute composite with different fiber volume fraction is presented in Fig. 4.6a. Unfortunately no agreement with experimental data is observed. Therefore, additional adjustment of β coefficient is necessary. Taking into account, that Hirsch's model with $\beta = 1 - \alpha$ (see Fig. 4.2a) has a good correlation with the experimental data in the range $0 < V_f < 0.12$ and the proposed model (Eq. 4.11) based on data fitting which works good at $V_f \approx 0.4$ it is possible to surmise that β largely depends on V_f . Thus, using the fitting technique it was estimated that the proposed model with $\beta = (1 - \alpha - 5V_f)$ gives reasonable agreement with experimental data. Finally, the following model can be proposed for estimation of the modulus of composite reinforced with randomly oriented natural fibers:

$$E_c = \alpha [V_f E_f^L + (1 - V_f) E_m] + (1 - \alpha - 5V_f) \left[\frac{1}{V_f / E_f^T + (1 - V_f) / E_m} \right], \quad (4.12)$$

Indeed, if $V_f \rightarrow 0$, then $\beta = (1 - \alpha - 5V_f)_{V_f=0} = 1 - \alpha$ and the model approaches to Hirsch's model, but if $V_f \rightarrow 0.4$, then $\beta = (1 - \alpha - 5V_f)_{V_f=0.4} = -(1 + \alpha)$, which corresponds to the proposed model in this section in Eq. 4.11. The comparison of the developed model (Eq. 4.12) with experimentally obtained data (Table 4.2) is presented in Fig. 4.6b. Reasonable agreement can be achieved with following parameters if $\alpha = 0.22$, $E_f^L = 41$ GPa, $E_f^T = 4$ GPa, $E_m = 800$ MPa for PP/Jute composite.

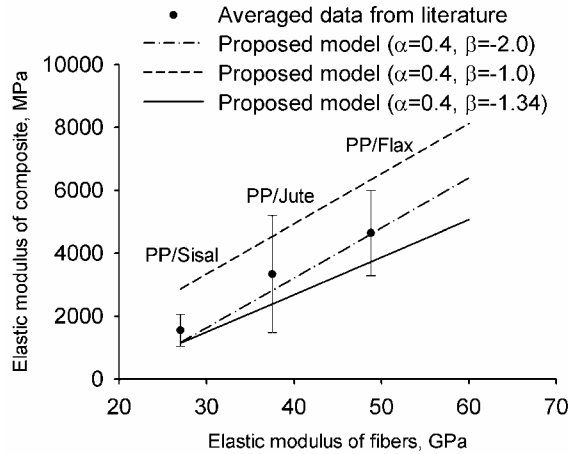


Figure 4.3 Adjustment of β coefficient in proposed model (Eq. 4.10).

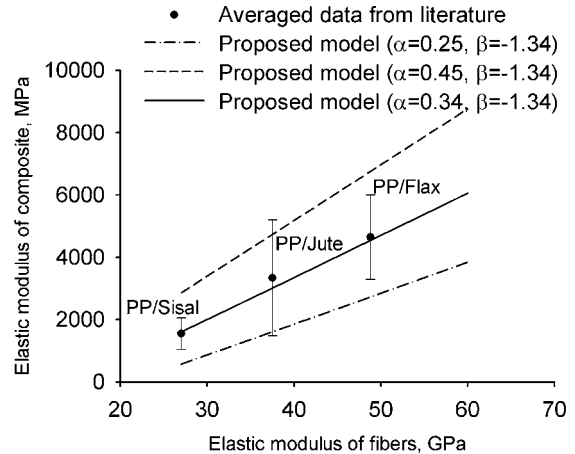


Figure 4.4 Adjustment α of coefficient in proposed model (Eq. 4.10).

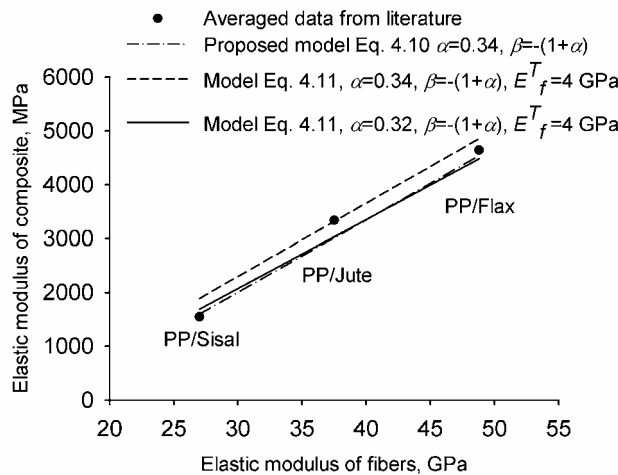


Figure 4.5 Comparison of the proposed theoretical model with experimentally obtained data.

The Figure 4.7 shows the developed model results in the wider range of fiber volume fraction than it has been used for fitting in above. The parameters $E_f^L=41$ GPa, $E_f^T=4$ GPa, $E_m=800$ MPa and $\alpha=0.22$ are used. The function gradually rises up to $V_f \approx 0.47$ and then goes down. At $V_f \approx 0.81$ the curve change its sign. Such a behavior can be supported by the fact that an addition of strong fibers into weak PP matrix certainly can produce a positive effect on the stiffness of a composite, but there is a certain limit of this improvement. Indeed, the increasing amount of fibers in composite, the amount of matrix resin decreases. Matrix becomes discontinuous and loses the ability to transfer applied load between fibers. Usually this happens due to poor impregnation of fibers with polymer resin as a result of technological problems. In production of composites with high values of fiber volume fraction the polymer resin can hardly be transferred between densely compacted fibers due to its high viscosity. In natural fiber reinforced composites (especially in thermoplastic ones) this problem is even more strengthened due to hydrophobicity of natural fibers, which also produces additional negative effect on fibers' wetting. Therefore a natural fiber composite at high values of fiber volume is only separated fibers, which are poorly connected to each other by drops of polymer resin. Of course, the stiffness of such combination is low or even

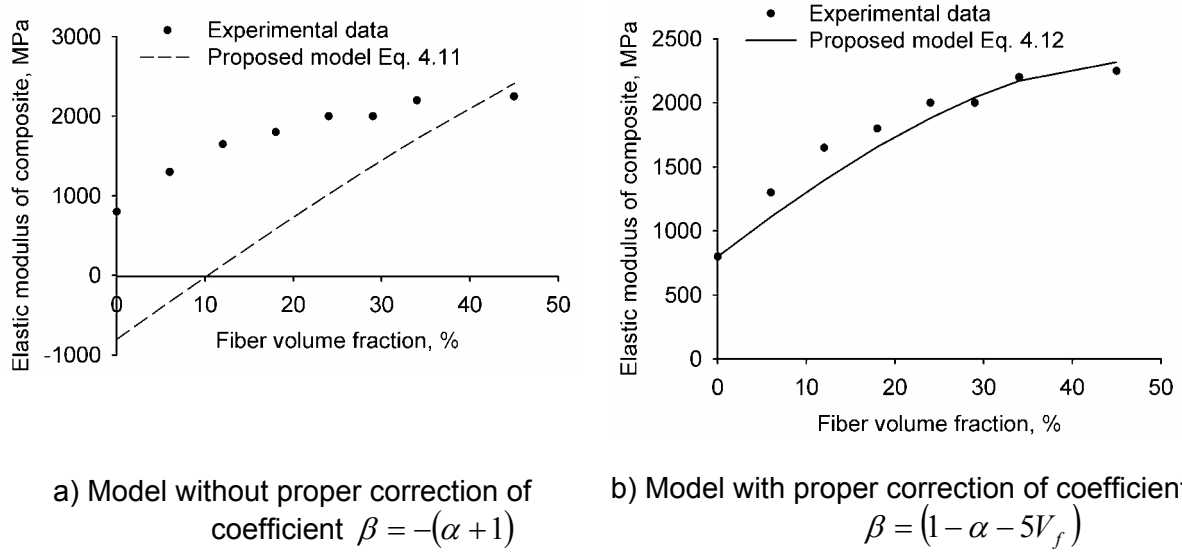


Figure 4.6 Comparison of theoretically predicted and experimentally obtained elastic modulus of PP/Jute composite with different fiber volume fraction.

does not exist (like if non-impregnated non-woven natural fiber mat would be loaded). This effect is different for every natural fiber composite and depends on many parameters, such as: type of fibers, type of polymer matrix, presence of compatibilizer (adhesion improvement agent) and processing conditions (especially temperature, which has strong effect on viscosity of polymers). For natural fiber composite under consideration (PP/Flax) the negative effect for stiffness due to high fiber volume fraction is in the range of $0.47 < V_f < 0.80$ (see Fig. 4.7). The effect of drop of modulus in natural fiber composites with extremely high fiber volume fraction was also observed by [157]. Namely it is reported 10 – 150 % decrease in mechanical properties of PP/Hemp composite while increasing fiber volume fraction from 57 to 68 wt. %.

In order to prove the reliability of the finally developed model (Eq. 4.12), an additional testing can be performed using different experimental data. The data obtained by [82] for low density polyethylene (LDPE) with randomly distributed Sisal fibers (see in Table 4.3) can be used for that purpose. The comparison is presented in Fig. 4.8. Reasonable agreement can be achieved at $\alpha = 0.1$ with known other parameters $E_f^L = 15$ GPa, $E_f^T = 4$ GPa, $E_m = 40$ MPa.

It can be concluded that the empirical coefficient α depends on a particular combination of fibers and matrix, in other words it depends on interaction between the components in a composite. It is also possible to estimate theoretical limit of the fiber volume fraction, beyond which the further increase of fiber volume fraction negatively affects the composite properties.

The function Eq. 4.12 has one point of extremum in range of $0 < V_f < 0.80$, which can be determined by following condition: $\partial E_c / \partial V_f = 0$. Values of α for some of the combinations of fibers and matrices together with the theoretical limit of fiber volume fraction V_f are presented in Table 4.4. In principle α can be estimated for any natural fiber composite with randomly distributed fibers. In order to estimate value of α it is necessary to perform mechanical testing of a composite in order to determine its modulus of elasticity. It can be advised to perform the testing of a composite with different fiber volume fraction in order to have more data points and therefore α can be estimated more reliably. However, in some cases one data point is sufficient. Together with the determined modulus of a composite it is necessary to know the longitudinal and transverse moduli of fibers, the

modulus of polymer matrix and fiber volume fraction. With all the mentioned values known the Eq. 4.12 can be solved with respect to α .

The developed model (Eq. 4.12) also can be used as a tool for estimation of the elastic modulus of a composite material if the elastic modulus of fibers is known, and vice versa. For example, with the known elastic modulus of Hemp fibers with the help of the model it is possible to extrapolate the elastic modulus for composite with 40 vol. % of randomly oriented Hemp fibers and polypropylene matrix (see Fig. 4.9). With the same success it is possible to reconstruct the elastic modulus of the Kenaf fibers if elastic modulus

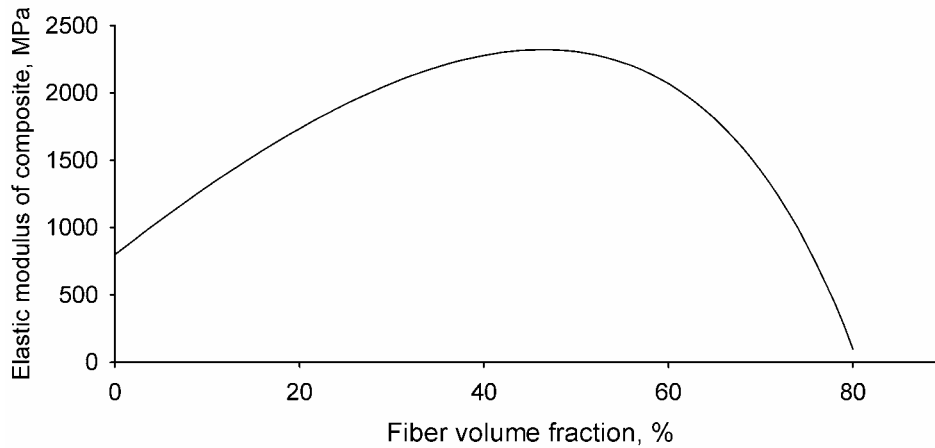


Figure 4.7 The graph of the proposed model (Eq. 4.12) in range of fiber volume fraction $0 < V_f < 0.80$, (PP/Flax composite: parameters $E_f^L=41$ GPa, $E_f^T=4$ GPa, $E_m=800$ MPa and $\alpha=0.22$).

Table 4.3 Experimentally obtained data for LDPE/Sisal composite reinforced with randomly oriented fibers (after [82]).

Fiber volume fraction	Modulus of composite, MPa
0	140
0.06	210
0.14	240
0.21	290

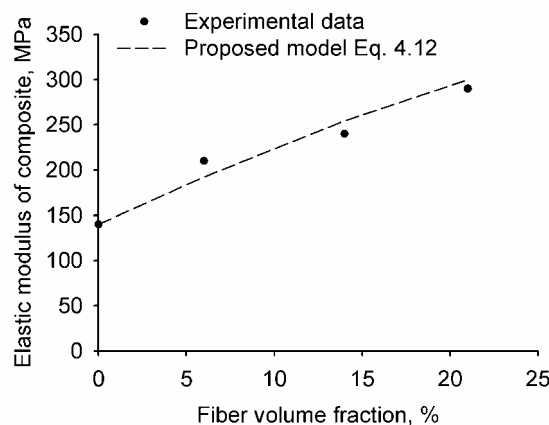


Figure 4.8 Theoretically estimated (using Eq. 4.12 with $\alpha=0.1$, $E_f^L=15$ GPa, $E_f^T=4$ GPa, $E_m=40$ MPa) and experimentally obtained elastic modulus of LDPE/Sisal composite.

Table 4.4 Values of the empirical coefficient α in Eq. 4.12 determined for some types of natural fiber in combinations with matrices.

Fiber – matrix combination	α	Predicted theoretical limit of $V_f, \%$
Flax / PP	0.32	55-60
Jute / PP	0.22	45-50
Sisal / LDPE	0.1	35-40

of the composite reinforced with 40 vol. % of Kenaf fibers and PP matrix is known (see Fig. 4.9). In this case it is assumed that the bonding properties of the PP to the mentioned fibers are the same. Properties of the materials can be taken from Table 4.1 ($E_f^T=4$ GPa) as an input properties for estimation and $\alpha=0.32$. As it was mentioned α should be estimated for each combination of fibers and matrices, but if there is lack of information the same α can be used for the estimation (of course with lower reliability of estimation).

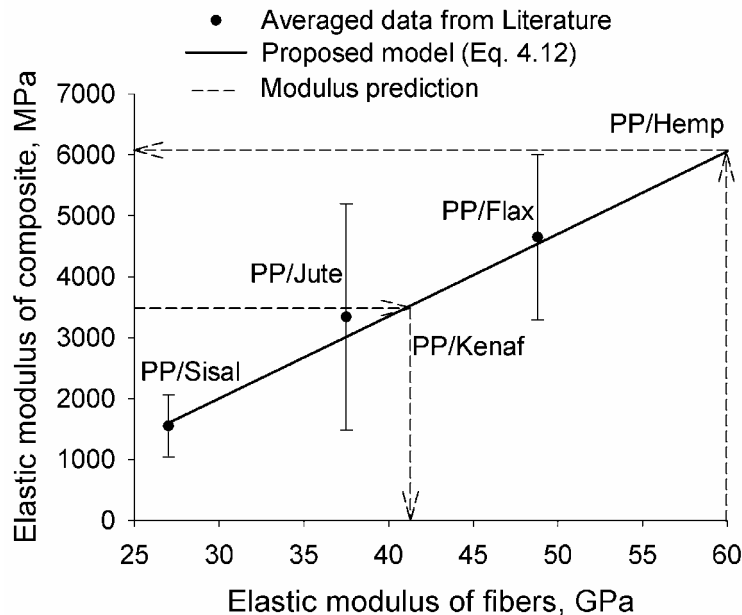


Figure 4.9 Modulus prediction (Eq. 4.12, $\alpha=0.32$, $E_m=800$ MPa, $E_f^T=4$ GPa, Table 4.1) for PP/Hemp and PP/Kenaf composites reinforced with 40 vol. % of randomly distributed fibers.

4.5 Conclusions

A number of theoretical models for estimation of the modulus of the natural fiber composite have been tested on available experimental data. The main objective was to find a reliable one to estimate the modulus of natural fiber composite in its dependence on fiber volume fraction (using constant properties of fibers and matrix). It was found that none of the existing models is suitable for prediction of modulus of natural fiber composite.

A new theoretical model (Eq. 4.12) based on Hirsch's model has been proposed. The behavior of the developed model has been tested on available experimental data. Good agreement with the experimental data has been achieved with properly adjusted empirical coefficient α . The adjustment of the α coefficient for a particular composite has to be done using experimentally obtained data. Thus the properly tuned proposed model can be used to correlate the modulus of natural fiber composite to fiber volume fraction.

Chapter 5

Heterogeneity simulation

5.1 Introduction

In chapter 3 the analysis technique suitable for heterogeneous composites was developed, based on which it was determined that non-woven natural fiber composites have a large variation in properties due to heterogeneity of fiber mat. The properties of different non-woven fiber mats were discussed. It was found that fiber clusters with various sizes and intensities are stochastically distributed in non-woven mats. The sizes and intensities of fiber clusters are considered as the parameters of mat heterogeneity. The parameters of heterogeneity for different fiber mats were determined based on representative sets of fiber clusters.

Heterogeneity simulation is needed in order to incorporate the derived parameters of the heterogeneity of a fiber mat into the structural analysis. Heterogeneity simulation is a technique that allows a virtual generation of non-uniformity in material. In other words, heterogeneity simulation is able to recreate the in-plane structure of the non-uniformity in a fiber mat with the predetermined parameters. It is assumed that the variation in properties of a fiber mat through its thickness is constant, i.e. homogenized. Simulated heterogeneity represents the variation of properties at any in-plane location in a mat (or composite). The development of such technique is essential for successful finite element (FE) simulations of plane or shell structures made from heterogeneous materials. This technique should take into account the derived parameters of material (mat or composite) heterogeneity and should give random distribution of the properties.

Generated heterogeneity should satisfy certain conditions. The smoothness and discontinuity are the primary conditions since the generated heterogeneity supposed to be used in subsequent FE analysis. Smoothness is important because even modern FE solvers are quite sensitive to high difference in properties of adjacent finite elements. This might lead to instability or poor convergence of calculations. Discontinuity condition of the heterogeneity secures the ability of the technique to determine the local value of heterogeneity at any point within certain specified limits. Certainly, computational complexity of the used mathematical equations should be not very high, since the number of finite elements in a model sometimes is very high. Complex calculation in this case might negatively affect the speed performance of the analysis.

5.2 Heterogeneity generation approach

In principle heterogeneity of the natural fiber mat is quite complex. The fibers are distributed not only in-plane, but in thickness as well (see an example in Fig. 5.1). Since the natural fiber mats are usually suited to be impregnated with resin to form plane thin sheets or structures with relatively thin walls, the in-plane distribution of fibers is more important than distribution through thickness. Thus, in structures where walls are relatively thin in comparison to other dimensions, the heterogeneity of the material can be assumed as in-plane, i.e. two-dimensional (2D). The heterogeneity through the thickness of composite is assumed to be constant. Most of the structures currently made of composites meet these assumptions.

The heterogeneity generation procedure should be able to describe the in-plane non-uniformity of material. This means that some points in plane of the model should have different values of properties which can be later correlated to real material properties (in this case the local amount of fibers in mat). Obviously, the heterogeneity in natural fiber mat or

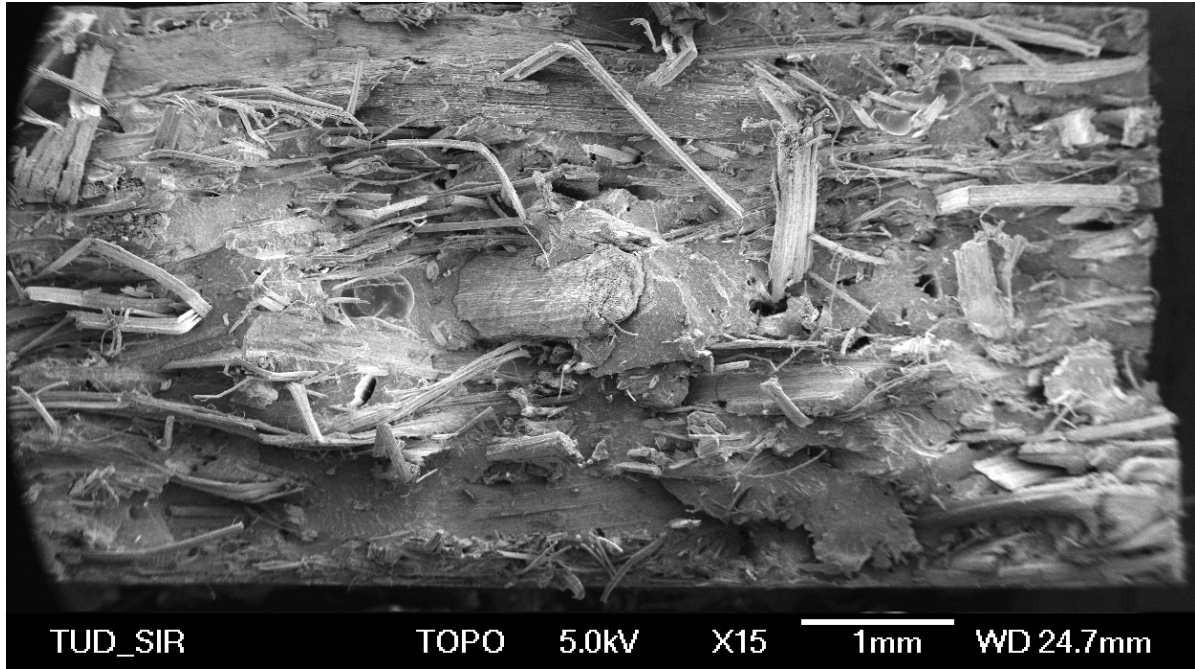


Figure 5.1 Distribution of fibers through the thickness of PP composite reinforced with non-woven Flax fiber mat.

composite can be represented by three-dimensional surface. In most of the cases Cartesian coordinate system can be used. Two-coordinate system is necessary to describe the position of points in the plane of the model. So, each point has two coordinates (X and Y) and the value parameter (Z) which represents the local property of the fiber mat, the amount of fibers, for example. Obviously, this description corresponds to the description of a three-dimensional $z = f(x, y)$ surface. This function should give the value of local property of material at the point with given coordinates.

The function of heterogeneity should satisfy criteria mentioned in section 5.1 (smoothness, discontinuity and simplicity). Moreover, it should take into account parameters of fiber mat heterogeneity determined in Chapter 3.

There are numbers of methods to describe mathematically the free-form 3D surface with given characteristics. Some of the methods are based on one complex equation, but the others – on a set of simple ones and hybrid methods. The advanced method from the first group is polynomial (spline) description, where the shape of the surface is described through power functions with certain coefficients at the power members [33]. An example of polynomial function is as follows:

$$y = C_n x^n + C_{n-1} x^{n-1} + \dots + C_1 x + C_0, \quad (5.1)$$

where C_0, C_1, \dots, C_n - are the constants, which describe the shape of the function. The most popular are cubic polynomial functions, which are called Beziars. The generated surface can be constructed from polynomial functions by description of polynomial functions for all three coordinated (X, Y, Z), thus:

$$\begin{aligned} X &= C_n^x t^n + C_{n-1}^x t^{n-1} + \dots + C_1^x t + C_0^x \\ Y &= C_n^y t^n + C_{n-1}^y t^{n-1} + \dots + C_1^y t + C_0^y . \\ Z &= C_n^z t^n + C_{n-1}^z t^{n-1} + \dots + C_1^z t + C_0^z \end{aligned} \quad (5.2)$$

In a similar way it is possible to construct so-called Bezier and B-spline surfaces. The advantage of such description is that the resulting surface can be very complex and can be described discontinuously. Hence, the heterogeneity of natural fiber mat is very complex (see Fig. 3.5 where a digital image of fiber mat is presented), so a very high-order polynomial function should be applied in order to generate a corresponding surface (for image brightness for example). This leads to the extreme complexity in adjustment of coefficients at the power members in Eq. 5.2 to achieve the surface with the desired parameters. Therefore, another method utilizing an application of a hybrid method seems to be more suitable.

According to the analysis of natural fiber mat, its heterogeneity is caused by the presence of fiber clusters. These fiber clusters are considered as elementary units of heterogeneity (see in Chapter 3) and they are described by parameters **size** and **intensity**. This allows decomposing the complex mat properties surface (which describes the heterogeneity of whole mat) into smaller surfaces (which describe the surface shape of each cluster separately). In other words the complex surface of heterogeneity is considered as a sum of small surfaces, which are represent the clusters shapes.

In some areas of fiber mat there are clusters and in the others there are voids, thus let **clusters** and **voids** are the **primitive elements of mat heterogeneity**. The clusters represent local increase of amount of fibers relative to their average amount in mat, but the voids – its local decrease. The average amount of fibers in a mat can be easily estimated beforehand. Such definition of decomposition of complex heterogeneity allows avoiding the contradiction of “zero” heterogeneity. This means that hypothetic fiber mat without non-uniformity contains not zero, but certain amount of fibers (apparently equal to its average value).

The mathematical description of the primitive elements shape with given quantitative parameters in this case is simple and therefore more controllable. Moreover, the shape of the primitive elements can be easily changed simply by choosing different shape function.

The spectral analysis was employed in Chapter 3 for the estimation of the parameters of fiber clusters. This analysis employs the decomposition of a complex function to a number of harmonics described with sine or cosine function. The period of different harmonics was correlated to the size of fiber clusters. Therefore sine or cosine functions can be successfully chosen to describe the shape of the primitive elements. The following function is chosen in order to describe the shape of the primitive elements:

$$f = \begin{cases} \pm \frac{A}{2} \left(\cos\left(\pi \frac{2x'}{L}\right) + 1 \right), & -L \leq x' \leq L, \\ 0, & x' < -L, \quad x' > L \end{cases}, \quad (5.3)$$

where A – the amplitude, L – the size. The endless cosine function is shifted up on $A/2$ value and limited to one full period, which is equal to $2L$ in order to form smooth bell-shaped curve. The first part of the equation describes the shape of the curve within limits, while the second one describes the curve beyond the specified limits.

The graphical representation of this function is given in Fig. 5.2. This function is smooth and simple to operate with. The amplitude (A) determines the height of the curve and the size (L) determines its width (see Fig. 5.2).

The obtained curve “generatrix” can be revolved 360 degrees around the vertical axis which goes through its peak in order to generate the surface that will describe the 3D shape of heterogeneity primitives (cluster or void). The first part of Eq. 5.3 might have a positive or a negative sign. This is necessary to generate a convex or concave surface. The hump (convex surface shape) will be formed if the function has a positive sign, but the cavity (concave surface shape) will be formed in case of a negative sign.

The shape of both types of surfaces describes the local gradual change in material properties. In general it could be almost any kind of property: physical, mechanical, acoustical, etc. Since the natural fiber mats (or composites) are under analysis, these

surfaces represent the local change in the amount of fibers at different locations in a mat or composite.

Thus, the hump signifies the local stepless increase of material property relatively to its average value. Therefore in that particular location the amount of fibers is considered to be higher than the average amount of fibers estimated through the whole mat. The cavity, on the contrary, signifies the local stepless decrease of material property, i.e. low amount of fibers. The hump and cavity (see Fig. 5.3) are considered as a primitive attributes of heterogeneity.

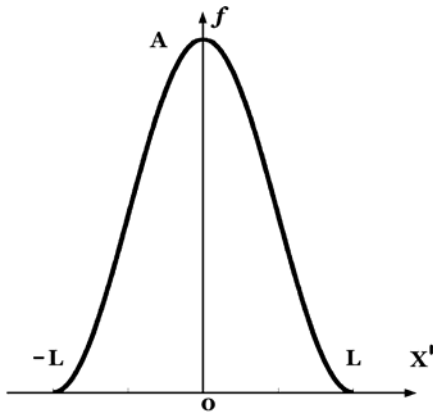


Figure 5.2 Shape-function for heterogeneity primitive's description.

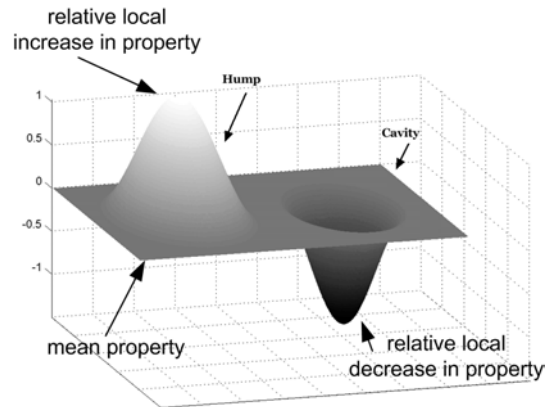


Figure 5.3 Hump and cavity as primitive attributes of heterogeneity.

As a result the heterogeneity generation procedure can manage them easily as elementary units. The parameters of the primitive attributes can be flexibly changed in order to achieve the desired result.

The fiber clusters and voids with different parameters are stochastically distributed in the mat. Therefore the next step is to develop the heterogeneity generation procedure which generates the primitive attributes with specified parameters and allocates them in plane. The allocation can be performed randomly or regularly. The random allocation of the primitive attributes is more preferable with respect to the accuracy and conformity of the generated heterogeneity to the heterogeneity of a real fiber mat but it is less controllable and more complex than regular allocation. The random allocation method requires availability of extensive statistical information about the number of heterogeneity primitives of a certain size in each square unit in a mat and the law of their distribution. The complexity of accomplishing of these tasks limits the usage of random allocation method. The regular allocation method does not require the mentioned statistical parameters, therefore it is more attractive to use at the beginning. The regular allocation method has been chosen, assuming that the inaccuracy in properties distribution would be within acceptable (engineering) error. The switch to the random allocation procedure can be considered as a further development of the technique.

The basis of the regular allocation method is a grid construction. Since Cartesian coordinate system is commonly used in practice it is reasonable to draw the grid lines parallel to the axes of coordinate system. Thus, the angle at intersection of grid lines in different directions is equal to 90 degrees. The grid lines have regular step size in both directions. The step size is equal to $2L$ (see Eq. 5.3, Fig. 5.4).

The intersections of grid lines are considered as origins for primitive attributes of heterogeneity. The origin of the primitive attribute is defined by its axis of symmetry, which passes through the origin of its local coordinate system $x^1 = 0$ (see Eq. 5.3, Fig. 5.2). Two types of heterogeneity primitives are alternating in both perpendicular directions. So the humps alternate with cavities. This procedure can be performed infinitely to cover a plane of any dimensions with the primitives.

In Chapter 3 it was shown, that in every mat with randomly distributed fibers it is possible to highlight a representative set of heterogeneity harmonics. Each set contains harmonics with certain sizes and corresponding intensities, which can be correlated to heterogeneity primitives. Since all fiber clusters present in a mat are different, the statistical parameters (mean and standard deviation) of harmonics sizes and intensity are obtained (see in Table 3.3). This allows us to generate stochastically the sizes and intensities of primitives. Gaussian distribution with known mean and standard deviation parameters can be successfully employed in this case. The application of stochastic procedure is essential since it can reduce the pattern in generated heterogeneity appeared due to a regular grid.

An example of heterogeneity with alternated primitive attributes generated with stochastic (according to normal distribution) amplitudes and size is presented in Fig. 5.4. In this figure the average size (width) of the primitives (both humps and cavities) (L) is equal to 10 mm and the average amplitude (A) is equal to 1 for humps, and for cavities to -1. Let's call the generated surface "the low-order" heterogeneity because it contains primitives (or harmonics) of only one mean size (L).

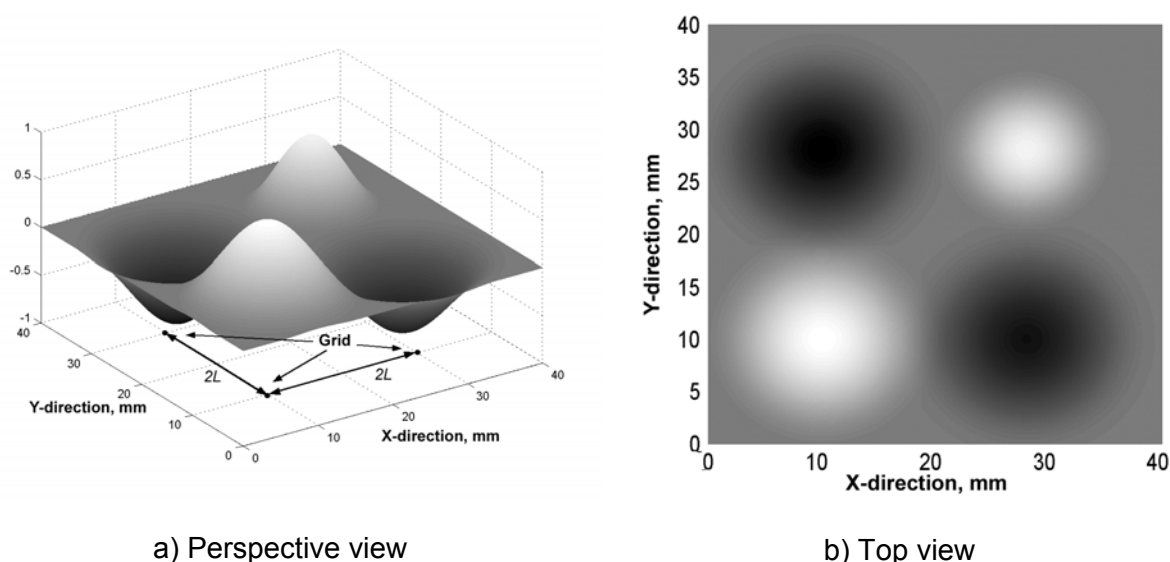


Figure 5.4 Example of generated heterogeneity using regular allocation method.

It was determined that a fiber mat contains a certain set of primitives with different sizes. Thus, it is necessary to generate several low-order heterogeneities (harmonics) with different parameters (size and intensity of primitives and grid step size) simultaneously. This is the advantage of the regular allocation method of primitives. The procedure for each low-order heterogeneity generation can be performed several times for the same plane independently. The resulting high-order heterogeneity should be calculated as a sum of all low-order heterogeneities (harmonics). It is important to note, that the intensity of high-order heterogeneity should be in range from -1 to +1. This can be achieved if the sum of the average intensities (A) of low-order heterogeneities is equal to 1, thus each low-order heterogeneity should have $A_n \leq 1$. An example of resultant heterogeneity generated with two size of primitive attributes ($L_{1mean} = 20$ mm, $A_{1mean} = 0.8$ and $L_{2mean} = 8$ mm, $A_{2mean} = 0.2$) is presented in Fig. 5.5. Such high-order heterogeneity already has quite complex structure, but it can be made even more complex by simple addition of more low-order heterogeneities with different parameters. This allows to generate the high-order heterogeneity of almost any complexity. The number of simultaneously generated low-order heterogeneities is not limited. The more low-order heterogeneities are generated the better correlation between real and simulated heterogeneity of fiber mat will be.

The parameters of heterogeneity of natural fiber mat derived in Chapter 3 (see Table 3.3) can be used for the generation of low-order heterogeneities. Several harmonics were highlighted in fiber mats under investigation. Each of the harmonics determines L_{mean} , $L_{st.dev.}$ and A_{mean} , $A_{st.dev.}$ parameters of certain low-order heterogeneity. The resultant high-order heterogeneity will be the closest possible to achieve, but the procedure of its calculation is rather complex and, therefore, time consuming. In order to simplify the procedure of the high-order heterogeneity generation the number of involved low-order heterogeneities (in other words harmonics) can be reduced. This number can be determined through limitation of the involved harmonics. The size parameter of the harmonics is used for that purpose. The boundaries of sizes depend on at least two parameters: the scale of the structure that will be modeled with FE analysis and the limitation in sizing of FE mesh. The scale of structure under investigations limits the largest in size harmonics (limit from the top) and the sizes of finite elements define the smallest in size harmonics. In other words, it is worthless to use those harmonics with size much larger than dimensions of the structure since their contribution is small. Also, there is no sense to generate heterogeneity with the size harmonics much smaller than size of finite elements because the properties within one element are constant. The relation of finite element size in dependence to harmonics size will be established later.

Thus, simulated high-order heterogeneity represents a relative change in the local properties of a fiber mat. In order to implement the established variation in local properties of the material into FE analysis it is necessary to establish a correlation between the simulated heterogeneity and certain mechanical properties of the composite material.

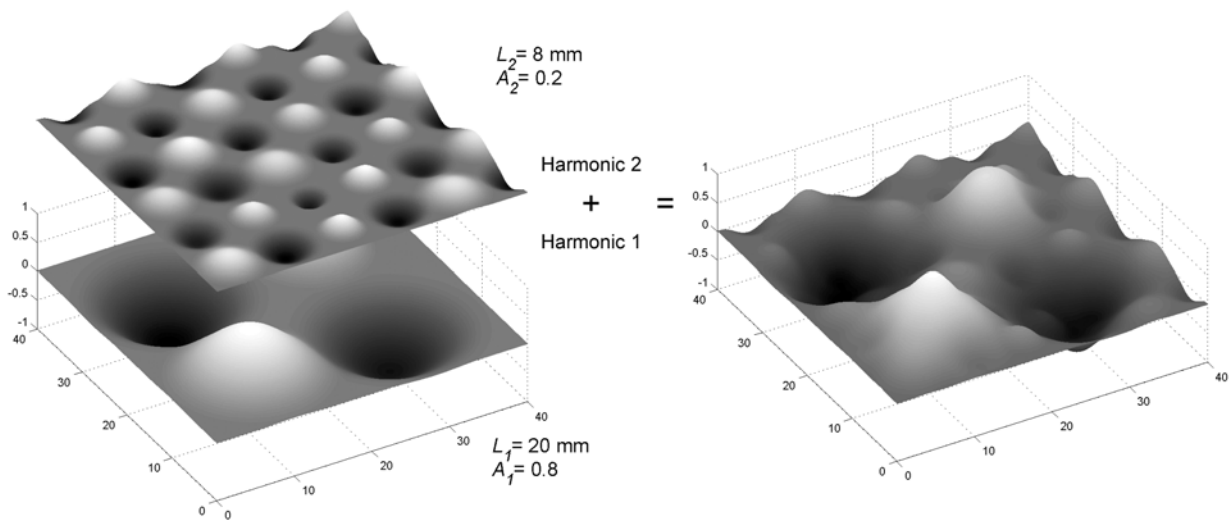


Figure 5.5 Example of a high-order heterogeneity generated with the two first-order heterogeneities with different parameters.

5.3 Verification

The heterogeneity generation procedure described in Section 5.2 should generate the heterogeneity as close to the original fiber mat as possible. In principle, the developed technique is based on decomposition of complex heterogeneity to heterogeneity primitives and should give a sufficient result. This technique operates with the heterogeneity primitives (clusters and voids) which are determined from the original fiber mat (or composite). The shape of the heterogeneity primitives is circular in-plane (see Fig. 5.3b). One can find that the clusters in the original fiber mat have quite complex shape, which is in general far from

circular and the distribution of clusters in a mat is irregular. However, in the developed technique these two parameters are compensated with stochastically distributed parameters of the generated heterogeneity primitives. The size and intensity of heterogeneity parameters in each of low-order heterogeneities are randomly generated. Moreover, the usage of several low-order heterogeneities to generate high-order heterogeneity introduces the additional element of contingency into the technique.

Verification of the generated heterogeneity can be performed using the procedure described in Chapter 3, but in place of the image of fiber mat the generated image (or numerical array) of the heterogeneity can be analyzed. Linear excerpts of the image brightness distribution similar to those described can be derived from the generated heterogeneity. The spectral analysis can be applied afterwards in order to determine the parameters of the generated heterogeneity and compare with those experimentally obtained. The actual verification will be presented further in this thesis.

5.4 Correlation with mechanical properties of composite

In Chapter 3 the heterogeneity of natural fiber mats (and composites) was discussed. The heterogeneity represents variation of local amount of fibers along the material. The local amount of fibers in a composite material is represented by the local fiber volume fraction. Thus, the generated 3D heterogeneity can be correlated to the variation of a fiber volume fraction and then, to mechanical properties of a composite.

Since the generated heterogeneity is a normalized function which has boundaries at -1 and +1 it needs to be correlated to the fiber volume fraction boundaries in composite. Thus the value of -1 is associated with the lowest local fiber volume fraction while the value of +1 – with the highest one. The lowest and the highest local values are the boundaries of fiber volume fraction which can be determined for any composite using the following technique.

A microphotograph of a composite cross-section can be used. PP/Flax composite reinforced with 30 vol. % of randomly distributed fibers (provided by Symalit® GMT, Switzerland) has been used as a case study. The cross-section of a plane sheet of this material has been analyzed with a laser confocal microscope (see an example in Fig. 5.6). It can be seen that the fibers are randomly distributed in the PP matrix, but their amount at different locations of the cross-section is different.

The determination of boundaries of fiber volume fraction in the cross-section of the composite is based on the image analysis. In principle, the fiber volume fraction can be determined by counting the sum of the areas occupied by fibers within certain chosen effective area in a cross-section of the composite. It is important to note that the size of the chosen effective area is of primary importance. From the one hand it should be small enough to estimate the fiber volume fraction in small areas of the composite – local volume fraction, but on the other hand it should be large enough to obtain a reliable result. For example, the average fiber volume fraction in a composite can be determined by counting the sum of areas occupied by fibers on a large effective area in a specified cross-section.

In order to avoid uncertainties related to the determination of the effective area a different estimation approach of fiber volume fraction is proposed. The technique is based on the assumptions made in Chapter 3, regarding the distribution of fibers through the thickness of a composite, since natural fiber composites are usually being produced and used in form of sheets. In most applications the thickness of a composite sheet is relatively small in comparison to its in-plane dimensions. Therefore, the heterogeneity in properties of sheet-formed natural fiber composite can be characterized by in-plane heterogeneity only, while the heterogeneity through its thickness is neglected (explanation of this assumption see in Chapter 3). Thus, it is assumed that the sheet made of natural fiber composite has different in-plane properties at different locations. The actual property at every in-plane point (due to in-plane heterogeneity) is determined by the homogenized property of the material determined through its thickness.

A technique determining the amount of fibers (fiber volume fraction) based on this assumption can be applied. A local coordinate system in Fig. 5.6 is introduced in order to

define in-plane and through-thickness directions in the sheet formed natural fiber composite. The X-axis is along the in-plane direction of a composite sheet while Y-axis is perpendicular to the sheet's plane and represents its thickness. Fibers in the cross-section of the composite can clearly be seen. Their contribution to the composition of the material can be determined along the Y-direction at any point with a specified coordinate. Therefore, a virtual vertical line (along Y-direction) can be drawn at any point with specified coordinate (see Fig. 5.6). The amount of fibers at any point along the X-direction can be determined by the sum of lengths of the fibers cross-sectional areas which the virtual line crosses (the sum of lengths of thick parts on a virtual line in Fig. 5.6). The length can be measured in either pixels or millimeters. With the known dimensions of the cross-section a fiber volume fraction can be easily determined. During this procedure the virtual line moves along X-direction with certain distance steps (0.1mm has been used). The fiber volume fraction is calculated at every step. The graph of the variation of fiber volume fraction for the presented cross-section of PP/Flax composite is shown in Fig. 5.7. The determined average fiber volume fraction is 27.8 % (which is rather close to declared value of 30 % in the manufacturer's material specification). The boundaries of fiber volume fraction are also can be determined: $V_{f\min} = 11.5\%$ and $V_{f\max} = 53.9\%$. These values can be used as boundaries for generation of the properties heterogeneity in such composite. As a result, the generated heterogeneity will represent the function of fiber volume fraction variation in a plane of a composite sheet.

The model developed in Chapter 4 (Eq. 4.12) can be applied for estimation of the modulus of natural fiber composite with respect to a fiber volume fraction. An example of variation of Young's modulus in PP/Flax composite with parameters: $E_f^L = 41$ GPa, $E_f^T = 4$ GPa, $E_m = 800$ MPa and $\alpha = 0.22$ is presented in Fig. 5.7. The resulting estimated variation of Young's modulus in a composite varies in range of 1950 – 6100 MPa.

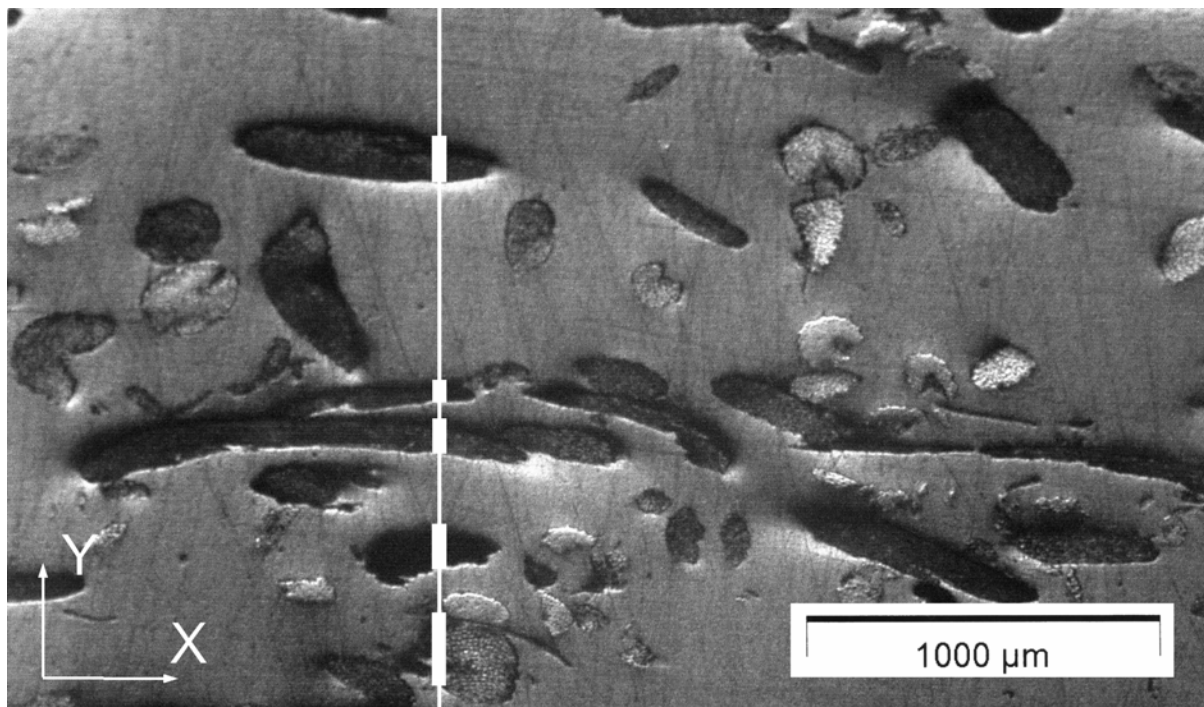


Figure 5.6 Cross-section of a specimen of PP composite reinforced with 30 vol. % of Flax fibers in form of a non-woven mat. The vertical line corresponds to one of the analyzed directions of fibers distribution.

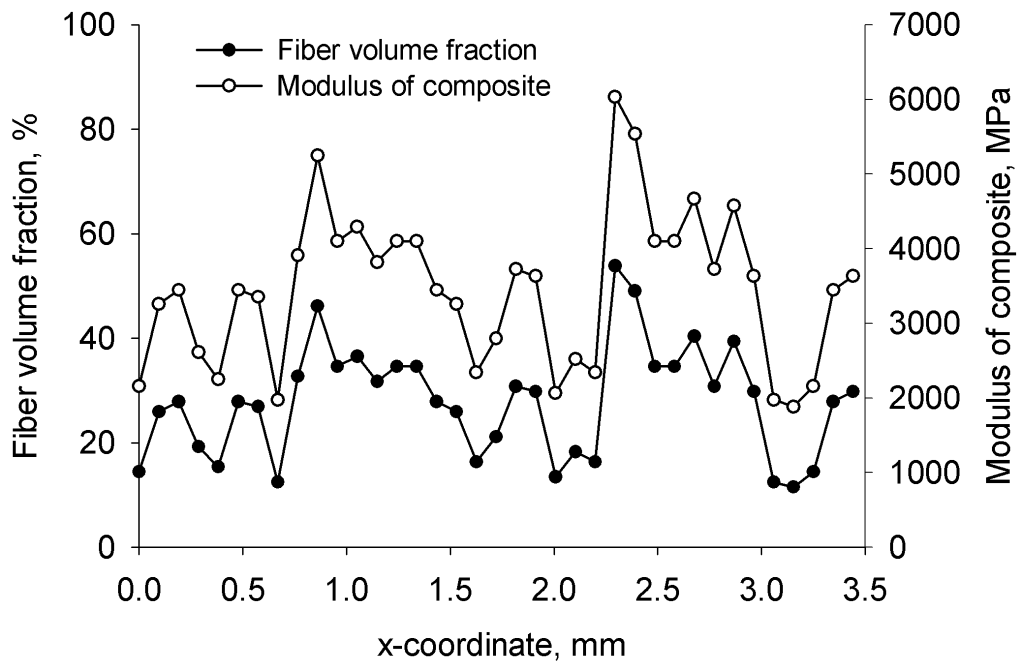


Figure 5.7 Variation of fiber volume fraction in the cross-section of PP composite reinforced with 30 vol. % of Flax fibers in form of non-woven mat (see Fig. 5.6), and the corresponding estimated variation of Young's modulus (estimated by using Eq. 4.12).

5.5 Conclusions

In this chapter the technique for heterogeneity generation has been developed. This technique is based on the applying the decomposition of complex heterogeneity into several primitives. It makes possible to describe the complex heterogeneity of the natural fiber mats by using simple equations. Moreover, the usage of this approach gives one the possibility to adjust the parameters of the heterogeneity (to be generated). The primitives are defined as the elementary units of complex heterogeneity. Each primitive describes the local change of the properties in a material. The primitives are arranged in correspondence with the regular grid which step size depends on the parameters of primitives. The bell-shaped cosine function has been chosen to describe the shape of the primitives and, correspondingly, the law of local material properties variation. The bell-shaped function can be positive as well as negative. The positive function produces a hump – local improvement of material properties while the negative one produces a cavity – local worsening of material properties. The amplitude and the size of hump and cavity (the parameters of the heterogeneity primitives) can be different. For example, the parameters of the heterogeneity of fiber mats determined in Chapter 3 can be taken in this case as the parameters of the heterogeneity primitives. In that table parameters of each harmonic of heterogeneity should be used to generate a separate low-order heterogeneity. According to developed technique the high-order heterogeneity is the sum of the low-order heterogeneities. As a result, the high-order heterogeneity represents a relative variation of properties of a heterogeneous material with the desired parameters. It varies within the boundaries of -1 and +1.

Further, the generated high-order heterogeneity has been correlated to certain material properties of natural fiber composites. The fiber volume fraction is one of the most important characteristics of any composite equally with the type of fibers and type of matrix polymer because mechanical properties of a composite have quite strong relationship with the fiber volume fraction. It is obvious, that local mechanical properties of a composite are

very sensitive to its variation. Therefore fiber volume fraction has been chosen to be correlated with the generated heterogeneity. Then, further the developed in Chapter 4 material model can be successfully used to estimate the local modulus of elasticity of a composite. As a result the modulus of elasticity of a composite can be varied according to the generated heterogeneity. This variation can be further implemented in FE simulation of structures made of heterogeneous materials.

A technique to determine the boundaries of fiber volume fraction in real composite has been proposed. It is based on the analysis of a digital image of the composite's cross-section. The boundaries of the fiber volume fraction for PP/Flax composite reinforced with 30 vol. % of randomly reinforced fibers has been determined according to the introduced assumptions.

Finally, summarizing the proposed technique, the following steps are necessary to perform the generation of heterogeneity in mechanical properties of a composite successfully:

- 1) Estimate the parameters of material's heterogeneity;
- 2) Generate the high-order heterogeneity with certain parameters of primitives;
- 3) Estimate the boundaries of fiber volume fraction variation in a real composite;
- 4) Estimate the empirical coefficient in the proposed theoretical model for the modulus of the composite estimation;
- 5) Put into correspondence the boundaries of the generated heterogeneity with the boundaries of fiber volume fraction determined in real composite.

Chapter 6

Finite element implementation

6.1 Introduction

The use of computer simulation to understand structural behavior is inevitable nowadays. There are a lot of commercial and non-commercial computational packages available. Orientation towards the commercial software is of primary interest, since this software is rather reliable and widely available. The purpose of the currently available computational simulation software packages is different. Nowadays such software packages as mechanical simulations, computational fluid dynamic, thermal analysis and multipurpose are available. Packages for mechanical simulations using the finite element (FE) method usually allow simulation of the structural behavior under mechanical, thermal and coupled loading conditions. These packages are dominant on the market. Some of the finite element packages can be directly connected (as plug-in) to the most popular computer aided design (CAD) packages. The plug-in type finite element packages use the drawn CAD geometry of the model and allow one to specify the material properties and boundary conditions through a native user-friendly interface of CAD software. Structural simulations performed using such packages are fast, reliable and suitable for simple simulations. However, in such packages most of the calculation procedures, for example, material models and the finite element mesh are usually hidden from the user and, therefore, cannot be traced or modified. These packages are operating as a “black box”, and it is rather difficult to control the calculation process. Accordingly, these packages can be used only for a rapid analysis of structures with simple (usually linear) material behavior. The non-linear stand-alone finite element packages have much more flexibility in description of material models, boundary conditions and optimization of the finite element mesh than any plug-in packages. On the one hand this gives a full control over the simulation process, but on the other hand the reliability of the simulations is completely in the competence of user (engineer). In other words, an engineer has to know what he (or she) is doing.

In Chapters 3 and 4 of this thesis a new approach to determine the properties of heterogeneous natural fiber composite has been developed. According to that approach local mechanical properties of a composite material can be varied with the given parameters of heterogeneity. In this chapter the finite element implementation of the developed approach will be described. The developed approach requires a full FE mesh access to assign the mechanical properties to finite elements. Therefore, a powerful stand-alone FE simulation package is required. In FE formulation heterogeneity can be implemented as the difference in the properties of adjacent finite elements through the model. Thus, the properties of finite elements are not constant, but depend on the element’s location in a model and, of course, on heterogeneity parameters. Further, the FE solver should be able to operate with complex distribution of material properties in a model. It should be noted, that not every stand-alone finite element package allows such flexibility. There are commercial packages like MSC.MARC, Ansys and ABAQUS which give the user a great flexibility to control and modify model description and calculation process through the external user’s subroutines. The user’s subroutines are extremely powerful. They allow to supplement standard build-in models of the package with the additional user’s parameters, and even completely substitute them with the user specified ones. Since in our laboratory the MARC (MSC Software) finite element package is available, the implementation of the developed approach and all simulations further will be performed with the help of this package.

6.2 Development of the user's subroutine

Thus, the developed material model has to be connected to a finite element code through user's subroutine. According to the conventions of MSC.MARC [136] all users' subroutines should be written in FORTRAN. Therefore the developed approach should be programmed in FORTRAN.

The call of the external functions from the user's subroutine during MARC simulation can be performed via MARC model description. The FE model description is in the form of a text file (input file) with a fixed format of commands. In general the input file can be divided into several blocks, like geometrical parameters (mesh description, connectivity of nodes and finite elements), boundary conditions, material properties, analysis parameters (type of analysis, friction, contact and etc.) and output (post variables). Performing standard analysis (without user's subroutines) the FE code reads the input text file of the model description (all blocks), calculates the given model and then, gives an output (see Fig. 6.1). However if it is necessary to perform an advanced analysis, certain user's subroutines can be included almost in every stage of the analysis. There exist different types of user's subroutines. They are: geometry and mesh modification, boundary conditions modification, material properties modification, constitutive relation modification and advanced output. Since the developed heterogeneous model is based on the material properties description at a particular location, at least two types of subroutines will be used.

First of all the geometrical parameters of the finite element model i.e. a connectivity matrix should be derived. This can be done through the user's subroutine UCONN (geometry modification type subroutine) which is used for connectivity of the finite elements modification [136]. But, here this procedure will be used only for the determination of the numbers and coordinates of the nodes, which belong to a particular finite element. This subroutine is to be called just after the connectivity matrix is built and therefore a direct access to internal MARC arrays with nodes coordinates and elements description is available. The coordinates of nodes are used for determination of the location of the finite element and appropriation of its mechanical properties according to the generated heterogeneity.

Further, according to the developed heterogeneous material model the assigned properties of the finite elements should be available for the FE solver. The subroutine HOOKLW (material properties modification type) [136] is used for that purposes.

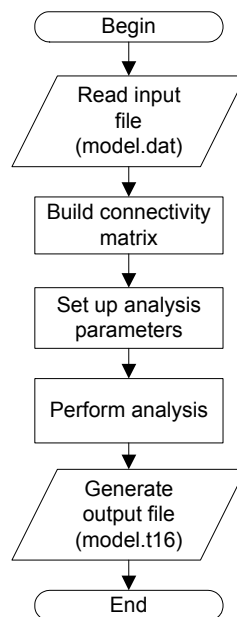


Figure 6.1 Algorithm of standard finite element analysis with MSC.MARC.

This subroutine allows the modification of the elastic properties of the finite elements via the direct input of stiffness matrix specified by user.

The user's subroutine PLOTV (advanced output) is used for the output of additional information, like heterogeneity distribution and assigned properties of finite elements. The algorithm of the analysis is presented in Fig. 6.2.

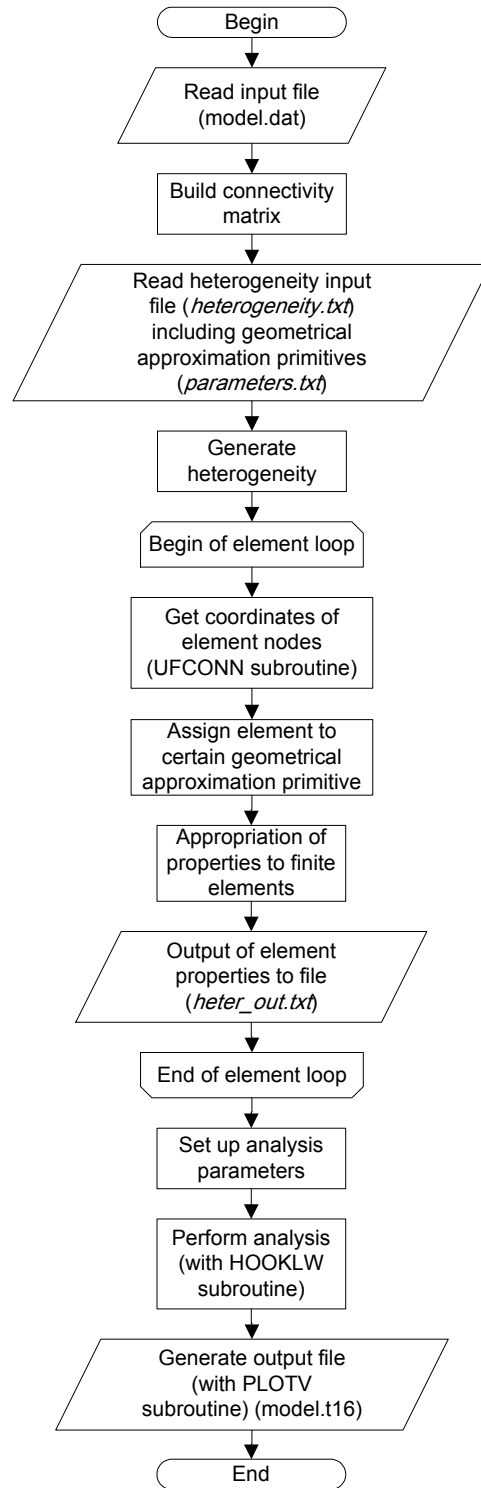


Figure 6.2 Algorithm of the finite element analysis using MSC.MARC with the implemented approach to simulate structures made from heterogeneous materials.

The subroutines UCONN, HOOKLW and PLOTV available in MSC.MARC package are only gates to access all necessary information from FE model and create an output. The subroutine for heterogeneity generation, the assignation of properties to the finite elements and generation of an output has to be programmed. The investigations in Chapter 3, Chapter 4 and Chapter 5 are taken as the basis to develop the subroutine.

6.3 Implementation procedure

In order to perform the FE analysis of a structure with a complex shape successfully a simplified FE model is usually used. In reality all structures are three-dimensional (3D) and in some cases it is possible to make certain assumptions and simplify them to reduce the calculation complexity. For example, structures made from composites due to certain design objectives and technological limitations are usually thin-walled. It makes them applicable to be modeled as shell structures. Such assumptions help to reduce not only a computational complexity, but also to reduce errors due to unimportant details like facets and hatches which are usually present in real structures. As a matter of fact, a quite large number of real-life structures can be modeled as shell structures. This is especially attributed to the structures made from plastics and composites reinforced with fibers using compression or injection molding technique. Such structures usually have large flat or slightly curved thin walls, which can be modeled using shell finite elements.

The approach to the model heterogeneous material is described in Chapter 5 has been developed for in-plane properties of a composite (thus, two-dimensional (2D) case). The variation in its properties is described only by two coordinates (x, y) in Cartesian coordinate system. However, most of the real-life structures, even those which can be modeled as shell structures, are still 3D. Thus, in order to perform FE simulation of 3D shell structures using developed material model it is necessary to approximate the complex 3D structure with certain locally defined 2D geometrical primitives. The main issue of 2D geometrical approximation primitives is that their local mathematical description uses only 2 independent coordinates to confirm the developed approach. For example, a plane can be described by using 2 independent coordinates (x, y) in a locally defined 3D Cartesian coordinate system and therefore can be successfully used. However, for example, cylindrical approximation as geometrical approximation primitive can also be used. A cylindrical surface is not a 2D surface in Cartesian coordinate system; therefore, it is described there by using three coordinates (x, y, z) , but if local cylindrical coordinate system is defined, this surface can be described by using only two independent coordinates (x, θ) and one constant (R) . These two variables (x, θ) can be easily linked to the developed approach by using the coordinate system transformation. This gives the excellent possibility to use cylindrical surfaces as geometrical approximation primitive as well. Cylindrical primitive is rather useful due to the adjustable curvature (R parameter), which allows approximation of cylindrical surfaces that might be present in a structure.

Several examples of a typical structures and their possible approximation with plane and cylindrical primitives are presented in Fig. 6.3. Simple flat structures can be approximated using only one plane (Fig. 6.3a). Tubular or ring-type structures can be approximated by a cylindrical primitive (Fig. 6.3b). However, more complex structures, consisting of more elements can be approximated using several geometrical primitives like plane and cylindrical surfaces at the same time (Fig. 6.3 c,d). The geometrical approximation primitives are suggested to choose in the way to cover as large area of the structure's surface as possible.

It is suggested to use a parameter D_{\max} , which is introduced for each geometrical primitive. Parameter D_{\max} represents the maximum distance from a geometrical approximation primitive to a structure's surface (see Fig. 6.3a - 6.3d), or in other words, to finite elements present in a mesh. This parameter determines the "roughness" of the geometrical approximation. Thus, small out-of-plane structural elements within D_{\max} distance

that present in a large surface of a structure are assigned with that surface to the same approximation primitive. An example is presented in Fig. 6.3e. In that figure a crate is shown. This structure can be successfully approximated by using only one plane geometrical primitive if the height of its walls is not higher than specified $2D_{max}$.

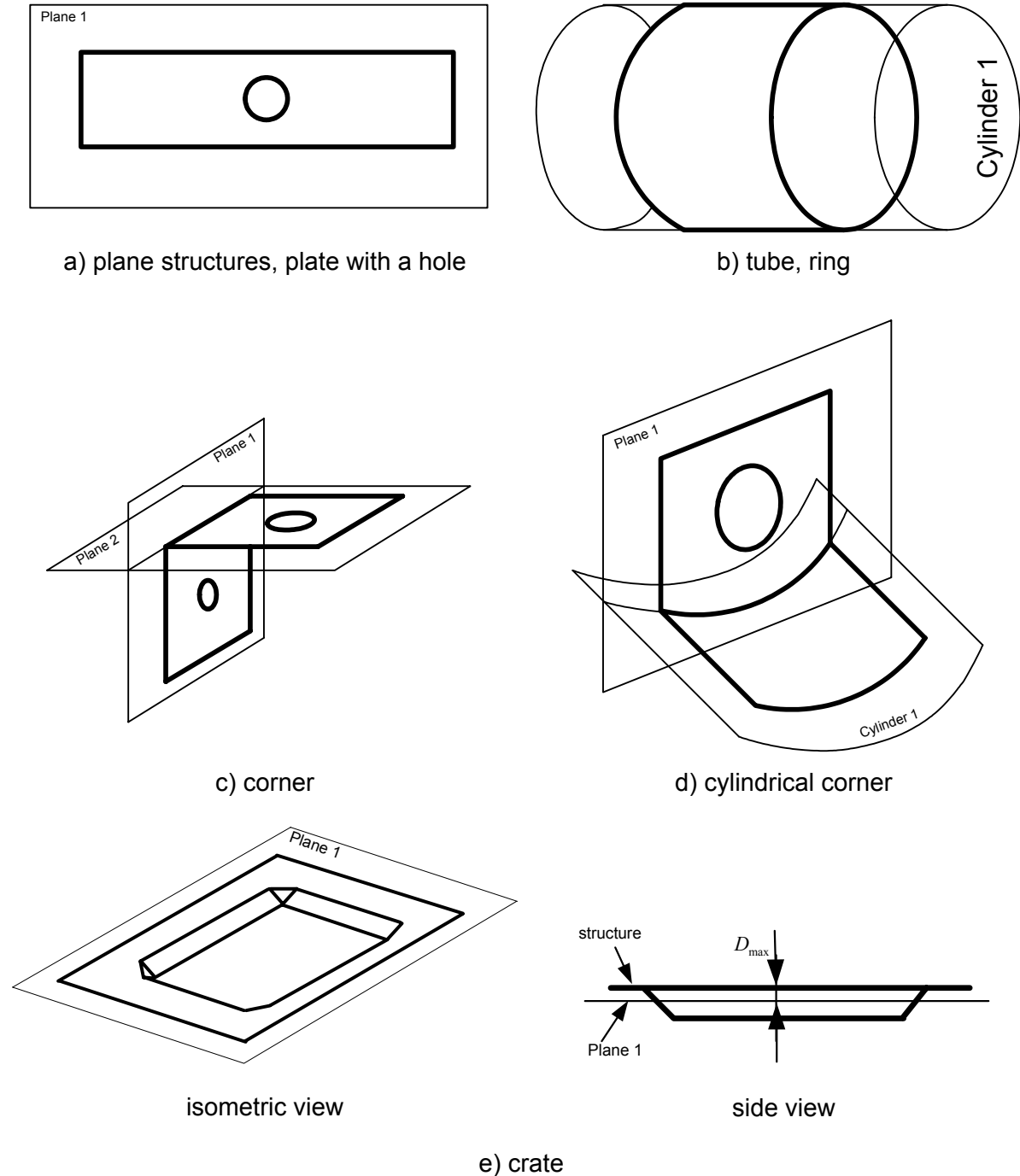


Figure 6.3 Examples of approximation of structure with geometrical primitives.

6.3.1 General approximation of the finite the element model with geometrical primitives

A general technique to apply the in-plane variation in properties of a material to 3D structures is not a standard procedure, therefore has been specially developed. It is based on the approximation approach of a FE model with locally defined 2D geometrical approximation primitives like planes and cylindrical surfaces as depicted in Fig. 6.3. Mathematically the approximation is implemented by using the following procedure. First of all, as in any FE analysis the structure is subdivided into finite elements. Then user has to define the geometrical approximation primitives (its coordinates and type). Each specified primitive has its own local 2D coordinate system. Then, the main task is to properly assign the finite elements to a certain geometrical approximation primitive. In order to do that it is necessary to transform the global 3D coordinates of finite element nodes (they are known from model description) to the local 2D coordinate system of each geometrical primitive and then check how close the element is to a certain primitive. Obviously, the finite element is assigned to the closest geometrical approximation primitive with respect to the defined D_{\max} parameter.

Approximation with plane. The approximation with plane primitive is rather simple. The global (3D) to local coordinates of finite element (apparently its nodes) transformation can be done as follows:

$$\begin{aligned} P'_x &= (P_x - r_x) \cdot i'_x + (P_y - r_y) \cdot i'_y + (P_z - r_z) \cdot i'_z \\ P'_y &= (P_x - r_x) \cdot j'_x + (P_y - r_y) \cdot j'_y + (P_z - r_z) \cdot j'_z, \\ P'_z &= (P_x - r_x) \cdot k'_x + (P_y - r_y) \cdot k'_y + (P_z - r_z) \cdot k'_z \end{aligned} \quad (6.2)$$

where $P'(P'_x, P'_y, P'_z)$ - the resulting coordinates of a point in local coordinate system, $P(P_x, P_y, P_z)$ - the given coordinates of this point in global coordinate system, $\bar{i}'(i'_x, i'_y, i'_z)$, $\bar{j}'(j'_x, j'_y, j'_z)$, $\bar{k}'(k'_x, k'_y, k'_z)$ - are the basis unit vectors, which determine the orientation of the local coordinate system relative to global and $\bar{r}(r_x, r_y, r_z)$ - is the vector, which determines the position of the origin of the local coordinate system with respect to the global coordinate system and can be determined as follows:

$$\begin{aligned} r_x &= O'_x \\ r_y &= O'_y, \\ r_z &= O'_z \end{aligned} \quad (6.3)$$

where $O'(O'_x, O'_y, O'_z)$ - the coordinates of origin of local coordinate system (specified in global coordinate system). Schematically it is shown in Fig. 6.4.

It should be noted that the orientation of approximation plane and therefore its local coordinate system is chosen in a way to have a local FE mesh in the plane $X'O'Y'$, so only P'_x and P'_y will be used for the heterogeneity generation procedure. This means that if a point (or node) perfectly corresponds to approximation plane, then anyway $P'_z = 0$. In other case, when the point (or node) does not correspond to approximation plane (if $P'_z \neq 0$), then P'_z is neglected. However, to reach the minimum distortion of generated further heterogeneity it is desirable that the approximation plane should coincide with a local surface of a structure as much as possible.

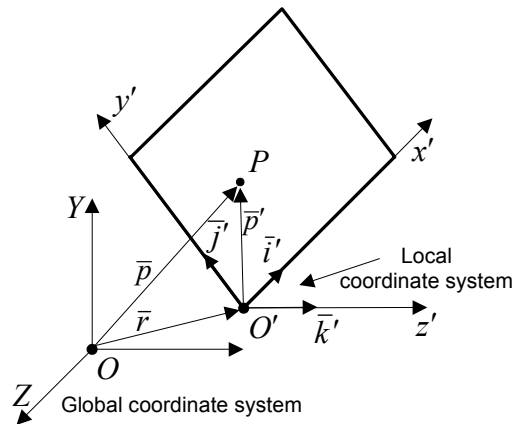


Figure 6.4 Local and global coordinate systems for plane approximation.

Approximation with cylindrical surface. A local cylindrical coordinate system is the basis of such geometrical approximation. Here the 2D heterogeneity should be spread over a cylindrical surface. Due to this, one of the coordinates of heterogeneity which goes along the generatrix curve (arc or circle) of cylindrical surface (see Fig. 6.5) and will be represented by curvilinear coordinate (\tilde{y}), but the other coordinate (\tilde{x}), which goes along directrix line will be linear. The local Cartesian coordinate system hence is chosen to describe the orientation of the cylindrical surface relatively global coordinate system. This allows an easier transformation of the 3D coordinates of the finite elements to a local curvilinear coordinate system $\tilde{O}(\tilde{x}, \tilde{y})$. Thus, first the transformation from global coordinate system to local Cartesian coordinate system should be done using transformation described by Eq. 6.2. The second transformation from local Cartesian coordinate system to curvilinear can be done using the following equation:

$$\begin{aligned} \tilde{P}_x &= P'_x \\ \tilde{P}_y &= R \cdot \arctan\left(\frac{P'_z}{P'_y}\right), \end{aligned} \quad (6.4)$$

where $\tilde{P}(\tilde{P}_x, \tilde{P}_y)$ - the resulting coordinates of a point in local curvilinear coordinate system, R - the radius of cylinder, $P'(P'_x, P'_y, P'_z)$ - the given coordinates of a point in local Cartesian coordinate system. According to the described transformation the 2D heterogeneity can be generated in coordinates $\tilde{O}(\tilde{x}, \tilde{y})$ and will fit on cylindrical surface without any distortions. Schematically it is shown in Fig. 6.5.

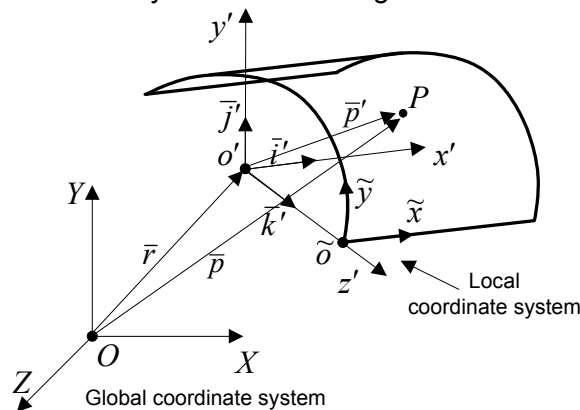


Figure 6.5 Local and global coordinate systems for cylindrical surface approximation.

6.3.2 Detailed description of the approximation procedure

The algorithmic scheme of the approximation procedure is presented in APPENDIX 2. Here the procedure starts from reading of the parameters of the approximation primitives. The parameters are written in an input file PARAMETERS.TXT (see an example in Fig. 6.6). This allows to change them fast and reliable. This file has a fixed format and includes the following parameters:

- a) N – number of primitives. It describes the maximum number of primitives that are used to approximate the structure. This is common a parameter for both types of geometrical approximations;

For the plane approximation primitive:

- b) COORD X, Y, Z – translation of the origin of the local coordinate system (in local coordinate system). This is an additional parameter, which can be used if it is necessary for any reason to shift the origin of the local coordinate system;
- c) ORIGIN OrigNodeNumber – the node number, where the origin of the local coordinate system will be placed;
- d) NODE1 XStart – the node number, which is used for specification of the beginning of X axis of the local coordinate system (N_1);
- e) NODE2 XEnd – the node number, which is used for specification of the end of X axis of the local coordinate system (N_2);
- f) NODE3 YStart – the node number, which is used for specification of the beginning of the pseudo \hat{Y} axis of the local coordinate system (N_3) (pseudo \hat{Y} axis will be described later);
- g) NODE4 YEnd – the node number, which is used for specification of the end of pseudo \hat{Y} axis of the local coordinate system (N_4);

For the cylindrical approximation primitive

- a) described above;
- b) COORD X, Y, Z – translation of the origin of the local coordinate system (in local coordinate system). This is an additional parameter, which can be used if it is necessary for any reason to shift the origin of the local coordinate system;
- c) NODE1 XStart – the node number, which is used for specification of the beginning of X axis of the local coordinate system. This node is also being used to describe an arc of the cylinder (generatrix). It determines the beginning of arc (N_1);
- d) NODE2 XEnd – the node number, which is used for specification of the end of X axis of the local coordinate system and describes the directrix or the cylinder (N_2);
- e) NODE3 ArcMiddle – the node number, which is used to describe the arc of the cylinder (generatrix). It determines the middle of arc (N_3);
- f) NODE4 ArcEnd – the node number, which is used to describe arc of the cylinder (generatrix). It determines the end of arc (N_4);

If more than one approximation primitive is defined in this file (parameter N), then for every primitive parameters b-g (for plane) or b-f (for cylinder) entries in an input text file should be defined.

```

-----Number of new coordinate systems-----
15
-----type of new coordinate system-----
plane
---Nodes---
displacement 1
  -20.00  -20.00   0.00
threshold
15.0
Origin 1
4356
Node 1.1 X axis start
4356
Node 1.2 X axis end
4338
Node 1.3 Y axis start
4363
Node 1.4 Y axis end
4384
-----type of new coordinate system-----
plane
---Nodes---
displacement 2
  -20.00  -20.00   0.00
threshold
10.0
Origin 2
946
Node 2.1 X axis start
946
Node 2.2 X axis end
181
Node 2.3 Y axis start
946
Node 2.4 Y axis end
862

```

Figure 6.6 Example of PARAMETERS.TXT file.

After the parameters of geometrical approximation primitives are read from the file, the transformation of their coordinates can be calculated using the following procedure. At this stage the local coordinate systems of each of specified geometrical approximation primitive have to be determined. Obviously, any local coordinate system can be described by three basis vectors (\bar{i}' , \bar{j}' , \bar{k}') and one point – origin O' . Basis vectors \bar{i}' and \bar{j}' are specified by the user through selection of appropriate two nodes (for each vector) in the FE model. It is important to note that chosen nodes N_1 and N_2 directly define the \bar{i}' vector, but the nodes N_3 , N_4 and N_1 define only a plane in which vector \bar{j}' will be calculated afterwards. Therefore, nodes N_3 and N_4 define only pseudo $\hat{\bar{j}}'$ vector. Thus, the defined plane corresponds to a geometrical approximation primitive (plane type in this case). According to the defined plane the basis vector \bar{k}' can be calculated (as normal vector to the plane). After that, the right \bar{j}' basis vector can be obtained. For the cylindrical primitive the determination of the local coordinate system is more complex. The origin of the local coordinate system has to be placed at the center of the generatrix arc which, however, is not specified by the user, but has to be calculated using three specified finite element nodes. The nodes are chosen so, that they should be located anywhere along the curved surface of the FE model. Using these three nodes (N_2 , N_3 , N_4) the coordinates of center of the generatrix arc O' can be determined as well as its radius (R). One extra node (N_1) is used to determine the directrix line (along $N_1 N_2$) of the cylinder. Mathematically the procedure of

the local coordinate system determination for the plane and cylindrical approximation primitives is described below.

Plane geometrical approximation primitive. Direction of the $\bar{i}'(i'_x, i'_y, i'_z)$ basis vector can be determined as follows:

$$\begin{aligned} i'_x &= \frac{N_{2x} - N_{1x}}{L_i} \\ i'_y &= \frac{N_{2y} - N_{1y}}{L_i}, \\ i'_z &= \frac{N_{2z} - N_{1z}}{L_i} \end{aligned} \quad (6.5)$$

where $N_1(N_{1x}, N_{1y}, N_{1z})$ and $N_2(N_{2x}, N_{2y}, N_{2z})$ - the coordinates of the nodes, entered by user in parameters file, $L_i = \sqrt{(N_{2x} - N_{1x})^2 + (N_{2y} - N_{1y})^2 + (N_{2z} - N_{1z})^2}$ - the distance between of the nodes.

For the plane primitive the second pseudo $\hat{j}'(\hat{j}'_x, \hat{j}'_y, \hat{j}'_z)$ basis vector can be determined using the same technique as for \bar{i}' can be determined as follows:

$$\begin{aligned} \hat{j}'_x &= \frac{N_{4x} - N_{3x}}{L_j} \\ \hat{j}'_y &= \frac{N_{4y} - N_{3y}}{L_j}, \\ \hat{j}'_z &= \frac{N_{4z} - N_{3z}}{L_j} \end{aligned} \quad (6.6)$$

where $N_3(N_{3x}, N_{3y}, N_{3z})$ and $N_4(N_{4x}, N_{4y}, N_{4z})$ - the coordinates of the nodes, entered by user in parameters file, $L_j = \sqrt{(N_{4x} - N_{3x})^2 + (N_{4y} - N_{3y})^2 + (N_{4z} - N_{3z})^2}$ - the distance between the nodes. This vector is called pseudo \hat{j}' because the nodes N_3 and N_4 (chosen by user) are only supposed to be located in one plane with nodes N_1 and N_2 , determining the desired orientation of the plane primitive (but not actual axis direction). Thus the basis vector \bar{i}' and pseudo \hat{j}' may not have the right angle between them (90°) (see Fig. 6.7). However, this vector is necessary for the determination of the right third $\bar{k}'(k'_x, k'_y, k'_z)$ basis vector of local coordinate system. It can be determined via the cross product as follows:

$$\bar{k}' = \bar{i}' \times \hat{j}'. \quad (6.7)$$

And finally, the determination of the \bar{j}' basis vector to form the right hand triple can be done as follows:

$$\bar{j}' = \bar{k}' \times \bar{i}'. \quad (6.8)$$

The origin of the local coordinate system $O'(O'_x, O'_y, O'_z)$ is specified by the node *OrigNodeNumber* (entered by user) in the input file. Finally, the transformation of coordinates of nodes of any finite element to the local coordinate system of approximation primitive can be done using Eq. 6.2 and 6.3. Schematically the described procedure is presented in Fig. 6.7.

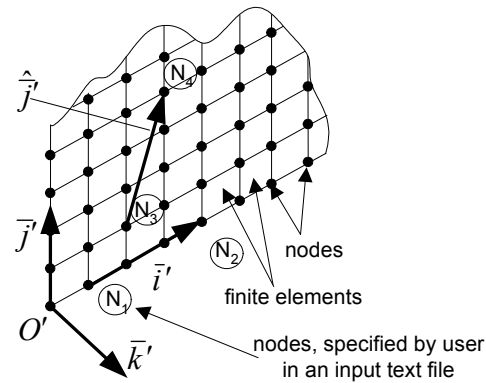


Figure 6.7 Construction of the local coordinate system for plane geometrical approximation primitive using finite element mesh.

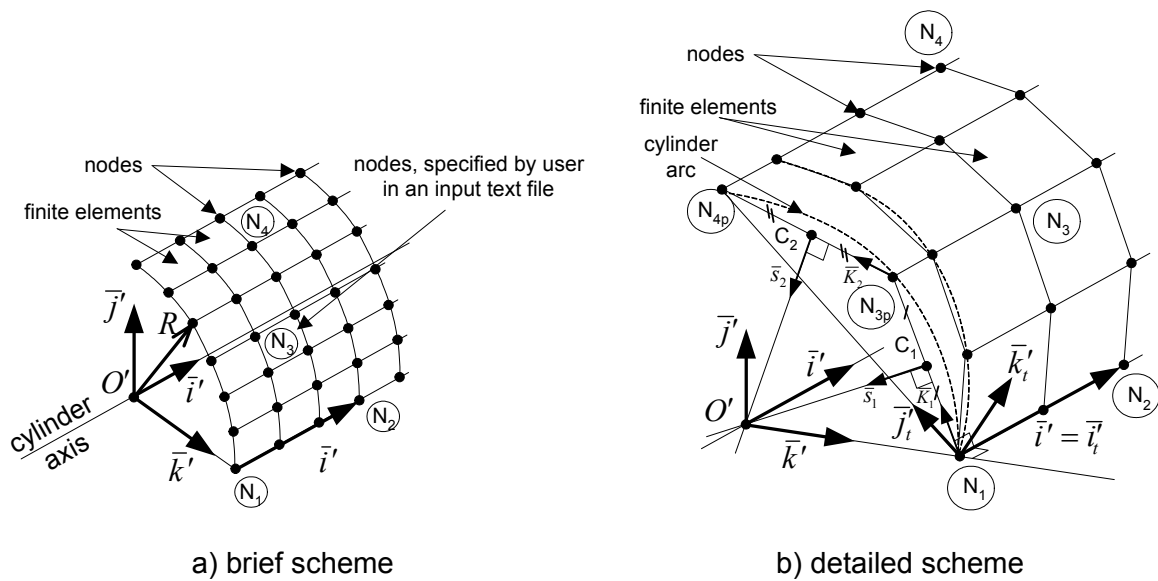


Figure 6.8 Construction of the local coordinate system for cylindrical geometrical approximation primitive using finite element mesh.

Cylindrical geometrical approximation primitive. The construction of the local coordinate system for cylindrical geometrical approximation primitive is more complex, since it is necessary to determine the origin of the cylinder generatrix (arc). The procedure is schematically presented in Fig. 6.8. The basis vector $\vec{i}'(i'_x, i'_y, i'_z)$ of the local coordinate system can be calculated using nodes N_1 and N_2 specified by user with the help of Eq. 6.5. In fact, this vector has been chosen to determine the direction of the axis and directrix line of the cylinder. The radius and origin of the cylinder generatrix arc can be determined using three points (nodes N_1, N_3 and N_4 specified by user), which however, should not lie on one line. Thus, the nodes N_1, N_3 and N_4 (further they will be called points) are freely chosen on that surface of FE model which is supposed to be approximated with cylindrical geometrical primitive. Obviously, they usually are not located in the plane perpendicular to the axis $\vec{i}'(i'_x, i'_y, i'_z)$ of the cylinder. Therefore the parameters of the arc cannot be directly determined. That is why it is necessary to project these points in the plane perpendicular to the directrix line of the cylinder. The plane which goes through the point $N_1(N_{1x}, N_{1y}, N_{1z})$ with normal vector equal to known $\vec{i}'(i'_x, i'_y, i'_z)$ can be used. Thus the projections of these points to that plane can be done as follows:

$$\begin{aligned}
 N_{3px} &= N_{3x} - i'_x \cdot D_{3p} \\
 N_{3py} &= N_{3y} - i'_y \cdot D_{3p} , \\
 N_{3pz} &= N_{3z} - i'_z \cdot D_{3p}
 \end{aligned} \tag{6.9}$$

$$\begin{aligned}
 N_{4px} &= N_{4x} - i'_x \cdot D_{4p} \\
 N_{4py} &= N_{4y} - i'_y \cdot D_{4p} , \\
 N_{4pz} &= N_{4z} - i'_z \cdot D_{4p}
 \end{aligned} \tag{6.10}$$

where

$$D_{3p} = i'_x(N_{3x} - N_{1x}) + i'_y(N_{3y} - N_{1y}) + i'_z(N_{3z} - N_{1z}), \tag{6.11}$$

$$D_{4p} = i'_x(N_{4x} - N_{1x}) + i'_y(N_{4y} - N_{1y}) + i'_z(N_{4z} - N_{1z}), \tag{6.12}$$

where D_{3p} and D_{4p} - the distances from the points N_3 and N_4 to the plane, $N_3(N_{3x}, N_{3y}, N_{3z})$, $N_4(N_{4x}, N_{4y}, N_{4z})$ - the coordinates of these points, $N_{3p}(N_{3px}, N_{3py}, N_{3pz})$, $N_{4p}(N_{4px}, N_{4py}, N_{4pz})$ - the projections coordinates of the points at the plane. Now, as a result, points N_1 , N_{3p} and N_{4p} are in the plane with normal $\bar{i}'(i'_x, i'_y, i'_z)$ (see Fig. 6.8b).

The center of generatrix arc and the radius of its curvature now can be determined using points N_1 , N_{3p} and N_{4p} . The two spans can be drawn between these points: N_1N_{3p} and $N_{3p}N_{4p}$. The center of the arc therefore is at the intersection of normal lines drawn from the middle points of these spans (see Fig. 6.8b). The middle point of spans N_1N_{3p} and $N_{3p}N_{4p}$ can be determined as follows:

$$\begin{aligned}
 C_{1x} &= \frac{N_{1x} + N_{3px}}{2} \\
 C_{1y} &= \frac{N_{1y} + N_{3py}}{2} , \\
 C_{1z} &= \frac{N_{1z} + N_{3pz}}{2}
 \end{aligned} \tag{6.13}$$

$$\begin{aligned}
 C_{2x} &= \frac{N_{3px} + N_{4px}}{2} \\
 C_{2y} &= \frac{N_{3py} + N_{4py}}{2} . \\
 C_{2z} &= \frac{N_{3pz} + N_{4pz}}{2}
 \end{aligned} \tag{6.14}$$

Any line can be represented by directing vector and coordinates of one point through which it goes. It appears that the spans N_1N_{3p} and $N_{3p}N_{4p}$ are located in the plane with normal vector \bar{i}' . Thus, determination of the normal lines to these spans can be done by taking a cross product of spans directing vectors (\bar{K}_1 and \bar{K}_2 correspondingly) and vector \bar{i}' . The resulting vectors \bar{s}_1 and \bar{s}_2 are the directing vectors of the perpendiculars. The directing vectors of spans are:

$$\begin{aligned}
 K_{1x} &= \frac{N_{3px} - N_{1x}}{L_{ch1}} \\
 K_{1y} &= \frac{N_{3py} - N_{1y}}{L_{ch1}}, \\
 K_{1z} &= \frac{N_{3pz} - N_{1z}}{L_{ch1}}
 \end{aligned} \tag{6.15}$$

$$\begin{aligned}
 K_{2x} &= \frac{N_{4px} - N_{3px}}{L_{ch2}} \\
 K_{2y} &= \frac{N_{4py} - N_{3py}}{L_{ch2}}, \\
 K_{2z} &= \frac{N_{4pz} - N_{3pz}}{L_{ch2}}
 \end{aligned} \tag{6.16}$$

where

$$L_{ch1} = \sqrt{(N_{3px} - N_{1x})^2 + (N_{3py} - N_{1y})^2 + (N_{3pz} - N_{1z})^2}, \tag{6.17}$$

$$L_{ch2} = \sqrt{(N_{4px} - N_{3px})^2 + (N_{4py} - N_{3py})^2 + (N_{4pz} - N_{3pz})^2}. \tag{6.18}$$

The directing vectors of perpendiculars are as follows:

$$\bar{s}_1 = \bar{K}_1 \times \bar{i}', \tag{6.19}$$

$$\bar{s}_2 = \bar{K}_2 \times \bar{i}'. \tag{6.20}$$

The determined perpendiculars appear to be located in one plane with normal vector equal to \bar{i}' . All the coordinates are three dimensional. Thus, theoretically it is possible to find the point of intersection. However, due to numerical errors the finding of intersection of two lines in space is not sufficiently accurate. Therefore, it is better to transform the task into a plane to increase the accuracy of this procedure and to avoid unforeseen circumstances of its numerical implementation.

The transformation can be done using a temporary local coordinate system with basis $\bar{i}'_t, \bar{j}'_t, \bar{k}'_t$. The origin of this coordinate system corresponds to point N_1 . This coordinate system has to be chosen in a way that vectors \bar{s}_1 and \bar{s}_2 should be in plane $X'_tO'_tY'_t$. It is already known that the vectors \bar{s}_1 and \bar{s}_2 are in the plane with known normal vector \bar{i}' , thus:

$$\bar{i}'_t = \bar{i}'. \tag{6.21}$$

The second pseudo basis vector $\hat{j}'_t(\hat{j}'_{tx}, \hat{j}'_{ty}, \hat{j}'_{tz})$ can be determined using points (N_1 and N_{4p}) which are in one plane with \bar{s}_1 and \bar{s}_2 as follows:

$$\begin{aligned}
 \hat{j}'_{tx} &= \frac{N_{4px} - N_{1x}}{L_{jt}} \\
 \hat{j}'_{ty} &= \frac{N_{4py} - N_{1y}}{L_{jt}}, \\
 \hat{j}'_{tz} &= \frac{N_{4pz} - N_{1z}}{L_{jt}}
 \end{aligned} \tag{6.22}$$

where $L_{jt} = \sqrt{(N_{4px} - N_{1x})^2 + (N_{4py} - N_{1y})^2 + (N_{4pz} - N_{1z})^2}$ - the distance between the points. This vector is called pseudo \hat{j}'_t because the points N_1 and N_{4p} are supposed to lie in one plane perpendicular to the vector \bar{i}'_t . Thus the basis vector \bar{i}'_t and pseudo \hat{j}'_t might not have between them the angle of 90° . However, this vector is necessary for determination of the right third $\bar{k}'_t(k'_{tx}, k'_{ty}, k'_{tz})$ basis vector for temporary local coordinate system, so that basis vectors $\bar{i}'_t, \bar{j}'_t, \bar{k}'_t$ form a right-hand triple. It can be determined as follows:

$$\bar{k}'_t = \bar{i}'_t \times \hat{j}'_t. \tag{6.23}$$

And finally, the determination of the right \bar{j}'_t temporary basis vector can be done as follows:

$$\bar{j}'_t = \bar{k}'_t \times \bar{i}'_t. \tag{6.24}$$

As a result the temporary local coordinate system is defined in such a way that vectors \bar{s}_1, \bar{s}_2 and points C_1, C_2 are all located in the plane with normal \bar{i}'_t (see Fig. 6.8b).

Further, the necessary transformation of vectors \bar{s}_1 and \bar{s}_2 , points C_1 and C_2 as well as coordinates of the origin N_1 to the local temporary basis vectors $\bar{i}'_t, \bar{j}'_t, \bar{k}'_t$ can be done using the following equation:

$$\begin{aligned}
 a'_{tx} &= a_x \cdot i'_{tx} + a_y \cdot i'_{ty} + a_z \cdot i'_{tz} \\
 a'_{ty} &= a_x \cdot j'_{tx} + a_y \cdot j'_{ty} + a_z \cdot j'_{tz}, \\
 a'_{tz} &= a_x \cdot k'_{tx} + a_y \cdot k'_{ty} + a_z \cdot k'_{tz}
 \end{aligned} \tag{6.25}$$

where the corresponding input coordinates of the vectors and points should be put in place of a_x, a_y, a_z in right part of the equation. The resulting coordinates of \bar{s}'_{1t} and \bar{s}'_{2t} , points C'_{1t}, C'_{2t} and N'_{1t} are being calculated at the left side of the equation as $a'_{tx}, a'_{ty}, a'_{tz}$.

The x-component of coordinates (abscissas) of the $\bar{s}'_{1t}, \bar{s}'_{2t}, C'_{1t}, C'_{2t}$ and N'_{1t} is equal to 0 in local temporary coordinate system due to the fact that initial vectors \bar{s}_1, \bar{s}_2 and points C_1, C_2 are located in one plane with normal \bar{i}'_t . Therefore, the intersection point of the lines with directing vectors $\bar{s}'_{1t}, \bar{s}'_{2t}$, which goes through points C'_{1t} and C'_{2t} correspondingly can be calculated by using the following equations:

$$\begin{aligned}
 a_1 &= s'_{1tz} \\
 b_1 &= -s'_{1ty} \\
 c_1 &= s'_{1ty} \cdot C'_{1tz} - s'_{1tz} \cdot C'_{1ty}
 \end{aligned} \tag{6.26}$$

$$\begin{aligned}
 a_2 &= s'_{2tz} \\
 b_2 &= -s'_{2ty} \\
 c_2 &= s'_{2ty} \cdot C'_{2tz} - s'_{2tz} \cdot C'_{2ty}
 \end{aligned} \quad , \quad (6.27)$$

$$\begin{aligned}
 O'_{tx} &= N'_{1tx} \\
 O'_{ty} &= \frac{b_1 \cdot c_2 - b_2 \cdot c_1}{a_1 \cdot b_2 - a_2 \cdot b_1} \\
 O'_{tz} &= \frac{c_1 \cdot a_2 - c_2 \cdot a_1}{a_1 \cdot b_2 - a_2 \cdot b_1}
 \end{aligned} \quad (6.28)$$

where $O'_t(O'_{tx}, O'_{ty}, O'_{tz})$ are the resulting coordinates of the lines intersection point (calculated in temporary local basis). Point O'_t is the center of the generatrix arc specified by three points N_1 , N_{3p} and N_{4p} . The reverse coordinates transformation can be applied in order to transform the coordinates of this point into the global coordinate system (coordinate system of the FE model):

$$\begin{aligned}
 O'_x &= O'_{tx} \cdot i'_{tx} + O'_{ty} \cdot j'_{tx} + O'_{tz} \cdot k'_{tx} \\
 O'_y &= O'_{tx} \cdot i'_{ty} + O'_{ty} \cdot j'_{ty} + O'_{tz} \cdot k'_{ty} \\
 O'_z &= O'_{tx} \cdot i'_{tz} + O'_{ty} \cdot j'_{tz} + O'_{tz} \cdot k'_{tz}
 \end{aligned} \quad (6.29)$$

where, $O'(O'_x, O'_y, O'_z)$ - the coordinates of the center of the generatrix arc in global coordinate system. This point can be also used as the origin for local coordinate system of cylindrical geometrical primitive approximation. The radius of the cylinder can be determined using the following equation:

$$R = \sqrt{(N_{1x} - O'_x)^2 + (N_{1y} - O'_y)^2 + (N_{1z} - O'_z)^2} \quad (6.30)$$

The description of the cylindrical primitive is now completed. The line drawn through point $O'(O'_x, O'_y, O'_z)$ with the directing vector $\bar{i}'(i'_x, i'_y, i'_z)$ is taken as the axis of the cylindrical surface with radius R . The determination of the rest basis vectors of local coordinate system for cylindrical approximation primitive can be calculated as follows:

$$\begin{aligned}
 k'_x &= \frac{N_{1x} - O'_x}{L_k} \\
 k'_y &= \frac{N_{1y} - O'_y}{L_k} \\
 k'_z &= \frac{N_{1z} - O'_z}{L_k}
 \end{aligned} \quad (6.31)$$

where $O'(O'_x, O'_y, O'_z)$ - the coordinates of the determined origin of the local coordinate system (in global coordinate system), N_1 - the coordinates of the user's specified node in the FE mesh, $L_k = R$ (determined in Eq. 6.30) - the distance between the local coordinate origin and the node N_1 . The last \bar{j}' basis vector can be determined using Eq. 6.8.

Finally the desired transformation of finite element nodes coordinates from the global coordinate system to the local for cylindrical primitive approximation can be done using Eq. 6.2 and Eq. 6.3 with the determined basis vectors $\bar{i}'(i'_x, i'_y, i'_z)$, $\bar{j}'(j'_x, j'_y, j'_z)$, $\bar{k}'(k'_x, k'_y, k'_z)$ and $\bar{r}(r_x, r_y, r_z)$.

Determination of the local coordinate systems of all approximation primitives that have been specified in an input file to approximate the FE model has to be done. After that each finite element should be checked as to which particular approximation primitive it belongs. It can be done through determination of the closest to a finite element approximation primitive. In other words, the distance from the finite element to every approximation primitive has to be determined. The shortest distance can be used as a sign to associate a finite element with a certain primitive. The reliable method is to use the center of gravity of a finite element for that purpose.

6.3.3 Association of finite elements to the geometrical primitives

The global coordinates of the center of gravity (C) of finite elements are determined from the available FE mesh. They should be transformed into the determined local coordinate system of each geometrical approximation primitive (C'). The coordinates transformation can be done using Eq. 6.2 and Eq. 6.3 for each approximation primitive with the determined basis vectors \bar{i}' , \bar{j}' , \bar{k}' of its local coordinate system. A shortest distance from the center of gravity of a finite element determined in the local coordinate system of the geometrical approximation primitive C' can be used as a parameter for association. This distance is determined between the center of gravity of finite element C' and its projection to the surface (plane or cylinder) C_p in the direction of its normal. Geometrical approximation primitive to which the determined distance is minimal is considered as the closest and then, the finite element is assigned to that particular primitive.

Distance to the plane geometrical approximation primitive. The distance from the center of gravity C' of a finite element to the plane approximation primitive can be calculated as follows:

$$D_{plane} = |k'_x \cdot (C'_x - O'_x) + k'_y \cdot (C'_y - O'_y) + k'_z \cdot (C'_z - O'_z)|, \quad (6.32)$$

where $C'(C'_x, C'_y, C'_z)$ - the coordinates of the center of gravity of a finite element in local coordinate system of a geometrical approximation primitive, $\bar{k}'(k'_x, k'_y, k'_z)$ - the normal vector of the plane (here it is equal to the \bar{k}' basis vector in local coordinate system), $O'(O'_x, O'_y, O'_z)$ - the coordinates of the origin of the plane primitive (specified as a FE node in the parameters text file). Schematically it can be represented as the distance from point C' (center of gravity of finite element in local coordinate system) to its normal projection to plane (C_p) (see Fig. 6.9a).

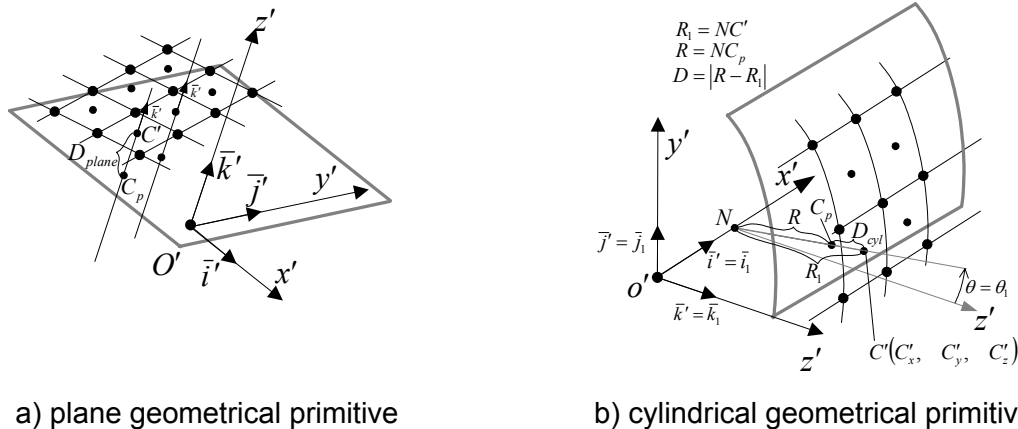


Figure 6.9 Determination of the distance between center of gravity of a finite element and approximation primitive.

Distance to the cylindrical geometrical approximation primitive. The determination of the distance from the center of gravity of a finite element to a cylindrical primitive is more complex. However, it is also based on finding of normal projection of its center of gravity C' to a cylindrical surface C_p (see Fig. 6.9b). Suppose, the center of gravity of element is located on a cylindrical surface with radius R_1 and its local coordinate system $(\bar{i}'_1, \bar{j}'_1, \bar{k}'_1)$ coincide with that local one $(\bar{i}', \bar{j}', \bar{k}')$, then the coordinates of the center of gravity C' in local cylindrical coordinate system can be determined as follows:

$$\begin{cases} R_1 = \sqrt{C_y'^2 + C_z'^2} \\ \theta_1 = \arctan\left(\frac{C_y'}{C_z'}\right), \end{cases} \quad (6.33)$$

where $C'(C'_x, C'_y, C'_z)$ - the coordinates of the center of gravity of a finite element in the local Cartesian coordinate system of the cylindrical geometrical primitive with the basis $(\bar{i}', \bar{j}', \bar{k}')$ (determined by Eq. 6.2). It is obvious that the cylindrical coordinate θ and X coordinates of the projection point C_p are equal to corresponding coordinates of the center of gravity C' . Thus, $\theta_1 = \theta$ and $X_1 = X$, but the $R_1 \neq R$ because the radii are different. Then, the distance from the center of gravity C' to its projection point on the surface C_p can be determined as the difference in radii as follows:

$$D_{cyl} = |R - R_1|. \quad (6.34)$$

Thus, the distances between the center of gravity of a finite element and every specified approximation primitive can be determined. It can be done for all specified approximation primitives. Then, a finite element should be attached to the closest approximation primitive where D_{plane} or $D_{cyl} = \min\{D_i\}$, where $i = 1..n$. The parameter D_{max} is considered for each of the geometrical approximation primitives. If $D_i > D_{max}$, then the element remains unassigned and therefore the value of the heterogeneity function for that element will be equal to zero.

It should be noted that the finite element implementation of approximations is totally the user's decision. Thus, before the run of FE analysis it is necessary to decide how to approximate the complex structure with the geometrical approximation primitives. Following questions should be raised: Which geometrical primitives should be chosen? What is the location of their local coordinate systems? What are the heterogeneity parameters for each geometrical approximation primitive? Only when all the questions are answered and required parameters are determined then the generation of the heterogeneous material properties can be successfully performed.

6.3.4 Heterogeneity generation procedure

The heterogeneity generation procedure is implemented according to the description in Chapter 4 of this thesis. The algorithm of this procedure is presented in APPENDIX 3. The parameters of heterogeneity are defined in an input text file HETEROGENEITY.TXT, which should be composed before running the simulation. This file has a fixed format and contains the following parameters:

- a) NPrimitive – the number of geometrical approximation primitives used in the model (see previous section);
- b) DIM X,Y – the maximum dimensions of the geometrical primitive, necessary for heterogeneity generation to set up the boundaries;

- c) NOrder – the number of the low-order heterogeneities to be used for high-order heterogeneity generation;
- d) SIZE Mean, Std – the size parameter, consisting of two components: L^l - the mean size and L_{std}^l - standard deviation of size. These values have to be entered for each l^{th} low-order heterogeneity (specified by “NOrder” parameter);
- e) AMPL Mean, Std – the amplitude consisting of two components: A^l - the mean size and A_{std}^l - standard deviation of size. These values have to be entered for each l^{th} low-order heterogeneity (specified by “NOrder” parameter);

Thus, if more than one geometrical approximation primitive have been specified all the parameters (positions b) - e) from the list in above) should be entered. If more than one low-order heterogeneity are specified (“NOrder” parameter), then for each low-order heterogeneity the same number of parameters “SIZE Mean, Std” and “AMPL Mean, Std” (positions d) - e) from the list in above) should be entered. These parameters are determined from spectral analysis of composite materials (see Table 3.3 in Chapter 3). An example of input file HETEROGENEITY.TXT is presented in Fig. 6.10

```

#Number of surfaces
22
----- SURFACE 1 -----
#maximum surface dimensions
X      70.0
Y     140.0
#Number of harmonics
2
#Length 1
23.43
#Deviation of length 1
3.87
#Amplitude 1
0.27
#Deviation of Amplitude 1
0.15
#Length 2
13.57
#Deviation of length 2
1.81
#Amplitude 2
0.43
#Deviation of Amplitude 2
0.1
----- SURFACE 2 -----
#maximum surface dimensions
X     190.0
Y     130.0
#Number of waves
2
#Length 1
23.43
#Deviation of length 1
3.87
#Amplitude 1
0.27
#Deviation of Amplitude 1
0.15
#Length 2
13.57
#Deviation of length 2
1.81
#Amplitude 2
0.43
#Deviation of Amplitude 2
0.1

```

Figure 6.10 Example of HETEROGENEITY.TXT file.

Origins of heterogeneity primitives' allocation. After all the necessary information has been read from the input file it is possible to define the grid for each of the low-order heterogeneities in every geometrical approximation primitive. The nodes of the grid will be used as origins for the heterogeneity primitives (hump or cavity). The grid is regular in both directions (see Fig. 4.3) and it is generated using the “SIZE Mean” parameter L^l . The grid is specified in local coordinate system of an approximation primitive (Cartesian $O'(x', y')$ for a plane, Fig. 6.4 and curvilinear $\tilde{O}'(\tilde{x}', \tilde{y}')$ for a cylindrical geometrical approximation primitive, Fig. 6.5). The number of the grid nodes in both directions can be determined from the “DIM X,Y” parameters, which explicitly specify the physical dimensions of a locally defined geometrical approximation primitive. The coordinates of the grid nodes can be determined by using the following equation:

$$\begin{aligned} T_{ij_x}^l &= 2L^l \cdot i \\ T_{ij_y}^l &= 2L^l \cdot j \end{aligned} \quad (6.35)$$

where L^l – the mean size of the l -th low-order heterogeneity (in other words l -th harmonic) read from parameters file (“SIZE Mean” parameter), i, j - the indexes which determine the column and row (along abscissa and ordinate, correspondingly) of the grid node. Note that their maximum number is limited by the “DIM X,Y” parameters. If more than one of the low-order heterogeneities is used the grid is generated for each of heterogeneities separately with different parameters in different harmonics (multi-harmonic grid) (see an example in Fig. 6.11).

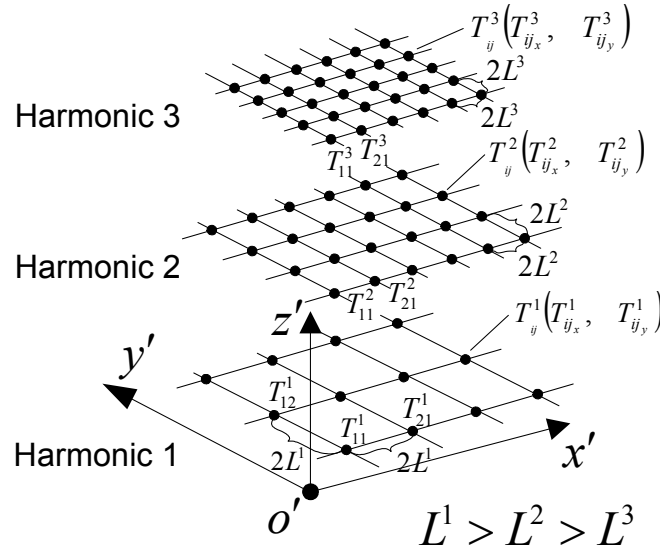


Figure 6.11 Multi-harmonic grid along approximation primitive.

Stochastic generation of heterogeneity primitives' parameters. The grid nodes are used as the origins for heterogeneity primitives. The shape (size and amplitude) of the heterogeneity primitives is according to Eq. 5.3. The parameters of the shape are stochastically generated for all heterogeneity primitives in each harmonic along the defined geometrical approximation primitive. The parameters “SIZE Mean, Std” and “AMPL Mean, Std”, obtained from the input file, are used for generation. The Gaussian (normal) distribution has been used. If more than one of low-order heterogeneities (harmonics) is used then the stochastic generation of its parameters is performed for each harmonic separately. As a

result, the size L_{ij}^l and the corresponding amplitude A_{ij}^l as the parameters of the shape function of the heterogeneity primitive (see Eq. 5.3) at (i, j) -th grid node in l -th low-order heterogeneity are generated. This procedure is repeated for all specified all low-order harmonics. As a result the individual set of parameters L_{ij}^l and A_{ij}^l is attached to each grid node $T_{ij}^l(T_{ij_x}^l, T_{ij_y}^l)$.

The sum of all harmonics of the low-order heterogeneities constitutes the high-order (multi-harmonic) heterogeneity (see the definition in Chapter 5). The resulting heterogeneity is generated in local 2D coordinate system of the geometrical approximation primitive (Cartesian $O'(x', y')$ for a plane and curvilinear $\tilde{O}'(\tilde{x}', \tilde{y}')$ for a cylindrical).

6.3.5 Appropriation of properties of the finite elements according to generated heterogeneity

The generated heterogeneity is a complex function which has different values at different locations along the surface of the geometrical approximation primitive. The values of the function determine a hypothetic property of finite elements. A hypothetic property can be in range of $-1 \dots +1$. This property later can be easily correlated to a real mechanical property of finite elements.

In previous section each finite element present in FE model is associated with a particular geometrical approximation primitive. Since the heterogeneity in each geometrical approximation primitive is determined within its local coordinate system, it is necessary to determine the coordinates of a finite element in that local coordinate system. The location of a finite element (eventually coordinates of its nodes), which is associated with a plane geometrical approximation primitive can be determined by using Eq. 6.2 and Eq. 6.3. If a finite element is associated with a cylindrical geometrical primitive, the determination of its location can be done by using Eq. 6.2 and Eq. 6.3 and Eq. 6.4.

The value of heterogeneity function at a particular finite element depends on the location of that element in a local coordinate system of an associated approximation primitive. Since triangle or quadrilateral finite elements have certain area, the properties of such finite elements cannot be determined by determining the value of heterogeneity function in one point only, but it should be determined as an integral value over the whole area of the finite element. The value of heterogeneity function at any point which is in the area of the finite element can be determined by coordinates of that point in local coordinate system of geometrical primitive, where this function is generated. Such determination cannot give a reliable result of the hypothetical properties for the entire finite element. Due to this an integral hypothetical property can be used. The integral hypothetical property of a finite element requires integration of heterogeneity function over area of a finite element. However, due to complexity of the heterogeneity function a large amount of calculations is required, which is rather difficult to be performed. Therefore, in order to reduce calculation complexity a pseudo-integration procedure is proposed.

The pseudo-integration procedure uses the principle of averaging values of heterogeneity function determined at several points located in the area of a finite element. Unlike integration, where infinite amount of points is used, the pseudo-integration procedure operates with the finite amount of points, the so-called sub-points. These points are regularly distributed in the area of the element. Such procedure essentially reduces the calculation complexity and, without a large effect on the accuracy of the result.

The number of sub-points necessary to reach sufficient accuracy depends on the size of finite element and, of course, on the scale of the generated high-order heterogeneity, i.e. L^l parameters. Thus, a bigger finite element usually requires more sub-points. And if in the generated high-order heterogeneity there are low-order heterogeneities with small size (L^l) (less or at the same level as the scale of the finite element) then, the number of sub-points should be also increased in order to increase the accuracy.

The procedure of determination of sub-points location in a finite element is schematically presented in Fig. 6.12. According to this procedure the sides of a finite element are subdivided into D equal parts by primary sub-points $n_1^s, n_2^s, \dots, n_i^s, \dots, n_D^s$, where i – is the point number, s – is the finite element side identifier (for triangle finite element $s=1\dots3$, for quadrilateral finite element $s=1\dots4$) and D - is the sub-division factor, which user has to specify. Then, for quadrilateral finite element the lines are drawn through the corresponding primary sub-points on the opposite sides of the element. The intersection of these lines gives the coordinates for the secondary sub-points, which are located inside the element area. The coordinates of the secondary sub-point can be calculated as follows:

$$\begin{aligned} a_1 &= P_{2y} - P_{1y} \\ b_1 &= P_{1x} - P_{2x} \\ c_1 &= P_{1y} \cdot P_{2x} - P_{1x} \cdot P_{2y} \end{aligned} \quad , \quad (6.36)$$

$$\begin{aligned} a_2 &= P_{4y} - P_{3y} \\ b_2 &= P_{3x} - P_{4x} \\ c_2 &= P_{3y} \cdot P_{4x} - P_{3x} \cdot P_{4y} \end{aligned} \quad , \quad (6.37)$$

$$\begin{aligned} M_x^{(p,r)} &= \frac{b_1 \cdot c_2 - b_2 \cdot c_1}{a_1 \cdot b_2 - a_2 \cdot b_1} \\ M_y^{(p,r)} &= \frac{c_1 \cdot a_2 - c_2 \cdot a_1}{a_1 \cdot b_2 - a_2 \cdot b_1} \end{aligned} \quad , \quad (6.38)$$

where P_1P_2 and P_3P_4 are the intersecting segments with coordinates of the ends $P_1(P_{1x}, P_{1y})$, $P_2(P_{2x}, P_{2y})$ and $P_3(P_{3x}, P_{3y})$, $P_4(P_{4x}, P_{4y})$ which coincide with the corresponding primary sub-points n_i^s according to Fig. 6.13, and $M^{(p,r)}(M_x^{(p,r)}, M_y^{(p,r)})$ - the resulting coordinates of the sub-point, where indexes $p=1\dots(D+1)$ and $r=1\dots(D+1)$. Equations 6.36 – 6.38 are used for all defined segments on sides of a finite element. The similar principle is used to determine the sub-points for triangle finite element.

It should be noted that all secondary sub-points as well as all primary sub-points are used for pseudo-integral hypothetical property determination of a finite element. The resulting coordinates of all sub-points are determined in the local coordinate system of geometrical approximation primitive, which corresponds to the coordinate system of the generated heterogeneity. Therefore, the value of low-order heterogeneity function at each of sub-points $M^{(p,r)}$ can be determined as follows:

$$h^{l,(p,r)} = \sum_{i=1}^{i_{\max}^l} \sum_{j=1}^{j_{\max}^l} \begin{cases} \pm \frac{A_{ij}^l}{2} \cos\left(\pi \frac{2\rho_{ij}^{l,(p,r)}}{L_{ij}^l} + 1\right), & -L_{ij}^l \leq \rho_{ij}^{l,(p,r)} \leq L_{ij}^l \\ 0, & \rho_{ij}^{l,(p,r)} < -L_{ij}^l, \rho_{ij}^{l,(p,r)} > L_{ij}^l \end{cases} \quad , \quad (6.39)$$

where $h^{l,(p,r)}$ - the value of low-order heterogeneity function at the $M^{(p,r)}$ sub-point in l -th low-order heterogeneity, L_{ij}^l and A_{ij}^l - the size and amplitude of the shape function (randomly generated) at (i, j) -th origin in l -th low-order heterogeneity. It should be noted that i_{\max}^l, j_{\max}^l are different for every low-order heterogeneity (l). They can be determined using the following equations:

$$i_{\max}^l = \text{abs}\left(\frac{DIM_x}{L^l}\right), \quad (6.40)$$

$$j_{\max}^l = \text{abs}\left(\frac{DIM_y}{L^l}\right), \quad (6.41)$$

where DIM_x and DIM_y – the specified dimensions of the geometrical approximation primitive in X and Y direction correspondingly (specified in an input file), L^l – the mean size of the heterogeneity primitives in l -th low-order heterogeneity (specified in an input file). The sign of the shape function (see Eq. 6.39) is positive at the (i, j) -th origin where $(i + j)$ is even number, otherwise the sign is negative, $\rho_{ij}^{l,(p,r)}$ – the distance from the $M^{(p,r)}$ sub-point to the (i, j) origin in l -th low-order heterogeneity which can be determined as follows (for both plane and cylindrical geometrical approximation primitive):

$$\rho_{ij}^{l,(p,r)} = \sqrt{\left(M_x^{(p,r)} - T_{ij_x}^l\right)^2 + \left(M_y^{(p,r)} - T_{ij_y}^l\right)^2}, \quad (6.42)$$

where $M^{(p,r)}(M_x^{(p,r)}, M_y^{(p,r)})$ is the coordinates of a sub-point and $T_{ij}^l(T_{ij_x}^l, T_{ij_y}^l)$ is the coordinates of the (i, j) -th grid node in l -th low-order heterogeneity.

The total value of high-order heterogeneity function at any of sub-points can be determined by using the following equation:

$$h^{(p,r)} = \sum_{l=1}^{NOrder} h^{l,(p,r)}, \quad (6.43)$$

where $h^{l,(p,r)}$ - the value of low-order heterogeneity function at the sub-point in l -th low-order heterogeneity, $NOrder$ – number of low-order heterogeneities, in other words harmonics, D - is the finite element sub-division factor. Then, the pseudo-integral hypothetic property of finite element can be calculated as follows:

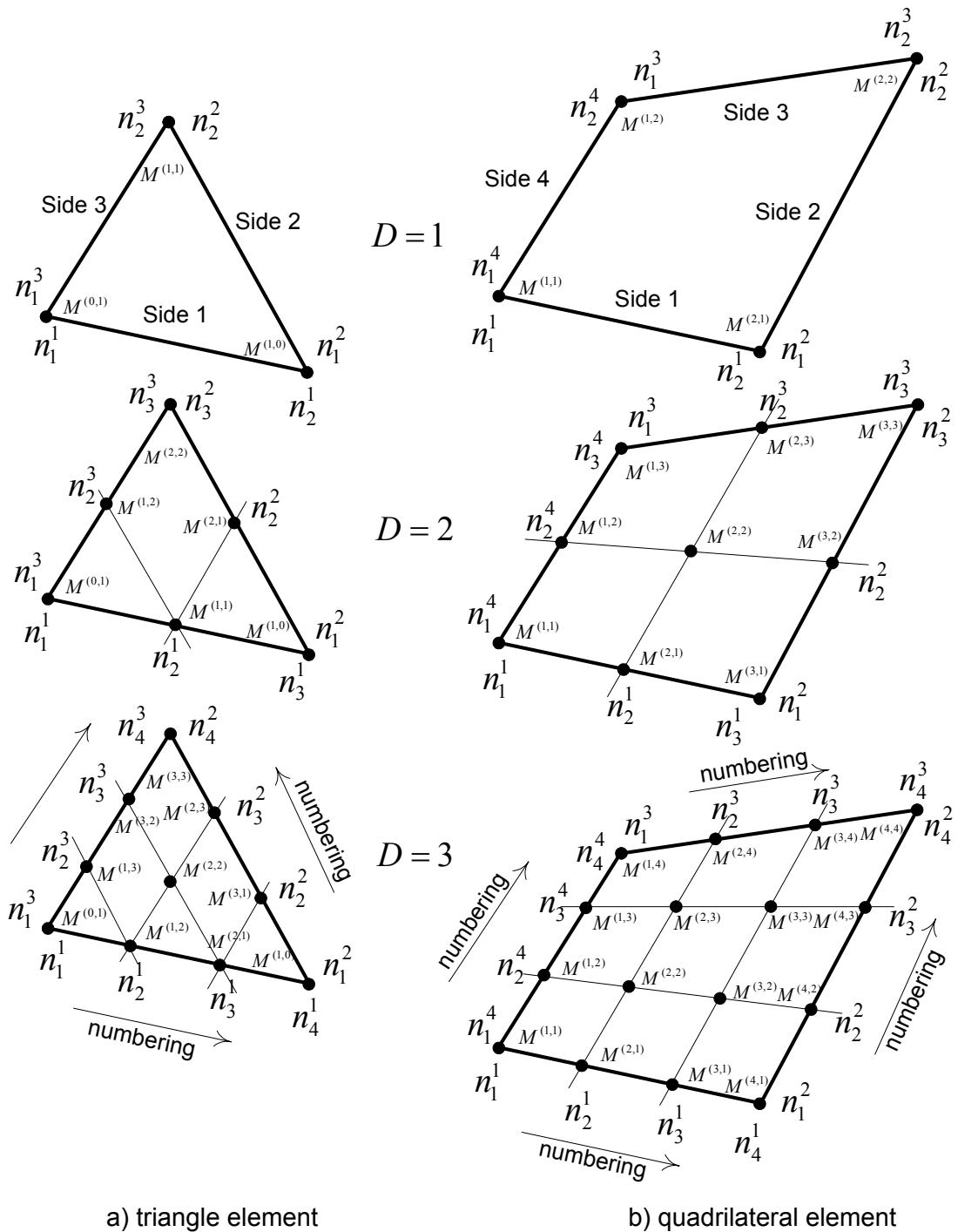
$$H = \frac{1}{N} \sum_{p=1}^{D+1} \sum_{r=1}^{D+1} h^{(p,r)}, \quad (6.44)$$

where $h^{(p,r)}$ - the total value of high-order heterogeneity function at the sub-point, N - the total number of sub-points in finite element, which can be calculated using the following equation:

$$N = \begin{cases} (D+1)!, & \text{triangle element} \\ (D+1)^2, & \text{quadrilateral element} \end{cases}, \quad (6.45)$$

where D - is the finite element sub-division factor.

An example of low-order heterogeneity is presented in Fig. 6.13. An example of high-order heterogeneity is presented in Fig. 6.14. The high-order heterogeneity should be generated for each approximation primitive separately. This can be done even by using different set of low-order heterogeneity for each of defined geometrical approximation primitives.



a) triangle element

b) quadrilateral element

Figure 6.12 Allocation of sub-points to determine the pseudo-integral property of finite element (D – subdivision factor).

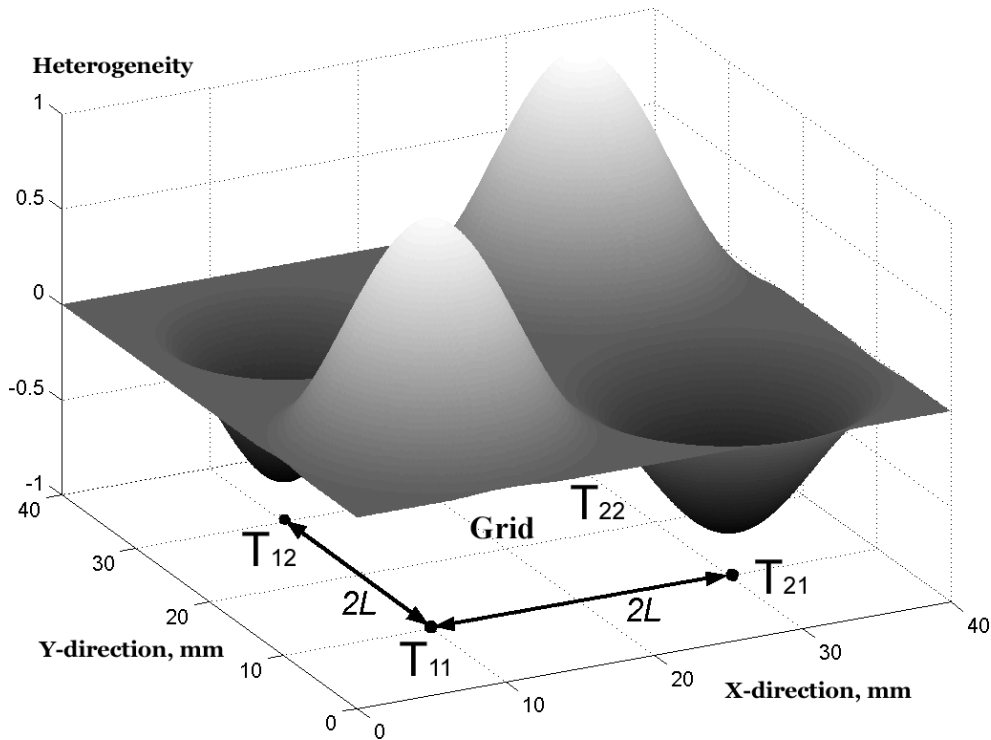


Figure 6.13 Example of the grid nodes allocation (T_{ij}^1) and the generated low-order heterogeneity ($L_{mean} = 20\text{mm}$, $A_{mean} = 1$).

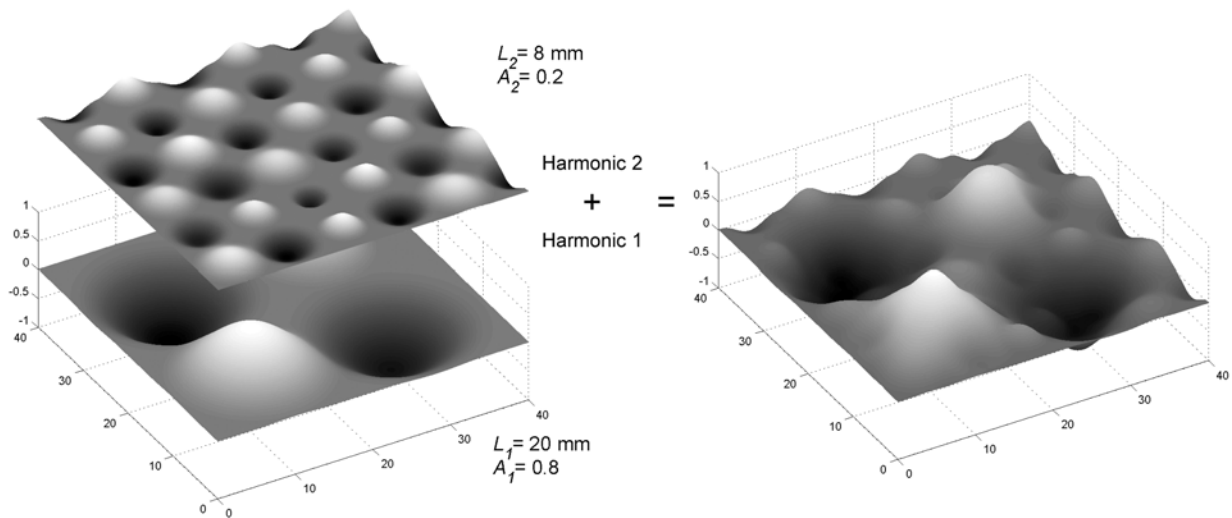


Figure 6.14 Composition of the high-order heterogeneity as a sum of low-order heterogeneities.

The determined hypothetic property H of a finite element now has to be correlated to its mechanical property. As it has already been mentioned in Chapter 5, the fiber volume fraction in a composite material can be correlated to the generated heterogeneity. The generated high-order heterogeneity is a function, which has different value in every finite element in a model. The variation of that function is in range from -1 to +1. The variation of the fiber volume fraction in composites is common to be represented by a value, which varies in range from 0 to 1, where 0 corresponds to 0% of fibers content and 1 to 100%. However, according to the performed studies (see Chapter 5) the variation of fiber volume fraction in a real composite varies around its mean value in a certain range. For example, for

polypropylene reinforced with 30 vol. % (mean value) flax fibers the determined variation of fiber volume fraction is in the range of 12 ... 60 vol.%. These limits should be put into correspondence with the limits of the generated heterogeneity (-1...+1) using the following equation:

$$V_f = \frac{V_{\min} + H(V_{\max} - V_{\min})}{100\%}, \quad (6.46)$$

where V_{\min} , V_{\max} - the lower and upper limits of the fiber volume fraction variation correspondingly. Finally, based on the determined fiber volume fraction the elastic material properties within a finite element can be determined by using Eq. 4.12 as suggested in Chapter 4.

6.4 Verification of the finite element implementation

6.4.1 Material model

The described above procedure of heterogeneous material properties generation is programmed in FORTRAN language and attached to MSC.MARC FEA code.

In order to verify the behavior of the developed material model, trials of FE simulation for a simple structure should be performed. Finite element model of a rectangular plate, which represents the working area of a standard ISO 527-1 [97] specimen (see Fig. 6.15) has been chosen for that purposes. In order to investigate the response of the heterogeneous material model, additionally several widths of simulated plates have been chosen. Rectangular plates with length of 100 mm and different widths were considered for FE simulations. The widths of the plates were chosen equal to 5 mm, 10 mm, 15 mm, 20 mm, 25 mm and 40 mm.

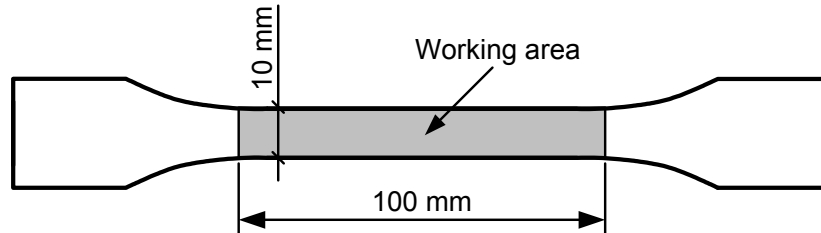


Fig. 6.15 Geometry of ISO-527-1 specimen and its working area [97].

During the work on this thesis a number of the parameters of heterogeneity of some natural fiber reinforced plastics have been estimated and published. Several natural fiber non-woven mats, like Flax, Duralin® Flax and Coir have been studied in [94]. The determined properties of Flax fiber mat using a specially developed technique are presented in Table 3.3 (see Chapter 3). It appears that there are four distinguishing groups of heterogeneity primitives present in that mat. Just for the trial testing of the developed heterogeneity generation procedure, two of them with high amplitudes parameter can be taken to generate the heterogeneity for this mat. The reduced number of groups of heterogeneity primitives can help to reduce the computational complexity of the FE task and better visualize the results. This problem has already been discussed in Chapter 5.

The harmonics with the largest amplitudes contribute much to the heterogeneity of mat and they are considered as dominant. The contribution of the other groups to heterogeneity of the mat is small. For the flax fiber mat the heterogeneity primitives corresponding to harmonics 1 and 2 (see Table 6.1) which have largest amplitudes are taken for the procedure of heterogeneity generation.

Table 6.1 Parameters of heterogeneity primitives in non-woven flax fiber mat (determined in Chapter 3).

Harmonics	Size L (st. deviation) , mm	Normalized intensity A (st. deviation)
1	23.43 (3.87)	0.27 (0.15)
2	13.57 (1.81)	0.43 (0.13)
3	9.10 (1.45)	0.10 (0.12)
4	5.91 (0.67)	0.20 (0.08)
5	3.8 (0.91)	0.15 (0.11)

The absolute boundaries of fiber volume fraction variation in polypropylene reinforced with 30% of randomly distributed Flax fiber mat were determined in Chapter 5 and discussed in paper [96]. The procedure of boundaries determination is based on the analysis of a cross-section image of this composite. The determined boundaries for this composite are: the minimum is equal to 12 vol. % and the maximum is equal to 60 vol. %.

As it is suggested in Chapter 4 the modulus of elasticity is one of the most important mechanical characteristics of any material and can be taken as a variable in accordance to the fiber volume fraction in composites. The correlation between fiber volume fraction and the modulus of elasticity for composite materials reinforced with natural fibers is suggested in Chapter 4 and published in papers [90, 96]. Representation of that model is according to Eq. 4.12 (Chapter 4). The input parameters in this equation are: the modulus of the flax fibers $E_f = 40.1$ GPa, and the modulus of polypropylene matrix: $E_m = 1050$ MPa. For this combination of fiber and matrix the $\alpha = 0.32$ can be taken [90].

6.4.2 Experimental results

In order to determine the mechanical properties of polypropylene reinforced with 30 vol.% of randomly distributed flax fibers, the experimental work was performed according to ISO-527 [97]. The tensile properties of this composite have been studied. The determined modulus of elasticity for tested composite is equal to 3293 MPa with a standard deviation equal to 177.4 MPa. The elastic strain limit is about 0.004. The experimental stress-strain diagrams (elastic part) are presented in Fig. 6.18a.

6.4.3 Simulation parameters

The plates were subjected to stretching according to scheme presented in Fig. 6.16. A gradually increasing displacement was applied during the simulation in order to achieve the maximum strain of the plates equal to 0.004. This value of strain corresponds to the elastic limit of the PP/Flax composite with 30% of randomly distributed flax fibers.

In order to highlight the influence of finite elements size on the simulation results each plate's geometry was simulated using three different finite element sizes. Quadrilateral plane-stress type 3 finite elements from MSC.MARC element library with sizes of sides of 1.25x1.25mm, 2.5x2.5 mm, 5x5 mm were used [135]. In total 18 combinations of plate dimensions and finite element size were simulated. In order to estimate statistical characteristics of the results, the simulation was performed 10 times for each combination.

Since the plates are flat, one plane-type geometrical approximation primitive has been defined by using four nodes. The origin of the local coordinate system is located at the

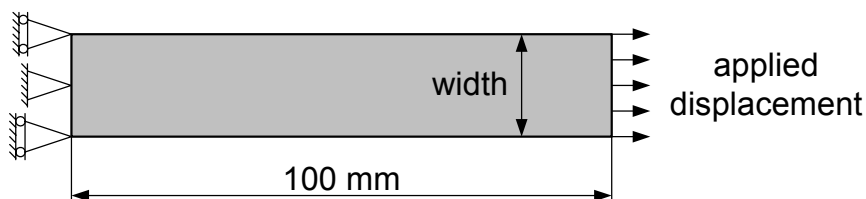


Figure 6.16 Loading scheme for simulations.

left lower corner of the FE model. The heterogeneity then is being generated in that geometrical approximation primitive with the parameters taken from Table 6.1 for non-woven flax fiber mat. The subdivision factor D has been taken equal to 4 for all of the plates. As a result, a certain hypothetical property is distributed in accordance with the generated heterogeneity. The fiber volume fraction is correlated with this hypothetical property using Eq. 6.46. Then, Young's modulus for each finite element has been calculated, using Eq. 4.12 (Chapter 4) in dependence to the local fiber volume fraction.

As a result, the distribution of Young's modulus through the finite elements was uniquely generated for each run of the simulation with the help of the developed subroutine. An example of generated heterogeneity for different model geometries is presented in Fig. 6.17.

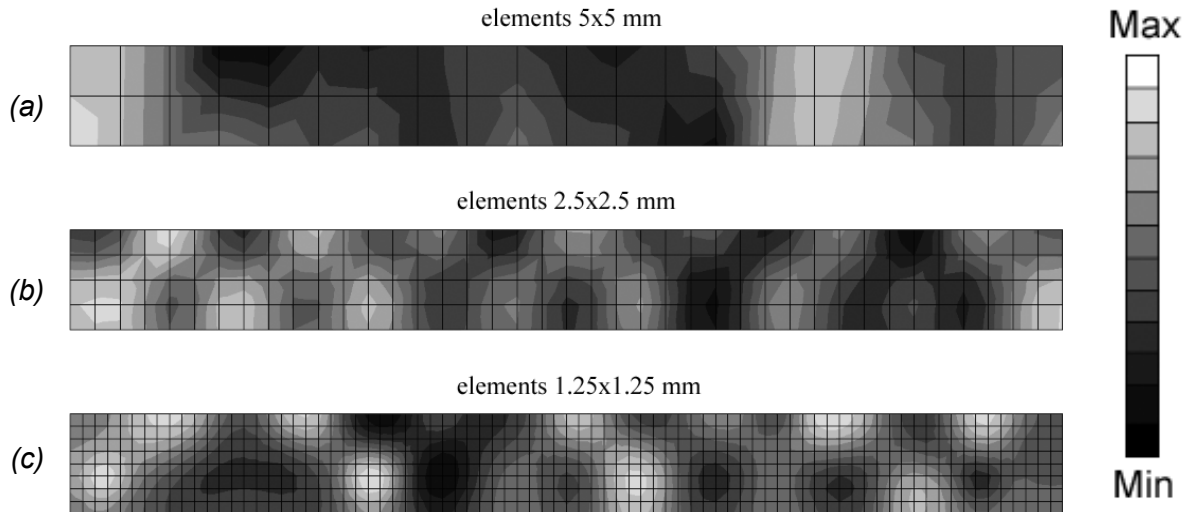


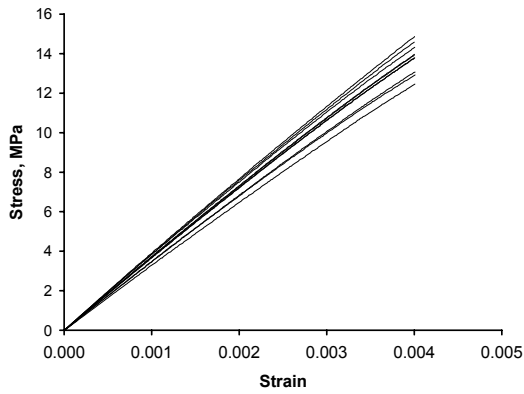
Figure 6.17 Examples of plates' heterogeneity with elements size: (a) 5x5 mm, (b) 2.5x2.5 mm, (c) 1.25x1.25 mm (plate width is equal to 10 mm).

6.4.4 Results of the simulation trials

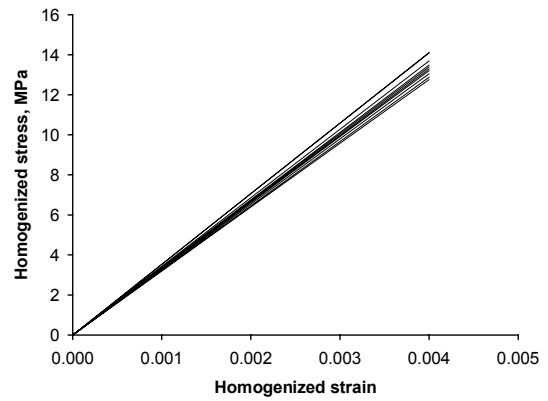
Reaction force and displacement for the plates were recorded during the simulation. The homogenized stress and strain for each simulated plate can be determined from resulting reaction force at certain applied displacement and by using known geometrical parameters of the plates. Stress-strain diagrams for the tested (a) and one for the simulated (b) plates are given in Fig. 6.18.

Since the geometry of the simulated plates and loading scheme is similar to the tensile experiment set-up, we can compare the results of the simulation with the experimental results [75]. The diagrams for homogenized stress and strain derived from the simulations are different for each simulated plate. This difference appeared due to the stochastic distribution of properties in the plates. Using simulated stress-strain diagrams a homogenized Young's modulus of the plates (like they would be homogeneous) was determined. This was done for each combination of the plate's width and the finite elements' size. The homogenized Young's modulus for each of the simulated plates is determined from the elastic part of stress-strain diagrams (curve inclination relatively the strain axis).

The scatter of the homogenized Young's modulus can be also determined since there are many stress-strain diagrams available. The results are presented in Fig. 6.19. The scatter of Young's modulus in these graphs is represented by bars which correspond to its minimum and maximum values. The numbers above the marks represent the standard deviation of the modulus.



a) experimentally tested specimens



b) simulated plates

Figure 6.18 Stress-strain diagrams for experimentally tested specimens [97] and simulated plates with dimensions of 100x10 mm and finite element size 1.25x1.25 mm.

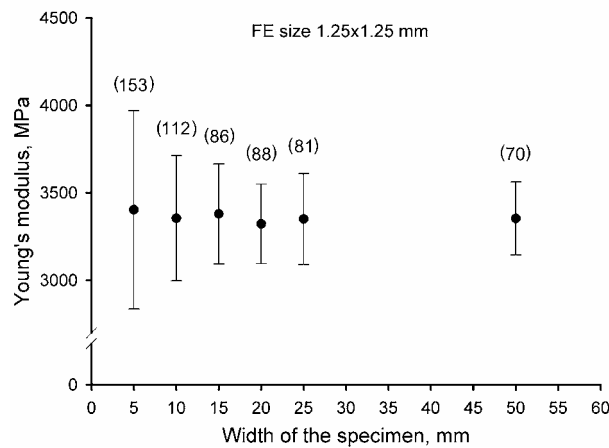
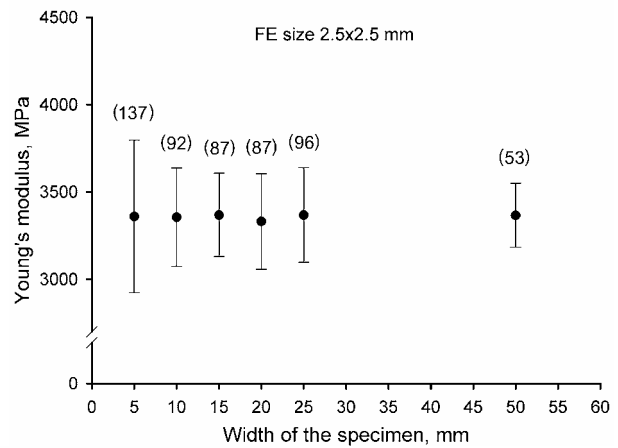
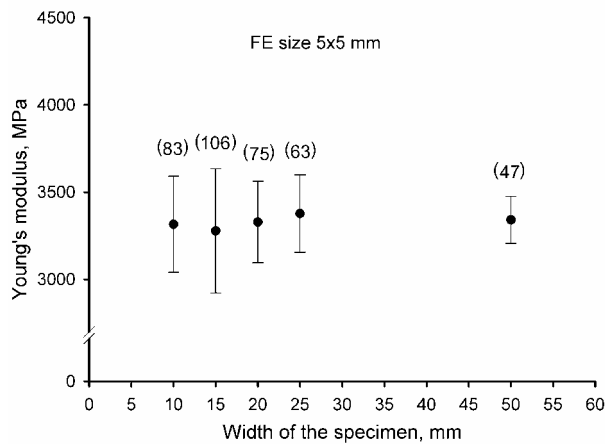


Figure 6.19 Homogenized Young's modulus of simulated plates (the bars show the maximum and minimum values, standard deviation is in parentheses).

6.4.5 Size-effect

It is easy to see Fig. 6.19 that the average value of the homogenized Young's modulus of the simulated plates remains the same for all simulated plates (with different geometry and mesh) and it is equal to 3350 MPa. However, the scatter of homogenized Young's modulus for different combinations of plate's width and finite element sizes is different. The scatter is high in relatively narrow plates and low in wide plates. There is a gradual decrease of the scatter of homogenized Young's modulus for the plates of 5 – 15 mm wide, but for the plates with a width of 20 mm and wider there is no significant change in the scatter. This can be correlated to the size of generated harmonics of 23.43 mm and 13.57 mm. The heterogeneity primitives with size 13.57 mm are dominant in this case (they have maximum averaged amplitude) and therefore they have the major influence on the heterogeneity topology. Therefore, the generated heterogeneity in narrow plates (less than 13.57 mm) cause weak areas with less fibers and strong areas with more fibers are placed in an alternate sequence along the plate length. The relatively weak areas will prevail in this case and they will determine the overall stiffness of the plate. Since the relatively weak areas have stochastic magnitude of fiber volume fraction in each plate the scatter of overall stiffness in narrow plates is large. However, if the width of plate is larger than the size of the dominant heterogeneity primitive (more than 13.57 mm in this case) relatively weak areas at some places in the material are counterpoised by relatively strong areas at the other places, which makes balance in the overall stiffness of the plate. The scatter in homogenized properties of the plates is smaller in this case.

6.4.6 Influence of the finite element's size

It appears that the size of finite elements does not influence the average value of the homogenized Young's modulus of simulated plates; however it influences its scatter. The scatter becomes higher with the decrease of finite elements in size. The heterogeneity primitives falling into the finite elements are being "averaged" or discretized over the area of finite element. Finite elements with a large surface area result in coarse discretization of the shape function of heterogeneity primitives. This leads to a smaller diversity in the properties of the relatively strong and relatively weak areas in the FE model, decreasing the scatter of homogenized properties of the plates. Thus, for successful simulations of structures using developed material model the appropriate size of finite elements should be estimated. The estimation of the size of finite elements is performed using the principles of signal processing. The function of the generated heterogeneity is discontinuously described by Eq. 6.39, 6.43, 6.44. Its value for each finite element is determined via the pseudo-integral procedure. This is similar to the sampling of an analog signal in signal processing. The heterogeneity function in this case is two-dimensional analog signal and the area of finite element is a sampling period. An example of sampling for one-dimensional case is shown in Fig. 6.20. There is a well-known Kotelnikov-Shannon Sampling Theorem [106, 142, 199], which determines the minimal sampling frequency necessary to restore the original analogue signal without losses. According to this theorem, an analogue signal with the spectrum limited with maximum frequency F_{\max} can be restored without losses by using its sampling values, if the sampling values are taken with frequency:

$$f_{discr} \geq 2F_{\max} \quad (6.47)$$

or in other form the period between samples is according to the following equation:

$$T_{discr} \leq \frac{1}{2F_{\max}}. \quad (6.48)$$

Following this theorem, the maximum linear size of finite elements for given heterogeneity (with determined set of harmonics with certain size parameters) will be at least twice as small as the smallest harmonic (L'). In other words:

$$S \leq \frac{1}{2} \min\{L^l\}, \quad (6.49)$$

where S - the recommended length of side of the finite elements, L^l - the harmonics sizes determined for the spectral analysis ($l=1 \dots NOrder$).

This allows to avoid the improper heterogeneity “averaging” by large finite elements, which greatly affects the scatter of the homogenized properties of the material, reducing the accuracy of the generated heterogeneity. However, if such fine meshing of the FE model is not possible, a coarser meshing can be used, but the scatter of the results in this case is not reliable.

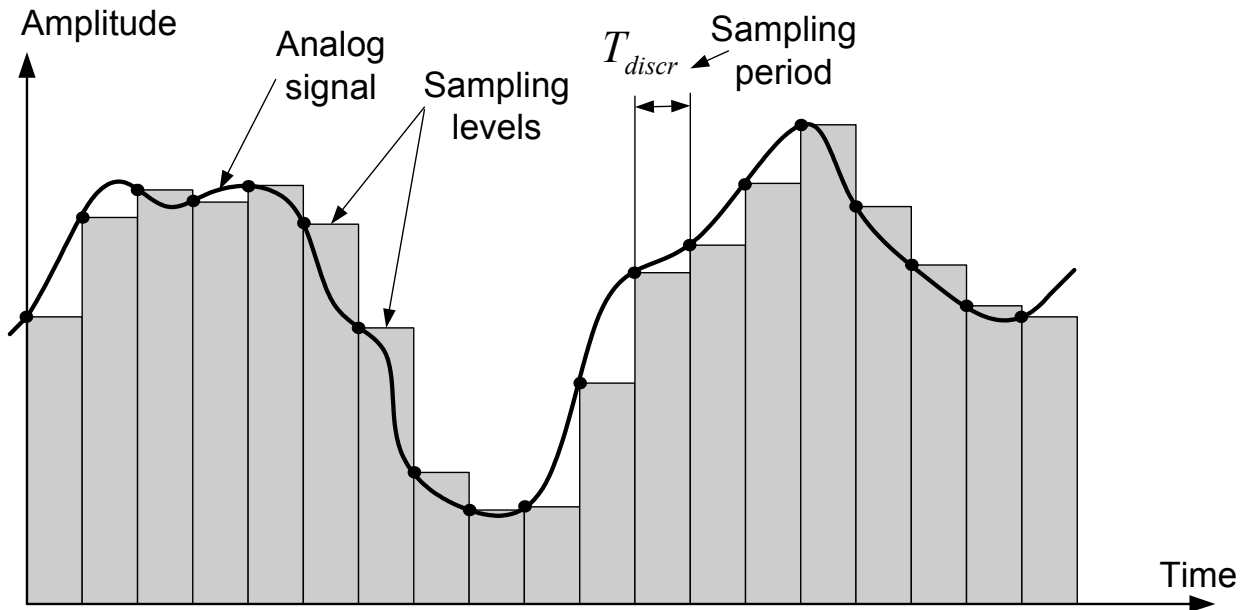


Figure 6.20 Sampling of analogue one-dimensional signal.

6.5 Conclusions

In this chapter the finite element implementation of the suggested approach to simulate heterogeneous natural fiber composites has been developed. The user subroutine has been written in FORTRAN and attached to the MSC.MARC. It is suggested that the complex FE model should be approximated with simple geometrical primitives (planes and cylinders) beforehand. The finite elements present in FE model are assigned to the closest geometrical approximation primitive. This is a rather important step which has to be carefully accomplished. However, some of elements will remain unassigned to any geometrical primitive. Each of geometrical primitive has its own threshold parameter (D_{max}), which defines the maximum distance from the primitive to finite elements. This happens in case if this distance is longer than that of the specified threshold.

Heterogeneity function in each geometrical approximation primitive is generated according to the developed procedure. For those finite elements in a model, which are associated with one of the geometrical primitives the value of heterogeneity function is determined. But for those unassigned finite elements this value is not determined, i.e. equal to 0. The pseudo-integral value of heterogeneity function which is later correlated to composite fiber volume fraction in that element determines the hypothetical property of the finite elements. For unassigned finite elements the fiber volume fraction is equal to the average fiber volume fraction determined in a composite.

In order to use the developed subroutine in FE simulations it is necessary to provide two input text files: a) parameters of the geometrical approximation primitives for FE model (nodes coordinates); b) parameters of the heterogeneity (harmonics) for each geometrical approximation primitive, and, separately, the maximum and the minimum local fiber volume fraction of a composite.

The developed subroutine can be successfully used to perform FE analysis of the structures made from heterogeneous materials. During simulation trials no numerical errors from the FE-code were reported. The convergence of the numerical solver was good.

The developed subroutine is tested in FE simulations of simple structures. The standard deviation of the Young's modulus derived from trial simulations of the composite plates with width of 10 mm and elements size equal to 1.25x1.25mm (see Fig. 6.19) is close to the same parameter derived from the experiment. The decrease of the finite elements in size with incorporation of more fine harmonics (instead of 2 dominant) in heterogeneity generation procedure can give even a closer correlation of properties between the simulated and tested plates. But, a decrease of the finite elements size leads to increase of the number of elements in model. A large number of elements, in its turn, leads to the complexity of a simulation task and requires more powerful calculation means.

The successful application of the developed approach is also presented in papers [91, 93], where various structures such as plates with different geometry and plates with holes are modeled.

Chapter 7

Structural simulation and experimental verification

7.1 Introduction

A novel approach to simulate the heterogeneous materials by using available commercial finite element code is proposed in the previous chapters of this thesis. This approach is applicable to model structures made from composite materials reinforced with natural fibers. It is based on the fact that reinforcement in these composites is not uniformly distributed and therefore there is large heterogeneity in mechanical properties of these composites. Special technique has been developed to analyze the heterogeneity. Digitized image of composite (or reinforcement) is used as the basis to derive parameters of the heterogeneity. It has been shown that heterogeneity has a complex structure and can be decomposed into simple primitives by using spectral analysis (Chapter 3). Determining parameters of heterogeneity primitives is essential for heterogeneity simulation. The technique for heterogeneity simulation, based on determined parameters and its correlation to mechanical properties of material, is developed in Chapter 5. The finite element implementation of the developed procedure is described in Chapter 6.

The usage of Finite Element Analysis for the prediction of the behavior of structures nowadays becomes a state-of-the-art technique. There are many commercial FE-codes available. Most of them allow to carry out both linear and nonlinear analysis. Some of them have implemented subroutines for composite materials, but there is not a single FE code suitable to analyze highly heterogeneous composite materials. Therefore a user's subroutine has been developed (Chapter 6) for widely used FE-code MSC.MARC. This subroutine uses the derived parameters of heterogeneity of composites material (or reinforcement) to simulate similar heterogeneity and to appropriate certain mechanical properties to finite elements in a FE model. As a result, the properties of the finite elements are distributed through the structure model according to the estimated heterogeneity of a composite.

In this chapter a validation of FE simulations including heterogeneous material model is discussed. The results of the simulations will be compared with the experimental results.

7.2 Testing and simulations of specimens

7.2.1 Materials

Experimental work has to be carried out in order to prove high variation of properties in natural fiber reinforced composites. Experimental data can be used to validate the FE simulations using the developed heterogeneous material model. A commercially available natural fiber composite material has been taken as a case-study. The material is semi-finished PP/Flax with 30 vol. % of fibers in the form of a non-woven mat (no compatibilizer was added). The material is supplied by Symalit® (Switzerland). The material was stored in normal conditions (20 °C, 50% relative humidity) before being processed. The material is provided in the form of sheets with the average thickness $t=4$ mm. During the production phase the composite sheet is cut in pieces with the preliminary estimated dimensions. Then it is heated up to 190-200 °C in an oven and rapidly placed in a mold heated up to 50 °C. Then the compression for about 30 s follows. A closed mold is used for manufacturing i.e. material cannot escape from the mold, but remains there. The size of pieces of the original semi-finished material as well as their positioning in the mold is determined experimentally to reach full filling during compression. Thus, it has been experimentally found that for the production of flat plates (400x400 mm) with different thicknesses it is possible to take two square pieces (one on top the other) of semi-finished material and place them in the center of the mold. The drawing of the material placement in the mold is schematically shown in Fig.

7.1. It should be noted that after the compression the volume fraction of fibers in all manufactured plates remains the same as it was in the semi-finished material. Three different thicknesses of manufactured plates are chosen in order to examine the influence of manufacturing process on the properties of the plates (see in Table 7.1).

After the composite plates were manufactured a preliminary visual observation of their surfaces showed that the reinforcement has a non-uniform structure and the fibrous reinforcement in the central area and areas outside the center has different distribution accordingly. In the central area the fibers distribution on the surface looks like in the original semi-finished material, i.e. randomly oriented, while in the area close to the edge of the plate the fibers are oriented in the direction of melted material flow. Therefore high anisotropy of the material near the edges is expected.

The X-ray photographs of manufactured plates presented in Fig. 7.2 and Fig. 7.3 show clearly the anisotropy of the plates. In the central area of the plate with thickness $t=4.6$ mm (see Fig. 7.2) the fibers orientation is rather random, which results in more or less quasi-isotropic properties of the composite (properties of composite do not depend on chosen direction), while in the area close to the edge, there is visible fiber orientation. It should be noted that in the central area of the plate the reinforcement has heterogeneous structure, similar to that observed in the scanned image of the flax fiber mat (see Fig. 3.3a in Chapter 3) and in the X-ray photograph of the semi-finished PP/Flax composite (see Fig. 3.4a in Chapter 3). It can be concluded that the observed heterogeneity in the manufactured plates is similar to heterogeneity of semi-finished composites examined earlier in this thesis.

Table 7.1 Geometrical parameters of the manufactured composite sheets.

Plate thickness	Initial geometry of semi-finished material (L_{orig}), (mm)	Resulting geometry of compressed sheets (L_{result}), (mm)
t=4.6mm	300x300	400x400
t=3.8mm	250x250	400x400
t=2.0mm	200x200	400x400

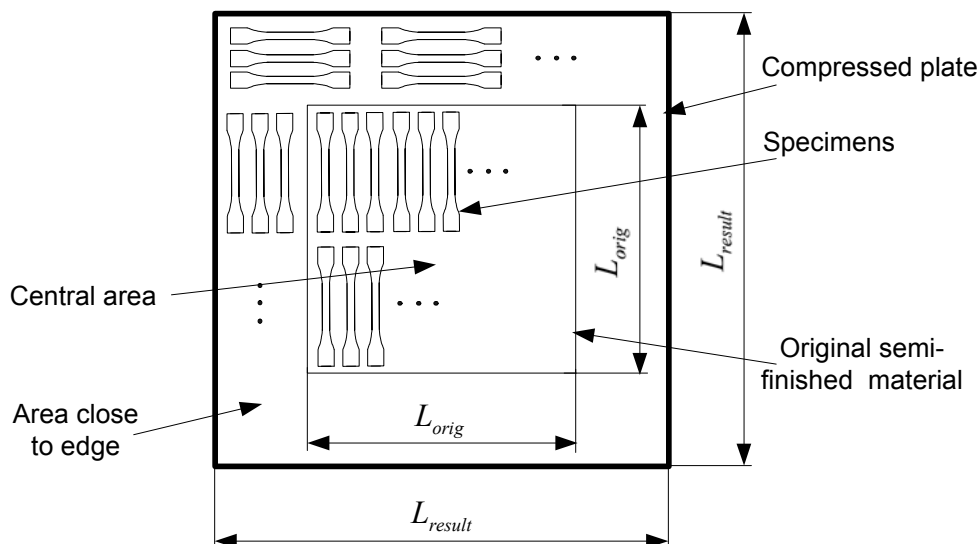
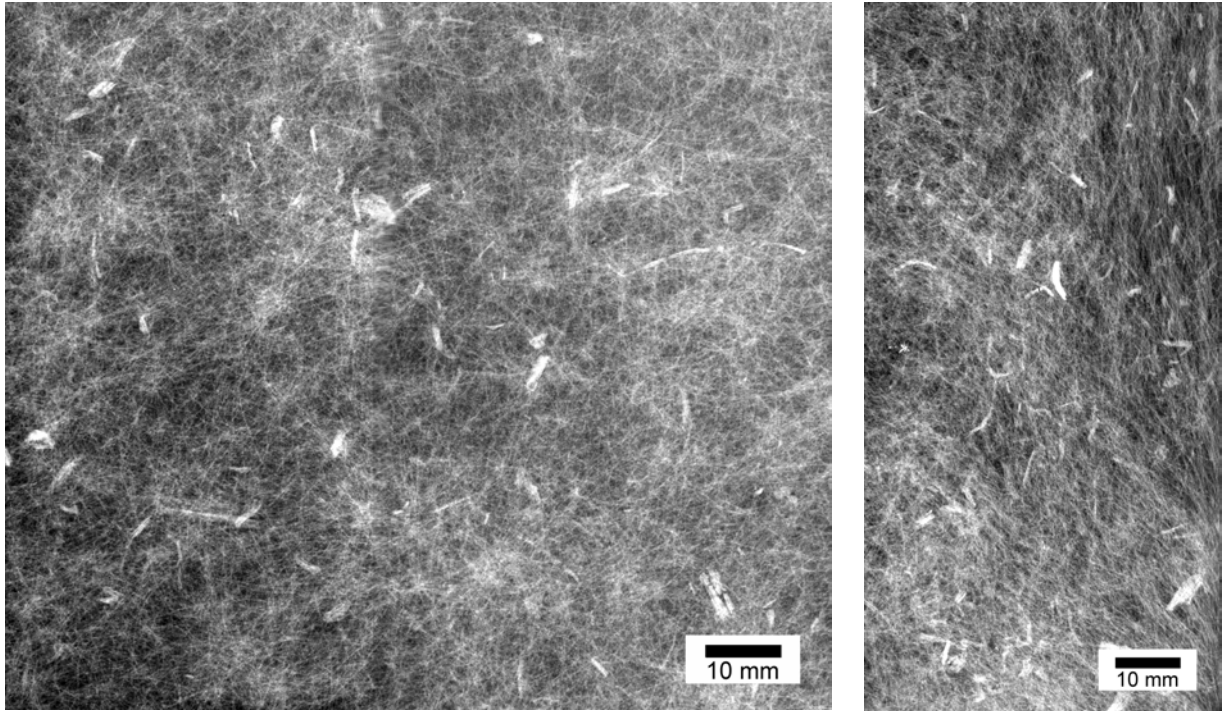


Figure 7.1 Placement of the semi-finished material in the mold just before compression and specimens' location.



a) central area

b) edge area

Figure 7.2 X-ray photograph of manufactured PP/Flax plate with the thickness $t=4.6$ mm.

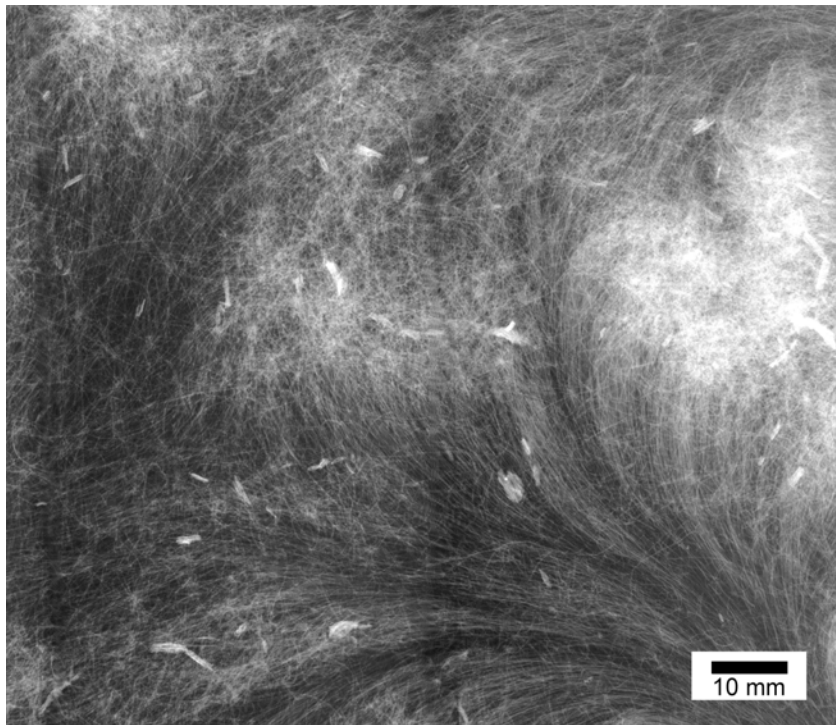


Figure 7.3 X-ray photograph of manufactured PP/Flax plate with thickness $t=2.0$ mm.

Therefore the heterogeneity of that area of plate can be estimated using the developed technique (see in Chapter 3). Fibers in the area close to the edge of the plate can hardly be considered as randomly oriented, therefore the heterogeneity in that area will not be estimated.

The X-ray photograph of manufactured composite plate with thickness $t=2.0$ mm (see Fig. 7.3) shows that there is no longer easy recognizable so-called “central” (quasi-isotropic) and “edge” (anisotropic) areas. This whole plate has extremely non-uniform fiber distribution. Moreover, some fibers are stuck in large clusters with randomly distributed fibers, while the other fibers between those clusters are oriented. Extremely high variation in the properties of such composite is expected.

7.2.2 Test setup

An experimental test to determine tensile properties of the composite plates according to ISO 527 standard has been carried out. Specimens were cut out from the manufactured plates with the geometry according to ISO 527-1 [75]. A computer numerically controlled cutting machine has been used for that purpose. Two sets of specimens, from the center and the edge parts of each plate were cut out because high difference in mechanical properties was expected. The approximate locations of the specimens in the composite plates are shown in Fig. 7.1. At least 10 specimens were tested in each set. Thickness along the length of each specimen was measured before testing. A Zwick testing machine was used at a test speed of 1 mm/min.

7.2.3 Results

The stress-strain diagrams for tested specimens are presented in Fig. 7.4. High scatter of experimental data is observed. This means that PP/Flax composite under investigation has high variation in their mechanical properties. The scatter in properties is different for those specimens cut out from the central and outside of the central area of the plates. The experimental results after the statistical analysis are presented in Table 7.2.

The research results of the heterogeneity in semi-finished PP/Flax composite have been already published in [97]. Large scatter in mechanical properties of the material has been found with the coefficient of Young’s modulus variation $V=0.06\dots0.14$ (specimens’ thickness is about $t=3.8$ mm). The manufactured PP/Flax composite plates also have a larger scatter ($V=0.08\dots0.19$ for plate with thickness $t=3.8$ mm) in their mechanical properties. This can be seen from the estimated high V coefficient of the modulus variation (see in Table 7.2), which is slightly higher for the manufactured composite plates.

Table 7.2 Tensile properties of PP/Flax (30 vol. % non-woven fiber mat).

Center				
Plate average thickness, mm	Modulus of elasticity (St.Dev.), MPa	Coefficient of modulus variation $V=E_{St.Dev}/E_{Mean}$	Strain at break (St.Dev.)	Ultimate tensile strength (St.Dev.), MPa
t=4.6	2628.10 (154.63)	0.06	0.016 (0.0029)	22.45 (3.90)
t=3.8	2937.57 (218.50)	0.08	0.013 (0.0025)	22.05 (3.61)
t=2.0	2792.05 (388.80)	0.14	0.010 (0.0016)	16.56 (2.35)

Edge				
Plate average thickness, mm	Modulus of elasticity (St.Dev.), MPa	Coefficient of modulus variation $V=E_{St.Dev}/E_{Mean}$	Strain at break (St.Dev.)	Ultimate tensile strength (St.Dev.), MPa
t=4.6	3079.62 (541.22)	0.18	0.017 (0.0041)	26.26 (9.41)
t=3.8	3467.04 (659.83)	0.19	0.014 (0.0040)	27.63 (10.00)
t=2.0	1868.56 (955.58)	0.51	0.012 (0.0010)	17.74 (4.09)

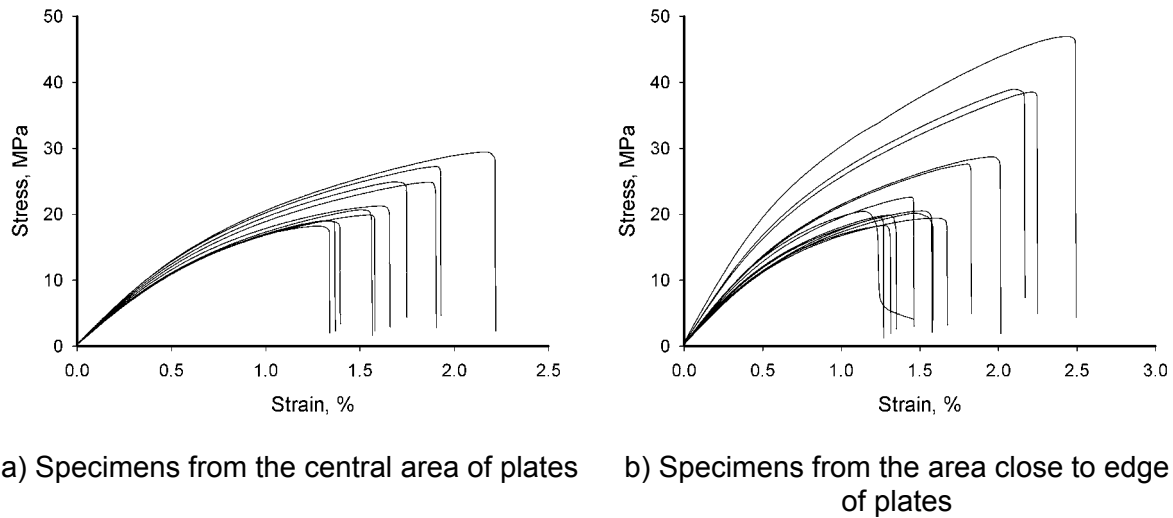


Figure 7.4 Stress-strain diagrams for PP/Flax (30 vol. % non-woven fiber mat) composite (plate thickness $t = 4.6$ mm).

As it was expected, the scatter in the properties is higher for the specimens cut out from the edge area of the plates. For these specimens the standard deviation of Young's modulus and tensile strength parameters is about 2-3 times higher than for the specimens cut out from the central area (see V in Table 7.2). Probably this happens due to the complex flow mechanics of the melted matrix material during processing. Natural fibers are much thicker than, for example, glass fibers, and, therefore, they have a great influence on the flow of the melted polymer. Moreover, the considered natural fiber reinforcement is in the form of a non-woven mat where fibers are randomly interwoven. This causes less freedom for fibers to flow with matrix polymer during molding in comparison with the loose fibers used in GMT, for example.

Mechanical properties of the manufactured plates with different thickness, hence, are not the equal. The scatter is much larger in thinner plates (see V in Table 7.2). There is also a significant drop in mechanical properties (if averaged) in the specimens cut out from the area close to the edge of thin ($t=2.0$ mm) plates. For example, the scatter of modulus in plates $t=2.0$ mm is about two times larger than in plates of $t=4.6$ mm. The same behavior for the tensile strength is observed. At first sight a large scatter and the drop in properties in the specimens cut out from the area close to the edge of plate are due to low fiber volume fraction and its extremely high variation in that area. Probably the melted semi-finished material placed in the center of the mold has to flow a lot, while fibers in the form of a non-woven mat, sticking together in the center, hardly move with the flow causing non-uniformity and the edge. However, additional research has to be performed in order to find the reasons of such non-uniformity.

X-ray photographs of the tested specimens have been made in order to analyze the structure of the reinforcement. They are shown in Fig. 7.5 – 7.7. Specimens 1C1 and 1C7 in Fig. 7.5 are cut out from the central area and 1S3 and 1S7 are cut out from the area close to the edge of the manufactured composites plates with thickness $t=4.6$ mm. According to the testing results, the specimen 1C1 is the stronger and stiffer (modulus $E=2869$ MPa and strength $\sigma_{ultim} = 27$ MPa) than the specimen 1C7 (modulus $E=2490$ MPa and strength $\sigma_{ultim} = 19$ MPa). In the presented photographs it is clear that the fibers in both specimens are randomly distributed. However, randomly distributed fibers form clusters which cause the variation of the fiber volume fraction along the specimens' surface (thus, the heterogeneity).

It is obvious that during the tensile testing the specimens are broken in the weakest area. Sometimes the weakest area can be recognized by a lower (than in other areas) amount of fibers in X-ray photographs. In the photographs of specimens 1C1 and 1C7 these parts can be easily observed (see Fig. 7.5). Thus, the difference in the mechanical performance of these specimens can be explained by a different amount of fibers in their weakest area.

The structure of the fibrous reinforcement in the specimens cut out from the area close to the edge of plate is rather different from the specimens cut out from the central area of the plates. In the photographs of the specimens 1S3 and 1S7 (see Fig. 7.5) it is easily observed that the fibers are no longer randomly distributed, but in some areas they are orientated, resulting in locally unidirectional composite. It is obvious that the behavior of composites reinforced with unidirectional fibers is much more different than those with the randomly distributed reinforcement. These composites are very stiff and strong if the load is transferred along the fibers, but they are weak, if the load is applied in transverse direction. In other words, unidirectional composites have anisotropic properties. In some areas in specimens there is a local anisotropy of properties, while in the other areas the properties can be considered as quasi-isotropic (fibers are randomly oriented). Nevertheless in all areas of these specimens the fiber clusters in the reinforcement can be seen. According to the results of testing, specimen 1S3 is stronger ($E = 4343$ MPa and $\sigma_{ultim} = 50$ MPa) than specimen 1S7 ($E = 2576$ MPa and $\sigma_{ultim} = 19$ MPa). The presence of fiber clusters certainly results in the variation of mechanical properties due to variable fiber volume fraction. But, it is clearly seen that in specimen 1S3 the dominant fiber orientation is parallel to the specimen's long side (and therefore, parallel to applied load). This is the best fiber orientation to resist the applied load. In specimen 1S7 the dominant fiber orientation is almost transverse to its long side (and therefore transverse to applied load). This results in weak specimen. Thus, in the specimens cut out from the area close to the edge of plate, not only heterogeneity due to non-uniform fibers distribution, but also anisotropy due to fibers orientation can be observed. Moreover, in this case the anisotropy has a major influence on the properties of the specimen.

In X-ray photographs of the specimens cut out from the plate with the thickness $t = 3.8$ mm (see Fig. 7.6) the structure of the reinforcement is rather similar to that observed in the plate with thickness $t = 4.6$ mm. However, the heterogeneity due to the fiber volume fraction variation is slightly higher. This can be explained from the fact that fiber clusters are easily recognizable, especially in specimens 2C1 and 2C2. Since the anisotropy in these specimens is not present, the fracture occurs at the areas, where fiber volume fraction is low.

The specimens 2S1 and 2S4 are cut out from the edge of the composite plate with the thickness $t = 3.8$ mm. The anisotropy in these specimens can be observed. Anisotropy in this case, has a major influence on the mechanical properties of specimens. For example, the fracture of the 2S4 specimens occurred in the area where fibers were randomly orientated (at the right side), while at its left side there was a clear fiber orientation in the direction parallel to the load.

Even more interesting X-ray photographs were obtained for the specimens cut out from the plate with thickness $t = 2.0$ mm (see in Fig. 7.7). In these photographs it is easy to see that a high heterogeneity and high anisotropy exists in all specimens regardless of their belonging to either central or peripheral (i.e. close to the edge) area of plates. The mechanical behavior of specimens with such structure of reinforcement is very difficult to describe. It is clear that their fracture is governed by anisotropy. The heterogeneity in these specimens is not significant for the fracture. Thus, the fracture of specimens 3C2, 3C4 and 3S2 (see Fig. 7.7) occurred in the areas where fibers are transverse to the applied load. Specimen 3C1 is broken in the central area due to random fiber orientation, while the fibers on its right and left sides are oriented parallel to the load. The structure of the reinforcement in specimen 3S8 is similar to that observed in 3C1. The phenomenon of specimen 3S6 is difficult to explain. It is broken in the area with high fiber volume fraction. Probably this happened due to a poor fiber impregnation with the matrix resulting in extremely weak

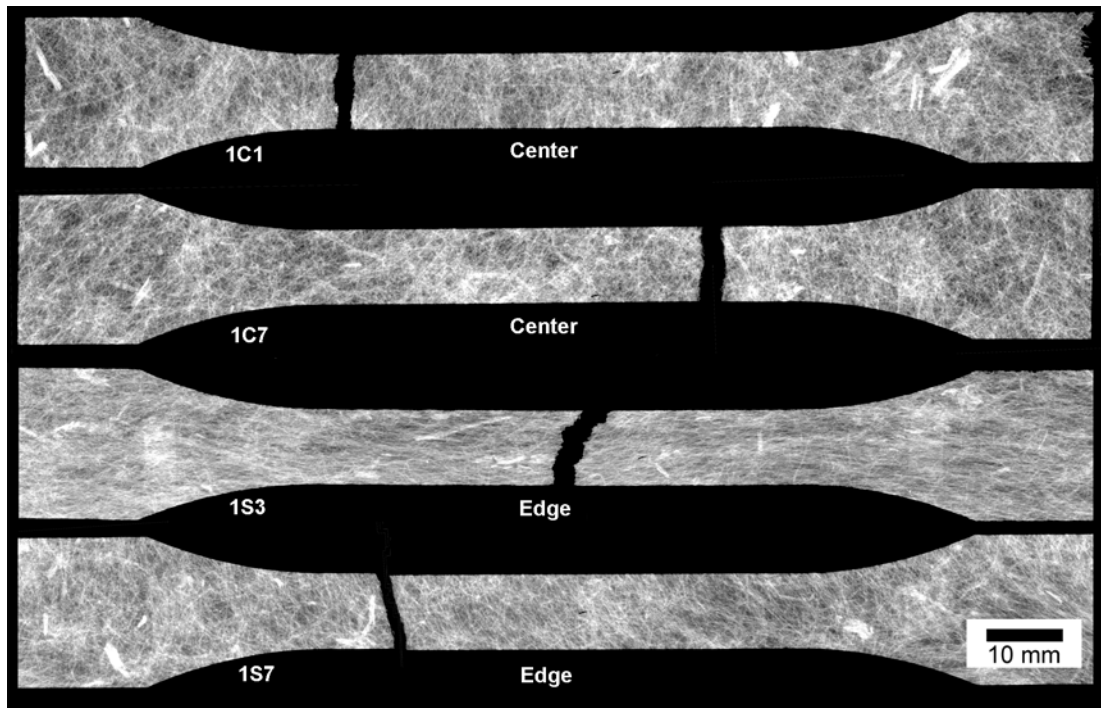


Figure 7.5 X-ray photographs of the specimens cut out from the central area (denoted as Center) and the area close to the edge (denoted as Edge) of a PP/Flax composite plate with the thickness $t=4.6$ mm.

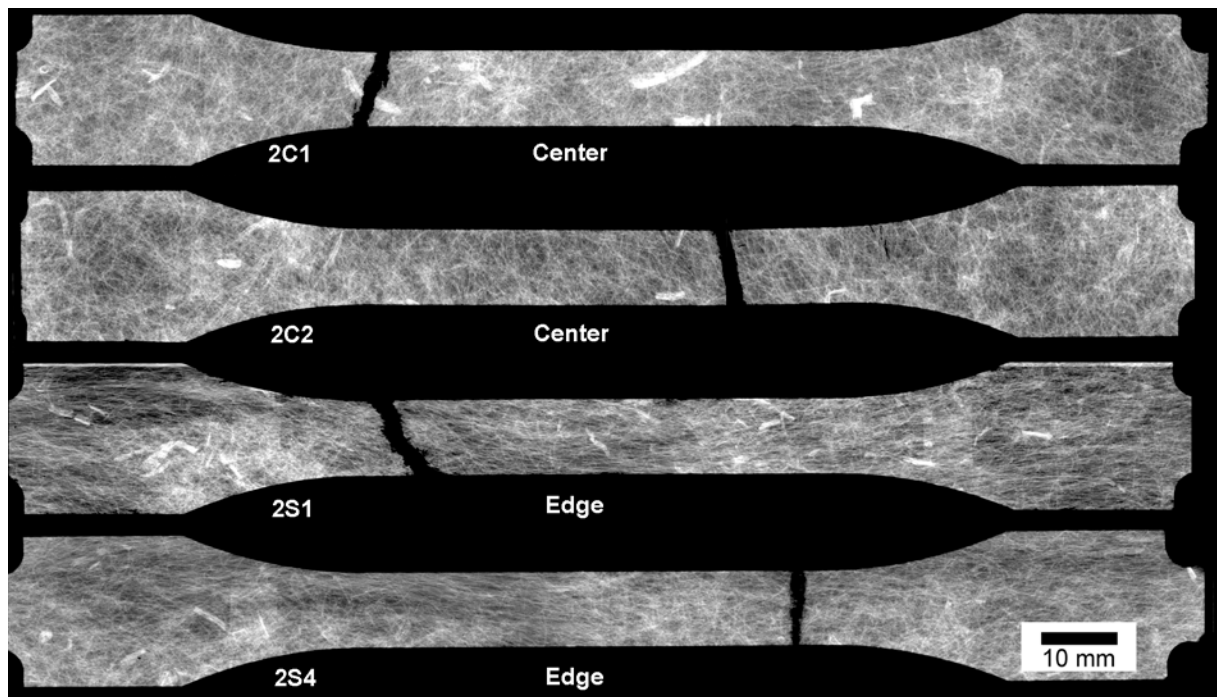


Figure 7.6 X-ray photographs of the specimens cut out from the central area (denoted as Center) and the area close to the edge (denoted as Edge) of a PP/Flax composite plate with the thickness $t=3.8$ mm.

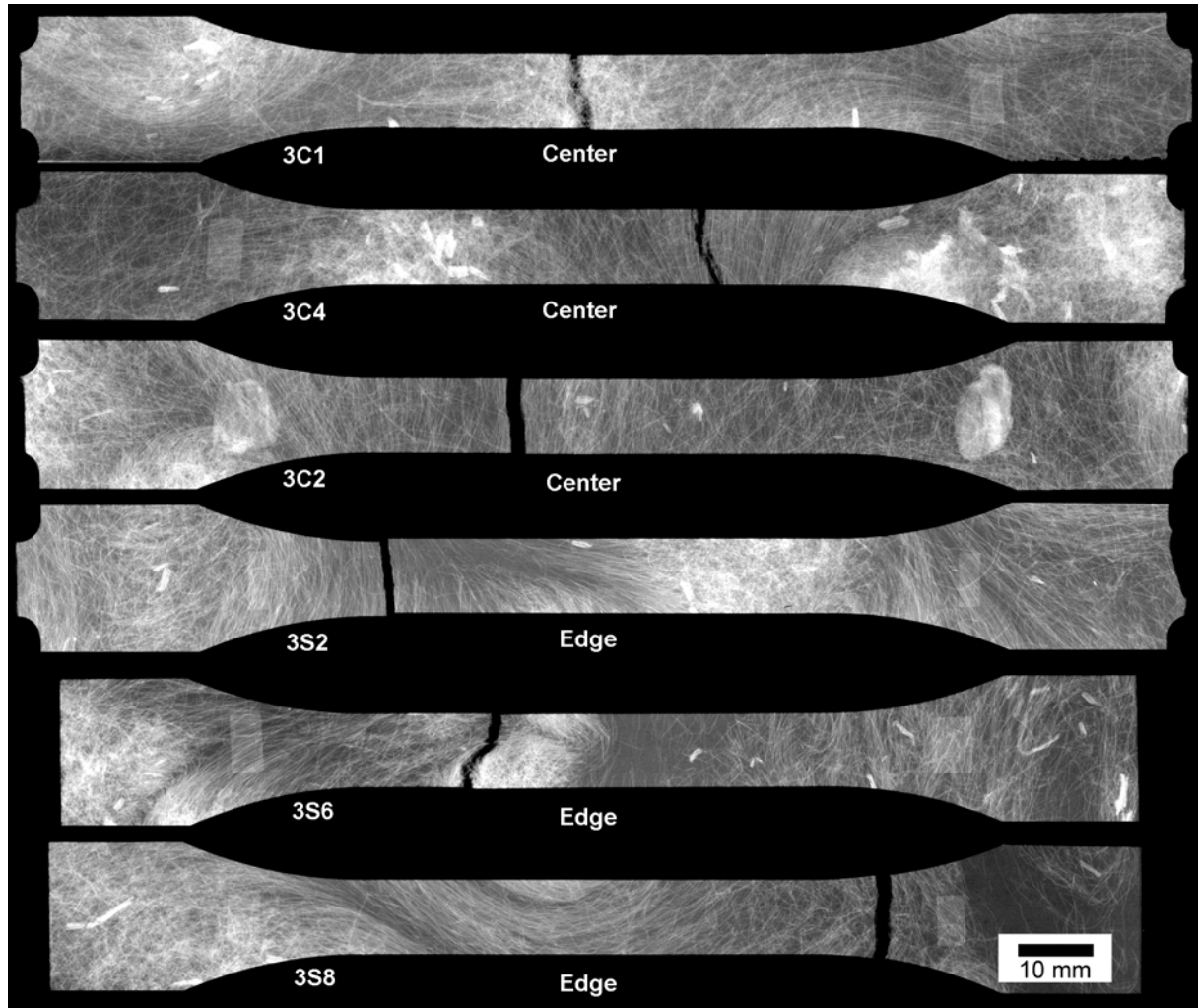


Figure 7.7 X-ray photographs of specimens cut out from the central area (denoted as Center) and the area close to the edge (denoted as Edge) of PP/Flax composite plate with thickness $t=2.0$ mm.

composite material. Unfortunately this cannot be seen in X-ray photographs. Additional research should be carried out in order to understand such behavior. The fracture governing factors with respect to the structure of the reinforcement in the discussed specimens are presented in Table 7.3.

In general, the results of X-ray photographs analysis are in line with the results of mechanical testing of the PP/Flax composite specimens. They confirm high influence of the reinforcement structure on the mechanical properties of composites. Thin composite plates have a high non-uniformity in the reinforcement structure probably due to the non-uniformity of the melted material flow during molding. In order to manufacture a thin plate smaller amount of initial material is placed in the mould in comparison with the production of thick plates. The melted matrix (near $190\text{ }^{\circ}\text{C}$) has to flow through narrow clearances of relatively cold ($50\text{ }^{\circ}\text{C}$) mold parts, which results in different viscosity of polymer during flow. At the same time stochastically interwoven fibers being highly compressed affect that flow even more. They can flow together with the polymer either in clusters or separately (see Fig. 7.2), which results in the extremely non-uniform structure of the reinforcement, sometimes with the local fiber orientation (local anisotropy). In thicker plates more initial material is used, which result in wider clearance between mold parts and thus melted matrix material with fibers, has more freedom to flow. Interwoven fibers in this case, disturb the flow less, resulting in a more uniform material (see Fig. 7.3). However, regardless to the plate thickness the anisotropy,

induced by flow of polymer matrix, is always present in the area close to the edge of the plates. It should be noted, that the anisotropy in properties of molded composites reinforced with non-woven fiber mats appears not only due to the high flow ratios and narrow clearance of the mold, but also depends on the viscosity of the melted material (matrix with fibers). The viscosity of the melted material depends on the temperature. Thus, due to the increase in temperature, the material flows better even in narrow clearance showing less anisotropy in resulting structure. Therefore not necessarily thin composite structures have higher anisotropy in properties. However, the temperature should be limited by that of natural fibers degradation (see in Chapter 2).

Thick composite plates (with thickness $t=4.6$ and $t=3.8$ mm) in the central area have heterogeneous properties with minimal anisotropy. Therefore, specimens cut out from that area of the plates will be taken for further analysis, while the other specimens will be just briefly discussed. Structure of the reinforcement in other specimens (cut out from the area close the edge area of thick plates and all specimens cut out from thin plate $t=2.0$ mm) does not correspond to the heterogeneity approach discussed in Chapter 3. The parameters of the heterogeneity of chosen specimens can be derived by using the developed technique (see in Chapters 3, 5). Their mechanical behavior can be predicted using developed heterogeneous materials model in the finite element simulations. The focus of the research in this thesis has been made on heterogeneity in the composite properties due to non-uniformity of randomly oriented fibers (thus, fiber volume fraction variation only). Therefore, variation of properties induced by oriented fibers (thus, anisotropy in reinforcement) will not be considered further. However, the problem of anisotropy can be considered for further development in the area of natural fiber composites reinforced with non-woven fibers.

Table 7.3 Fracture governing factors with respect to the structure of the reinforcement in PP/Flax composite specimens.

Plate thickness, mm	Specimen	Structure of the reinforcement	Reasons governing fracture
4.6	1C1	Random overall	Heterogeneity
	1C7	Random overall	Heterogeneity
	1S3	Oriented parallel overall	Anisotropy
	1S7	Oriented almost transverse overall	Anisotropy
3.8	2C1	Random overall	Heterogeneity
	2C2	Random on left side Oriented transverse on right side	Anisotropy, heterogeneity
	2S1	Oriented parallel overall On left side less fibers	Anisotropy
	2S4	Oriented parallel on left side Random on right side	Heterogeneity, anisotropy
2.0	3C1	Random in center Oriented parallel on left and right	Anisotropy
	3C4	Oriented parallel on left side Oriented transverse on right side	Anisotropy
	3C2	Oriented transverse overall	Anisotropy
	3S2	Oriented transverse on left side Random on right side	Anisotropy
	3S6	Oriented almost parallel on left side Oriented transverse on right side	Anisotropy, poor impregnation
	3S8	Oriented almost parallel overall	Anisotropy

7.2.4 Surface strain field analysis

Heterogeneity of PP/Flax composite is observed by contact-less strain measurement system “ARAMIS” (manufacturer GOM GmbH, Germany) at the same time with the standard tensile tests. This system consists of two digital cameras and a processing unit, which is attached to a PC. ARAMIS system captures the displacement of points on the object’s surface by using the principles of photogrammetry. Therefore, just before testing all the specimens were painted on one face with aerosol paint in order to create a black and white speckled pattern (see Fig. 7.8). The speckles in the pattern are randomly distributed. The cameras have to be calibrated before the actual measurements in order to provide their relative position to the image processing software. During the loading of a specimen, both cameras capture an image of the pattern painted on specimen’s surface at different load stages at the same time and store it in the memory of the processing unit. Several images are captured at different loading steps containing information about the displacements of speckled pattern, which is occurred due to material deformation. After that, a special image processing software on PC calculates the surface displacement field based on the captured pattern deformations. Displacement of points on specimen’s surface at different loading steps is obtained resulting in the surface displacement field. The difference in the surface displacement fields at different load steps gives the field of surface strain. The obtained strain field is composed from three components $\varepsilon_x, \varepsilon_y, \varepsilon_{xy}$, which represent the strains in two perpendicular in-plane directions and the shear component. The equivalent strain is always considered under “strain” further in this thesis (otherwise is specified) is calculated by using the following equation:

$$\bar{\varepsilon} = \sqrt{\frac{2}{3}(\varepsilon_x^2 + \varepsilon_y^2 + \varepsilon_{xy}^2)}, \quad (7.1)$$

where $\varepsilon_x, \varepsilon_y, \varepsilon_{xy}$ - are correspondingly in-plane principal (X, Y) and shear (XY) components of strain tensor.

The equivalent surface strain field at different load steps for some of the tested PP/Flax specimens is shown in Fig. 7.20 (see on page 128), Fig. 7.21 (see on page 129) and Fig. 7.22 (see on page 132). X-ray image of the specimen under investigation is presented at the top, so it is rather simple to compare the structure of the reinforcement with the observed surface strain field. The surface strain field of specimen 1C7 cut out from the central area of PP/Flax composite plate with thickness $t=4.6$ mm is shown in Fig. 7.20 (see on page 128). In those areas of the specimen, where there is a low amount of fibers (more black color in X-ray image) there is local concentration of surface strain. Indeed, composite becomes locally less stiff, if the local amount of fibers is low. Therefore, heterogeneity in the reinforcement causes the strain concentrations, which leads to the poor behavior of the specimen under load. The failure of specimens made of PP/Flax material during testing is always unpredictable. However, having X-ray image of specimen, sometimes it is possible to predict its potentially weak areas. As to the specimens cut out from the central area of thick plate ($t=4.6$ mm) it is rather difficult to determine potential failure areas in the X-ray image due to randomly distributed fibers, which form quasi-isotropic reinforcement. While in those specimens cut out from the area close to the edge of thick plates ($t=4.6$ and 3.8 mm) the reinforcement is no longer randomly oriented and therefore anisotropic allowing weak areas be easy recognized.

The X-ray image and the surface strain field of specimen cut out from the area close to the edge of thick plate ($t=3.8$ mm) is presented in Fig. 7.21 (see on page 129). It is easy to see that on its left side the reinforcement is anisotropic (fiber orientation is along the specimen), but on its right side the reinforcement is quasi-isotropic. Anisotropy, induced by fiber orientation, has major influence on the properties of the composites. In a unidirectional composite, maximum material performance can be achieved if the fibers are parallel to the applied load, whereas the minimum performance – when the fibers are transverse to the load. The performance of a composite with randomly distributed fibers, in principle, does not

depend on the direction of the applied load and it is somewhere in-between the maximum and minimum performances of a unidirectional composite. Thus, the strain field on the left side of specimen 2S4 (see Fig. 7.21 on page 129) is expected to be low due to high local stiffness of the composite (fibers are parallel to applied load), while on its right side the high strain concentration appears due to lower stiffness (quasi-isotropic composite) in comparison to the left side of the specimen.

Comparing the surface strain field of two specimens cut out from the central area (see Fig. 7.20 on page 128) and area close to the edge (see Fig. 7.21 on page 129) of plate, it is clear that strain non-uniformity is higher in that specimen cut out from the area close to the edge of plate. This confirms a strong correlation between the structure of reinforcement (heterogeneity and anisotropy) and the surface strain field. In the specimen cut out from the central area of the thick plate (see Fig. 7.20 on page 128) the surface strain concentrations have local character and do not occupy large area (maximum 2-3 mm in diameter). While in the specimen cut out from the area close to the edge of the thick plate (see Fig. 7.21 on page 129) the surface strain concentrations occupy larger area and they are more intense. In both cases the highest surface strain non-uniformity appears at the latest loading steps ($\varepsilon > 0.45\%$), which is beyond the elastic limit of the PP/Flax composite (equal to $\varepsilon = 0.4\%$, determined in [97]). A section through the center of strain image (along its long side) has been drawn in order to compare the results numerically (see Fig. 7.9a). The strain distribution along that section is shown in Fig. 7.9b. The remarkable thing is that the surface strain variation even at the low loading level can vary up to $\pm 50\%$ in relation to its mean value.

Just as an example, the surface strain in the specimens along with its X-ray image cut out from the thin plate ($t = 2.0$ mm) is presented in Fig. 7.22 (see on page 132). According to the X-ray photograph the structure of the reinforcement in this specimen is extremely non-uniform. On the left side of the specimen there is low amount of fibers and they are randomly oriented, resulting in locally quasi-isotropic composite. Whereas on its right side the amount of fibers is higher, but they are oriented transverse to the load, resulting in locally weak composite. The surface strain on the right side of the specimen is alike to the fibers' orientation. Thus, from the strain pictures at the latest loading steps ($\varepsilon > 1.05\%$) it is possible to recognize, that a strain field is in the form of "strips" about 2...5 mm wide, which go transverse through the specimen. The strips of high strain are alternating with the strips of low strain. The strain field conforms with the X-ray photograph showing that the fibers have certain orientation. In this example it can be seen that too high local amount of fibers, like on the upper left side of the specimen (see X-ray in Fig. 7.22 on page 132) may result in a soft spot in the material. This is probably, due to poor fibers' impregnation with the polymer matrix. The surface strain variation in this specimen is huge – up to 230% of its mean value (see Fig. 7.9c).

The investigations of manufactured plates confirm the hypothesis that the locally low amount of fibers (void in the reinforcement) in composite may result in locally weak composite, which was predicted in Chapter 2 and Chapter 3. Since the voids in non-woven reinforcement cannot be avoided, their presence has to be considered at the design stage. Using numerical simulations with the applied developed heterogeneous material model gives possibility to take these voids into consideration.

The manufacturing process also has significant influence on the properties of the plates. The experimental plates manufactured from PP/Flax composite have a large variation in properties. Different areas of the plates have their own variation in properties. Processing conditions (temperature, semi-finished material placement in a mold, etc.) can be adjusted in order to manufacture plates with different thickness and with more uniform properties. However, molding a complex structure, where all structural walls have different thickness, can be a rather complex task in view of optimizing the processing conditions to reach the low variation in properties. In this case post-analysis of local properties of the structure are required.



Figure 7.8 Example of painted specimen with stochastic black and white speckles.

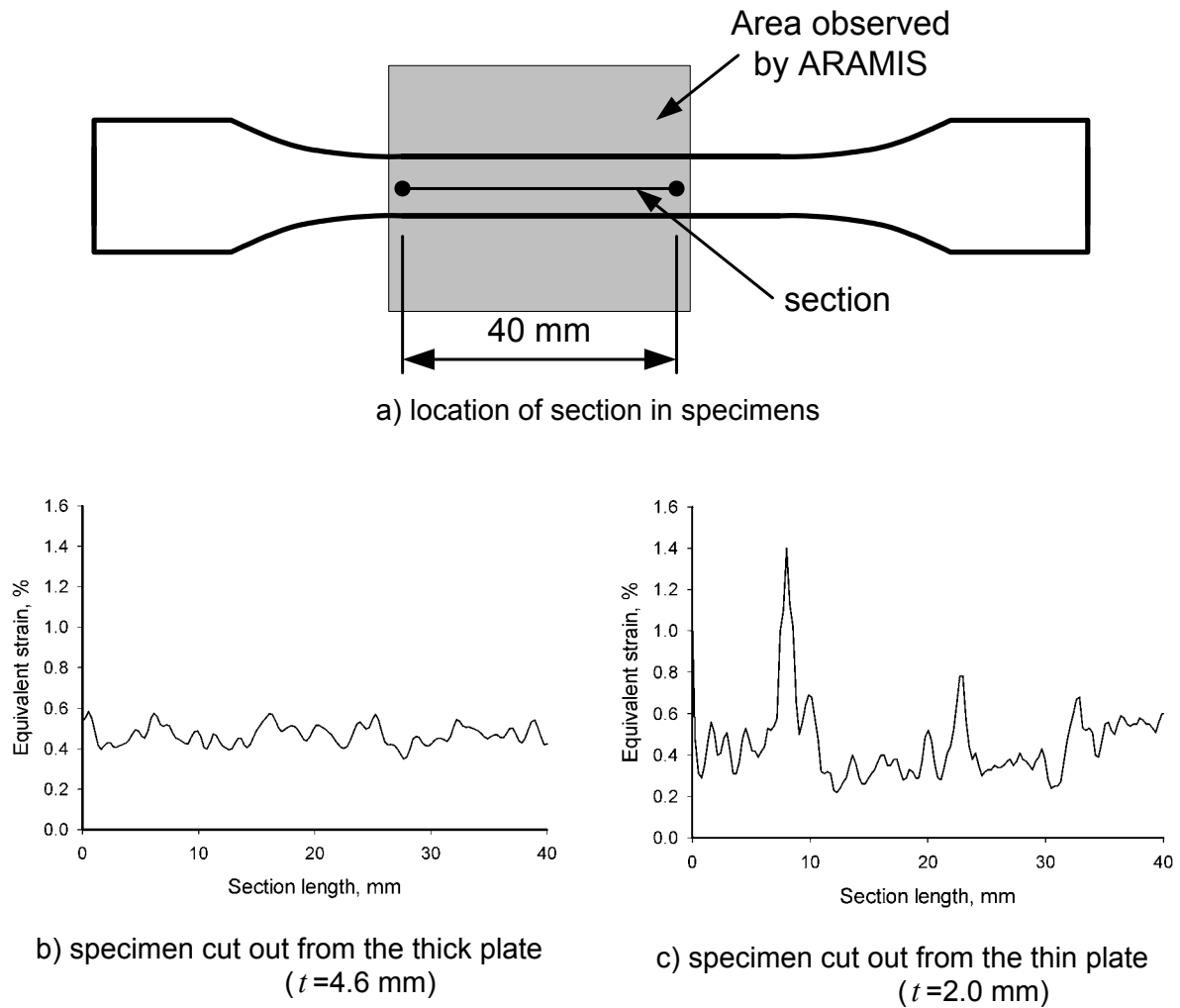


Figure 7.9 Variation of equivalent surface strain along a section drawn in specimens cut out from the central area of PP/Flax plates at applied homogeneous deformation $\varepsilon = 0.45\%$.

Underestimation of possible presence of local weak and strong areas in the manufactured structure (namely heterogeneity and anisotropy) might lead to its unpredicted failure. The exact definition of the possible problem areas in structure is difficult. However, it can be estimated and simulated using the developed heterogeneity analysis technique. Using that technique one can improve the reliability of structural design. Finite element simulations with developed material model for heterogeneous materials can be applied, using the assumption that the natural fiber reinforced composite has the heterogeneity in the properties due to fiber volume fraction variation. The heterogeneous FE simulations can help to avoid the unpredicted failure of the structure through a more reliable stress-strain state

simulation in comparison with the traditional approach. The anisotropy of the reinforcement is difficult to predict and analyze. Therefore the non-uniformity of properties in natural fiber reinforced composites due to anisotropy is out of the scope of this thesis.

7.2.5 Comparison of the FE analysis results with the experimental data

The surface strain obtained with the ARAMIS system can be used for comparison with the results obtained from the finite element simulations performed using the developed approach to simulate the heterogeneity in material's properties. The FE model of a plate (described earlier in Chapter 6) with dimensions 100x10mm and thickness 4.6 mm is simulated. This plate represents the geometry of working area of ISO-527 specimen used for the testing. Quadrilateral shell finite elements with the side length equal to 0.5 mm are used. The heterogeneity parameters of the material are estimated using the available X-ray image of PP/Flax specimens cut out from the central area of the manufactured composite plate with thickness $t=4.6$ mm. The specimens with minimal visual signs of anisotropy are taken. The estimated heterogeneity parameters are presented in Table 7.4. The dominant harmonic of heterogeneity (with maximum amplitude) in that material is number 8 with average period of 2.85 mm. This means that the expected variation in a stress-strain state mostly will have the period of that harmonic. The heterogeneity in simulated plate is generated by using the developed technique (see Chapter 4 and Chapter 5). The model suggested in Eq. 4.12 with the following parameters $E_f^L=41$ GPa, $E_f^T=4$ GPa and $E_m=800$ MPa, is used to correlate the generated heterogeneity with Young's modulus of the finite elements in the model. The coefficient in that model is tuned according to the experimental data presented in Table 7.2 and it is equal to $\alpha=0.32$.

Table 7.4 Parameters of heterogeneity in PP/Flax specimen ($t=4.6$ mm) estimated from its X-ray image, presented in Fig. 7.20 (see on page 128).

Harmonics	Size (St. dev.), mm	Normalized Amplitude (St. dev.)
1	15.49 (2.06)	0.06 (0.03)
2	11.15 (1.46)	0.16 (0.09)
3	7.44 (0.77)	0.04 (0.02)
4	6.13 (0.88)	0.07 (0.11)
5	4.77 (0.49)	0.14 (0.07)
6	4.16 (0.44)	0.07 (0.05)
7	3.59 (0.49)	0.08 (0.03)
8	2.85 (0.8)	0.39 (0.1)

The resulting strain field in the specimens obtained either from simulation or experiment has to be compared in equal loading conditions. In this case the loading condition is defined by the applied homogeneous deformations. Thus it has to be the same in both simulation and experiment. Due to the fact that FE simulations can be performed for the elastic region of material curve the applied homogeneous deformation should result in heterogeneous strains below the elastic limit of the material, otherwise the comparison is not reliable. The earlier determined by us elastic limit for the PP/Flax composites reinforced with 30 vol.% of non-woven fibers is at $\varepsilon=0.40\%$ [97]. Taking into the consideration the possible strain variation in the range of $\pm 150\%$ the applied homogeneous deformations of $\varepsilon=0.15\%$ can be taken. The result from ARAMIS at that stage ($\varepsilon=0.15\%$) is presented in Fig. 7.20 (see on page 128). The same homogeneous deformations are applied in FE simulations. During the simulations the plate is constrained at one side and the displacement of 0.15 mm is applied at the other (see the loading scheme in Chapter 6, Fig. 6.16). Taking into consideration the length of the simulated plate (100 mm), the required homogeneous

deformation of $\varepsilon = 0.15\%$ is achieved. A number of plates with individually simulated heterogeneities have been modeled.

The equivalent strain in one of the simulated plates is presented in Fig. 7.19b (see on page 128) as an example. Obviously, the X-ray image of the real specimen (see Fig. 7.20 on page 128) and the simulated heterogeneity in the plate (see Fig. 7.19a on page 128) look rather different in their heterogeneity. Thus, it is not possible to find the identical areas in both images due to stochastic distribution of fibers clusters in real specimen and generated heterogeneity primitives in simulated plate. However, the parameters of both heterogeneities (sizes and amplitudes of fiber clusters) should be compared using more scientific methods than visual observation.

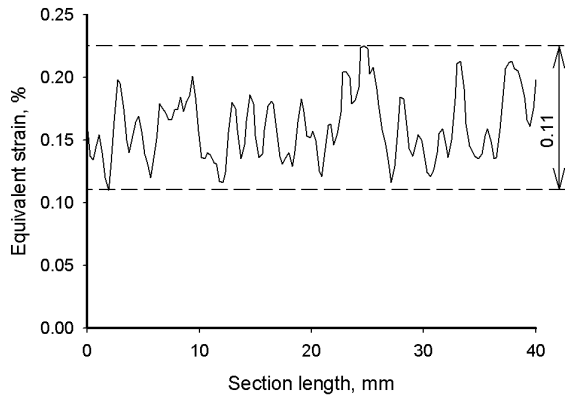
A section in the form of a line can be used in order to compare the strain distribution in experimentally tested specimens with that of the simulated plates. A section is a line drawn along the center line from left to right in a simulated plate and tested specimen. The experimentally obtained distribution of equivalent surface strain presented in Fig. 7.20 (see on page 128) at $\varepsilon = 0.15\%$ is used for the comparison. The equivalent strain distribution along chosen sections is presented in Fig. 7.10.

In that figure the estimated mean equivalent strain in tested ($\varepsilon = 0.16\%$) and simulated ($\varepsilon = 0.15\%$) specimens are rather close to each other. This shows that the average response of the FE model is correct.

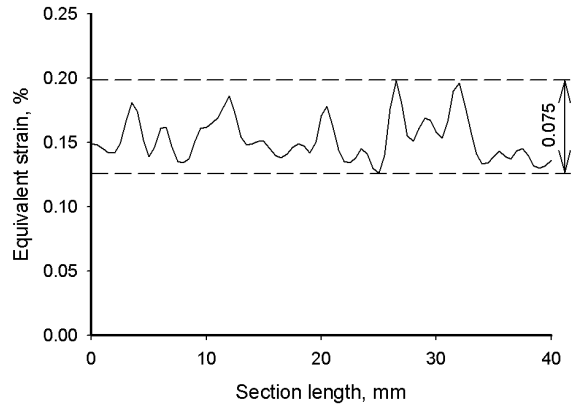
The variation of the equivalent strain along the section in tested and simulated specimens is slightly different. In experimentally obtained data the maximum magnitude of equivalent strain variation in the material can reach up to 147% (see Fig. 7.10a) and in simulations up to 134% (see Fig. 7.10b) relatively to its mean value. These high variations in the material cannot be neglected during the structural design. The amplitude of the strain variation is calculated between its maximum and minimum values. Thus, the amplitude of the strain variation in the tested specimen is about 0.11%, but in the simulated it is about 0.075%, thus slightly lower. This explains the oblateness of the histogram of FEA strain variation (see Fig. 7.10d). However, both strain distributions have the same stochastic distribution of values, which is corresponding to χ^2 -distribution (see Fig. 7.10e, Fig. 7.10f).

The waveforms of the observed variations of strain in experiment and simulations can be compared in order to check their similarity. Obviously, the strain variations can be considered as signals which can be analyzed with spectral analysis. According to the performed spectral analysis in the experimentally obtained strain variation there are four major harmonics, with periods equal to 15 mm, 8 mm, 4 mm and 2 mm, while in the simulated strain distribution the major harmonics are 12 mm, 5 mm and 3 mm, which is rather similar to those observed in the experimental strain. The agreement in the comparison of the waveforms is rather important because it shows similarity in the sizes of the simulated heterogeneity primitives with those actually present in real specimen and registered with ARAMIS. Based on the carried out comparison, the reasonable validation of the developed material model for heterogeneous materials is achieved.

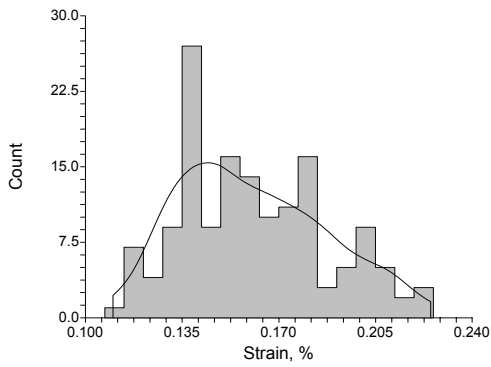
The difference in the amplitudes of the strain variations in Fig. 7.10a and Fig. 7.10b can be explained by the fact that ARAMIS system utilizes indirect principles of measurements of the surface strain. The accuracy of these principles, while measuring heterogeneous materials is questionable, because it is capable to observe strain only on the surface of an object. As it was discussed earlier, the distribution of fiber through the thickness of a composite reinforced with non-woven fibers is not uniform. If, for example, such composite would be possible to subdivide into hypothetical in-plane "layers", then each layer will have its own in-plane fiber distribution (and its own in-plane heterogeneity). When a composite specimen is loaded, the strain observed by ARAMIS corresponds to that in the layer closest to the observed surface of an object (note: ARAMIS measures only surface strain). Strain in the other hypothetical layers is hidden to ARAMIS's cameras, and therefore cannot be measured, but it has an indirect effect on the strain on the surface. This effect is also hardly measurable. The conclusion regarding the application of ARAMIS system for



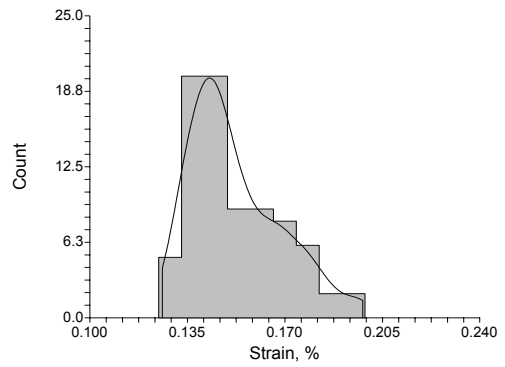
a) Strain distribution in ARAMIS



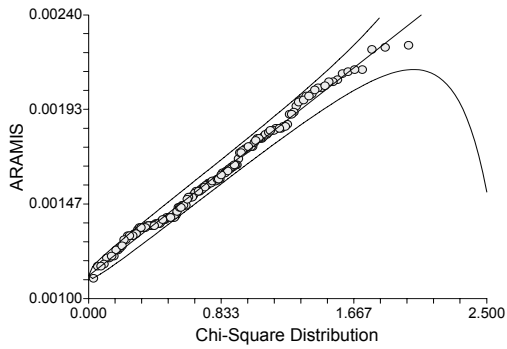
b) Strain distribution in FEA



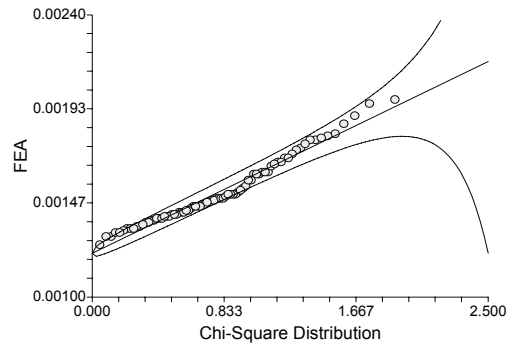
c) Histogram of ARAMIS strain



d) Histogram of FEA strain



e) χ^2 probability plot for ARAMIS results



f) χ^2 probability plot for FEA results

Harmonics length, mm	
ARAMIS	FEA
15	12
8	-
4	5
2	3

g) Spectral analysis results

Figure 7.10 Comparison of equivalent strain along a section in results obtained from ARAMIS and FE simulations for specimen with thickness ($t=4.6$ mm) at applied homogeneous strain of $\varepsilon=0.15\%$.

measurements of strain in heterogeneous materials, in particular for natural fiber composites reinforced with non-woven fiber mats, has to be very careful drawn due to non-uniformity through thickness of material.

Heterogeneity parameters of the composite plates for FE simulations in this work are estimated using the X-ray images of real specimens. It is obvious, that the X-ray image characterizes the in-plane heterogeneity of a composite by using integral amount of fibers, which are present in the core of the material. This means that in-plane heterogeneity in each of the hypothetical layers is accounted not layer-by-layer, but as a whole. Therefore using the developed technique the generated in-plane heterogeneity for FE simulations represents the integral value of non-uniformity through the thickness of finite elements. According to ARAMIS measurements, the amplitude of in-plane properties heterogeneity variation in the top hypothetical layer of the investigated specimens appears to be higher than it is estimated using X-ray images. High properties variation in the top layer result in high amplitude of the observed strain variation, but this does not mean that such high variation appears in the core of composite. The reason for the difference in the amplitudes of variation of the simulated and experimentally obtained strain is explained by different approaches for material property description involved.

In order to reach a better correlation of ARAMIS measurements with the structure of the reinforcement it is essential to use specimens thin enough to assume that there is no non-uniformity through the material thickness. The material description in this case becomes similar to that used in FE simulations, which will result in a better correlation of simulations and experiments. However, additional experimental work is needed in order to determine the proper thickness of specimens. It is evident that in experiments carried out earlier in this thesis with specimens cut out from a composite plate with different thicknesses the heterogeneity is extremely high in thin specimens due to not optimized technology. However, according to the X-ray images the local anisotropy in thin specimens governs the extreme non-uniformity their mechanical properties.

The problem of finding applicable thickness and accounting for local anisotropy in the composite specimens can be defined as challenging tasks for the further development in the area of natural fiber composites. The developed model for simulation of heterogeneous materials can be also improved towards better accuracy (will be suggested later).

7.3 Testing of the structure

An automotive structure made of PP/Flax composite has to be chosen for the approbation of the developed technique for simulation of structures made of heterogeneous materials. However, not every automotive component can be made of natural fiber reinforced composites due to limited mechanical properties of the material (as discussed in Chapter 2). Therefore, a suitable structure for the research purposes has to be selected. In this thesis the investigations of cost aspects of structure redesign are not considered, but the mechanical performance will be investigated.

Since the objective of the whole research project is to find a possibility to make structural automotive components by using natural fiber composites, the structure should be preferably load bearing. Moreover, due to the yet unresolved problem of moisture uptake of natural fibers the structure should be in the car interior. There are several structures in a car, which can satisfy the mentioned criteria. Door trim panels, a dashboard, seat squabs, seat bases, a rear parcel shelve are rather suitable. However, due to the lack of possibility to produce such components in our university laboratory (absence of moulds, presses etc.) cooperation with industry has been established. An automotive seat base component is chosen for investigations. This structure is located in the middle of the rear seat of a car. It is an interior and load bearing part. It is designed to carry the load of one person (100 kg) during normal service conditions and it is capable to carry a dynamic load of the same person during car collision (by preventing the seat squab from sliding). A photograph of this structure is in Fig. 7.11. Originally this structure is made of PP reinforced with 40 vol. % of

randomly oriented Glass fibers (GMT) using compression molding. The mass of GMT structure is 547 gram and average walls thickness is 2.6 mm.

7.3.1 Materials

The described seat base structure is experimentally made of PP/Flax composite with 30 vol. % of fibers in form of non-woven mat. The same semi-finished material (as for composite plates) investigated earlier from Symalit® (Switzerland) and compression molding production technique have been used. The natural fiber composite sheets were cut in pieces of desired dimensions, then heated in an oven up to 190 °C and rapidly placed in a heated mold (50 °C) and compression molded. The amount of initial material has been experimentally obtained to achieve good filling of the mold and to reach proper thickness of the resulting component. Several structures using natural fiber composite with different wall thicknesses were made. This was possible since a closed mold has been used. By putting different amount of initial material the resulting thickness of structure can be varied. Structures with 3 different wall thicknesses are made:

- a) the same as original GMT ($t = 2.6$ mm);
- b) 25% thicker relatively the original ($t * 1.25 = 3.25$ mm);
- c) 50% thicker ($t * 1.5 = 3.9$ mm) relatively the original one.

The reason of making different thickness is to check the possibility of simple material substitution without costly redesign of the structure and the mold. The bending stiffness and the weight of structure are the parameters to compare.

7.3.2 Testing procedure and general results

A loading scheme used for the test is presented in Fig. 7.12. Cylindrical restrainers ($\varnothing 12$ mm) support the structure at two sides in order to define the boundary conditions clearly (line contact). It is essential to have simple and well determined boundary conditions for FE simulations. The cylindrical indenter ($\varnothing 12$ mm) is used to apply load on the structure. A position controlled loading is applied during the test. The displacement of the indenter and the reaction force are recorded by the testing equipment. The force-displacement diagrams are obtained during testing and presented in Fig. 7.13. Structures with different wall thickness behave differently. Their loading diagrams are rather linear and have different slopes. Thus, the original structure made of PP/Glass composite with thickness $t = 2.6$ mm can be used as a reference. The resulted weight and stiffness of the structure made of different materials are presented in Table 7.5.



Figure 7.11 The rear seat base structure.

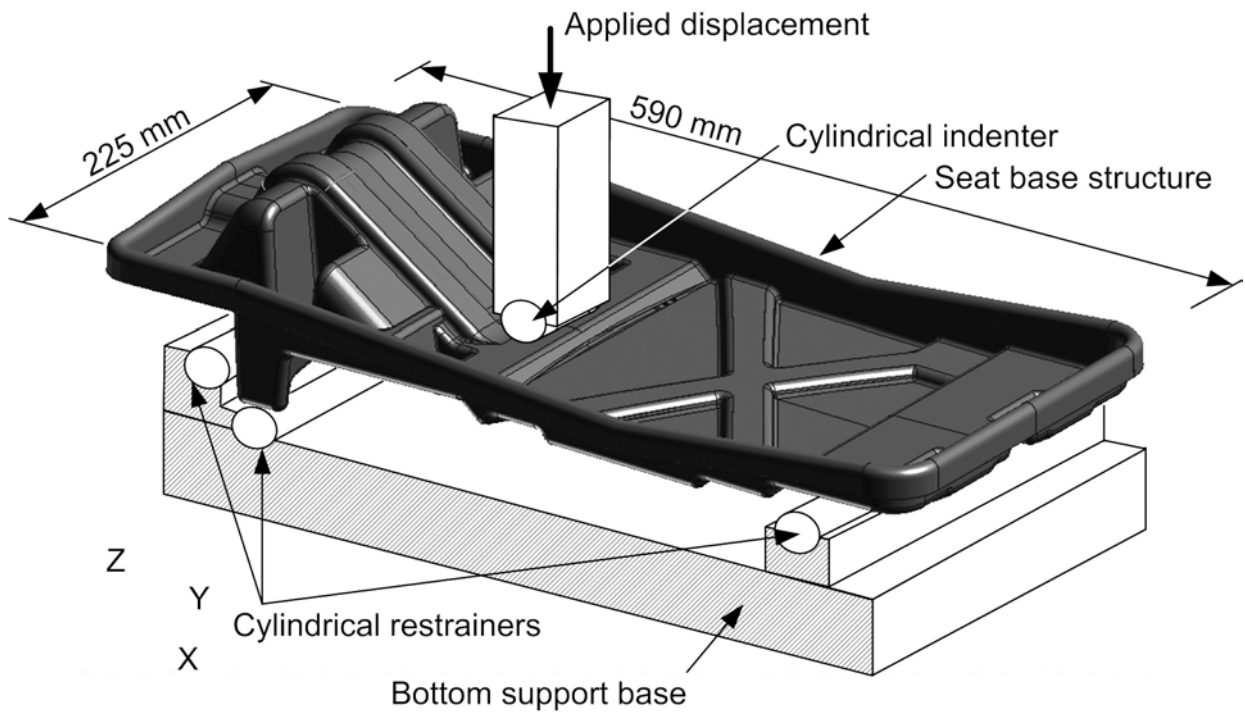


Figure 7.12 Loading scheme.

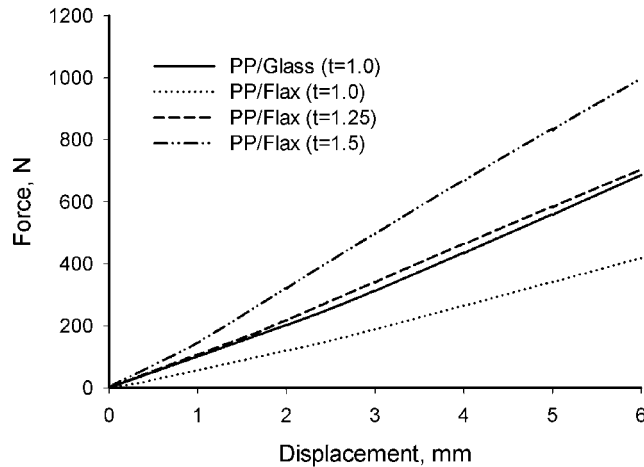


Figure 7.13 Reaction force diagrams of the seat base structure made of different materials and with different wall thickness.

Table 7.5 Mass-stiffness comparison of the seat base structures made of different materials and with different wall thickness.

Material (thickness)	Relative mass*	Relative stiffness*	Mass, gram
Glass/PP ($t=2.6$ mm)	1.00	1.0	575
Flax/PP (t)	0.88	0.61	506
Flax/PP ($1.25 \cdot t$)	1.08	1.03	621
Flax/PP ($1.5 \cdot t$)	1.26	1.45	724

* values are in comparison with Glass/PP ($t=2.6$ mm)

The seat base structure made of PP/Flax with thickness $t=2.6$ mm has about 40% less stiffness than that originally made of PP/Glass with the same thickness. Therefore, simple substitution of glass fiber composite with natural fiber does not provide sufficient stiffness to the structure. However, by increasing the thickness of the structure up to $1.25 \cdot t = 3.25$ mm, the stiffness of the structure made of PP/Flax reaches the same level as PP/Glass, but the weight is increased by about 8%. Obviously the mechanical properties of the used PP/Flax composite are relatively low. Indeed, according to the results of specimens testing, the Young's modulus of PP/Flax composite is about 3000 MPa, but PP/Glass is about 3570 MPa (the difference is about 15% in favor of PP/Glass). The used PP/Flax composite has lower amount of natural fibers (30 vol.%) and no fiber-matrix interface improvement (at least according to the manufacturer's data sheet). Therefore, according to reference survey presented in Chapter 2 it is expected that about 50% improvement in the Young's modulus of a composite can be obtained by improving the fiber-matrix bonding. The interface improvement can be achieved through, for example, using silane fiber treatment or maleic anhydride PP (MAPP). The thickness of PP/Flax structure can be reduced in this case and without worsening its stiffness and, then, weight savings, very important for fuel efficiency of a car, can be obtained.

However, even using a not improved PP/Flax composite there are some benefits of substituting a PP/Glass composite, e.g. a more sustainable material, provides better labor conditions (no skin irritation) and causes less wear of equipment.

7.3.3 Analysis of structure's heterogeneity

After the overall stiffness performance analysis of the seat base structure it is necessary to look at the heterogeneity in its reinforcement. The seat base structure made of PP/Flax composite with thickness $t=2.6$ mm will be used for heterogeneity estimation and for FE analysis. Heterogeneity in properties is expected. The digitized X-ray photograph (see Fig. 7.14) of the structure is used for the analysis. The investigations in the research purposes are focused not on the whole structure, but on a part of it due to complexity of the structure's geometry. In that structure there is a large flat area in the center (see Fig. 7.11) and there are ribs in the other locations.

The X-ray photograph of a structure made of fiber reinforced material gives a unique possibility to analyze the distribution and orientation of the reinforcement affected by a material flow during manufacturing. Sometimes, from such a photograph it is possible to estimate the mechanical properties of a structure and to assess its behavior without breaking. Indeed, in the X-ray photograph (see Fig. 7.14) the reinforcement is random and heterogeneous, however in some areas there is local anisotropy. Undoubtedly the anisotropy appears due to different properties of material flow during the compression molding. The anisotropy is well defined in those parts where the material has to flow over the ribs, or through narrow complex geometrical forms of the mold. The developed model can be applied to those areas where there are randomly oriented fibers. Thus, central area (see magnified image 3 in Fig. 7.14) in the structure is rather suitable because the absence of local anisotropy in the reinforcement.

7.3.4 Measurements of the surface strain field

The structural behavior can be experimentally measured by a contactless strain measurement system ARAMIS (GOM GmbH, Germany). This system has been used to evaluate the non-uniformity of surface strain in tensile loaded composite specimens showing partial success. The seat base structure made of PP/Flax (30 vol.% non-woven fiber mat) composite with wall thickness $t=2.6$ mm is subjected to position controlled loading by using the same loading conditions as described earlier (see Fig. 7.12), and with applied contactless strain measurement system. Due to the limited resolution of ARAMIS's cameras, only part of the structure is observed during the experiments. A smaller observation area can give better visualization of small surface strain non-uniformities and therefore result in more accurate and detailed results. Equivalent surface strain in the central area of the structure is obtained

(see Fig. 7.23 on page 133). Location of the observed area in the structure is also presented in that figure. The X-ray image of the same area is presented in Fig. 7.25 (see on page 136) to compare the non-uniformity of observed surface strain and the reinforcement distribution. Some correlation between measured surface strain concentrations and the local low amount of fibers (determined from the X-ray image) in the structure can be observed in Fig. 7.25 (see on page 136).

However, there are some exceptional areas in the measured surface strain field while being compared with X-ray image of the reinforcement. The areas of local disagreement are presented in Fig. 7.26 (see on page 136). In that figure the strain concentrations unexpectedly appear in those areas of the structure, where there is a high amount of fibers (according to the X-ray image). This phenomenon has already been discussed earlier in this thesis. The X-ray image shows the integral amount of fibers present in a particular local area, but not their distribution through the composite thickness. It is not possible to make a distinction between the fibers in the core of material and those on the surface. However, the used contactless strain measurement system (ARAMIS) gives the strain field observed only on the surface of the material as a result of the measurements.

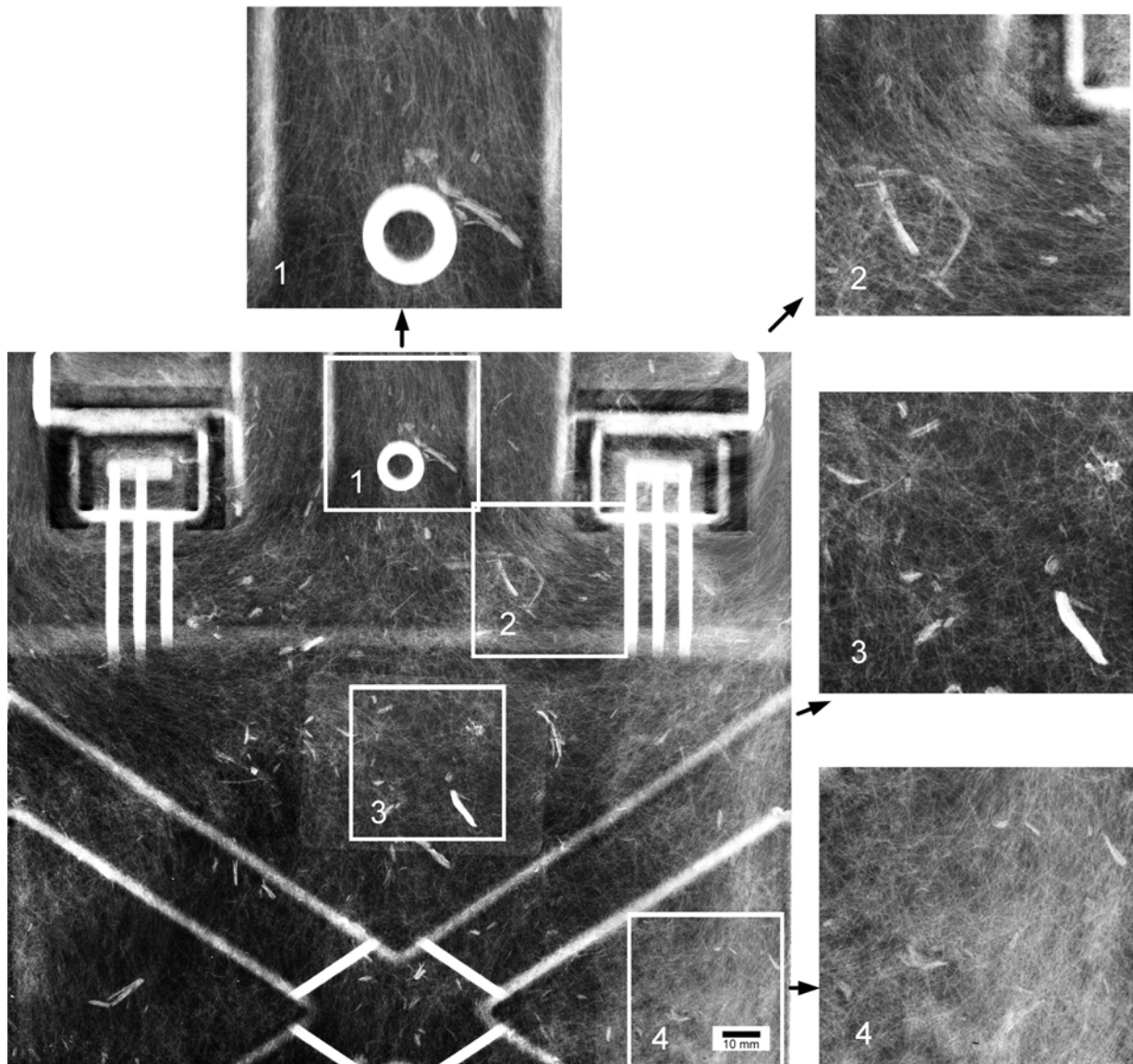


Figure 7.14 X-ray image of the seat base structure with thickness $t=2.6$ mm.

During the loading of the structure it is obvious that the fibers close to the surface behave differently from those in the core. And they have a major influence on the measured surface strain, while the strain in the material core can be rather different. As a result in Fig. 7.25 (see on page 136) there is high a local strain in that area where there is potentially stiff material (a lot of fibers, according to X-ray photograph). Therefore, a truly high local strain in the material core is not necessarily present. As follows, interpretation of the results derived from the ARAMIS has to be very careful.

The variation of the equivalent surface strain measured by ARAMIS (see Fig. 7.24b) can be numerically characterized by using a section drawn along the strain image (presented in Fig. 7.24a). The equivalent strain in that section varies in range of 0.038 - 0.13 %. This variation is rather high, since it reaches up to 170% of its mean value. Therefore, the appeared stress-strain state in some local areas can exceed the design limits unexpectedly if the design is performed with the assumption that the natural fiber composite has homogeneous properties. The variation of the stress-strain state in the structure in this case is underestimated. The usage of heterogeneous simulations can help to avoid such a problem and to improve the design.

7.4 Estimation of heterogeneity parameters for the structure

The developed technique (see in Chapter 3) is applied for the estimation of heterogeneity parameters of PP/Flax composite used for manufacturing of the seat base. Available digitized X-ray image of the structure (see Fig. 7.14) can be used for that purpose. The central area of the seat base structure is in focus. Estimated heterogeneity parameters are presented in Table 7.6. These parameters are implemented into FE simulations of the seat base structure for heterogeneity generation procedure.

Table 7.6 Heterogeneity parameters estimated in central part of seat base structure made of PP/Flax composite

Harmonics	Size (St. dev.), mm	Normalized Amplitude (St. dev.)
1	15.49 (2.06)	0.06 (0.03)
2	11.15 (1.46)	0.16 (0.09)
3	7.44 (0.77)	0.04 (0.02)
4	6.13 (0.88)	0.07 (0.11)
5	4.77 (0.49)	0.14 (0.07)
6	4.16 (0.44)	0.07 (0.05)
7	3.59 (0.49)	0.08 (0.03)
8	2.85 (0.8)	0.39 (0.1)

7.5 Simulation of the structure

7.5.1 Geometry and boundary conditions

Finite element simulations of the seat base structure are carried out in order to test the developed material model by complex geometry of FE model. Boundary conditions (BC) in the simulations are equal to those used during mechanical testing of this structure. In the experiments two cylindrical restrainers ($\varnothing 12\text{mm}$) are used to support the structure. The load is applied by a moving cylindrical indenter ($\varnothing 12\text{mm}$). In the FE model restrainers are specified as zero movement of appropriate nodes in vertical (Z) direction, but the indenter is specified as a rigid cylindrical surface, which goes into contact with the structure. During the simulation the surface moves downwards (-Z) in steps and deforms the structure. The displacement step size is equal to 1 mm. In total 6 steps were applied. The FE mesh with boundary conditions is presented in Fig. 7.27 (see on page 137). Mesh is carefully generated on the basis of available CAD model. The central area of the model is meshed using small

finite elements (approximately side length is equal to 0.25 mm), while the rest of the model is meshed using finite elements with average size of 2 mm. About 54000 of shell finite elements are used in simulations in total. Due to symmetry of the structure the computational complexity of the simulation can be reduced if only a half of the model is simulated. The 3D thick shell finite elements number 75 from standard MSC.MARC elements library are used [135]. The thickness of the finite elements is equal to that of the original seat base structure, thus $t = 2.6$ mm. The number of layers in shell elements is taken equal to 5.

7.5.2 Tuning of material model

The material model developed in Chapter 4 for elastic modulus of natural fiber composite estimation has to be tuned in order to confirm to experimental material properties. Therefore, the empirical coefficient α in the material model suggested in Chapter 4 (Eq. 4.12) has to be adjusted. Since the modulus of elasticity of flax fibers and polypropylene matrix are known and the average fiber volume percentage in the used PP/Flax composite is known to be equal to 30%, then, the Eq. 4.12 can be solved with respect to α . The experimentally obtained Young's modulus equal to 2792 MPa determined for composite plate with thickness $t = 2.0$ mm (see in Table 7.2) is used as a reference. As a result the $\alpha = 0.28$ is calculated using the data presented in Table 7.7 and the model Eq. 4.12 is implemented into the heterogeneity generation procedure.

Table 7.7 Calculation of the empirical coefficient α in the material model (see Eq. 4.12 in Chapter 4) for structure made of PP/Flax with 30 vol.% of randomly distributed fibers.

Material 30 vol.% Flax/PP	Modulus of fibers, GPa	Modulus of matrix, MPa	Experimentally obtained modulus, MPa	α	Theoretically estimated modulus, MPa (Eq. 4.12)
$t = 2.6$ mm	41	1050	2792*	0.28	2780

* Experimentally obtained modulus of composite plate with thickness $t = 2.0$ mm is taken as reference.

7.5.3 Approximation of the structure with geometrical primitives

The geometry of seat base structure is complex. According to the approach suggested in Chapter 6 the structure is approximated with a number of approximation primitives. Namely, 18 planes and one cylindrical surface are specified to approximate most of the large surfaces of a seat base structure. An example of definition of approximation primitive is presented in Fig. 7.28 (see on page 137). The parameters (namely node numbers) for the description of each approximation primitive are specified in the input text file *parameters.txt* (see Chapter 6). According to the developed technique the heterogeneity of material is simulated in each of the specified geometrical approximation primitives using the same parameters from the Table 7.6. These parameters are specified in the input text file *heterogeneity.txt* (see Chapter 5). An example of simulated heterogeneity in the FE model is presented in Fig. 7.29 (see on page 140). In that figure the variation of FE properties is represented by different colors. It should be noted that the simulated heterogeneity represents relative variation in properties of FE elements with boundaries from 0 to 1. The simulated properties of FE elements represent fiber volume fraction parameter. The boundaries for fiber volume fraction variation (Eq. 6.46 in Chapter 6) are chosen equal to $V_{\min} = 10\%$ and $V_{\max} = 60\%$ correspondingly (according to investigations in Chapter 4). Thus, the fiber volume fraction is simulated for each element according to the heterogeneity and then converted into Young's modulus of element using Eq. 4.12 with data from Table 7.7.

7.5.4 General FE simulation results

The FE analysis is performed in a linear elastic mode and the contact option is used. The friction can be neglected, since the contact between two bodies (deformable – seat base

and rigid - indenter) is performed in a way that there is no sliding contact between those two bodies.

Indenter acts on the surface of the structure during simulations. At each loading step normal contact reaction force is measured resulting in total applied force. The resulting force-displacement diagrams for simulated and experimentally obtained are presented in Fig. 7.15. The agreement of these two diagrams proves the correct overall behavior of the FE simulations. This means that the force-reaction response of the FE model is correct. The generated variation in material properties (mean value of modulus is equal to 2647 MPa) result in a FE model with the same stiffness as the manufactured PP/Flax structure. Therefore, the local behavior of the FE model can be compared to that obtained experimentally with ARAMIS.

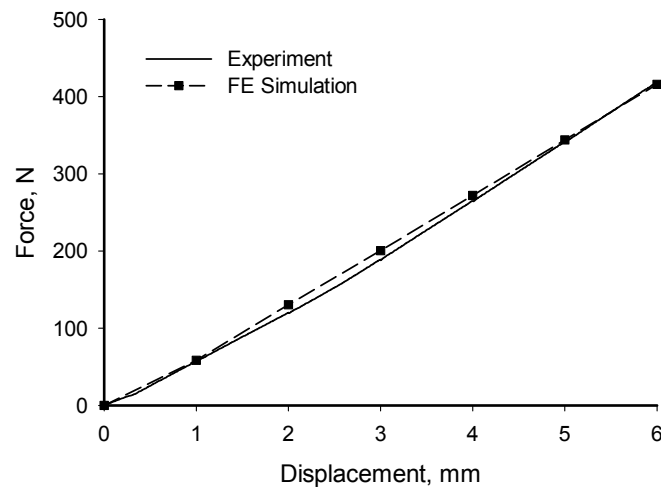


Figure 7.15 Simulated and experimentally obtained force-displacement diagrams of seat base structure made of PP/Flax composite with wall thickness $t = 2.6$ mm.

7.5.5 Comparison of the local behavior of FE model with the local experimental results

The central area of the seat base structure has been investigated by contactless strain measurement system ARAMIS. The clear influence of the material heterogeneity on local stress-strain state in the simulated model has been observed. This appears in non-uniformity of equivalent surface strain. Additional testing of the structure was performed using pre-described displacement loading conditions with glued strain gauges. This test allows to validate the ARAMIS's results (see Fig. 7.24 on page 133), which might be inaccurate due to non-uniformity of material, discussed earlier. The location of strain gauges is presented in Fig. 7.16. Strain gauges are glued to the top surface of the structure. In fact, a 90° rosette strain gauge (two strain gauges in perpendicular directions) has been used. Its orientation was chosen according to the principal directions (X and Y) of the coordinate system of ARAMIS system and global coordinate system of the FE model. The strain gauges have dimensions 3x2 mm (longer – measuring length). The PICAS amplifier (PEEKEL Instruments GmbH) was used to register the signals from the gauges. This equipment has an internal adjustable bridge which allows connecting external strain gauges according to the quarter-bridge scheme. The signal from amplifier was digitized with the analog-digital converter

(National Instruments Inc.) and stored in a PC. Since the strain gauges were glued in principal directions of a global coordinate system the results of their measurements represent two strain components ε_x and ε_y which occur on the surface of the structure during loading.

The strain components ε_x and ε_y are collected from FE model and ARAMIS results at the same location of the real seat base structure where strain gauges are glued. Since the gauges' average the strain over a certain area (in this case 3x2 mm), the results from FE calculations and ARAMIS are also averaged over the equal area. In the FE model certain strain components are taken from the top layer (number 1) of shell elements (they have 5 layers in total). The graphs of the results at different loading steps are presented in Fig. 7.17.

The results derived from both experiments and FE simulations are sufficiently similar to each other. The similarity is good enough for engineering applications. This confirms the correct local response of the FE model. Therefore further, the results of FE model for local equivalent strain can be compared to ARAMIS results in detail.

The central area of FE model is analyzed in order to compare the simulated strain field with that experimentally obtained. Equivalent strain (calculated by using Eq. 7.1) in the top layer (number 1) of finite elements along with generated heterogeneity is presented in Fig. 7.30b (see on page 140). Since the comparison of two stochastic images has to be performed, it is reasonable to use the technique of linear sections applied earlier for plate specimens. Linear sections are drawn through the FE model (see Fig. 7.30a on page 140) and exactly at the same place in ARAMIS results (see Fig. 7.24 on page 133) in order to compare these two results. Equivalent strain in FE model and in ARAMIS measurements along the defined section are presented in Fig. 7.18.

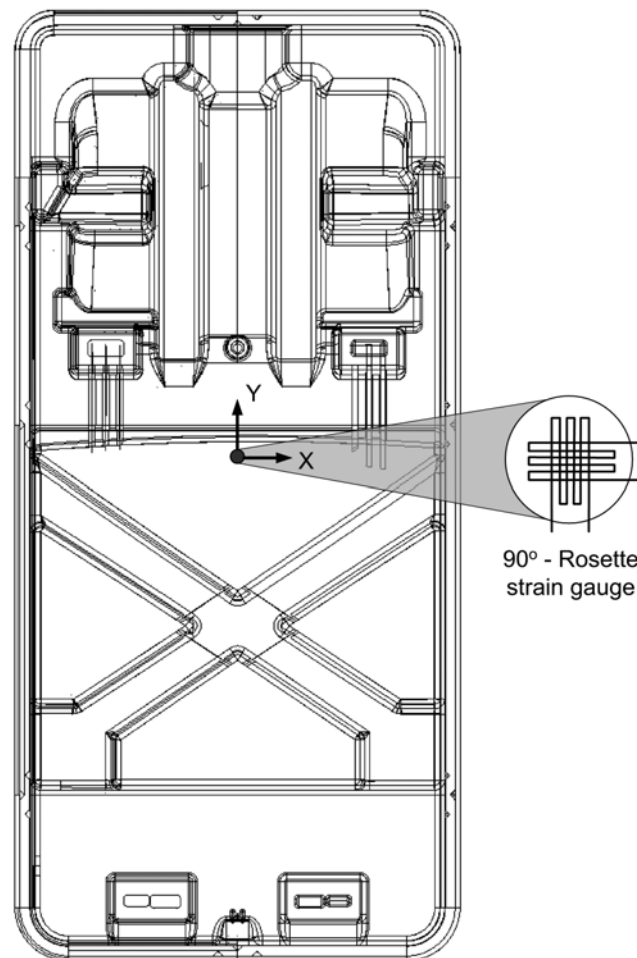


Figure 7.16 Location of strain gauges and their orientation

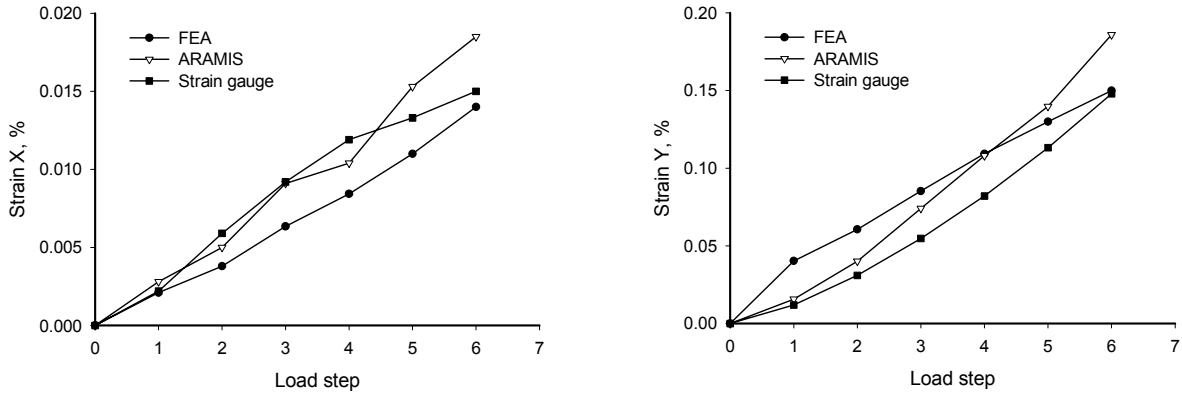


Figure 7.17 Comparison of surface strain derived from the strain gauges, ARAMIS and FE calculations.

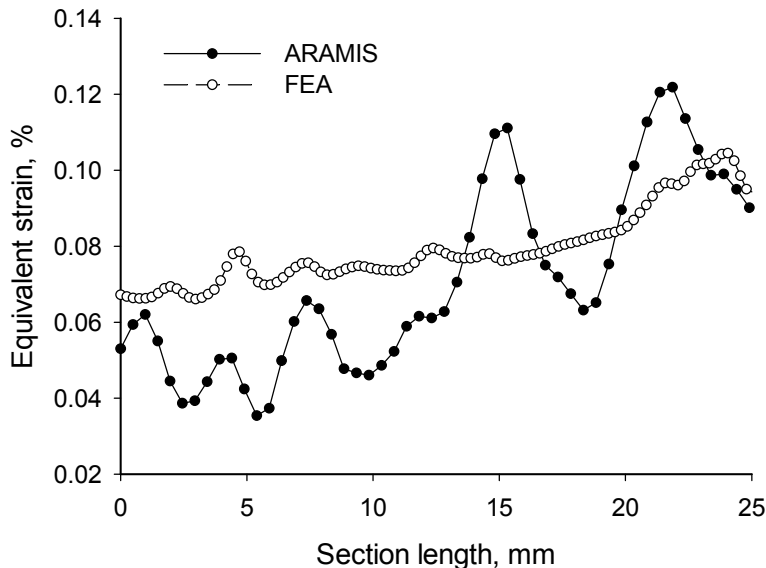


Figure 7.18 Equivalent strain distribution along the chosen section in FE model and ARAMIS results at 4-th load step (indenter displacement is at 4mm).

7.6 Discussion of the results and conclusions

It can be observed that there is a significant difference in equivalent strain distribution along the section in FE simulations and ARAMIS experiments (see Fig. 7.18), while there is a good agreement with the results of the strain gauges presented in Fig. 7.17. The results of a local strain represent the strain at a single point (which is in fact a small area) chosen in the structure and FE model, while the results in Fig. 7.18 represent a number of such points taken along the defined section. Thus, in principle, the results observed in the section are more informative. As it can be seen from Fig. 7.30a (see on page 140) the chosen section ends exactly at that point where the strain gauges are glued. The results of the strain observed in Fig. 7.17 are rather close to each other, so are the strain graphs (Fig. 7.18) at the right part of the sections (where “Section length” is equal to 25 mm). It could be just accidental. The significant difference of the results in the left part of the diagrams in Fig. 7.18 is observed. The overall behavior of the diagrams is similar, ascending from the beginning to the end, while the amplitude of the strain variation is not the same. The FE model shows a much lower strain variation (see Fig. 7.18).

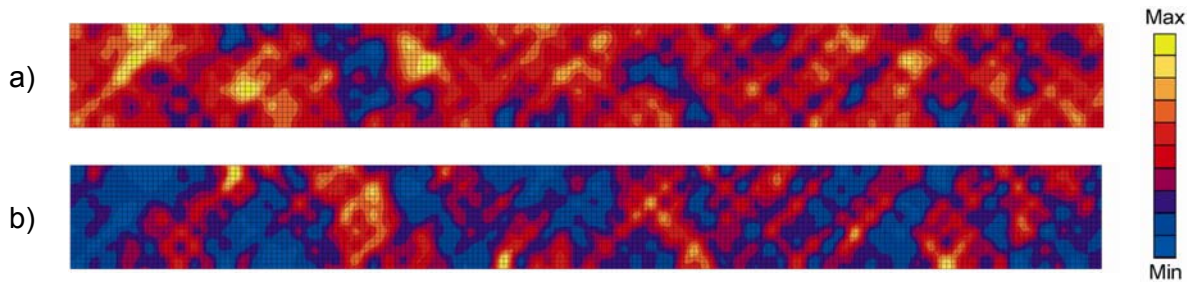


Figure 7.19 Example of (a) heterogeneity and (b) equivalent strain field in simulated PP/Flax plate.

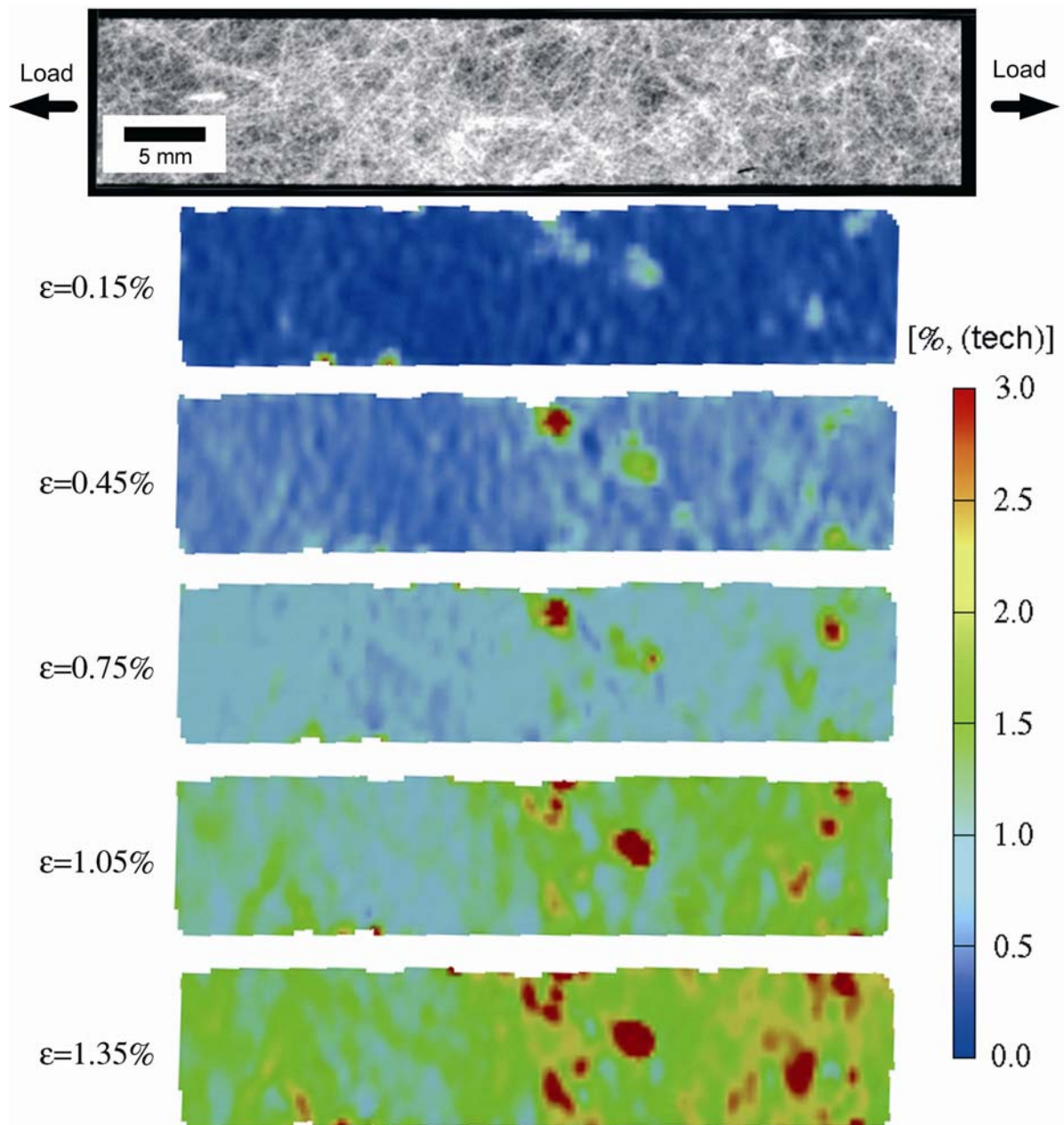


Figure 7.20 An equivalent surface strain field at different loading stages and the structure of the reinforcement in specimen (1C7) cut out from the central area of PP/Flax plate with thickness $t=4.6$ mm.

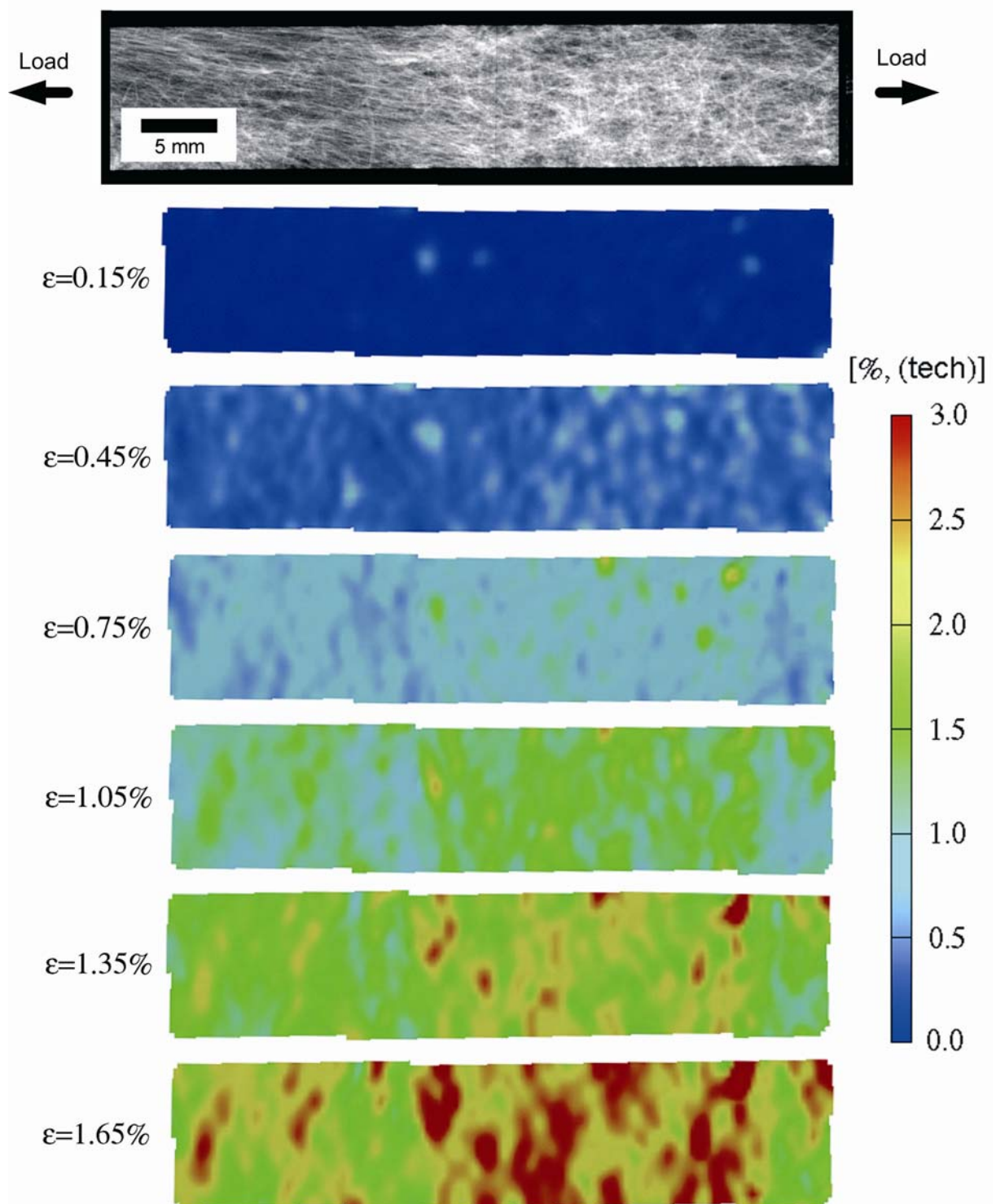


Figure 7.21 An equivalent surface strain field at different loading stages and the structure of the reinforcement in specimen (2S4) cut out from the edge area of PP/Flax plate with thickness $t=3.8$ mm.

This comparison is rather similar to that observed in testing and simulations of composite planes, discussed above. The conclusions derived from that comparison are also applicable to the current problem. The main explanation of the observed difference is due to limitations of the ARAMIS measurement system and material assumptions made during the development of the material model. The strain variation observed on the surface of the seat base with ARAMIS is due to the heterogeneity of the top hypothetical layer of a composite material which is not uniform through its thickness. The strain variations in the other hypothetical layers, certainly, contribute to that surface strain, but their effect cannot be accounted. Simply, in this case the non-uniformity of the strain variation on the surface of the structure measured by ARAMIS is overestimated, while in the FE simulations the composite material is considered to be uniform through the thickness which results in small variation of surface strain. Indeed, it is obvious that X-ray image integrally characterizes the heterogeneity through the thickness of material. In other words, the heterogeneity that is present in each hypothetical layer is accounted not by layer-by-layer, but all together, thus integrally. Therefore, the generated heterogeneity for FE simulations is integral through the thickness of the FE elements. Thus in the simulations, the variation of the equivalent strain on the surface of the FE model is considered as underestimated, due to homogenization of the non-uniformity through the thickness of material. The true amplitude of the surface strain, thus, can be considered somewhere between those two results.

The large difference in the results can be also supported by a complex stress-strain state in heterogeneous composite in case of flexural loading of the seat base structure. A reasonable agreement in the results obtained before in simulations of composite plates with the experimental data obtained for tensile specimens has been achieved. The tensile load is equally applied to all hypothetical layers resulting in stretching both faces of the tested specimens (and simulated plates). Therefore in that experiment and simulations all hypothetical layers of the composite material are loaded uniformly. This result in small divergence of the results obtained experimentally and those simulated.

It appears that the major trouble can come out especially when the stress-strain state in the core of the non-uniform material is also not uniform. Like, for example, in bending, which results in extremely different stress-strain state in core of the bended material (or structure) resulting in stretching at one face of specimen (or structure) and compression at the other. In this case the strain observed with ARAMIS hardly corresponds to that simulated (even in top layer in case of shell finite elements), because the response of the material which is not uniform through the thickness is not same as implemented in FE model (homogenized through thickness).

Therefore there are the limits in application of contactless strain measurement system to non-uniform composites through thickness. Thickness here is the major factor which influences the accuracy of the observed results. A possible solution to that problem can be recommended in the usage of thin specimens, where the non-uniformity through the thickness can be neglected (which is easier to simulate). Moreover, reduced thickness can help to prevent extremely not uniform stress-strain state through the material thickness under complex loading conditions. In all other cases (thick through the thickness non-uniform material, complex loading conditions) the results of ARAMIS observations will largely differ from reality. This is as far as from the site of measuring equipment can be done.

However, the material model used in FE simulations has the advantage of being improved according to the latest research, unlike the ARAMIS system. Moreover, the application of the ARAMIS system is not sufficiently verified in working with the heterogeneous materials. This statement is supported by the manufacturer of this system (GOM GmbH, Germany).

The following actions towards a better accuracy of the developed heterogeneity estimation technique and FE simulations can be proposed. First of all, instead of using of X-ray images of composite (which represent integral amount of fibers) the CT-scans at different hypothetical layers through the material thickness can be used in order to obtain separate heterogeneity parameters in each layer. In FE simulations layered composite shell elements can be used. These elements allow different properties definition for each layer. Furthermore

a unique heterogeneity based on the estimated parameters can be generated for each layer in composite finite elements separately. The anisotropy, which is present in a real composite, can be also taken into account. The mentioned modernizations of simulation procedure will definitely increase the calculation complexity (longer time of calculations), but the results are expected to be much more realistic.

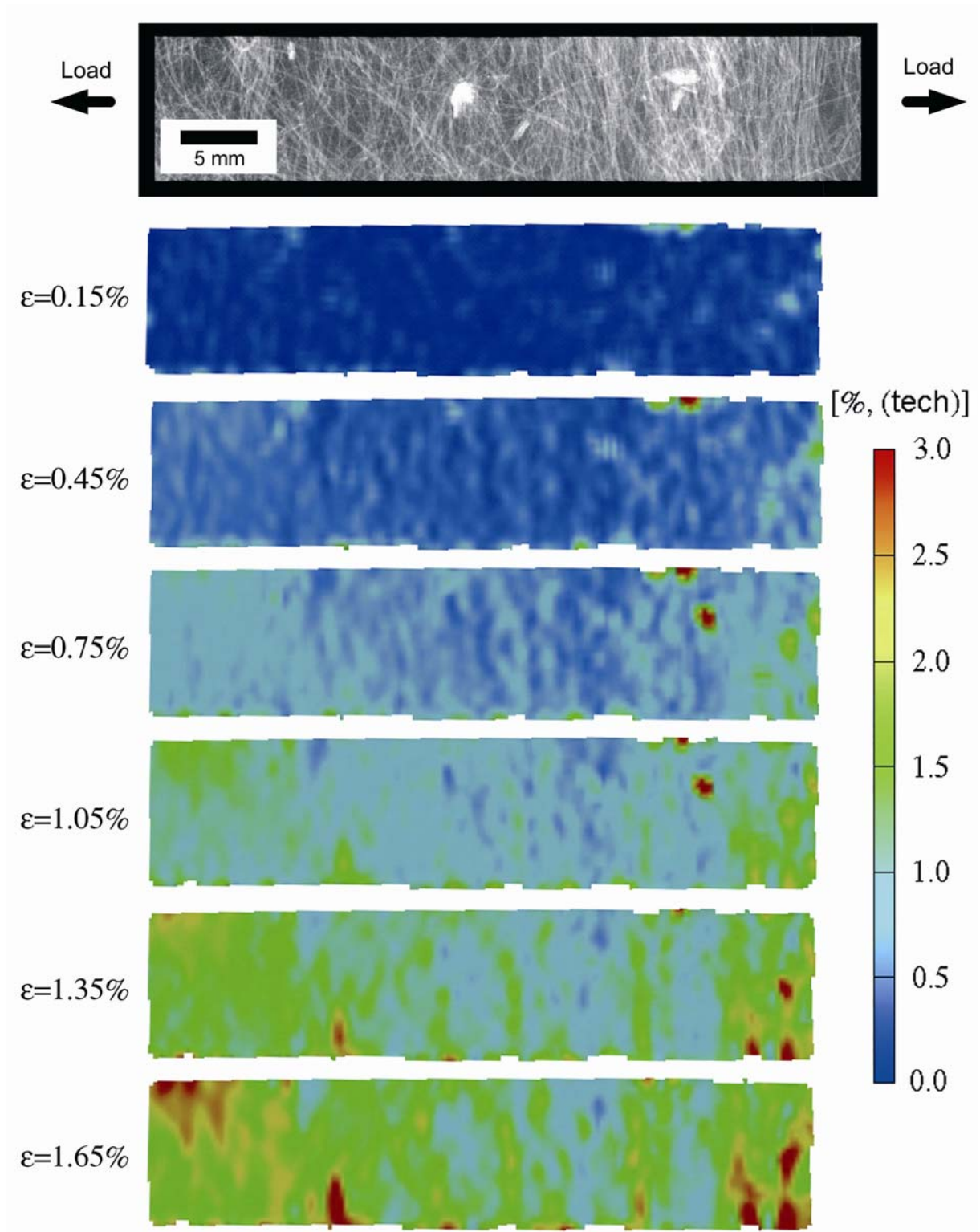


Figure 7.22 An equivalent surface strain field at different loading stages and the structure of the reinforcement in specimen (3C2) cut out from the central area of PP/Flax plate with thickness $t=2.0$ mm.

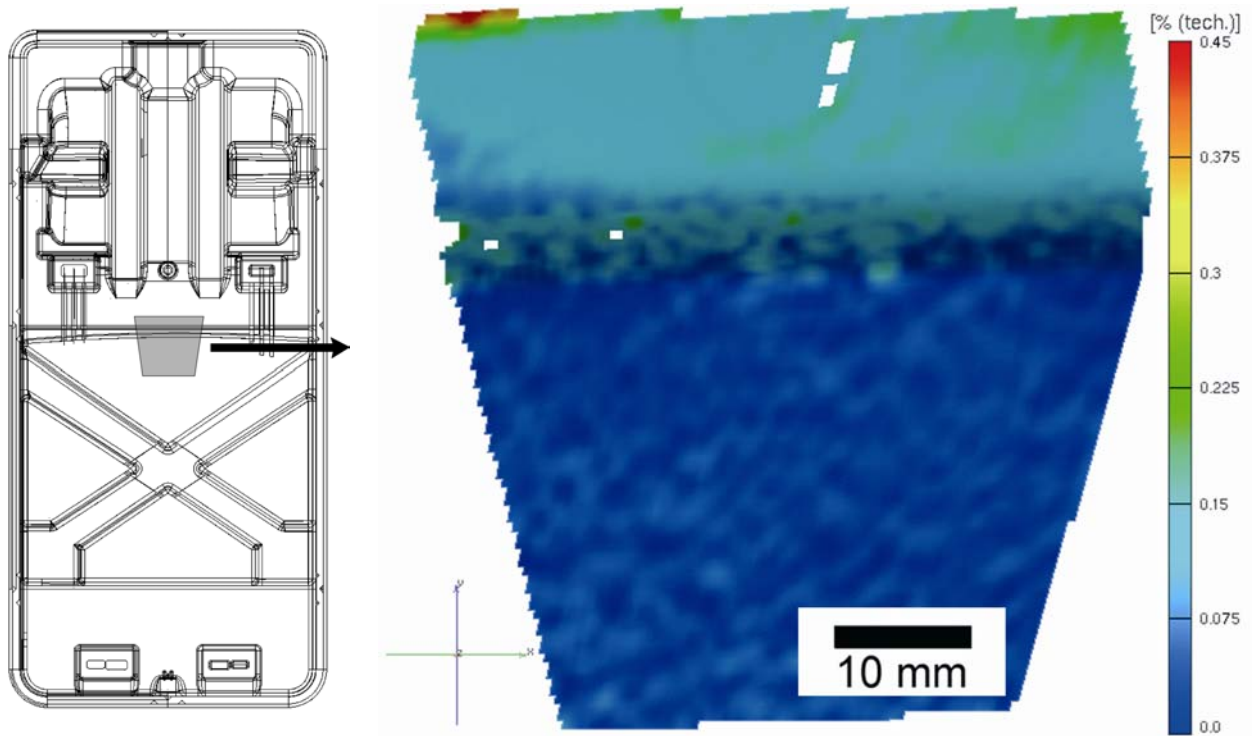


Figure 7.23 The equivalent surface strain in the central part of the seat base structure made of PP/Flax (30 vol.% of non-woven fiber mat) composite with thickness $t=(2.6 \text{ mm})$.

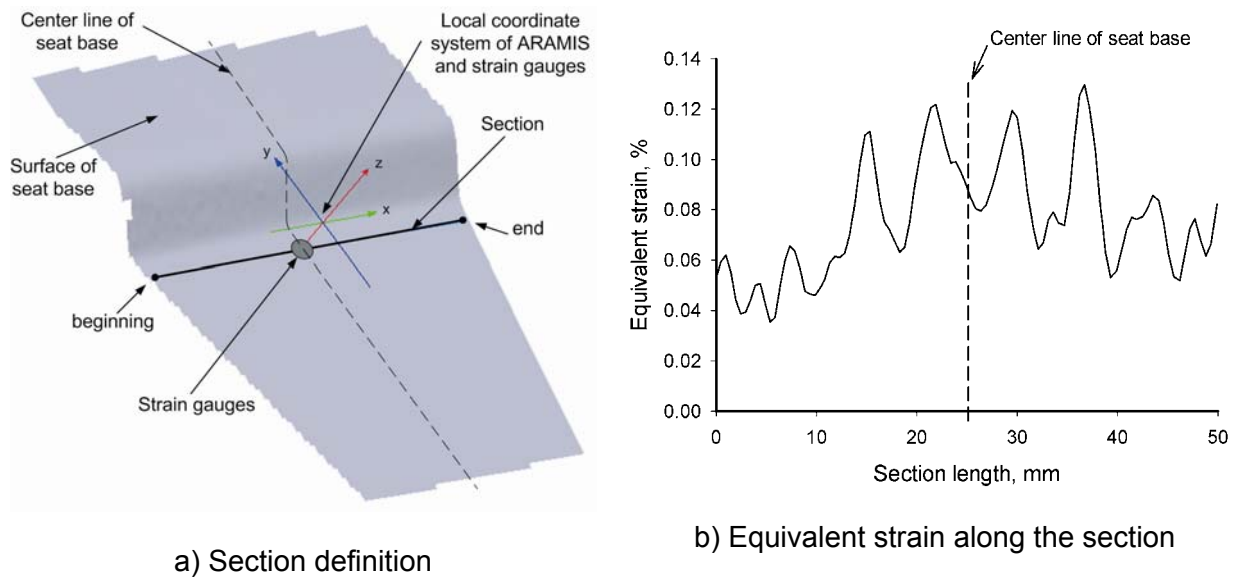


Figure 7.24 Equivalent surface strain distribution along a section chosen in ARAMIS results.

Chapter 8

Conclusions

The presented thesis contains the discussion of several topics, in particular: issues of automotive sustainable design, an overview of the properties of modern materials, study and analysis of heterogeneity in properties of natural fiber composites and the advanced numerical simulations of structures. The initial problem of improvement of passenger cars towards a better eco-design is discussed. In accordance with that, the definition of a car sustainability with respect to the influencing factors is made. A lightweight embodiment design is considered as the most efficient way towards car sustainability. Ways of possible improvement of a car design in view of modern materials application has been discussed.

It is suggested that advanced lightweight materials should be used in order to reduce the weight of the car, which leads to reduce in emissions. However, most of the advanced materials like magnesium alloys or conventional glass and carbon fiber composites are very expensive and in most the cases their application requires a large investment in manufacturing equipment. Currently they are applicable in either sports or luxury cars, where the price of the design is not the main issue. But in serial production of passenger cars price plays a crucial role in the design, therefore other modern materials, like natural fiber composites are considered as promising. They have reasonable mechanical performance, comparable with that of glass fiber composites, but at significantly lower price. The manufacturing technology applied is rather similar to that of conventional composites. Moreover, natural fiber composites are based on natural renewable resources, usually derived from plants, which makes a great contribution to the CO₂ balance, even if they are thermally recycled at the end of life. Additional advantages of the usage of natural fibers as reinforcement in composites are the added value to the main production of crops and clothes (where the plant stem either is not used or partly used) and better labor conditions (natural fiber composites while being machined do not irritate the skin and do not create the hazardous dust).

A detail overview of the mechanical properties of the natural fiber composites is presented. Composites with non-woven reinforcement are in focus. Several disadvantages in their properties with respect to the automotive requirements are found. They are: low impact property, high moisture sensitivity and high heterogeneity in their mechanical properties. However, it is found that the impact property and moisture sensitivity can be technological resolved at reasonable costs, unlike heterogeneity, which is inherent in the composites reinforced with natural fibers in the form of non-woven mats. This makes them difficult to apply in load bearing structures due to uncertain in mechanical properties. Numerical simulation tools, like finite element analysis, are commonly used to simulate the behavior of structures under the load. The standard approaches of the material's property description are implemented in these tools. However, the application of standard approaches in simulations of structures made of heterogeneous materials may lead to unreliable results. Therefore, a new approach is needed to implement heterogeneity in material's properties into structural simulations in order to improve the reliability of simulations.

A novel approach is developed in this thesis in order to implement the variation in material's properties (heterogeneity) into the numerical simulations of structures. The approach, in general, consists of the following procedures:

- a) Estimation of heterogeneity parameters;
- b) Heterogeneity generation;
- c) Correlation of the heterogeneity with mechanical properties of a composite;
- d) Approximation of a complex geometry of the structure with geometrical primitives.

The procedures are described in detail and accompanied with examples and recommendations. The studies of composite materials reinforced with natural fibers in form of non-woven mats constitute the basis of the developed approach.

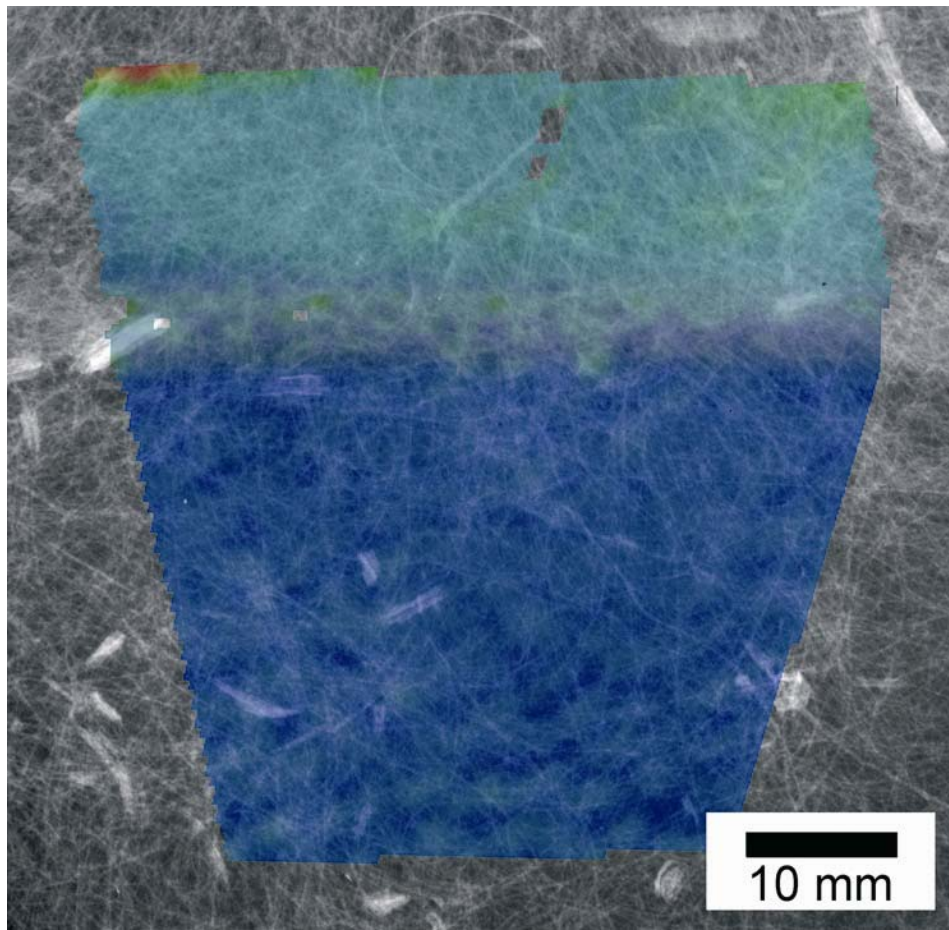


Figure 7.25 The equivalent surface strain field over X-ray image in central area of the seat base structure at the last load step (indenter moved to 6 mm).

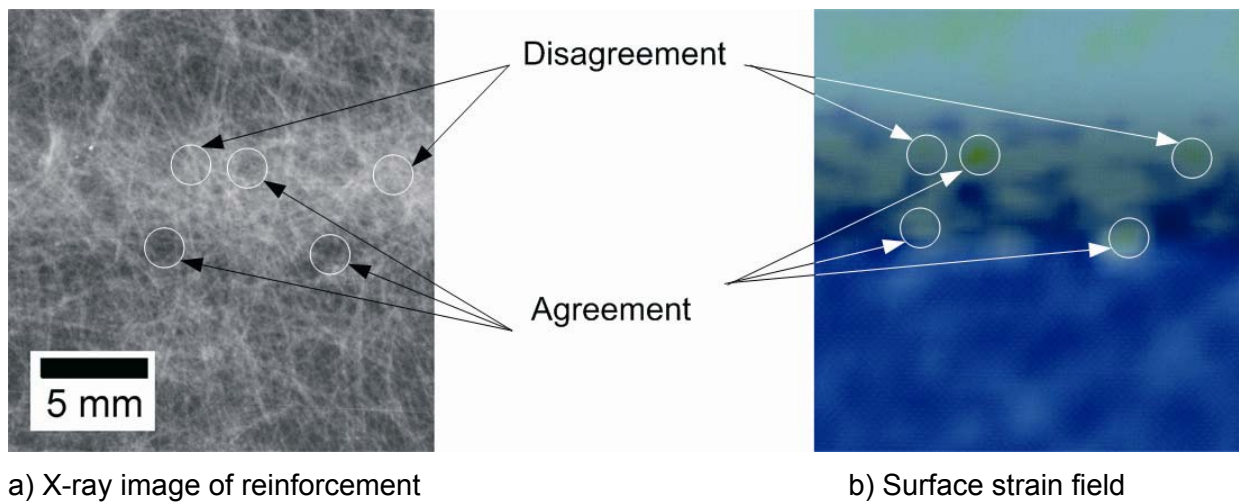


Figure 7.26 Local disagreement in the measured surface strain and the local amount of fibers in PP/Flax structure (derived from X-ray images). The thickness of structure is $t=2.6$ mm.

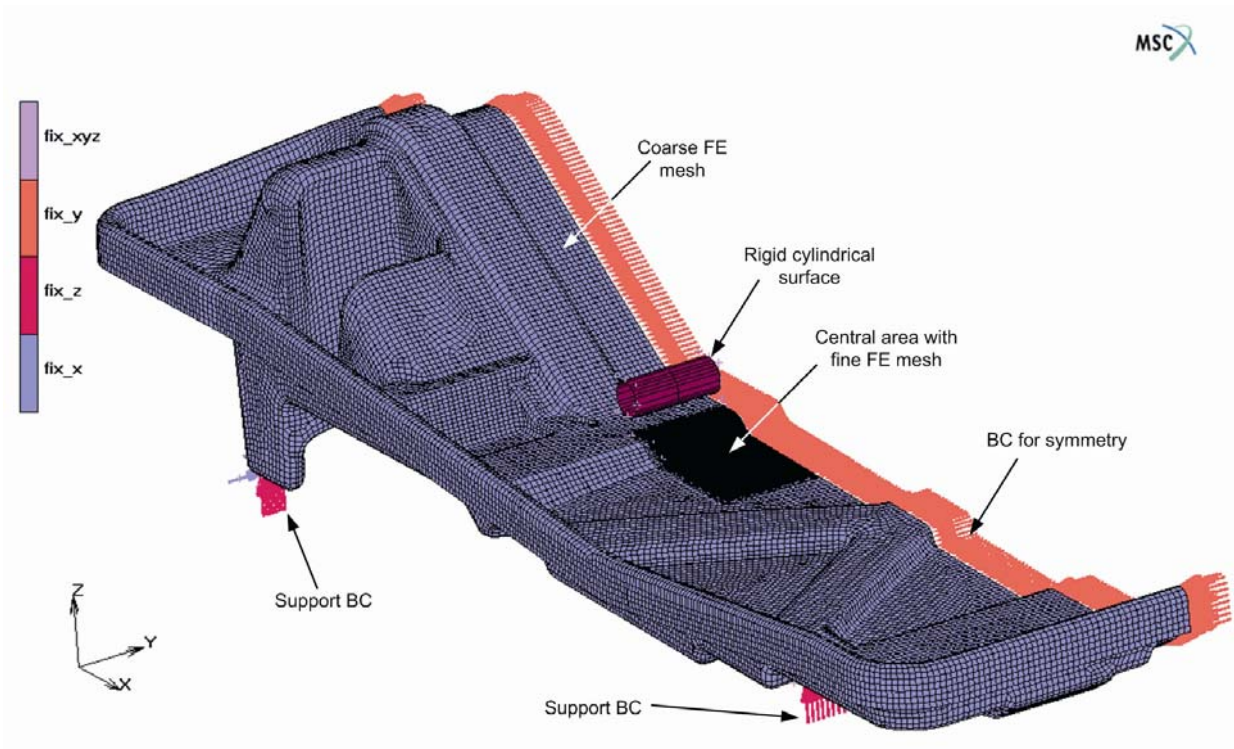


Figure 7.27 Finite element model and boundary conditions for seat base structure.

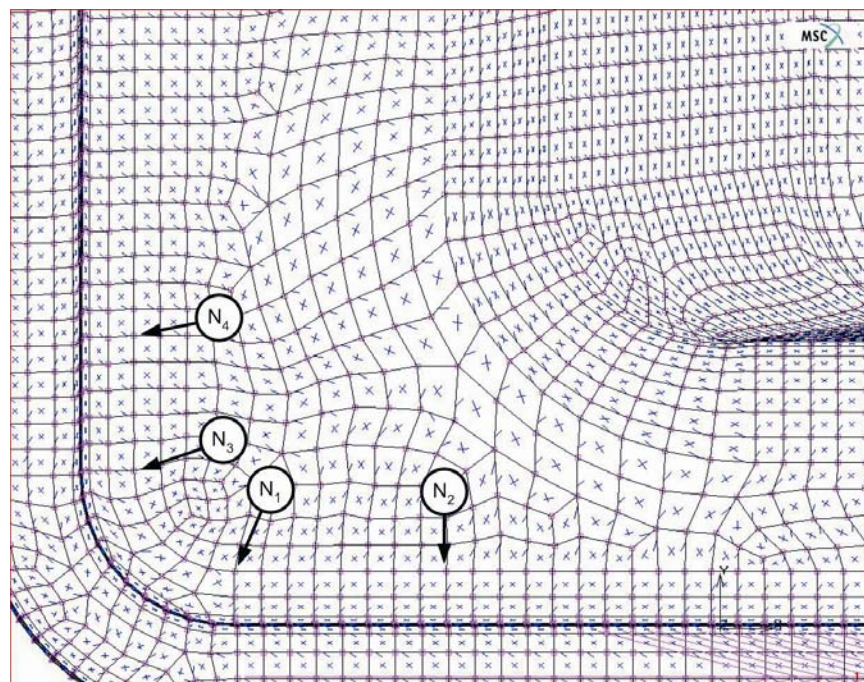


Figure 7.28 Example of one geometrical approximation primitive definition (procedure is according to that described in Chapter 6).

Estimation of heterogeneity parameters. In general the heterogeneity can be found in most materials even in such conventional materials like steel or aluminum (at crystals level). The scale and magnitude of heterogeneity is different for every material. Its magnitude is low in conventional materials due to small variation in properties of crystal, but in composite materials the magnitude of heterogeneity is high, because these materials consist of two or more materials with rather different properties (ductile matrix and stiff fibers). Thus, on a microscopic scale, if the representative volume element of material is taken as small as fibers cross-section, heterogeneity appears as the difference of the fibers' size and their bonding properties to the matrix. On a larger scale, if the size of the representative volume element is comparable to the size of fiber bundles – mesoscale, heterogeneity appears as the difference of properties of fiber bundles (fibers orientations and their amount in bundles). In natural fiber composites, especially in non-woven ones, the mesoscale heterogeneity is particularly outstanding. This can be explained by non-uniform distribution of fibers in the material.

In this thesis the heterogeneity of natural fiber composites is analyzed on mesoscale using the developed technique. The definition of the heterogeneity with respect to non-uniform distribution of fibers in the reinforcement is proposed. The heterogeneity primitives “cluster” and “void” are defined as the basic heterogeneity primitives. The heterogeneity primitives are randomly distributed in the reinforcement and their parameters “size” and “intensity” are stochastic. The size determines the linear dimensions of fiber cluster and the intensity – the amount of fibers in that cluster. The same parameters are used to describe the voids. In order to obtain a quantitative characteristic of the heterogeneity, the size and intensity of the heterogeneity primitives have to be determined. The technique of the determination is based on the analysis of the structure of the reinforcement by using the methods of signal processing. The digital image of the reinforcement derived by either optical scanning or X-raying is used for the analysis. The linear excerpts are stochastically chosen in the image. Each excerpt contains a relative variation of the image brightness, which is considered as a signal. The spectral analysis of the excerpts is performed in order to estimate harmonics in their signal. The set of several harmonics with major amplitudes is determined in each excerpt. The correlation technique is used to determine the representative excerpt. The determined set of harmonics is representative for the given image. The wavelength and amplitude characterize each harmonic and they are correlated with the parameters of the size and intensity of heterogeneity primitives correspondingly. This results in a quantitative characteristic of the heterogeneity.

Heterogeneity generation. The virtual heterogeneity generation using derived parameters of primitives is performed. A low-order heterogeneity is composed of the heterogeneity primitives of certain mean size allocated in a special manner. The complex heterogeneity, called a high-order heterogeneity, is composed as the sum of several low-order heterogeneities. The resulting high-order heterogeneity has similar characteristics to that originally observed in digital image of the reinforcement. The degree of similarity depends on the number of low-order heterogeneities used. The generated heterogeneity is a function, which describes the relative in-plane variation of a certain property of a composite material.

Correlation of the heterogeneity to mechanical properties of a composite. The generated heterogeneity is correlated with the mechanical properties of the composite material by using the developed material model. This material model allows to estimate the modulus of elasticity of a composite reinforced with randomly oriented natural fibers with the known modulus of fibers, matrix and fiber volume fraction. Thus, the generated high-order heterogeneity is first correlated with the variation of fiber volume fraction of composite and then, using the developed model, correlated to the modulus of elasticity.

The heterogeneity generation and modulus estimation model are programmed as a subroutine, which is incorporated into MSC.MARC finite element code in order to perform simulations of structures. This subroutine is able to vary the elastic properties of finite elements in accordance to the generated heterogeneity.

Approximation of a complex geometry of structure with geometrical primitives.

The heterogeneity generation procedure is able to simulate the variation of properties in the structures with simple geometry (plane or cylinder). Therefore, a method of approximation of the complex geometry of a structure with simple geometrical primitives is developed. Heterogeneity is generated in each of geometrical primitives and then assigned to the finite elements on a model according to some special rules. This method allows to perform numerical simulations of structures made of heterogeneous materials with virtually any imaginable shape.

Experimental work is carried out in order to determine the mechanical properties of several natural fiber composites including polypropylene/flax and polypropylene/glass composites with randomly distributed fibers. Not only basic mechanical properties are determined, but also the parameters of their heterogeneity are estimated. The heterogeneity of the mentioned composites is estimated by using X-ray images. Their testing is performed using an advanced contactless strain measurement system (ARAMIS) to determine the variation in the surface strain. The ARAMIS system allows to measure the strain field on the surface of an object with the help of two cameras and specially developed software. A better understanding of material's properties can be achieved while using this system for measurements, which is rather crucial for heterogeneous materials. The non-uniformity in strain field in specimens made of heterogeneous polypropylene/flax composite is obtained and compared to the structure of reinforcement, namely X-ray image. Reasonable correlation of the strain variation and heterogeneity of reinforcement is observed.

Structural simulations have been performed using the developed approach for the simulation of structures made of heterogeneous materials. The heterogeneous composite plates with the geometry similar to the geometry of the tested specimens are simulated. The parameters of heterogeneity are obtained according to the developed techniques using X-ray images. The surface strain in simulated plates is compared to that experimentally obtained. A reasonable agreement is observed. However, the amplitude of the surface strain variation in simulated plates is slightly lower than that obtained in experiments. A reasonable explanation of this disagreement is discussed where the major problem is due to difficulties with measurement and assumptions of material description in simulations. On one hand, in FE simulations the heterogeneity is implemented as variation of mechanical properties of the adjacent finite elements, describing in-plane heterogeneity in material properties. According to analyzed microphotograph of the cross-section of a natural fiber composite there is also heterogeneity through the thickness. It appears due to non-uniform fibers' distribution through the material thickness. Heterogeneity through material thickness is homogenized and therefore neglected in the finite element model, while it is not in a real composite. Therefore the currently developed material model slightly underestimates the amplitude of strain variation appeared in heterogeneous material. On the other hand the ARAMIS system observes the strain variation only on the surface of an object. The variation of strain in the core of the material cannot be measured. The reinforcement close to the observed surface of an object greatly affects the surface strain. Therefore, the strain measurement of ARAMIS is valid only for the thin top "layer" of a composite, which is absolutely not representative for a thick composite. Hence, the developed approach can be improved in the sense of better material description, but the measurement principles can not. In order to increase the accuracy of the experimental contactless strain measurements it is suggested that thinner specimens, where the influence of heterogeneity through thickness is minimal should be used.

An automotive component is manufactured from natural fiber composite as a result of cooperation with industrial partners. An experimental setup for flexural testing of the structure is built. The testing is performed using ARAMIS system and strain gauges (for verification). Structures made of polypropylene/flax and polypropylene/glass are tested. It is found that the flexural stiffness of the structures reinforced with flax fibers can be at the same reach that of reinforced with glass fibers, but with thicker walls resulting in a heavier structure. However, it is suggested that the improvement of mechanical properties of polypropylene/flax composite should be applied in order to make a thinner structure and decrease weight.

Conclusions

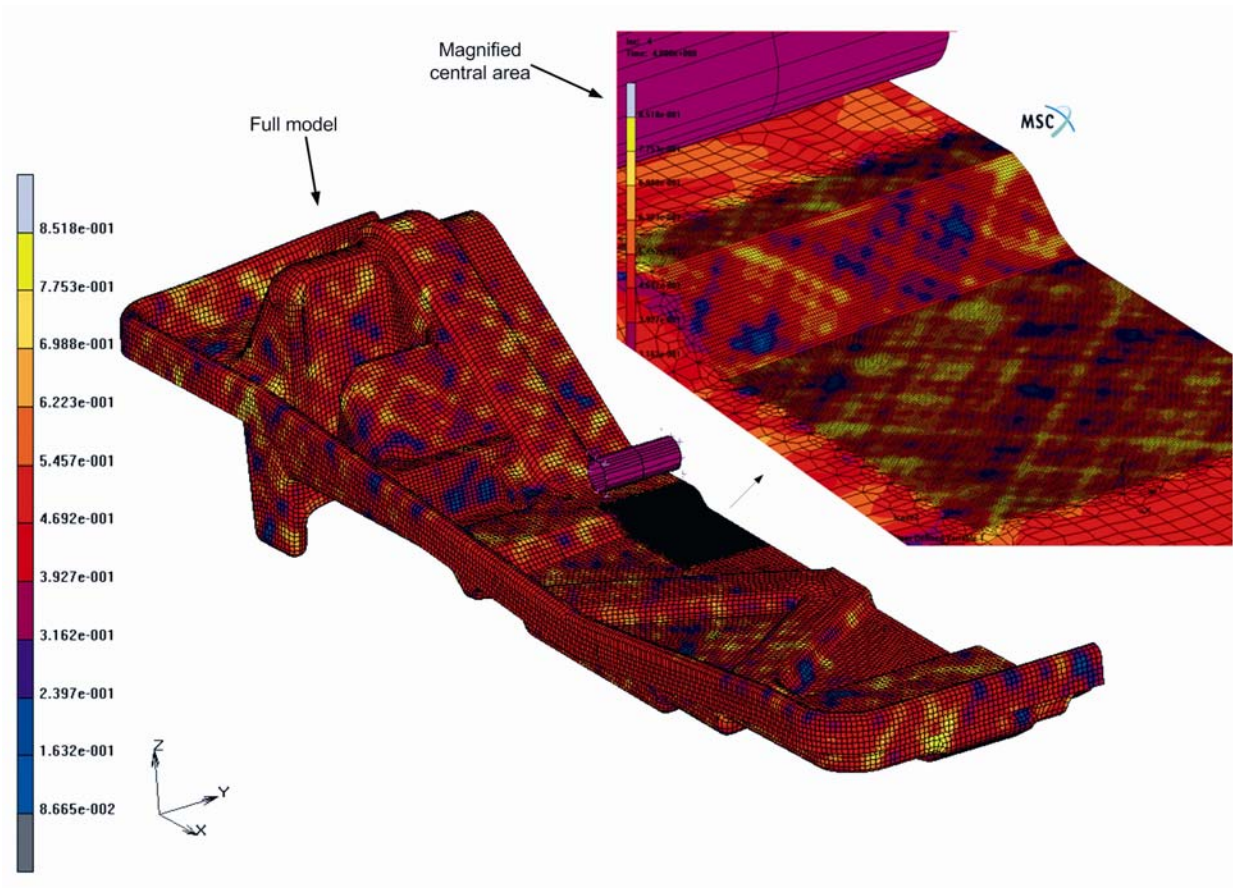
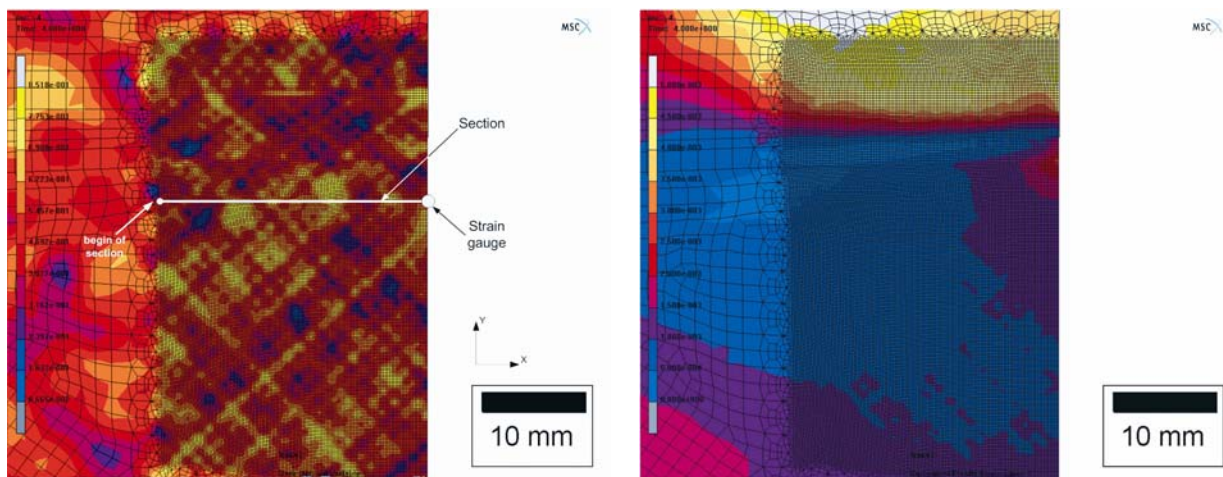


Figure 7.29 Example of the simulated heterogeneity in the seat base structure. Different color of finite elements represents different fiber volume fraction in composite material.



a) Generated heterogeneity, defined section and strain gauge location

b) Equivalent surface strain

Figure 7.30 Results of FE simulations of seat base structure (central area). Chosen section and location of strain gauge are also shown.

The chosen automotive structure is simulated using the novel developed approach. The results of the simulations are compared to those obtained experimentally. Similar problems of amplitude of strain variation as in tests with tensile specimens are observed.

Further improvements of the developed approach are suggested and the limitations of the contactless strain measurement system in application to heterogeneous material model are discussed. All the novel methods developed in this thesis contribute towards a better engineering design and reliability of the structures made of heterogeneous materials.

General design recommendations are drawn with respect to the automotive application of natural fiber composites as a result of the carried investigations (published in [95]). Thus, the several main issues should be considered:

- **Environmentally friendly design.** Natural fibers are considered as renewable resource, and therefore their application reduces the usage of the non-renewable resources. Secondly, natural fibers can be incorporated into biodegradable plastic matrix resulting in pure biocomposite. Application of natural fibers positively contributes to CO₂ balance. When grow they absorb CO₂. Therefore, even if at the end of life the recycling into energy (burning, release CO₂) of the component is considered, the presence of natural fibers reduces the environmental impact.
- **Cheap design.** The price of raw natural fibers is very low. Some natural fibers for composite reinforcement are coming out as waste material of the main processes. Additional processing of natural fibers like combing, weaving, etc. in order to reach the best properties of a composite, leads to increase in their price. Having the cheapest design as an objective, the natural fibers in form of non-woven mats have to be considered as the reinforcement.
- **Designable mechanical properties.** Natural fiber composites like any composite can be designed in a way that their properties can be tailored and in wide range from tough to brittle. Matrix polymer and its bonding properties with the natural fibers directly contribute to the fracture toughness of the composite. Composite with long (20 – 30 mm) natural fibers have a better toughness, but their manufacturing is costly. Hybrid natural fiber composites (with addition of small amount of glass fibers or regenerated cellulose fibers like Lyocell®) have a better combination of toughness, strength and price. However, their application in structures subjected to impact loads should be avoided.
- **Moisture sensitivity.** Natural fibers due to their hydrophilicity absorb moisture very well. This is their main disadvantage. Due to the capillary effect the moisture goes deep into a composite, resulting in deterioration of its mechanical properties. The surface of the composite becomes rough, fibers start to degrade and the fiber-matrix interface becomes weak. A protective coating layer, which could be a paint or a thin extra layer of matrix polymer could help to prevent the moisture influence on the structure made from natural fiber composites. However, natural fiber composites are not suitable for extremely moisture-affected structures.
- **Heterogeneity in mechanical properties.** During the engineering design phase a sufficient mechanical performance of the structure with a design reliability should be achieved. A deep understanding of structural loading conditions is required. Maximum stress areas should be of primary attention. Considering that the mechanical performance of natural fiber composites is comparable to that of glass fiber composites, their application in highly loaded structures should be avoided. Basic mechanical properties of a natural fiber composite can be used in order to perform engineering design of non-loaded or lightly loaded structures. But for medium loaded or critical structures heterogeneity estimation is required. The influence of heterogeneity in material properties on behavior of a structure can be quite significant and unpredictable, especially in critical areas.
- **Experimental testing.** Heterogeneity scale should be considered during the experimental testing of natural fiber composites. Thus, the size parameters of the heterogeneity primitives have to be estimated. The dimensions of test specimens

should be properly chosen in order to eliminate the influence of material's heterogeneity on the results.

- **Simulations.** The finite element simulation of the structures performed using the developed approach for heterogeneous material description can provide essential information about the stress-strain state. For example, during the simulation it can be found that a real stress concentration in the heterogeneous structure could be much higher than theoretically predicted (using traditional approach). The contribution of heterogeneity to overall structural performance is even higher in case where the physical dimensions of the structure are on the same scale or even smaller than the scale of material's heterogeneity. This might lead to unpredicted failure due to underestimated stress-strain state. In order to avoid such failure an additional safety coefficient due to heterogeneity should be considered. In other words, sometimes it is necessary to make the structure stronger than it is estimated using common engineering techniques, while the finite element simulations with applied heterogeneous material model can help engineers to evaluate stress-strain state more accurate and therefore, optimally use the material. The size of the finite elements in this case should be properly chosen taking heterogeneity into account.

References

- 1 Adam, H. (1997) Carbon fibre in automotive applications, *Mater Design*, 18(4/6):349-355.
- 2 Advanced Automotive Technology: Visions of a Super-Efficient Family Car, Report of U.S. Congress, Office of Technology Assessment, OTA-ETI-638, Washington, DC: U.S. Government Printing Office, 1995.
- 3 Aghion, E.; Bronfin, B.; Eliezer, D. (2001) The role of the magnesium industry in protecting the environment, *J Mater Process Tech*, 117:381-385.
- 4 Alma, M.H.; Maldas, D.; Shiraishi, N. (2002) Resinification of NaOH-catalyzed phenolated wood-phenol mixture with formalin for making molding materials, *J Adhesion Sci Technol*, 16(8):1141-1151.
- 5 Andersson, M.; Tillman, A.M. (1989) Acetylation of jute: Effects on strength, rot resistance, and hydrophobicity, *J Appl Polym Sci*, 37(12):3437.
- 6 Aurich, T.; Mennig, G. (2001) Flow-induced fiber orientation in injection molded flax fiber reinforced polypropylene, *Polym Composite*, 22:680-689.
- 7 Automotive Fuel Economy. Potential Effects of Increasing the Corporate Average Fuel Economy Standards, Report of United States General Accounting Office, GAO/RCED-00-194, Washington, D.C. 20548-0001, August 2000.
- 8 Barnes, T.A.; Pashby, I.R. (2000) Joining techniques for aluminium spaceframes used in automobiles Part I – solid and liquid phase welding, *J Mater Process Tech*, 99:62-71.
- 9 Belgacem, M.N.; Bataille, P.; Sapiha S. (1994) Effect of corona modification on the mechanical properties of polypropylene/cellulose composites, *J Appl Polym Sci*, 53(4):379-385.
- 10 Benevolenski, O.I.; Karger-Kocsis, J.; Mieck, K.-P.; Reussmann, T. (2000) Instrumented perforation impact response of polypropylene composites with hybrid reinforcement flax/glass and flax/cellulose fibers, *J Thermoplast Compos*, 13(6):481-496.
- 11 Bernal, C.; Cabral, H.; Vázquez, A. (2002) Mechanical properties of jute-PP composites, *Proc. of the 10th European Conference on Composite Materials – ECCM-10, Composites for the future*, Sol H. and Degrieck J. (eds.), June 3-7, 2002, Brugge, Belgium, paper 452.
- 12 Bezdek, R.H.; Wendling, R.M. (2005) Potential long-term impacts of changes in US vehicle fuel efficiency standards, *Energ Policy*, 33:407-419 (not used)
- 13 Biagiotti, J.; López-Manchando, M.A.; Arroyo M.; Kenny, J.M. (2003) Ternary composites based on PP-EPDM blends reinforced with flax fibers. Part II: Mechanical properties/morphology relationship, *Polym Eng Sci*, 43(5):1031-1043.
- 14 Biodegradable Polymers in North America & Europe (PO81), Market Research Report, MarTech Reports, USA, July 1998, p. 289.
- 15 Birch, S. (1994) Aluminium spaceframe technology, *Automotive Eng*, 102(1):8-12.
- 16 Bisanda, E.N.; Ansell, M.P. (1992) Properties of sisal-CNSL composites, *J Mater Sci*, 27:1690.
- 17 Bismarck, A.; Aranberri-Askergorta, I.; Springer, J.; Lampke T.; Wielage, B.; Stamboulis, A.; Shenderovich I.; Limbach, H.-H. (2002) Surface characterization of flax, hemp and cellulose fibers; Surface properties and the water uptake behavior, *Polym Composite*, 23(5). (not used)
- 18 Bledzki, A.K.; Faruk, O.; (2004) Wood fiber reinforced polypropylene composites: compression and injection molding process, *Polym-Plast Technol*, 43(3):871-888.
- 19 Bledzki, A.K.; Gassan, J. (1998) Natural Fiber Reinforced Plastics in *Handbook of Engineering Polymeric Materials*, N. P. Cheremisinoff (ed.), pp. 787-810.
- 20 Bledzki, A.K.; Gassan, J. (1999) Composites reinforced with cellulose based fibres, *Prog Polym Sci* 24:221-274.
- 21 Bledzki, A.K.; Reihmane, S.; Gassan J. (1996) Properties and modification methods for vegetable fibers for natural fiber composites, *J Appl Polym Sci*, 59(8):1329-1336.

- 22 Brody, H.; Ward, I.M. (1971) Modulus of short carbon and glass fiber reinforced composites, *Polym Eng Sci*, 11:139-151.
- 23 Bruijn de, J.C.M. (2000) Natural Fibre Mat Thermoplastic Products from a Processor's Point of View, *Appl Compos Mater*, 7:415-420
- 24 Brungs, D. (1997) Light weight design with light metal castings, *Mater Design*, 18(4/6):285-291.
- 25 Buggy, M.; Farragher, L.; Madden, W. (1995) Recycling of composite materials, *J Mater Process Tech*, 55:448-456.
- 26 Cabrera, N.; Alcock, B.; Loos, J.; Peijs, T. (2004) Processing of all-polypropylene composites for ultimate recyclability, *Proceedings of the I MECH E Part L, P I Mech Eng L-J Mat*, 218:145-155.
- 27 Carle, D.; Blount, G. (1999) The suitability of aluminium as an alternative material for car bodies, *Mater Design*, 20:267-272.
- 28 Caulfield, D.F.; Feng, D.; Prabawa, S.; Young, R.A.; Sanadi, A.R. (1999) Interphase effects on the mechanical and physical aspects of natural fiber composites, *Die Angew Makromol Chem*, 272:57-64 (Nr. 4757).
- 29 Caulfield, D.F.; Stark, N. (1998) Dynamic and mechanical properties of agro-fiber based composites, *Proc. of Workshop on Progress in woodfibre-plastic composites: Emergence of a new industry*, Mississauga, Ontario, Canada, June 1, 1998, Eds.: J.J. Balatinecz, T.E. Redpath. Publisher: Materials and Manufacturing Ontario, 2655 North Sheridan Way, Suite 250, Mississauga, Ontario, Canada L5K 2P8.
- 30 Chen, H.L.; Porter, R.S. (1994) Composite of polyethylene and kenaf, a natural cellulose fiber, *J Appl Polym Sci*, 54(11):1781.
- 31 Cheon, S.S.; Lee, D.G.; Jeong, K.S. (1997) Composite side door impact beams for passenger cars, *Comp Struct*, 38:29-39.
- 32 Chou, T.W.; Nomura, S. (1981) Fiber orientation effects of the thermoplastic properties of short fiber composites. *Fibre Sci Technol*, 14:279-291.
- 33 Cohen, E.; Riesenfeld, R.F.; Elber, G. (2001) Geometric modeling with splines: an introduction, ISBN 1-56881-137-3, Natick : Peters, 2001, p. 616.
- 34 Cox, H.L. (1952) The elasticity and strength of paper and other fibrous materials, *Brit J Appl Phys*, 3:72-79.
- 35 Cunliffe, A.M.; Jones, N.; Williams, P.T. (2003) Recycling of fibre-reinforced polymeric waste by pyrolysis: thermo-gravimetric and bench-scale investigations, *J Anal Appl Pyrol*, 70:315-338.
- 36 Cyras, V.P.; Iannace, S.; Kenny, J.M.; Vázquez, A. (2001) Relationship between processing and properties of biodegradable composites based on PCL/starch matrix and sisal fibers, *Polym Composite*, 22:104-110.
- 37 Dahlke, B.; Larbig, H.; Scherzer, H.D.; Poltrock, R. (1998) Natural fiber reinforced foams based on renewable resources for automotive interior applications, *J Cell Plast*, 34(4):361.
- 38 Daimler-Benz High Tech Report 2, The Corporate Units in the Daimler-Benz Group (1995).
- 39 Dam van, J.E.G.; Vilsteren van, G.E.T.; Zomers, F.H.A.; Shannon, W.B.; Hamilton, I.T. (1994) Increased application of domestically produced plant fibres in textiles, pulp and paper production, and composite materials, Report of Directorate-General XII Science Research and Development, EUR 16101 EN, ATO-DLO, Wageningen, The Netherlands, 1994.
- 40 Dargay, J.; Gately, D. (1997) Vehicle ownership to 2015: implications for energy use and emissions, *Energ Policy*, 25(14/15):1121-1127.
- 41 Dash, B.N.; Rana, A.K.; Mishra, H.K.; Nayak, S.K.; Tripathy, S.S. (2000) Novel low-cost jute-polyester composites. III. Weathering and thermal behavior, *J Appl Polym Sci*, 78(9):1671-1679.
- 42 Devi, L.U.; Bhagawan, S.S.; Thomas, S. (1997) Mechanical properties of pineapple leaf fiber-reinforced polyester composites, *J Appl Polym Sci*, 64:1739-1748.

- 43 Directive 2000/53/EC of the European Parliament and the Council of end-of-life vehicles, Office Journal of the European Communities, October 21st, 2000, ABI. EG Nr. L 269 S. 34L 269/34
- 44 Ellison, G.C.; McNaught, R. (2000) The use of natural fibres in nonwoven structures for applications as automotive component substrates, Research & Development Report of Ministry of Agriculture Fisheries and Food Agri – Industrial Materials, Reference NF0309, 10 Whitehall Place London SW1A 2HH, February 2000.
- 45 Felix J.M.; Gatenholm, P. (1991) The nature of adhesion in composites of modified cellulose fibers and polypropylene, *J Appl Polym Sci*, 42(3):609.
- 46 Felix, J.M.; Gatenholm, P. (1993) Controlled interactions in cellulose-polymer composites. 1: Effect on mechanical properties, *Polym Composite*, 14:449.
- 47 Friedrich, K.; Schumann, S. (2001) Research for a new age of magnesium in the automobile industry, *J Mater Process Tech*, 117:276-281.
- 48 Fu, S.-Y.; Lauke, B. (1999) Strength anisotropy of misaligned short-fiber-reinforced polymers, *Compos Sci Technol*, 59:699-708.
- 49 Gaines, L.; Cuenca, R.; Stodolsky, F.; Wu, S. (1996) Potential automotive uses of wrought magnesium alloys, Proc. of Conference Automotive Technology Development, Detroit, Michigan, USA, October 28 - November 1, 1996
- 50 Garkhail, S.K.; Heijenrath, R.W.H.; Peijs, T. (2000) Mechanical properties of natural-fibre-mat-reinforced thermoplastics based on flax fibres and polypropylene, *Appl Compos Mater*, 7:351-372.
- 51 Gassan, J.; Bledski, A.K. (2001) Thermal degradation of flax and jute fibers, *J Appl Polym Sci*, 82:1417-1422.
- 52 Gassan, J.; Bledzki, A.K. (1996) Einfluß von haftvermittlern auf das feuchteverhalten naturfaserverstärkter kunststoffe, *Die Angew Makromol Chem*, 236(1):129-138. (in German)
- 53 Gassan, J.; Bledzki, A.K. (1997) Effect of moisture content on the properties of silanized jute-epoxy composites, *Polym Composite*, 18(2):179-184.
- 54 Gassan, J.; Bledzki, A.K. (1999) Possibilities for improving the mechanical properties of jute/epoxy composites by alkali treatment of fibres, *Compos Sci Technol*, 59:1303-1309.
- 55 Gauthier, R.; Joly, C.; Coupas, A.C.; Gauthier, H.; Escoubes, M. (1998) Interfaces in polyolefin/cellulosic fiber composites: chemical coupling, morphology, correlation with adhesion and aging in moisture, *Polym Composite*, 19(3):287-300.
- 56 Gayer, U.; Schuh, T. (1996) Automotive application of natural fibers composite, Proc. of The 1-st International Symposium on Lignocellulosic Composites, UNESP-Sao Paulo State University (1996).
- 57 Gensewich, C. (1999) Pultrusion von konstruktionswerkstoffen aus nachwachsenden rohstoffen, Proc. of the 2-nd International Wood and Natural Fibre Composites Symposium, Kassel 1999.
- 58 George, J.; Bhagawan, S.S.; Thomas, S. (1995) Short Pineapple-leaf-fiber-reinforced low-density polyethylene composites, *J Appl Polym Sci*, 57:843.
- 59 George, J.; Ivens, J.; Verpoest, I. (1999) Mechanical properties of flax fiber reinforced epoxy composites, *Die Angew Makromol Chem*, 272:41-45 (Nr. 4747).
- 60 George, J.; Joseph, K.; Bhagawan, S.S.; Thomas, S. (1993) Influence of short pineapple fiber on the viscoelastic properties of low-density polyethylene, *Mater Lett*, 18(3):163.
- 61 Ghosh, P.; Biswas, S.; Datta, C. (1989) Modification of jute fibre through vinyl grafting aimed at improved rot resistance and dyeability, *J Mater Sci*, 24:205-212.
- 62 Goa, S.; Zeng, Y. (1993) Surface modification of ultrahigh molecular weight polyethylene fibers by plasma treatment. I. Improving surface adhesion, *J Appl Polym Sci*, 47:2065-2071.
- 63 Gotch, T. (1991) Reinforced plastics in automotive applications, *J Reinf Plast Comp*, 35(9):11-20.

- 64 Hagstrand, P.-O.; Oksman, K. (2001) Mechanical properties and morphology of flax fiber reinforced melamine-formaldehyde composites, *Polym Composite*, 22(4):568-578.
- 65 Halpin, J.C. (1969) Stiffness and expansion estimates, for oriented short fiber composites, *J Compos Mater*, 3:720-724.
- 66 Halpin, J.C.; Pagano, N.J. (1969) The laminate approximation for randomly oriented fibrous composites, *J Compos Mater*, 3:720-724.
- 67 Hikita, K. (2002) Development of weight reduction technology for door trim using foamed PP, *JSAE Rev*, 23:239–244.
- 68 Hill, C.A.S.; Abdul Khalil, H.P.S. (2000) Effect of fiber treatments on mechanical properties of coir or oil palm fiber reinforced polyester composites, *J Appl Polym Sci*, 78:1685-1697.
- 69 Hine, P.J.; Davidson, N.; Duckett, R.A.; Ward, I.M. (1995) Measuring the fiber orientation and modelling the elastic properties of injection-moulded long-glass-fiber-reinforced nylon, *Compos Sci Technol*, 53:125-131.
- 70 Hirsch, T.J. (1962) Modulus of elasticity of concrete affected by elastic moduli of cement paste matrix and aggregate, *J Am Concrete I*, 59:427-451.
- 71 Hornsby, P.R.; Hinrichsen, E.; Tarverdi, K. (1997) Preparation and properties of polypropylene composites reinforced with wheat and flax straw fibres: Part II Analysis of composite microstructure and mechanical properties, *J Mater Sci*, 32:1009-1015.
- 72 Hull, D. (1996) An introduction to composite materials, 2nd ed. Cambridge, UK : Cambridge University Press, 1996, ISBN 0-521-38190-8 , p, 326
- 73 Huque, M.M.; Habibuddowla, Md.; Mohamood, A.J.; Jabbar Mian, A. (1980) Graft copolymerization onto jute fiber: Ceric ion-initiated graft copolymerization of methyl methacrylate, *J Polym Sci Pol Chem*, 18:1447-1458.
- 74 Ismail, H. R.; Rosnah, N. (1997) Curing characteristics and mechanical properties of short oil palm fibre reinforced rubber composites, *Polymer*, 38(16):4059.
- 75 ISO-527, Plastics – determination of tensile properties, Nederlands Normalizatie Instituut (1993).
- 76 Jambor, A.; Beyer, M. (1997) New cars – new materials, *Mater Design*, 18(4/6):203-209.
- 77 Jayaraman, K. (2003) Manufacturing sisal–polypropylene composites with minimum fibre degradation, *Comp Sci Technol*, 63:367-374.
- 78 Jayaraman, K. (2004) Mechanical performance of woodfibre–waste plastic composite materials, *Resources, Conservation and Recycling*, 41(4):307–319.
- 79 Johnson, D.A.; Urich, J.L.; Rowell, R.M.; Jacobson, R.; Caufield, D.F. (1999) Weathering characteristics of fiber-polymer composites, *Proc. of The 5-th International Conference on Woodfiber-Plastic Composites*, May 26–27, 1999 The Madison concourse Hotel Madison, Wisconsin, USA, pp.203-209.
- 80 Joseph, K.; Thomas, S.; Pavithran, C. (1996) Effect of chemical treatment on the tensile properties of short sisal fibre-reinforced polyethylene composites, *Polymer*, 37(23):5139-5149.
- 81 Joseph, P.V.; Joseph, K.; Thomas, S. (1999) Effect of processing variables on the mechanical properties of sisal-fiber-reinforced polypropylene composites, *Compos Sci Technol*, 59:1625-1640.
- 82 Kalaprasad, G.; Joseph, K.; Thomas, S. (1997) Theoretical modelling of tensile properties of short sisal fiber-reinforced low-density polyethylene composites, *J Mater Sci*, 59:4261-4267.
- 83 Kandachar, P.V.; Brouwer, R.; (2001) Applications of bio-composites in industrial products, *Proc. of the Symposium on Advanced Fibers, Plastics, Laminates, and Composites*, Wallenberger, F.T.; Weston, N.E.; Ford, R.; Wool, R.P.; Chawla, K. (eds.), MRS, Volume 702, Japan, 2001.
- 84 Karger-Kocsis, J. (2000) Swirl mat and long discontinuous fiber mat reinforced polypropylene composites-status and future trends, *Polym Composite*, 21(4):514-522.

- 85 Karmaker, A.C.; Youngquist, J.A. (1996) Injection molding of polypropylene reinforced with short jute fibers, *J Appl Polym Sci*, 62:1147-1151.
- 86 Karnani, R.; Krishnan, M.; Narayan, R. (1997) Biofiber-reinforced polypropylene composites, *Polym Eng Sci*, 37(2):476-483.
- 87 Kasai, J. (1999) Life cycle assessment, evaluation method for sustainable development, *JSAE Rev*, 20:387-393
- 88 Kaveline K.G.; Skrypnik, I.D.; Kandachar, P.V. (2002) The stochastic modeling of the properties of composite materials based on renewable resources with random distributed reinforcement, *Proc. of Conference Advances in Computational Engineering & Sciences*, Atluri, S.N. and Pepper, D.W. (eds.), ICES'02, Reno, USA, 2002 CD-ROM
- 89 Kaveline, K.G. (2001) Literature survey on renewable materials, Internal report DE-136, Delft University of Technology, Delft, The Netherlands. 27 p.
- 90 Kaveline, K.G.; Ermolaeva, N.S.; Kandachar, P.V. (2001) Estimation of elastic modulus for natural fibers reinforced polypropylene composites, *Proc. 23-rd Riso International Symposium on Materials Science*, Lilholt, H; Madsen, B.; Toftegaard, H.L.; Cendre, E.; Megnis, M.; Mikkelsen, L.P.; Sorensen B.F. (eds.), Riso National Laboratory, Roskilde, Denmark, 2002, pp. 215-224. (ISBN 87-550-3091-2)
- 91 Kaveline, K.G.; Ermolaeva, N.S.; Kandachar, P.V. (2002) Examination and modelling of heterogeneous materials containing natural fibers, *Proc. of Light Materials for Transportation Systems*, Frazier, W.E.; Hahn, Y.D.; Kim N.J; Lee, E.W. (eds.), LIMAT-03, Honolulu, USA, (2003) CD-ROM
- 92 Kaveline, K.G.; Ermolaeva, N.S.; Kandachar, P.V. (2003) Numerical modelling of properties for sustainable development of products in natural fiber composites, *Proc. of 2nd International Conference on Eco-Composites*, Peijs, T. and Goutianos S. (eds.), EcoComp-03, Queen Mary, University of London, UK (2003), CD-ROM.
- 93 Kaveline, K.G.; Ermolaeva, N.S.; Kandachar, P.V. (2004) Simulation of heterogeneous natural fiber reinforced composites with holes, *Proc. of The 2nd International Workshop on Green Composites* (eds. Goda, K.; Takagi, H.), IWGC-2, Ube, Japan, 2004 pp. 29-37.
- 94 Kaveline, K.G.; Ermolaeva, N.S.; Kandachar, P.V. (2005) Investigation of stochastic properties of the natural fiber mats, *Comp Sci Technol*, (submitted)
- 95 Kaveline, K.G.; Kandachar, P.V.; Spoomaker J.L. (2004) Design with materials containing natural fibers, *Proc. of The 11th European Conference on Composite Materials – ECCM-11*, Rhodes, Greece, 31 May-3 June 2004, paper c223, CD-ROM.
- 96 Kaveline, K.G.; Skrypnik, I.D.; Ermolaeva, N.S.; Kandachar, P.V. (2003) The simulation of the heterogeneity in properties of composite materials with randomly distributed reinforcement, *Proc. of The 5-th International Symposium on Advanced Composites 2003*, Corfu Imperial hotel, Corfu, Greece, (2003). CD-ROM
- 97 Kaveline, K.G.; Spoomaker, J.L.; Kandachar, P.V. (2002) Flax fiber reinforced synthetic polymer experimental properties investigation, *Proc. of the 10th European Conference on Composite Materials – ECCM-10 Composites for the future*, Sol H. and Degrieck J. (Eds.), June 3-7, 2002, Brugge, Belgium, paper 190. CD-ROM
- 98 Kazayawoko, M.; Balatinecz, J.J.; Woodhams, R.T. (1997) Diffuse reflectance Fourier transform infrared spectra of wood fibers treated with maleated polypropylenes, *J Appl Polym Sci*, 66(6):1163.
- 99 Kennerley, J.R.; Kelly, R.M.; Fenwick, N.J.; Pickering, S.J.; Rudd, C.D. (1998) The characterisation and reuse of glass fibres recycled from scrap composites by the action of fluidised bed process, *Compos Part A-Appl S*, 29A:839-845.
- 100 Kessler, R.W.; Becker, U.; Kohler, R.; Goth, B. (1998) Steam explosion of flax — a superior technique for upgrading fibre value, *Biomass and Bioenergy*, 14(3):237-249.
- 101 Kessler, R.W.; Kohler, R. (1996) New strategies for exploring flax and hemp, *Chemtech*, pp.34-40.
- 102 Khan, M.A.; Hinrichsen, G.; Drzal, L.T. (2001) Influence of novel coupling agents on mechanical properties of jute reinforced polypropylene composite, *Compos Interf*, 20(18):1711-1713.

- 103 Knothe, J.; Schlößer, T. (2000) Natural fibre reinforced plastics in automotive exterior applications - naturfaserverstärkte kunststoffe in kfz-anwendungen, Proc. of The 3-rd International Wood and Natural Fibre Composites Symposium, Kassel, September 19-20th, 2000.
- 104 Kokta, B.V.; Maldas, D.; Daneault, C.; Beland, P. (1990) Composites of poly(vinyl chloride) and wood fibers. Part II: Effect of chemical treatment, *Polym Composite*, 11(2):84-89.
- 105 Kokta, B.V.; Maldas, D.; Daneault, G.C. (1989) Composites of polyvinyl chloride - wood fibers: IV. Effect of the nature of fibers, *J Vinyl Addit Techn*, 11(2):90-99.
- 106 Kotelnikov V.A. (1933) On throughput of air and wire in electric communication, Proc. of The 1-st All-Union congress on technical reconstruction of electric communications and development of low-current industry, All-Union Energetic Committee, USSR, 1933 (in Russian)
- 107 Kroschwitz, J.I. (1990) *Polymers: fibres and textiles*. New York: Wiley, 1990.
- 108 Kymäläinen, H.-R.; Hautala, M.; Kuisma, R.; Pasila, A. (2001) Capillarity of flax/linseed (*Linum usitatissimum* L.) and fibre hemp (*Cannabis sativa* L.) straw fractions, *Ind Crop Prod*, 14:41-50.
- 109 Leao, A.L.; Rowell, R.; Tavares, N. (1998) Application of natural fibers in automotive industry in Brazil – Thermoforming process, In: *Science and Technology of Polymers and Advanced Materials*, P. N. Prasad, J. E. Mark, S. Kandil, Z. H. Kafafi, Eds., Plenum Press, New York 1998, p. 755.
- 110 Lee, B.J.; McDonald, A.G.; James, B. (2001) Influence of fiber length on the mechanical properties of wood-fiber/polypropylene prepreg sheets, *Mater Res Innov*, 4:97–103.
- 111 Liao, B.; Huang, Y.; Cong, G. (1997) Influence of Modified Wood Fibers on the mechanical properties of wood fiber-reinforced of polyethylene, *J Appl Polym Sci*, 66:1561-1568.
- 112 Lilholt, H.; Lawther, J.M. (2000) Natural organic fibers, In: *Comprehensive composite materials*, Vol.1 Fiber reinforcement and general theory of composites, Kelly, A.; Zweben, C.; Chou, T.-W. (eds.), Elsevier, 2000.
- 113 Luo, S.; Netravali, A.N. (1999) Mechanical and thermal properties of environment-friendly "green" composites made from pineapple leaf fibers and poly(hydroxybutyrate-co-valerate) resin, *Polym Composite*, 20:367-378.
- 114 Magurno, A. (1999) Vegetable fibres in automotive interior components, *Die Angew Makromol Chem*, 272:99-107 (Nr. 4751).
- 115 Maldas, D.; Kokta, B.V. (1993) Performance of hybrid reinforcements in PVC composites. II: Use of surface-modified mica and different cellulosic materials as reinforcements, *J Vinyl Addit Techn*, 15(1):38-44.
- 116 Maldas, D.; Kokta, B.V.; Daneault, C. (1989) Influence of coupling agents and treatments on the mechanical properties of cellulose fiber-polystyrene composites, *J Appl Polym Sci*, 37(3):751-775.
- 117 Maldas, D.; Shiraishi, N.; Harada, Y. (1997) Phenolic resol resin adhesives prepared from alkali-catalyzed liquefied phenolated wood and used to bond hardwood, *J Adhesion Sci Technol*, 11(3):305–316.
- 118 Mannan-Kh., M.; Latifa, B.L. (1980) Effects of grafted methyl methacrylate on the microstructure of jute fibres, *Polymer*, 21:777-780.
- 119 Marco de, I.; Legretta, J.A.; Laresgoiti, M.F.; Torres, A.; Cambra, J.F.; Chomon, M.J.; Caballero, B.; Gondra, K. (1997) Recycling of the products obtained in the pyrolysis of fibre-glass polyester SMC, *J Chem Technol Biot*, 69:187-192.
- 120 Materials database www.io.tudelft.nl/research/dfs/idemat/index.htm
- 121 Materials database www.matls.com
- 122 Matuana, L.M.; Park, C.B.; Balatinecz, J.J. (1996) The effect of low levels of plasticizer on the rheological and mechanical properties of polyvinyl chloride/newsprint-fiber composites, *J Vinyl Addit Techn*, 3(4):265-273.

- 123 Mieck, K.-P.; Lützkendorf, R.; Reussmann, T. (1996) Needle-punched hybrid nonwovens of flax and PP fibers—textile semiproducts for manufacturing of fiber composites, *Polym Composite*, 17(6):873-878.
- 124 Mieck, K.-P.; Reussmann, T. (1995) Flachs versus glas, *Kunstst-Plast*, 3:366-370. (in German)
- 125 Mieck, K.-P.; Reussmann, T. (1999) Strong and impact resistant, *Kunstst-Plast Eur*, 89(12):a102-a105.
- 126 Misra, M.; Tripathy, S.S.; Nayak, S.K.; Mohanty, A.K. (2002) The influence of chemical surface modification on the performance of sisal-polyester biocomposites, *Polym Composite*, 23(2):164-170.
- 127 Mitra, B.C.; Basak, R.K.; Sarkar, M. (1998) Studies on jute-reinforced composites, its limitations, and some solutions through chemical modifications of fibers, *J Appl Polym Sci*, 67:1093-1100.
- 128 Mittal, K.L. (1992) Silanes and other coupling agents. Netherlands: VSP BV, 1992.
- 129 Mohan, R., Shridhar, M.K.; Rao, R.M. (1983) Compressive strength of jute-glass hybrid fibre composites, *J Mater Sci Lett*, 2:99-102.
- 130 Mohanty, A.K. (2002) Sustainable bio-composites from renewable resources: Opportunities and challenges in the green materials world, *J Polym Environ*, 10(1/2):19-26.
- 131 Mohanty, A.K.; Drzal, L.T.; Misra, M. (2002) Engineered natural fiber reinforced polypropylene composites: influence of surface modifications and novel powder impregnation processing, *J Adhesion Sci Technol*, 16(8):999-1015.
- 132 Mohanty, A.K.; Misra, M.; Drzal, L.T. (2001) Surface modifications of natural fibers and performance of the resulting biocomposites: An overview, *Compos Interface*, 8(5):313-343.
- 133 Mohanty, A.K.; Misra, M.; Hinrichsen, G. (2000) Biofibres, biodegradable polymers and biocomposites: An overview, *Macromol Mater Eng*, 276/277:1–24.
- 134 Mohanty, A.K.; Singh, B.C. (1987) Redox-initiated graft copolymerization onto modified jute fibers, *J Appl Polym Sci*, 34(3):1325.
- 135 MSC.MARC Manual vol.B Element Library, MSC.Software, 2003.
- 136 MSC.MARC Manual vol.D User Subroutines and Special Routines, MSC.Software, 2003.
- 137 Mueller, D.H.; Krobjilowski, A.; Schachtschneider, H.; Muessig, J.; Cescutti, G. (2002) Acoustical properties of reinforced composite materials and layered structures basing on natural fibers, *Proc. of The INTC-International Nonwovens Technical Conference*, Atlanta, GA/USA, 24-26. September 2002.
- 138 Nair, K.C.M.; Thomas, S. (2003) Effect of interface modification on the mechanical properties of polystyrene-sisal fiber composites, *Polym Composite*, 24(3):332-343.
- 139 Naira, K.C.M.; Kumara, R.P.; Thomas, S.; Schit, S.C.; Ramamurthy, K. (2000) Rheological behavior of short sisal fiber-reinforced polystyrene composites, *Compos Part A-Appl S*, 31:1231-1240.
- 140 Nevell, T.P.; Zeronian, S.H. (1985) *Cellulose chemistry and its applications*. New York: Wiley, 1985.
- 141 Noland, R.B. (2005) Fuel economy and traffic fatalities: multivariate analysis of international data, *Energ Policy*, 33(17):2183-2190.
- 142 Nyquist, H. (1928) Certain topics in telegraph transmission theory, *Trans. AIEE*, 47:617-644.
- 143 O'Dell, J.L. (1997) Natural Fibers in Resin Transfer Molded Composites, *Proc. of The 4-th International Conference on Woodfiber-Plastic Composites*, May 12-14, 1997, The Madison Concourse Hotel, Madison, Wisconsin; Forest Products Society, proc. no 7277, ISBN 0-935018-95-6/1997, pp. 280-285.
- 144 O'Regan, D.F.; Akay, M.; Meenan, B. (1999) A comparison of Young's modulus prediction in fiber-reinforced polyamide injection mouldings. *Compos Sci Technol*, 59:419-427.

- 145 Oever van den, M.J.A.; Bos, H.L.; Kemenade van, M.J.J.M. (2000) Influence of the physical structure of flax fibres on the mechanical properties of flax fibre reinforced polypropylene composites, *Appl Compos Mater*, 7:387-402.
- 146 Oksman, K. (2000) Mechanical properties of natural fibre mat reinforced thermoplastic, *Appl Compos Mater*, 7:403-414.
- 147 Oksman, K.; Sandlund, E. (1998) Vacuum infusion moulding of natural fibre composites, *Proc. of The 2-nd International Symposium on Natural Polymers and Composites-ISNaPol/98*, May 10-13, 1998, Sao Paulo, SP, Brazil, paper 79.
- 148 Oksman, K.; Wallström, L.; Berglund, L.A.; Filho, R.D.T. (2002) Morphology and mechanical properties of unidirectional sisal-epoxy composites, *J Appl Polym Sci*, 84: 2358-2365.
- 149 Olesen, P.O.; Plackett, D.V. (1999) Bio-fibres for new materials and products, *Proc. of The 2-nd International Symposium on Materials from Sustainable Natural Resources*, Erfurt, Germany, September 1-2, 1999.
- 150 Online textbook on statistics <http://www.statsoft.com/textbook/stathome.html>
- 151 Pal, S.K.; Mukhopadhyay, D.; Sanyal, S.K.; Mukherjea, R.N. (1983) Studies of jute fiber composites with polyesteramide polyols as interfacial agent, *J Appl Polym Sci*, 28(10): 3029-3040.
- 152 Pal, S.K.; Mukhopadhyay, D.; Sanyal, S.K.; Mukherjee R.N. (1988) Studies on process variables for natural fiber composites - effect of polyesteramide polyol as interfacial agent, *J Appl Polym Sci*, 35(4):973-985
- 153 Patel, S.H.; Gonslves, K.E.; Stivala, S.S.; Reich, L.; Trivedi, D.H. (1993) Alternative procedures for the recycling of sheet molding compounds, *Adv Polym Technol*, 12:35-45.
- 154 Patil, Y.P.; Gajre, B.; Dusane, D.; Chavan, S.; Mishra, S. (1990) Effect of maleic anhydride treatment on steam and water absorption of wood polymer composites prepared from wheat straw, cane bagasse, and teak wood sawdust using Novolac as matrix, *J Appl Polym Sci*, 77(13):2963-2967.
- 155 Peijs, T. (2003) Composites for recyclability, *Materials Today*, ISSN: 1369 7021 © Elsevier Science Ltd 2003, April 2003, pp. 30-35.
- 156 Pervaiz, M.; Sain, M.M. (2003) Carbon storage potential in natural fiber composites, *Resour Conserv Recy*, 39:325-340.
- 157 Pervaiz, M.; Sain, M.M. (2003) Sheet-molded polyolefin natural fiber composites for automotive applications, *Macromol Mater Eng*, 288:553-557.
- 158 Pickering, S.J.; Kelly, R.M.; Kennerley, J.R.; Rudd, C.D.; Fenwick, N.J. (2000) A fluidised-bed process for the recovery of glass fibres from scrap thermoset composites, *Compos Sci Technol*, 60:509-523.
- 159 Plotkin, S.E (1997) Prospects for improving the fuel economy of light-duty vehicles, *Energ Policy*, 25(14/15):1179-1188.
- 160 Plotkin, S.E (2001) European and Japanese fuel economy initiatives: what they are, their prospects for success, their usefulness as a guide for US action, *Energ Policy*, 29:1073-1084.
- 161 Pott, G.T. (2001) Reduction of moisture sensitivity in natural fibres, *Proc. of the Symposium on Advanced Fibers, Plastics, Laminates, and Composites*, Wallenberger, F.T.; Weston, N.E.; Ford, R.; Wool, R.P.; Chawla, K. (eds.), MRS, Volume 702, Japan, 2001, pp. 87-100.
- 162 Pott, G.T. (2004) Reduction of moisture sensitivity in natural fibres, in *natural fibers, plastics, and composites natural fibers, plastics and composites*, Ed, F.T. Wallenberger, N.Weston, Kluwer Academic Publishers, ISBN 1-4020-7643-6, 2004.
- 163 Pott, G.T.; Pilot, R.J.; Hazendonk van, J. M. (1997) Upgraded natural fibres for polymer composites, in *Proc. of the 5th European Conference on Advanced Materials and Processes and Applications (EUROMAT 97)*, Vol. 2. Polymers and Ceramics, Maastricht, 21-23 April 1997, p. 107.
- 164 Prasad, S.V. (1989) Natural-fiber-based composites. In: Kelly A, editor. *Concise encyclopedia of composite materials*. New York: Pergamon; 1989.

- 165 Rana, A.K.; Mandal, A.; Mitra, B.C.; Jacobson, R.; Rowell, R.M.; Banerjee, A.N. (1998) Short jute fiber-reinforced polypropylene composites: Effect of compatibilizer, *J Appl Polym Sci*, 69:329-338.
- 166 Ray, D.; Sarkar, B.K.; Rana, A.K.; Bose, N.R. (2001) The mechanical properties of vinylester resin matrix composites, reinforced with alkali-treated jute fibres, *Compos Part A-Appl S*, 32:119-127.
- 167 Ray, P.K.; Chakravarty, A.C.; Bandyopadhyay, S.B. (1976) Fine structure and mechanical properties of jute differently dried after retting, *J Appl Polym Sci*, 20:1765-1767.
- 168 Reussmann, T.; Mieck, K.-P. (1999) Dynamic-mechanical analysis of natural fiber reinforced plastics, *Adv Eng Mater*, 1(2):140-141.
- 169 Riedel, U.; Nickel, J. (1999) Natural fibre-reinforced biopolymers as construction materials – new discoveries, *Die Angew Makromol Chem*, 272:34-40 (Nr. 4756).
- 170 Roe, P.J.; Ansell, M.P. (1985) Jute-reinforced polyester composites, *J Mater Sci*, 20(11):4015.
- 171 Romhány, G.; Karger-Kocsis, J.; Czigány, T. (2003) Tensile fracture and failure behavior of thermoplastic starch with unidirectional and cross-ply flax fiber reinforcements, *Macromol Mater Eng*, 288(9):699-707.
- 172 Rong, M.Z.; Zhang, M.Q.; Liu, Y.; Yang, G.C.; H.M. Zeng, (2001) The effect of fiber treatment on the mechanical properties of unidirectional sisal-reinforced epoxy composites, *Compos Sci Technol*, 61:1437-1447.
- 173 Ronga, M.Z.; Zhang, M.Q.; Liu, Y.; Yang, G.C.; Zeng, H.M. (2001) The effect of fiber treatment on the mechanical properties of unidirectional sisal-reinforced epoxy composites, *Compos Sci Technol*, 61:1437-1447.
- 174 Rosato, D.V. (1996) Injection molding higher performance reinforced plastic composites, *J Vinyl Addit Techn*, 2(3):216-220.
- 175 Rosenthal, J. (1992) A model for determining fiber reinforcement efficiencies and fiber orientation in polymer composites, *Polym Composite*, 13:462-466.
- 176 Rout, J.; Misra, M.; Tripathy, S.S.; Nayak S.K.; Mohanty, A.K. (2001) The influence of fiber surface modification on the mechanical properties of coir-polyester composites, *Polym Composite*, 22(4):468-476.
- 177 Rowell, R.M.; O'Dell, J.; Basak, R.K.; Sarkar, M. (1999) Applications of jute in resin transfer molding, *Proc. of International Seminar on Jute and Allied Fibres: Changing Global Scenario*, National Institute of research on jute and allied fiber technology, Mitra, B.C. (ed.) Indian Council of Agricultural Research 12, Regent Park, Calcutta-700040, India 1999, Ijira Association, pp. 89-96.
- 178 Ruys, D.; Crosky, A.; Evans, W.J. (1999) Ecologically sustainable composite materials for low energy city vehicles, *Proc. of The Waste and Byproducts as Secondary Resources for Building Materials Conference*, vol. 1, New Delhi, India, 1999, pp. 328-334.
- 179 Saeb, D.N.; Jog, J.P. (1999) Natural fiber polymer composites: A review, *Adv Polym Tech*, 18(4):351-363.
- 180 Safonov V.V. (1991) Treatment of textile materials. Moscow: Legprombitizdat, 1991. (in Russian)
- 181 Sahoo, P.K.; Samantaray, H.S.; Samal, R.K. (1986) Graft copolymerization with new class of acidic peroxy salts as initiators. I. Grafting of acrylamide onto cotton-cellulose using potassium monopersulfate, catalyzed by Co(II), *J Appl Polym Sci*, 32(7):5693.
- 182 Samal, R.K.; Mukul, C.; Ray, M.C. (1997) Effect of chemical modifications on FTIR spectra. II. Physicochemical behavior of pineapple leaf fiber (PALF), *J Appl Polym Sci*, 64(11):2119-2125.
- 183 Samal, R.K.; Sahoo, P.K.; Samantaray, H.S. (1986) Graft copolymerization with new class of acidic peroxy salts as initiators. I. Grafting of acrylamide onto cotton-cellulose using potassium monopersulfate, catalyzed by Co(II), *J Appl Polym Sci*, 32(7):5693-5703

- 184 Samal, R.K.; Samantaray, H.S.; Samal, R.N. (1986) Graft copolymerization with a new class of acidic peroxy salts as initiator. V. Grafting of methyl methacrylate onto jute fiber using potassium monopersulfate catalyzed by Fe(II), *J Appl Polym Sci*, 37(11):3085.
- 185 Sanadi, A.R.; Caulfield, D.F. (2000) Transcrystalline interphases in natural fiber-PP composites: effect of coupling agent, *Compos Interface*, 7(1):31-43.
- 186 Sanadi, A.R.; Caulfield, D.F.; Jacobson, R.E.; Rowell, R.M. (1995) Renewable agricultural fibers as reinforcing fillers in plastics: Mechanical properties of kenaf fiber-polypropylene composites, *Ind Eng Chem Res*, 34:1889.
- 187 Sanadi, A.R.; Prasad, S.V.; Rohadgi, P.K. (1986) Sunhemp fibre-reinforced polyester Part 1 Analysis of tensile and impact properties, *J Mater Sci*, 21(12):4299.
- 188 Sati, M.; Agnelli, J.A.M. (1989) The effect of chemical treatment of wood and polymer characteristics on the properties of wood-polymer composites, *J Appl Polym Sci*, 37(7):1777.
- 189 Satyanarayana, K.G.; Pillai, C.K.S.; Sukumaran, K.; Pillai, S.G.K.; Rohatgi, P.K.; Vijayan, K. (1982) Structure property studies of fibres from various parts of the coconut tree, *J Mater Sci*, 17:2453.
- 190 Schäfer, A.; Jacoby, H.D. (2004) Vehicle technology under CO₂ constraint: a general equilibrium analysis, *Energ Policy*, (article in press).
- 191 Schaper, S. (2001) Experiences of an automotive OEM in plastic recycling. Unattended side-effects of the EU End-of-Life-Vehicle directive presentation, AUDI AG, Germany, presentation on Identiplast 2001, Brussels, Belgium, 23rd - 24th April 2001.
- 192 Schick, M.J. (1977) Surface characteristics of fibres and textiles. Part II. New York: Marcel Dekker, 1977.
- 193 Schinner, G.; Brandt, J.; Richter, H. (1996) Recycling carbon fibre-reinforced thermoplastic composites, *J Thermoplast Compos*, 9(3):239-245.
- 194 Schlößer, T.; Knothe, J. (1997) Naturfaserverstärkte fahrzeugteile, *Kunstst-Plast 1997*, 9:1148. Hanser Verlag, München 1997 (in German).
- 195 Schneider, J.P.; Myers, G.E.; Clemons, C.M.; English, B.W. (1995) Biofibers as reinforcing fillers in thermoplastic composites, *J Vinyl Addit Techn*, 1(2):103-108.
- 196 Schuh, T.G. (2000) Renewable materials for automotive applications, report of Daimler-Chrysler AG, Stuttgart, 2000.
- 197 Semsarzadeh, M.A. (1986) Fiber matrix interactions in jute reinforced polyester resin, *Polym Composite*, 7(1):23.
- 198 Semsarzadeh, M.A.; Lottfali, A.R.; Mirzadeh, H. (1984) Jute reinforced polyester structures, *Polym Composite*, 5(2):141-142.
- 199 Shannon, C.E. (1949) Communication in the presence of noise, *Proc. Institute of Radio Engineers*, 37(1):10-21.
- 200 Sih, G.C.; Carpinteri, A.; Surace, G. (1995) *Advanced Technology for Design and Fabrication of composite Materials and Structures*, Kluwer Academic publishers: 1995.
- 201 Simonsen, J.; Rials, T.G. (2000) Investigating interphase development in woodpolymer composites by inverse gas chromatography, *Compos Interface*, 7(2):81-92.
- 202 Singh, B.; Gupta, M.; Verma, A. (1996) Influence of fiber surface treatment on the properties of sisal-polyester composites, *Polym Composite*, 17(6):910-918.
- 203 Singh, B.; Verma, A.; Gupta, M. (1998) Studies on adsorptive interaction between natural fiber and coupling agents, *J Appl Polym Sci*, 70:1847-1858.
- 204 SMC Automotive Alliance, *J Reinf Plast Comp*, 36, November (1992).
- 205 Spengler, E. (1996) Verkleidungsteile aus fasermatten, *Kunstst-Plast*, 3:314-316. (in German)
- 206 Stamboulis, A.; Baillie, C.A.; Garkhail, S.K.; Melick van, H.G.H.; Peijs, T. (2000) Environmental durability of flax fibres and their composites based on polypropylene matrix, *Appl Compos Mater*, 7:273-294.
- 207 Stodolsky, F.; Vyas, A.; Cuenca, R.M. (1995) Lightweight materials in the light-duty passenger vehicle market: Their market penetration potential and impacts, *Proc. of the Second World Car Conference*, University of California at Riverside, Jan. 22-24, March 1995.

- 208 Sustainability profile of the Automotive industry, UNEP Report on the automotive industry as a partner for sustainable development, Association des Constructeurs Européens d' Automobiles (ACEA), ISBN: 92-807-2177-1, 2002.
- 209 Takase, S.; Shiraishi, N. (1989) Studies on composites from wood and polypropylenes. II, *J Appl Polym Sci*, 37(3):645.
- 210 Thomason, J.L.; Cheney, T.; Williams, J. (2002) Injection mouldable 'long' natural fiber reinforced polypropylene for automotive applications, Proc. of the 10th European Conference on Composite Materials – ECCM-10 Composites for the future Sol, H. and Degrieck, J. (eds.), June 3-7, 2002, Brugge, Belgium.
- 211 Tobias, B.C. (1997) Evolving technologies for the competitive edge, Proc. of The International SAMPE Symposium and Exhibition, SAMPE, Covina, CA, 1997, Vol. 42 Issue 2, pp. 996.
- 212 Toll, S. (1992) Interpolative aggregate model for short-fiber composites, *J Compos Mater*, 26:1767-1783.
- 213 Varghese, S.; Kuriakose, B.; Thomas, S. (1994) Stress relaxation in short sisal-fiber-reinforced natural rubber composites, *J Appl Polym Sci*, 53:1051.
- 214 Varma, I.K.; Ananthakrishnan, S.R.; Krishnamurthy, Z.S. (1989) Composites of glass/modified jute fabric and unsaturated polyester resin, *Composites*, 20(4):383-388.
- 215 Velde van de, K.; Kiekens, P. (2001) Thermoplastic polymers: overview of several properties and their consequences in flax fibre reinforced composites, *Polym Test*, 20:885-893.
- 216 Velde van de, K.; Kiekens, P. (2001) Thermoplastic pultrusion of natural fibre reinforced composites, *Compos Struct*, 54:355-360.
- 217 Velde van de, K.; Kiekens, P. (2003) Effect of material and process parameters on the mechanical properties of unidirectional and multidirectional flax/polypropylene composites, *Compos Struct*, 62:443-448.
- 218 Voorn van, B.; Smit, H.H.G.; Snike, R.J.; Klerk de, B. (2001) Natural fibre reinforced sheet moulding compound, *Compos Part A-Appl S*, 23:1271-1279.
- 219 Wallentowitz, H.; Rappen, J.; Gossen, F. (1996) Fuel saving potential by weight reduction and optimizing of ancillary components: Simulation and Bench Test. VDI Berichte Nr. 1307.
- 220 Wambua, P.; Ivens, J.; Verpoest, I. (2003) Natural fibres: can they replace glass in fibre reinforced plastics? *Compos Sci Technol*, 63(9):1259-1264.
- 221 Weidmann, G.; Lewis, P.; Reid, N. (1990) Structural materials, ISBN 0-7506-1901-5, The Open University, 1990, p.430.
- 222 Westerlind, B.S.; Berg, J.C. (1988) Surface energy of untreated and surface-modified cellulose fibers, *J Appl Polym Sci*, 36(3):523-534.
- 223 Weyenberg van de, I.; Ivens, J.; Coster de, A.; Kino, B.; Baetens, E.; Verpoest, I. (2003) Influence of processing and chemical treatment of flax fibres on their composites, *Compos Sci Technol*, 63(9):1241-1246.
- 224 Winter, E.F.M.; Sharp, M.L.; Nordmark, G.E.; Banthia, V.K. (1990) Design considerations for aluminium spaceframe automotive structures, SAE technical series, Report No 905178, pp. 465-471.
- 225 Wötzel, K.; Wirth, R.; Flake, M. (1999) Life cycle studies on hemp fibre reinforced components and ABS for automotive parts, *Die Angew Makromol Chem* 272:121-127 (Nr. 4763).
- 226 Wright, J.R.; Mathias, L.J. (1993) New lightweight materials: Balsa wood-polymer composites based on ethyl-(hydroxymethyl)acrylate, *J Appl Polym Sci*, 48(12):2241.
- 227 Yap, M.G.S.; Que, Y.T.; Chia, L.H.L.; Chan, H.S.O. (1991) Thermal properties of tropical wood-polymer composites, *J Appl Polym Sci*, 43:2057-2065.
- 228 Yuxuan, L.; Zhongqin, L.; Aiqin, J.; Guanlong, C. (2003) Use of high strength steel sheet for lightweight and crashworthy car body, *Mater Design*, 24:177-182.
- 229 Yuxuan, L.; Zhongqin, L.; Aiqin, J.; Guanlong, C. (2004) Experimental study of glass-fiber mat thermoplastic material impact properties and lightweight automobile body analysis, *Mater Design*, 25:579-585.

References

- 230 Zárate, C.N.; Aranguen, M.I.; Reboredo, M.M.; (2000) Resol-vegetable fibers composites, *J Appl Polym Sci*, 77:1832-1840.
- 231 Zhu, W.H.; Tobias, B.C.; Coutts, R.S.P. (1995) Banana fibre strands reinforced polyester composites, *J Mater Sci Lett*, 14(7):508.

APPENDIX 1

Mechanical properties of some of natural fiber composites

Table 1. Experimentally obtained modulus of elasticity for some of natural and synthetic fiber reinforced composites.

Composite*	Reference	Tensile modulus, GPa	Density, kg/cm ³	Comments
Thermoplastics				
PP + 30% Flax	[186]	6	1.07	Non-woven
PP + 20% Flax	[50]	4-4.8	1.03	L _f = 3-25mm
PP + 30,40,50,60% Flax	[123]	4,6,7,8	1.02 – 1.24	Dew retted fibers
PP + 40,50% Kenaf	[28, 29, 85, 186]	6, 9.3 (8.3)	1.07	Untreated, (MAPP)
PP + 50 wt. % Jute	[186]	7.8	1.08	Non-woven
PE + 50 % Kenaf	[29]	4.57 (3)	1.16	Untreated, (MAPP)
PP + 57-68 wt.% Hemp	[156, 157]	3.6 – 1.5	1.23	Non-woven, needle punched mat
PP + 25–50 wt. % Flax	[146]	2.9 – 6.5	1.00 – 1.13	Different manufacturers
PP + 50% Sisal	[28]	5.5 (6) [5.9]	1.17	Untreated, (2% MAPP), (4% MAPP)
LD-PE + 10,20,30 wt. % Sisal	[80]	1.4 (1.7), 2.0 (2.3), 3.0 (3.3)	0.96 - 1.05	Untreated, (alkali treated). L _f = 2-10 mm
MaterBi + 20, 40, 60 % Flax	[171]	2.6, 5.9, 9.3	1.34 – 1.42	Thermoplastic biopolymer (starch based), Unidirectional fibers
PP + 20% Flax	[13]	2.45 (1.78)	1.02	No rubber, (matrix 70% PP, 30% rubbery additive). Injection molded
PP + 40 wt. % Kenaf	[86]	2.8 (3.4) [4.3]	1.07	Untreated, (2% MAPP), [5% MAPP]. L _f = 1.58mm. Injection molded
PP + 40 wt. % Flax	[84]	6	1.07	NMT
PP + 40 wt. % Glass	[84]	5.3 – 6	1.56	GMT
PP + 50 wt. % Jute	[85]	7.48 (7.56)	1.17	Untreated, (6% MAPP). L _f = 0.39 mm Injection molded.
PP + 30,40,60 wt.% Jute	[165]	4.6, 6.5, 11	1.07 – 1.21	3% MAPP. L _f =10mm
PP + 40 wt.% Glass	[29]	9	1.24	GMT
PP + 40 wt.% Glass	[146]	5.4	1.24	GMT
Thermosets				
UP + 30% Flax	[147]	5.1	1.16	Non-woven
Epoxy + 30% Flax	[59]	7.8	1.23	Non-woven
Epoxy + 25,43,50,60,75 % Sisal	[173]	8.0, 8.5, 9.0, 9.5, 10.0	1.19 – 1.26	UD fibers
Melanie formaldehyde + 22 wt.% Flax	[64]	10-13	1.49	Non-woven
UP + 15% Jute	[143]	1.8-3.7 (2.4-3.2)	1.10	Untreated, (Glycol treated)
UP + 15% Glass	[143]	7.0	1.26	
UP + 22 wt.% Flax + 38 wt% + chalk filler	[218]	7-12	1.4	L _f = 6,13,25,38 mm
UP + 22 wt.% Glass	[218]	8-11	1.4	Chopped fibers
UP + 50 % Sisal	[202]	1.15 (2.06) [1.75]	1.26	Untreated, (Methacrylamide treated), [silane treated]. Non-woven mats
UP + 60 wt. % Jute	[177]	2.8 – 3.1	1.26	RTM
UP + 60 wt. % Glass	[177]	5.4 – 6.0	1.92	RTM

APPENDIX 1

Table 1 continue:

UP + 45 wt. % Coir	[68]	3.6 (4.16)	1.18	Not treated (Silane treat). Non-woven mats
UP + 45 wt. % Glass	[68]	5.8	1.7	Non-woven mats
UP + 30 wt. % Pineapple fiber	[42]	2.3 (2.7)	1.09	Untreated, (silane treated). $L_f = 30\text{mm}$
UP + 30 wt.% palm leaf fibers	[110]	0.8 (1.9), [2.3]		$L_f = 5\text{mm}$, ($L_f = 10\text{ mm}$), [$L_f = 30\text{ mm}$]
Epoxy + 28, 46 % Sisal	[148]	14, 20	1.16	UD fiber, RTM
Epoxy + 32 % Flax	[148]	15	1.23	UD fiber, RTM
Epoxy + 48 % Glass	[148]	31	1.71	UD fiber, RTM

* fiber volume percentage is given (otherwise mentioned)

Table 2. Experimentally obtained strength of some of natural and synthetic fiber reinforced composites.

Composite*	Reference	Tensile strength, MPa	Density, kg/cm ³	Comments
Thermoplastics				
PP + 30% Flax	[186]	52	1.07	Non-woven
PP + 20% Flax	[50]	30-35	1.03	$L_f = 3\text{-}25\text{mm}$
PP + 30, 40, 50, 60% Flax	[123]	40, 45, 50, 60	1.02 – 1.24	Dew retted
PP + 40, 50 % Kenaf	[28, 29, 85, 186]	56, 33 (65)	1.07	Untreated, (MAPP)
PP + 50 wt.% Jute	[186]	72	1.08	Non-woven
PE + 50 % Kenaf	[29]	12 (27)	1.16	Untreated, (MAPP)
PP + 57-68 wt.% Hemp	[156, 157]	47-41	1.23	Non-woven, needle punched mat $L_f = 75\text{ mm}$
PP + 25–50 wt. % Flax	[146]	21 – 56	1.00 – 1.13	Non-woven
PP + 50% Sisal	[28]	37 (65) [67]	1.17	Untreated, (2% MAPP), (4% MAPP)
PP + 30 wt.% Sisal	[78]	25-27	1.07	Non-woven
LD-PE + 10, 20, 30 wt. % Sisal	[80]	15 (18), 22 (24), 31 (34)	0.96 - 1.05	Untreated, (alkali treated); $L_f = 2\text{-}10\text{ mm}$
MaterBi + 20, 40, 60 Flax	[171]	48, 73, 78	1.34 – 1.42	Thermoplastic biopolymer (starch based) UD fibers
PP + 20% Flax	[13]	32 (20)	1.02	No rubber, (matrix 70% PP, 30% rubbery additive). Injection molded
PP + 40 wt. % Kenaf	[86]	27 (41) [49]	1.07	Untreated, (2% MAPP), [5% MAPP]. $L_f = 1.58\text{ mm}$; Injection molded
PP + 40 wt.% Flax	[84]	50-70	1.07	NMT
PP + 40 wt.% Glass	[84]	80 – 100	1.56	GMT
PP + 50 wt.% Jute	[85]	30 (60)	1.17	Untreated, (6% MAPP). Injection molded, $L_f = 0.39\text{ mm}$
PP + 30, 40, 60 wt. % Jute	[165]	47, 57, 73	1.07 – 1.21	3% MAPP. $L_f = 10\text{mm}$
PP + 40 wt.% Glass	[29]	110	1.24	Non-woven
PP + 40 wt.% Glass	[146]	77	1.24	GMT
Thermosets				
UP + 30% Flax	[147]	44	1.16	Non-woven
Epoxy + 30% Flax	[59]	54	1.23	Non-woven
Epoxy + 25,43,50,60,75 % Sisal	[173]	160, 200, 250, 300, 330	1.19 – 1.26	UD fibers
Melanie formaldehyde + 22 wt.% Flax	[64]	37-43	1.49	Non-woven
UP + 15% Jute	[143]	26-45 (28-43)	1.10	Untreated, (Glycol treated)

APPENDIX 1

Table 2 continue:

UP + 15 % Glass	[143]	91-114	1.26	Random
UP + 22 wt.% Flax 38 wt.% chalk filler	[159]	40-80	1.4	L _f = 6, 13, 25, 38 mm
UP + 22 wt.% Glass	[159]	35-75	1.4	Chopped
UP + 50 % Sisal	[202]	30 (40) [34]	1.26	Untreated, (Methacrylamide treated), [silane treated]. Non-woven mats
UP + 17, 33 wt.% Coir	[176]	21, 24	0.96 – 1.08	L _f = 150 mm, Non-woven mats
UP + 60 wt. % Jute	[177]	27 – 44	1.26	RTM
UP + 60 wt. % Glass	[177]	85 – 117	1.92	RTM
UP + 45 wt. % Coir	[68]	40 (36)	1.18	Untreated, (silane treated). Non-woven mats
UP + 45 wt.% Glass	[68]	94	1.7	Non-woven mats
UP + 30 wt. % Pineapple fiber	[42]	52 (73)	1.09	Untreated, (silane treated). L _f = 30 mm
UP + 30 wt.% palm leaf fibers	[110]	15.6 (35), [53]	-	L _f = 5mm, (L _f = 10 mm), [L _f = 30 mm]
Epoxy + 28, 46% Sisal	[148]	169, 211	1.16	UD fiber
Epoxy + 32 % Flax	[148]	132	1.23	UD fiber, RTM
Epoxy + 48 % Glass	[148]	817	1.71	UD fiber

* fiber volume percentage is given (otherwise mentioned)

Table 3. Experimentally obtained Impact strength of some of natural and synthetic fiber reinforced composites.

Composite*	Reference	Notched izod, J/m	Charpy, kJ/m ²	Comments
Thermoplastics				
PP + 30 % Flax	[186]	20	-	Non-woven
PP + 20% Flax	[50]		6-13	L _f = 3-25 mm
PP + 40, 50% Kenaf	[28, 29, 85]	29, 34 (37)	-	Untreated (MAPP)
PP + 50 wt.% Jute	[186]	31		Non-woven
PE + 50% Kenaf	[29]	58 (110)		Untreated (MAPP)
PP + 57-68 wt.% Hemp	[156, 157]	111 – 84	11.9 – 8.5	Non-woven, needle punched mat. L _f = 75 mm
PP + 25–50 wt. % Flax	[146]	38-403	-	Non-woven
PP + 50% Sisal	[28]	68 (66) [62]	-	Untreated, (2% MAPP), [4% MAPP]
PP + 30 wt.% Sisal	[78]		50-60	Non-woven
PP + 20% Flax	[13]	-	3 (7)	No rubber, (matrix 70% PP, 30% rubbery additive). Injection molded
PP + 40 wt. % Kenaf	[86]	40 (41) [44]	-	Untreated, (2% MAPP), [5% MAPP]. L _f = 1.58 mm, Injection molded
PP + 40 wt. % Flax	[84]		20-25	NMT
PP + 30,40,60 wt. % Jute	[165]	27, 31, 32	-	3% MAPP. L _f = 10 mm
PP + 40 wt. % Glass	[29]	107	-	GMT
PP + 40 wt. % Glass	[146]	410	-	GMT
PP + 40 wt. % Glass	[84]	-	75 – 120	GMT
Thermosets				
Epoxy + 30% Flax	[59]	10	-	Unidirectional fibers
UP + 15% Jute	[143]	32-40 (29-38)	-	Untreated, (Glycol treated). Non-woven mat, RTM
UP + 15% Glass	[143]	343-377	-	Non-woven mat, RTM
UP + 22 wt.% Flax + 38 wt.% chalk filler	[218]	-	3 (7)	L _f = 13 (38) mm

APPENDIX 1

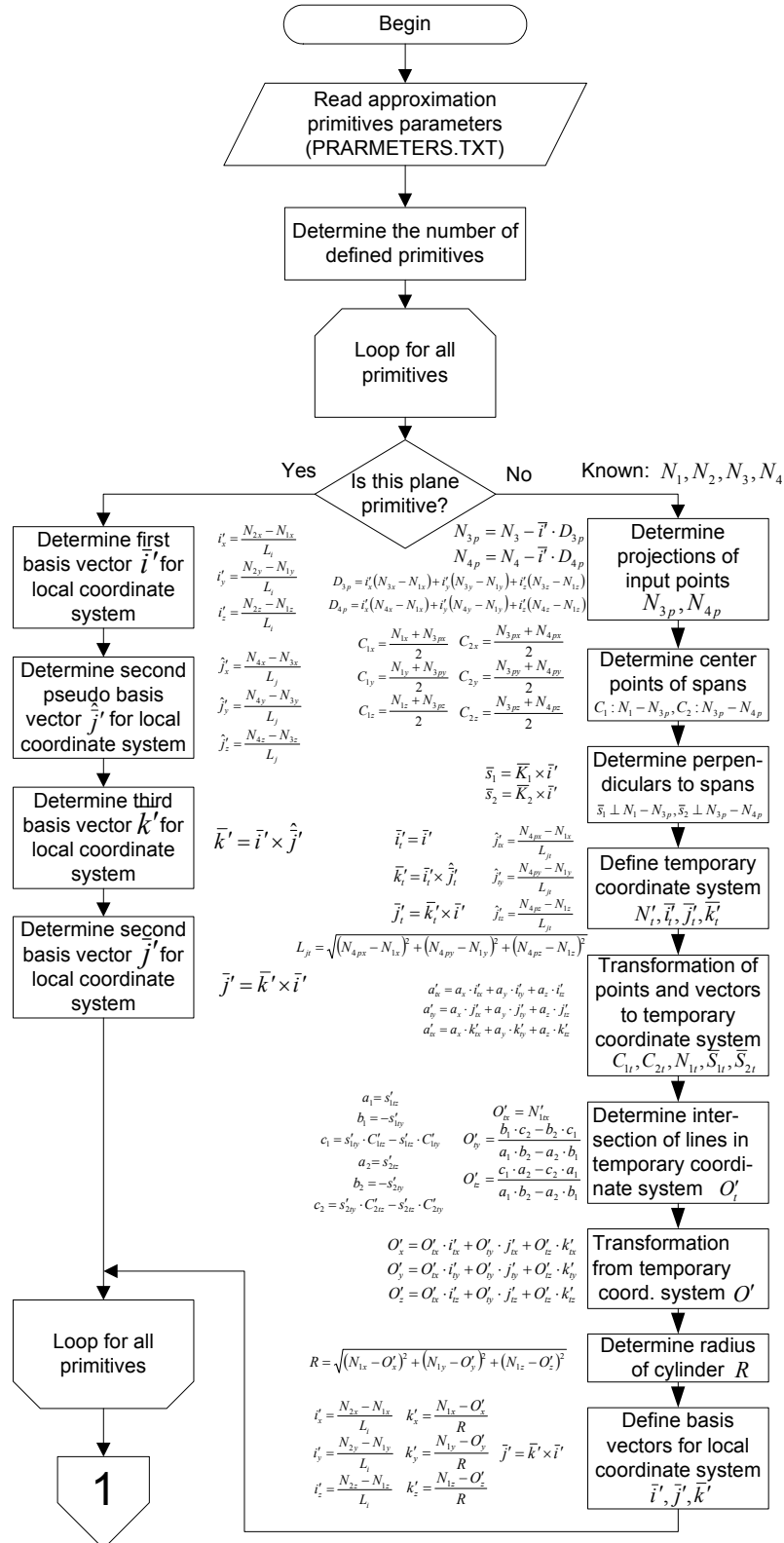
Table 3 continue:

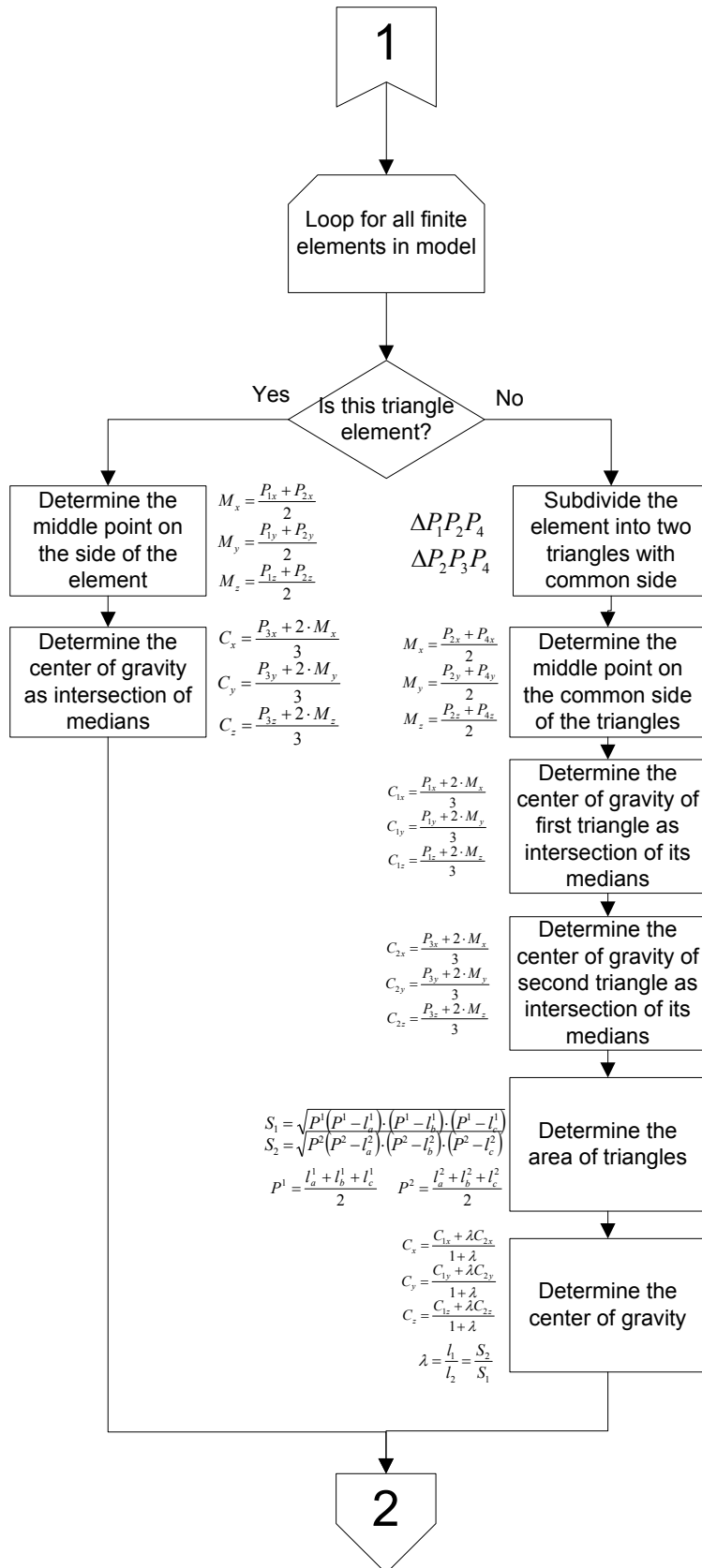
UP + 22 wt.% Glass	[218]	-	40-70	Random
UP + 17, 33 wt. % Coir	[176]	433, 568	-	L _f = 150 mm. Non-woven mats
UP + 60 wt.% Jute	[177]	32-40	-	RTM
UP + 45 wt.% Coir	[68]	-	16.5 (16.4)	Untreated, (silane treated). Non-woven mats
UP + 30 wt. % Pineapple fiber	[42]	-	25	silane treated L _f = 30 mm

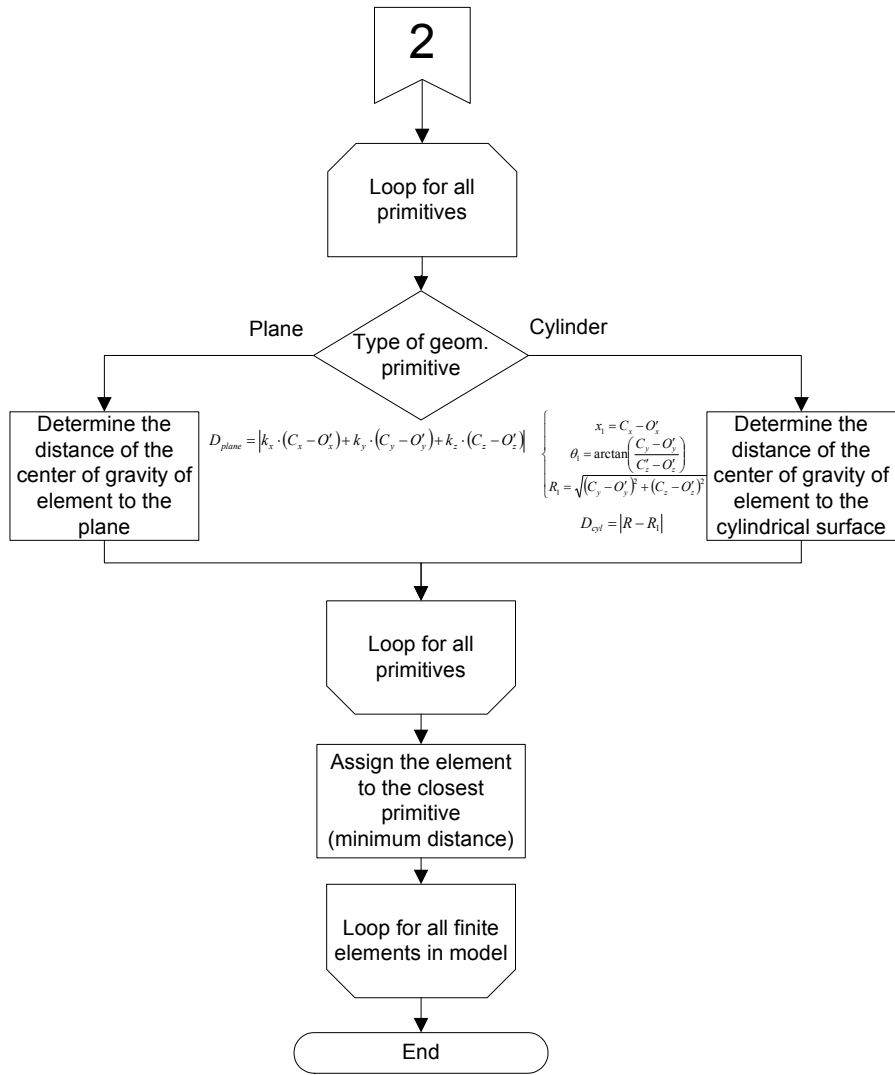
* fiber volume percentage is given (otherwise mentioned)

APPENDIX 2

Algorithm of the finite elements' association with geometrical primitives.

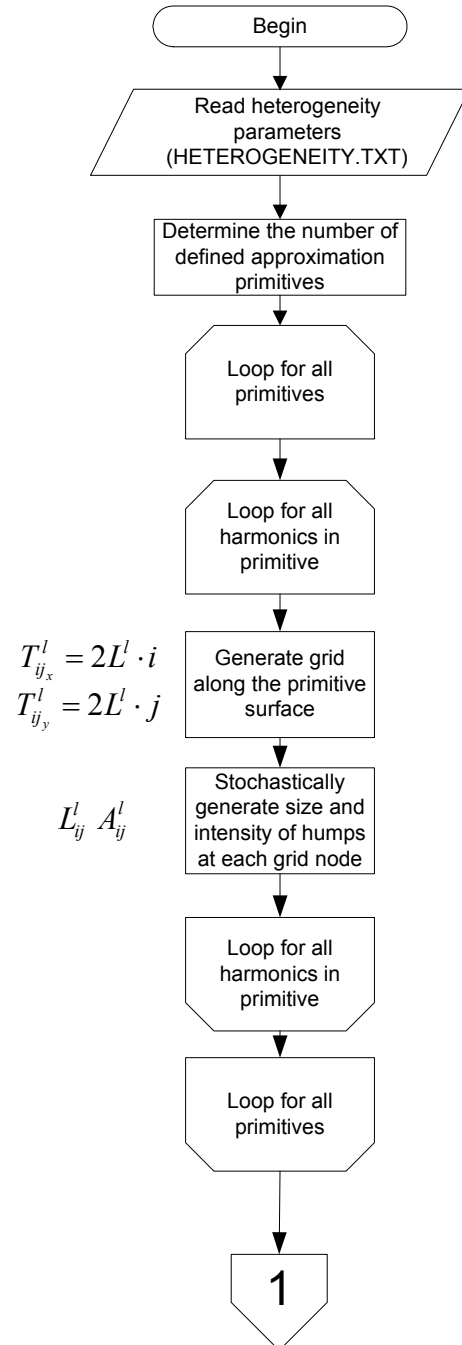


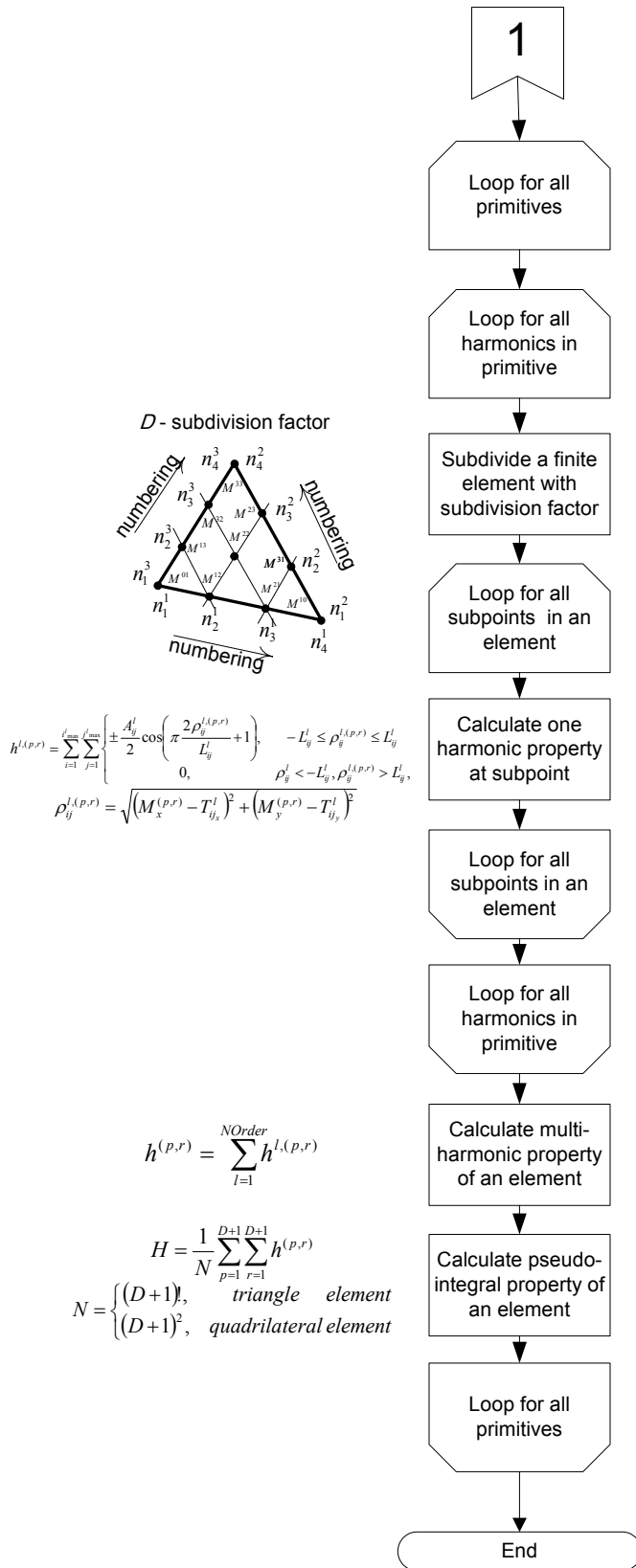




APPENDIX 3

Algorithm of heterogeneity generation procedure





Acknowledgements

The completion of this research work would be not possible without a valuable help of a number of people. Therefore I would like to express my gratitude to them.

First of all I would like to express my sincere gratitude to my supervisor Jan Spoormaker for giving me the opportunity to carry out this PhD project in the Netherlands and for his valuable supervision even after his retirement.

I am also indebted to Natalia Ermolaeva for her priceless coaching through the whole of my stay at the Delft University of Technology. She was my daily supervisor. She provided me with valuable scientific support during our talks where she could always direct me in the right way. Most of the papers related to this thesis have been published with her contribution. Special thanks for her enthusiasm in the countless reading of my paper articles and this thesis to improve the readability of the text. I would also like to express my thanks to Ihor Skrypnyk, who has provided me with the software which enabled fast preliminary checking of the early research findings.

Thanks to all my DIOC-16 colleagues who have put very good questions during our project meetings. With the help of these questions it was possible to improve my work.

My special thanks to Kees van Koert, Rogier Mandos and Martijn de Koninck from Polynorm BV, who have kindly provided the component made of natural fiber composite for the testing. Without that component the verification of my model would be problematic. I would like to thank our laboratory technician Fred den Elzen for his help in preparing the experiments.

This work would be very difficult to accomplish without the emotional support of my lovely wife Marina, who heroically withstood the hardships of this work. During this time she gave birth to our son Anton, lots of thanks for her patience, trust and understanding.

I also would like to express my gratitude to all my Russian-Ukrainian friends in Delft for providing me and my family with homelike atmosphere in a foreign country.

Finally I am most grateful to my mother and father, who played a crucial role in making important decisions in my life and have inspired me to move forward.

Curriculum vitae

Kirill Gennadjevich Kavelin was born on 7-th of May 1977 in the city of Izhevsk, Russia. In 1984 he began secondary education at school No 35 in his home city. On the 7-th year of his study a special group with intensive study of mathematics, physics, programming and foreign language has been formed in that school in co-operation with Izhevsk State Technical University. He joined that group after successfully passed tests. In 1994 he graduated from the secondary school and has been granted with privilege to follow 2-year course on Faculty of Robotics at Izhevsk State Technical University without entrance exams (which were normally required). In 1997, after four years of study, he received Bachelor's degree with honours in Machinery and Technology. In 1997 he has got an offer to follow a Masters course on Faculty of Mechanical Engineering at Budapest University of Technology and Economics (Hungary), which he has accepted. Following two years until 1999 he studied in Budapest and as a result of the study he received Master's degree with honours in Mechanical Engineering. He chose to perform investigations of behaviour of composite materials for his master's thesis. After that he has returned Izhevsk with an idea to join Faculty of Robotics at Izhevsk State Technical University as a PhD student. At the same time, due to financial situation and motivations to explore things in reality he has decided to join one of the industrial companies in Izhevsk. Unfortunately no open engineering positions were available at that moment and he agreed on the position of a master in an assembly workshop. However, after some time he realised that this work did not correspond with his objectives and left no time for the research at the University. Therefore he decided to terminate his contract at the factory and move closer to science. In late 1999 he joined Faculty of Robotics at Izhevsk State Technical University as a part-time docent. As a result more time for the research within the PhD study has appeared. However, the conducted research work in the field of friction joints in application to paper-making machinery proposed by his supervisor seemed had little chance to be applied in reality due to economical difficulties in the whole country. Absence of the research challenge and the desire to exploit the experience gained during his study in Budapest in the field of composite materials encouraged him to search for a new research project abroad. In 2000 he joined Industrial Design Faculty at TU Delft as a PhD student. The following four years for him were full of inspiration and creativity to perform the research in the field of natural fiber composites in applications to automotive structures, which is resulted in this Thesis. During his work at TU Delft he got married with Marina and become a father of Anton.

РЕФЕРАТ

Данная работа выполнена в рамках программы, целью которой является разработка методов, направленных на повышение эффективности использования материальных и энергетических ресурсов в продуктах повседневного спроса. Необходимость в этой программе возникла вследствие повышенного интереса современного общества к защите окружающей среды. Современные требования общества обязывают промышленный прогресс разрабатывать экологически чистые технологии. В качестве предмета исследования был взят концептуальный автомобиль под названием Dutch-EVO. Одна из главных инновационных идей проекта - это разработать такие методы применения современных легких и экологически чистых материалов при проектировании исследуемого автомобиля, с помощью которых удастся существенно снизить его энергопотребление, а также уменьшить отрицательное влияние его производства и эксплуатации на экологию окружающей среды. Разработанные методы и технологии предполагается использовать для улучшения конструкций других современных автомобилей и повышения их экологичности. Для этого в рамках программы был начат проект под названием "Исследование методов применения современных материалов в автомобильных конструкциях". Целью данного проекта является исследование самых современных конструкционных материалов, доступных на рынке, на предмет выгодности (эффективности) их использования в автомобилях.

В процессе исследований было проведено сравнение таких современных материалов как магниевые сплавы и композиты, с обычными материалами, такими как сталь и алюминиевые сплавы, широко применяющимися в автомобильных конструкциях на данный момент. В качестве критериев сравнения были выбраны не только стоимость и простые механические характеристики данных материалов, но также и их комплексные характеристики, такие как потенциальная возможность снижения веса автомобиля и возможность его чистой утилизации. В результате было выявлено, что зачастую применение новых материалов сопровождается необходимостью полного переоборудования технологических процессов. Материальные затраты, необходимые на переоборудование, также приняты во внимание.

В рамках данного исследования были проанализированы сложные связи между технологическими, экономическими и экологическими аспектами производства и утилизации материалов. В результате анализа композитные материалы на основе полимерной матрицы усиленной натуральными волокнами показали хорошие результаты. Поэтому они рассматриваются как многообещающие и наиболее выгодные материалы для автомобильных конструкций будущего. Применение выбранных композитных материалов в конструкционных и декоративных целях рассматривается как важная задача на пути повышения экономичности и экологичности автомобилей.

В работе проведено детальное исследование механических характеристик различных полимерных композитных материалов усиленных натуральными волокнами. Влияние таких факторов, как тип волокон, их длина, количество, направленность и т.д. на их механические характеристики принято во внимание. В результате исследований было выявлено, что применение случайно ориентированных натуральных волокон в виде нетканых матов в данных композитах наиболее эффективно. Низкая стоимость данных композитных материалов в сочетании с их низким удельным весом и хорошими механическими характеристиками являются привлекательными для производителей автомобилей, так как снижение массы автомобиля при низкой стоимости используемых материалов является ключевым моментом современного автомобильного производства. В частности, уже сейчас некоторые передовые автомобильные гиганты начали применение этих композитов в своих разработках. Однако, область применения полимерных композитных материалов усиленных натуральными

волокнами в форме нетканых матов ограничена вследствие их низкой ударной прочности, сильного влияния влаги на их механические характеристики, а также наличия проблемы с достижением требуемого качества поверхности изделий. На данный момент они применяются только в ненагруженных и малонагруженных конструкциях, а также в декоративных целях. Однако, все перечисленные проблемы носят сугубо технологический характер и с дальнейшим развитием технологии производства этих композитов могут быть разрешены. Было также выявлено еще одно их неотъемлемое свойство - большая неравномерность в механических характеристиках, которая обусловлена неоднородностью в распределении волокон в нетканых матах. Проблема неоднородности может быть также решена технологически (путем большего контроля за качеством распределения), но такое решение приводит к значительному подорожанию полученных волоконных матов и, как следствие, всего композитного материала. Таким образом, предпочтительнее использовать эти композитные материалы "как есть". Однако, в этом случае есть большая вероятность ненадежного определения их механических характеристик при использовании стандартных экспериментальных методов, разработанных ранее для композитных материалов с синтетическими волокнами.

Как известно, в проектировании конструкций используются усредненные характеристики материалов, получаемые в результате серии экспериментов. Поэтому, в частности, чтобы устранить влияние неоднородности свойств материала, вводят коэффициенты запаса. Большой разброс свойств композитных материалов с натуральными волокнами приводит к тому, что в расчеты конструкций необходимо вводить очень большие коэффициенты запаса, что, в свою очередь, приводит к неэффективному использованию материала и неоправданному увеличению веса конструкции.

Поэтому для успешного и эффективного использования в автомобильных конструкциях композитных материалов с натуральными волокнами, имеющих большую неоднородность в свойствах, необходимо разработать методы оценки и методы проектирования с учетом этой неоднородности. В частности, характеристики неоднородности могут быть включены в ставшие сейчас популярными конечноэлементные расчеты. Новые методы расчета существенно помогут инженерам в проектировании конструкций.

Новая методика определения характеристик неоднородности свойств в полимерных композитах усиленных натуральными волокнами в форме нетканых матов предложена в данной работе. Методика основана на определении спектральных характеристик неравномерной плотности матов, полученных с их цифровых изображений. Цифровые изображения матов предлагается получать при помощи сканирования незалитого в пластик мата или рентгеновского снимка листа готового композита. В результате исследований было выявлено, что неравномерность в свойствах композитов из натуральных волокон обусловлена локальным изменением количества (объемной доли) волокон вдоль поверхности материала. Это наглядно отражается на цифровом изображении полученного с рентгеновского снимка композита в виде локального изменения яркости участков изображения. Так, в одних областях изображения натуральные волокна образуют своего рода кластеры (уплотнения), в то время как в других присутствуют разреженности (пустоты). Локальные уплотнения и пустоты в волоконном мате хаотично распределены вдоль его поверхности. Неравномерность распределения волокон по толщине материала также выявлена с помощью анализа микрофотографии композитного материала. Однако, эта неравномерность не может быть выявлена при помощи рентгеновских снимков, поэтому на начальном этапе принято допущение не рассматривать эту неравномерность.

Для того, чтобы упростить описание сложной по структуре неоднородности в композите, ее предложено описать при помощи примитивов неоднородности. В качестве примитивов использованы простые математические функции, в отдельности описывающие форму и интенсивность локальных уплотнений или разреженностей

вдоль поверхности волокнистого мата или композита. Такой подход позволяет исключить использование функций высокого порядка для описания сложной структуры неоднородности материала.

Для определения параметров примитивов неоднородности был применен спектральный анализ. Для анализа было использовано несколько линейных распределений яркости (выборки), снятых с рентгеновского снимка композита. На полученных спектрограммах были выделены определенные гармоники. Известно, что каждая гармоника характеризуется по крайней мере двумя характеристиками: длиной волны и амплитудой. Было выявлено, что эти характеристики напрямую связаны с параметрами “размера” и “интенсивности” примитивов неоднородности. Так, “размер” примитивов связан с длиной волны, которая определяет их физические размеры в плоскости материала, а “интенсивность” определяет объемную долю волокон в примитивах (степень сгущенности или разреженности) и поэтому связана с амплитудой. В снятом спектре для данной выборки набор гармоник с большими амплитудами считается характеристическим. Набор характеристических гармоник для всего мата определяется методом корреляции гармоник в спектрах нескольких выборок, снятых с одного изображения. Таким образом, набор этих гармоник довольно точно отражает свойства неоднородности волокнистого мата или композита.

Очевидно, что для того, чтобы успешно проводить конечноэлементные расчеты конструкций, сделанных из неоднородных материалов, необходимо внедрить оцененную неоднородность в модель конструкции. Используя стандартные методы подготовки модели, предлагаемые производителями расчетных пакетов, очень сложно обеспечить заданную неоднородность на практике. Поэтому была разработана специальная процедура для генерирования неоднородности.

Разработанная в данной работе процедура генерирует неоднородность в плоскости композита с использованием заранее определенных характеристик примитивов. Параметры характеристических гармоник и общие статистические характеристики используются для генерации неоднородности. В пределах одного примитивного элемента неоднородности происходит плавное локальное увеличение или уменьшение значения функции неоднородности. Это изменение описано простой математической функцией в пространстве. Каждая гармоника из характеристического набора используется для генерации неоднородности первого порядка. Одновременно вдоль поверхности композита генерируется несколько неоднородностей первого порядка с использованием параметров заранее определенных характеристических гармоник. Результирующая неоднородность высокого порядка получается суммированием неоднородностей первого порядка. Было установлено, что сгенерированная неоднородность высокого порядка имеет характеристики, близкие к характеристикам, наблюдаемым в реальном композитном материале. Степень их сходства напрямую зависит от числа участвующих в генерации гармоник первого порядка. Сгенерированная неоднородность представляет собой изменение объемной доли волокон вдоль волокнистого мата или плоскости композитного материала. Объемная доля волокон в композитном материале напрямую влияет на его механические характеристики. Для того, чтобы установить эту взаимосвязь, необходимо произвести поиск подходящей теоретической модели.

Известно, что модель материала для проведения линейных расчетов конструкций может быть ограничена до одного параметра – модуля упругости. Поэтому на начальном этапе предложено связать сгенерированную неоднородность объемной доли волокон композитного материала именно с модулем упругости. Для выражения связи модуля упругости композита с объемной долей волокон требуется надежная теоретическая модель.

В данной работе рассмотрено несколько существующих теоретических моделей. Тестирование каждой из них проведено с использованием надежных экспериментальных данных для полимерных композитов с натуральными волокнами в форме нетканых матов. Все теоретические модели используют несколько параметров для определения модуля упругости композита, а именно: модули упругости

полимерной матрицы и волокон, объемную долю волокон, а также несколько эмпирических коэффициентов. По итогам тестирования существующих моделей было выявлено, что для рассматриваемых композитов ни одна не дает результат с необходимой точностью. Поэтому было предложено модифицировать ту модель, которая дает наиболее точный результат. После предложенной модификации модель давала надежный результат, близкий к экспериментальному. Модифицированная модель в дальнейшем использована в процедуре генерации неоднородности композитного материала в конечноэлементной модели в виде изменяющегося модуля упругости конечных элементов.

Также, для успешного моделирования различных композитных конструкций с учетом неоднородности материала была разработана технология внедрения сгенерированной неоднородности материала в стандартный программный пакет для расчетов конструкции методом конечных элементов. Разработанная технология основана на том принципе, что подавляющее число композитных конструкций, как правило, тонкостенные и могут быть смоделированы, используя принцип оболочек. В таком подходе допускается не моделировать распределение свойств по толщине материала. Поэтому, используя метод конечных элементов, неоднородность в оболочечных конструкциях можно представить только как изменение механических свойств смежных конечных элементов. В данном случае модуль упругости конечных элементов варьируется в зависимости от их местонахождения в модели, сгенерированной неоднородности и механических характеристик составляющих компонентов композитного материала. Зачастую оболочечные конструкции имеют довольно сложную геометрию. Поэтому для того, чтобы все конечные элементы имели свойства в соответствии со сгенерированной неоднородностью, в данной работе был разработан специальный метод.

Разработанный метод основан на примитивных геометрических элементах (плоскость и цилиндр), с помощью которых сложный трехмерный объект может быть аппроксимирован с достаточной для механических расчетов точностью. Неоднородность материала может быть сгенерирована вдоль поверхности каждого геометрического элемента в отдельности. Примитивные геометрические элементы назначаются пользователем на основе построенной конечноэлементной модели с использованием разработанных принципов. Используя разработанную методику, можно моделировать как двухмерные, так и трехмерные оболочечные конструкции. Методика запрограммирована на языке Фортран и встроена в коммерческий пакет для конечноэлементных расчетов MSC.MARC.

Разработанный подход к описанию свойств неоднородных композитных материалов апробирован на проведенных стандартных экспериментах. Образцы, использованные для испытаний на растяжение, были вырезаны из листа композитного материала на основе полипропиленовой матрицы усиленной натуральными волокнами в форме нетканого мата. Композитный лист был получен с помощью процесса горячей формовки. Во время проведения экспериментов для наблюдения за неоднородностью поверхностных деформаций образцов была использована бесконтактная оптическая система. Предварительно неоднородность распределения волокон в образцах была исследована с помощью рентгеновских снимков. Далее было проведено сопоставление поверхностных деформаций образцов с распределением в них волокон. Анализ показал хорошую корреляцию этих двух результатов. Далее параметры неоднородности распределения волокон (набор характеристических гармоник) были определены с рентгеновских фотографий. Полученные параметры были включены в конечноэлементный расчет точно таких же по геометрии образцов с использованием разработанного подхода. В результате сравнения поверхностных деформаций экспериментально протестированных и смоделированных образцов также выявлена хорошая корреляция.

С помощью моделирования стандартных образцов с различной конечноэлементной сеткой (изменялся размер конечных элементов) было также исследовано влияние размера конечных элементов на результат моделирования. На

основании этого был предложен метод для определения оптимального размера конечных элементов.

Далее автомобильная конструкция использовалась для полномасштабного апробирования разработанной методики моделирования конструкций, сделанных из неоднородных материалов. Конструкция основания заднего автомобильного сиденья была изготовлена в рамках сотрудничества с промышленным предприятием. Для этого были использованы два различных композитных материала: полипропилен усиленный стеклянными волокнами в случайной ориентации и полипропилен усиленный льняными волокнами в форме нетканых матов. Предварительно жесткость конструкций на изгиб исследовалась экспериментально, с использованием стандартной испытательной машины со специально разработанным приспособлением.

Было обнаружено, что конструкция, сделанная из композитного материала с натуральными волокнами, при определенных параметрах изготовления имеет жесткость, сравнимую с жесткостью конструкции, сделанной из стекловолоконного композита. Однако, вес конструкции выполненной из композита с натуральными волокнами был сравним с весом конструкции, сделанной из стекловолоконного композита. В результате не было ожидаемого выигрыша в весе конструкции из композита с натуральными волокнами. Поэтому был сделан вывод, что необходимо улучшить свойства этого композита, чтобы достичь оптимального его использования в данной конструкции. Это можно сделать, например, введя компонент, улучшающий адгезию между полимерной матрицей и волокнами и тем самым увеличивая модуль упругости материала. Для исследования и оценки неравномерности поверхностных деформаций, возникающей вследствие неоднородности материала конструкции, были проведены эксперименты с использованием системы бесконтактного измерения поверхностных деформаций. Сравнивая результат с ранее сделанными рентгеновскими фотографиями конструкции было выявлено, что полученное распределение поверхностных деформаций не всегда надежно. Для выявления причин обнаруженного феномена поперечный срез композита с натуральными волокнами исследовался под электронным микроскопом. Предположительно, неравномерность распределения натуральных волокон по толщине композитного материала оказывает значительное влияние на результат измерения поверхностных деформаций из-за неравномерной несущей способности разных "слоев" материала. Так, в результате изгибной деформации распределение нагрузки в толщине композита также неравномерно, что и оказывает большое влияние на поверхностные деформации. Этот эффект предлагается исследовать в следующих работах.

Для проверки достоверности бесконтактно полученных результатов были проведены дополнительные эксперименты с использованием тензодатчиков, наклеенных на конструкцию. В результате этих экспериментов было выявлено, что бесконтактная система измерения деформаций имеет определенные ограничения в измерении деформаций в сложно-нагруженных неоднородных вдоль поверхности конструкциях, материал по толщине которых также неоднороден.

Далее, используя разработанный в данной работе метод, были определены параметры неоднородности использованного для изготовления конструкции композитного материала на основе натуральных волокон. Для этого были использованы рентгеновские снимки конструкции. Конечноэлементная модель конструкции была построена на основе имеющейся геометрии. Результаты моделирования были сравнены с экспериментальными результатами. После проведения моделирования обнаружено частичное сходство полученных результатов с ранее полученными экспериментальными результатами. Сравнение производилось по неоднородности поверхностных деформаций. Некоторые причины различия в полученных результатах обсуждаются в данной работе.

Обобщив разработанные методики, мы получаем новый подход к моделированию конструкций из неоднородных композитных материалов. Его составляющими являются: определение параметров неоднородности материала, генерация неоднородности, настройка теоретической модели расчета модуля

упругости композитного материала (используя экспериментальные данные), а также метод аппроксимации сложной формы конструкции примитивными геометрическими элементами и, наконец, назначение свойств конечным элементам модели. С помощью разработанного подхода достигается более высокая надежность расчетов конструкций, сделанных из неоднородных композитных материалов, через более точное описание их локальных механических характеристик. Более того, имея известные свойства неоднородности, возможно более надежное экспериментальное тестирование образцов из неоднородных композитов. В частности, возможно исключить влияние размеров образцов на результаты тестирования.

В результате проведенной исследовательской работы был разработан и апробирован новый подход к определению свойств неоднородных композитных материалов на основе натуральных волокон. Разработанные в данной работе методики являются важным шагом на пути к более глубокому пониманию сложной механики таких материалов, а также дают возможность моделировать конструкции, сделанные из материалов с неоднородными свойствами, позволяя оптимально использовать материал. В заключении приведены общие принципы проектирования конструкций с использованием неоднородных композитных материалов на основе натуральных волокон.

Кирилл Кавелин